TESIS DE LA UNIVERSIDAD DE ZARAGOZA

2017

6

Carmen Arnal Bordetas

In deep study of new tuberculosis vaccine candidates based on *phoP* and *fadD26* mutations

Departamento

Microbiología, Medicina Preventiva y Salud Pública

Director/es

Martín Montañés, Carlos
Gonzalo Asensio, Jesús Ángel
Arbués Arribas, Ainhoa

ISSN 2254-7606

Prensas de la Universidad Universidad Zaragoza

ISSN 2254-7606

Universidad Zaragoza
1542

Tesis Doctoral

IN DEEP STUDY OF NEW TUBERCULOSIS VACCINE CANDIDATES BASED ON *PHOP* AND *FADD26* MUTATIONS

Autor

Carmen Arnal Bordetas

Director/es

Martín Montañés, Carlos
Gonzalo Asensio, Jesús Ángel
Arbués Arribas, Ainhoa

UNIVERSIDAD DE ZARAGOZA

Microbiología, Medicina Preventiva y Salud Pública

2016

FACULTAD DE MEDICINA

Departamento de Microbiología, Medicina Preventiva y Salud Pública de la Universidad de Zaragoza

In deep study of new tuberculosis vaccine candidates based on *phoP* and *fadD26* mutations

Tesis doctoral para optar al grado de Doctor presentada por:

Carmen Arnal Bordetas

Licenciada en Bioquímica

Directores:

Carlos Martín Montañés

Jesús Ángel Gonzalo Asensio

Ainhoa Arbués Arribas

Universidad Zaragoza
1542

D. CARLOS MARTÍN MONTAÑÉS, Catedrático de Microbiología del Departamento de Microbiología, Medicina Preventiva y Salud Pública de la Universidad de Zaragoza.

D. JESÚS ÁNGEL GONZALO ASENSIO, Doctor en Bioquímica y Biología Molecular y Celular por la Universidad de Zaragoza. Profesor Ayudante Doctor del Departamento de Microbiología, Medicina Preventiva y Salud Pública de la Universidad de Zaragoza.

Dª AINHOA ARBUÉS ARRIBAS, Doctora en Bioquímica y Biología Molecular y Celular por la Universidad de Zaragoza.

Directores de la Tesis Doctoral presentada por Carmen Arnal Bordetas bajo el título:

"In deep study on new tuberculosis vaccine candidates based on *phoP* and *fadD26* mutations"

EXPONEN:

Que dicha Tesis ha sido realizada bajo su dirección y cumple las condiciones para optar al grado de Doctor por la Universidad de Zaragoza.

Por lo tanto, emiten el presente **INFORME FAVORABLE.**

Zaragoza, Septiembre de 2016

Fdo: Carlos Martín Montañés

Fdo: Jesús Ángel Gonzalo Asensio

Ainhoa A.

Fdo: Ainhoa Arbués Arribas

Esta Tesis Doctoral ha sido elaborada en el Departamento de Microbiología, Medicina Preventiva y Salud Pública adscrito al programa de doctorado del Departamento de Bioquímica y Biología Molecular y Celular, siendo Carmen Arnal Bordetas beneficiaria de una beca predoctoral concedida por el Departamento de Ciencia, Tecnología y Universidad de la Diputación General de Aragón (referencia: B149/2010).

Parte de este trabajo es fruto de una estancia de cuatro meses en el Instituto de Farmacología y Biología Estructural (IPBS, CNRS) de Toulouse bajo la supervisión del Doctor Olivier Neyrolles, dentro del Proyecto Europeo (NEWTBVAC 241745 FP7 HEALTH EU), "Discovery and preclinical development of new generation tuberculosis vaccines"), cofinanciado por una beca de la CAI (Caja de Ahorros de la Inmaculada) perteneciente al programa CAI Europa y una beca para estancias de corta duración de la EMBO (European Molecular Biology Organization).

Este trabajo ha sido realizado dentro de los siguientes proyectos de investigación.

- Proyectos del Ministerio de Economía y Competitividad: "Estudios de los mecanismos de virulencia regulados por PhoP en *Mycobacterium tuberculosis*. Aplicación a la construcción de una nueva generación de vacunas" (referencia: BIO2008-01561) y Proyecto del Ministerio de Economía y Competitividad: "Estudio de los mecanismos de protección de MTBVAC y su uso potencial como vacuna recombinante polivalente" (referencia: BIO2011-23555).
- Proyectos de la Unión Europea del VII programa marco: "Discovery and preclinical development of new generation tuberculosis vaccines" (referencia: HEALTH-2009-2.3.2-2) y "New TBVAC" (referencia:I-2010/002 Project 241745).

"To be nobody but yourself
in a world that's doing its
best to make you somebody
else, is to fight the hardest
battle you are ever going to
fight. NEVER STOP FIGHTNG."

-E. E. Cummings.

A Adrián. Gracias por ser tan buen compañero y amigo, por estar a mi lado, por tenderme la mano cuando me caigo, por creer en mí cuando ni yo misma lo hago.

A mi Familia, mi Ohana, mi Piña, porque sois parte indispensable de mi motor, porque crecemos juntes y nos hacemos más fuertes, porque estáis ahí en las buenas y en las malas.

A mis padres, a mi Madre, porque tu ausencia llena cada línea de este trabajo. Porque te llevo siempre muy dentro, hasta la raíz.

Este trabajo está escrito con la fuerza de vuestro amor.

Quería agradecer a Carlos Martín la oportunidad de entrar en este grupo y al mundo de la investigación. Por todo el trabajo y dedicación de estos años, con sus parones y sus arrancadas, no ha sido fácil pero al final, aquí está el resultado.

Al Grupo de Genética de Micobacterias por todo lo aprendido de ciencia y de la vida en este trecho de vida que he compartido con vosotres. Gracias por esos capazos que alegraban el día, las risas, los cafés y los ratos, a veces eternos, compartidos en el P3.

A Cris y Henar, porque a pesar de ser tan diferentes encontré dos personas muy importantes donde menos lo esperaba. Habéis hecho de estos años algo mucho más llevadero, a pesar de las distancias, a pesar de las idas y venidas. Gracias prendas, por los ánimos, la fuerza, las risas y los lloros.

A mi equipo, mis sicaritas, porque aprendimos juntas algo muy importante y es que da igual cuántas veces nos caigamos, siempre nos volvemos a levantar con fuerza. En especial a Natalia, compañera de equipo y de vida, parte imprescindible de mi camino, que sigamos así por mucho tiempo.

I would like to thank all the people from Dr. Olivier Neyrolles's group for receiving and helping me during my 4 month stay. Also thanks to Dr. Christophe Guilhot and Dª Catherine Astarie-Dequeker for the support during my stay in Toulouse. It was a pleasure working with you.

Index

Summary

The first objective of the present work was to characterize the interactions of the attenuated live vaccine candidate against tuberculosis MTBVAC with the host. In this study, comparative proteome analysis of the secreted fractions of MTBVAC and its *M. tuberculosis* parental strain Mt103 was performed through Western-Blot and fluorescence two-dimensional difference gel electrophoresis (DiGE) techniques. Two protein datasets preferentially expressed either on MTBVAC or Mt103 were obtained. These results allowed us to show the higher secretion of the Twin Arginine Translocation (TAT) secretory system substrates in MTBVAC and to confirm the complete absence of the virulence factors ESAT-6 and CFP-10 from its secretome.

Intracellular trafficking of MTBVAC was the other aspect of the interaction with the host to be studied. Being MTBVAC a double *phoP* and *fadD26* mutant, the individual contribution of each mutation to the final phenotype was also a matter of study. Infections with the correspondent GFP-expressing strains were performed in two different cell models: a cell line of mouse alveolar macrophages (MHS) and human macrophages derived from monocytes (hMDM), and the results were analyzed through microscopy techniques. Results obtained suggest that MTBVAC, as an attenuated strain, is not able to arrest phagosomal maturation at early stages of the process, but it does arrest the maturation before the mycobacterial-containing phagosome evolves to a lysosomal stage. This strategy prevents MTBVAC to be degraded in the phagolysosome. Nevertheless impaired ESAT-6 and CFP-10 secretion in MTBVAC does not allow it to escape to the cytosol, presenting a persistence phenotype in which MTBVAC is “trapped” in a late endosome. The individual *phoP* and *fadD26* mutations of MTBVAC are predicted to have a synergistic effect on the intracellular trafficking phenotype of the vaccine candidate.

The second objective was the exhaustive study of the PhoP regulon in order to attempt to determine the signal modulating its expression. To achieve this objective, two different approaches were applied: i) to study the expression of different PhoP-

regulated genes through a reporter system based on genetic fusions of PhoP-regulated promoters to the GFP protein, ii) to directly measure the expression of the selected PhoP-regulated genes through RNA extraction and qRT-PCR techniques. In both cases, the wild-type strain H37Rv and its *phoP* mutant were exposed to the intracellular environment either through *in vitro* culture conditions mimicking it (acidic pH, ions, temperatures, hypoxia, etc.) or after infection of phagocytic and non-phagocytic cells. The *pks2* promoter was chosen to be the most representative reporter of the PhoP-regulon activity, demonstrating the relevant role of low pH to activate the PhoP regulon. None of the conditions suggests an exclusive signal activating the PhoP-regulon, insinuating that it is a multifactorial event occurring during the entrance of the bacteria inside the macrophage; nevertheless, the response of the regulon when exposed to acid pH demonstrates that it is a key factor in the induction of PhoP-regulated genes. Based on our results, a time-dependent expression of the different genes at different times post-infection was suggested. The first genes activated by PhoP are those related with lipid metabolism and oxidative stress, probably to protect bacteria against new stresses inside the phagosome. Secondly, after 3-5 days, genes related with the ESX-1 secretory system are upregulated and consequently, ESAT-6 and CFP-10 are secreted, inducing the phagosomal rupture and the escape of the bacteria to the cytosol. In the successive time points, Mcr7 ncRNA becames highly induced, inhibiting the TAT secretory system, and consequently restricting the secretion of components from the Antigen 85 complex in order to “hide” from the host response in its new cytosolic location. This mechanism would allow virulent mycobacteria to overcome the immune control favoring bacterial dissemination.

A third objective of this thesis was to construct an hyper-attenuated vaccine based on MTBVAC to be used in individuals in risk of immunosuppression where BCG vaccination in not indicated. A third mutation in the *zmp1* (Rv0198c) gene was introduced in the vaccine strain MTBVAC (live attenuated strain with deletions in genes *phoP* and *fadD26*) in order to hyper-attenuate this strain maintaining protection against tuberculosis. Using a double recombination strategy was possible to generate a triple mutant in genes *phoP*, *fadD26* and *zmp1*. Preliminary results show that the triple

mutant did not improve the attenuation, the immunological response or the protection when compared with MTBVAC; further studies in the guinea pig model are necessary to gain any conclusion.

Resumen

El primer objetivo de este trabajo fue caracterizar las interacciones con el hospedador del nuevo candidato a vacuna viva atenuada contra la tuberculosis, MTBVAC. En este estudio se comparó la proteómica de la fracción secretada de MTBVAC y su cepa parental Mt103 a través de las técnicas de western-blot y electroforesis fluorescente diferencial en dos dimensiones (DiGE). Se obtuvieron dos conjuntos de datos de proteínas secretadas mayoritariamente por MTBVAC o Mt103 respectivamente. Gracias a estos resultados se observó el alto porcentaje de sustratos del sistema de secreción TAT (Twin Arginine Translocation) entre la fracción secretada por MTBVAC, y se pudo confirmar la ausencia de los factores de virulencia ESAT-6 y CFP-10 en dicho secretoma.

El tráfico intracelular de MTBVAC fue otro aspecto a estudiar de la interacción del candidato a vacuna con su hospedador. MTBVAC es un mutante doble en los genes *phoP* y *fadD26*, por lo que se quiso estudiar también la contribución individual de cada mutación al fenotipo final. Se llevaron a cabo infecciones con las correspondientes cepas GFP^+ en dos modelos celulares diferentes: la línea celular de macrófagos alveolares de ratón (MHS) y macrófagos primarios humanos derivados de monocitos (hMDM); los resultados se analizaron mediante técnicas de microscopía. Los resultados obtenidos sugieren que MTBVAC, como cepa atenuada que es, no es capaz de detener la maduración del fagosoma en etapas tempranas del proceso, sin embargo la detiene antes de llegar a la fase lisosomal. Mediante esta estrategia MTBVAC evita ser degradada rápidamente en el fagolisosoma. Sin embargo, debido a haber perdido la habilidad de secretar ESAT-6 y CFP-10, MTBVAC no es capaz de escapar al citosol de la célula hospedadora, presentando un fenotipo de persistencia en el cual MTBVAC está “atrapada” en un estadio endosomal tardío. Las mutaciones en los genes *phoP* y *fadD26* de MTBVAC parecen tener un efecto sinérgico sobre el fenotipo del tráfico intracelular del candidato a vacuna.

El segundo objetivo fue el estudio exhaustivo del regulon PhoP para tratar de determinar la señal que activa y modula su expresión. Para ello se utilizaron dos estrategias: i) estudiar la expresión de diferentes genes regulados por PhoP a través de un sistema reportero basado en fusiones genéticas de promotores de dichos genes con la proteína GFP, ii) medida directa de la expresión de varios genes regulados por PhoP a través de la extracción de RNA y la técnica de qRT-PCR. En ambos casos, la cepa parental H37Rv y su mutante *phoP* fueron expuestos a un ambiente intracelular, bien sometiéndolas a condiciones *in vitro* que trataban de mimetizar las condiciones intrafagosomales (pH ácido, iones, temperatura, hipoxia, etc.) o bien infectando con dichas cepas células fagocíticas y no fagocíticas. Se eligió el promotor de *pks2* como reportero más representativo de la actividad del regulón PhoP, demostrando el importante rol que tiene el pH acido en la activación de dicho regulón. Ninguna de las condiciones probadas muestra una señal única que active el regulón PhoP, sugiriendo que es un proceso multifactorial que tiene lugar durante la entrada de la bacteria al interior del macrófago. Sin embargo, la respuesta del regulón tras la exposición a pH ácido demuestra que el pH es un factor clave en la inducción de los genes regulados por PhoP. Basándonos en los resultados obtenidos, se propone una dinámica de expresión de los genes regulados por PhoP dependiente del tiempo post-infección. Los primeros genes activados por PhoP son aquellos relacionados con el metabolismo lipídico y el estrés oxidativo, probablemente para proteger a la bacteria frente al ambiente hostil del interior del fagosoma. Tras 3-5 días, los genes relacionados con el sistema de secreción ESX-1 son activados y en consecuencia, la bacteria secretará ESAT-6 y CFP-10 induciendo con ello la ruptura del fagosoma y su escape al citosol. A partir de este punto, la actividad del RNA no codificante Mcr7 es altamente inducida por PhoP, lo cual conlleva la inhibición del sistema de secreción TAT y consecuentemente se ve restringida la secreción de los componentes del complejo Antígeno 85 con el objetivo de “esconderse” de la respuesta de la célula hospedadora ahora que la bacteria se encuentra en el citosol. Este mecanismo permite a las bacterias virulentas evadir el control inmunológico del hospedador y en el organismo.

El tercer objetivo de la presente tesis fue construir una vacuna hiper atenuada basada en MTBVAC para ser usada en la población con riesgo de inmunosupresión, para la que BCG está contraindicada. Se introdujo una tercera mutación en el gen *zmp1* (Rv0198c) de MTBVAC (vacuna viva atenuada con mutaciones en los genes *phoP* y *fadD26*) con la intención de hiper atenuar la cepa manteniendo su eficacia protectora frente a tuberculosis. Se usó una estrategia de doble recombinación para generar el triple mutante en los genes *phoP*, *fadD26* y *zmp1*. Resultados preliminares muestran que el triple mutante no mejora la atenuación, la capacidad de generar respuesta inmunológica o la eficacia protectora de MTBVAC; estudios más exhaustivos en otros modelos animales (cobayas) son necesarios para llegar a alguna conclusión.

Introduction

In 2014, tuberculosis (TB) ranked alongside Human Immunodeficiency Virus (HIV) as a leading cause of death from an infectious agent worldwide. Nowadays, 9.6 million people are estimated to have fallen ill with TB and 1.5 million died in 2014 (including 0.4 million deaths among HIV-positive people) according to the World Health Organization (WHO) [1]. This plague affects virtually every nation and every ethnicity.

TB is caused by *Mycobacterium tuberculosis* (Mtb) and usually attacks the lungs (pulmonary TB) but can also affect almost any organ (extra-pulmonary TB). The pathogen is extremely well adapted to humans and its success could be due to its ability to persist for years inside the host [2]. However most of the infection cases will not develop into disease; asymptomatic, latent infection is the most common. About one in ten of these latent infections will eventually progress to active disease, which, if untreated, kills more than half of its victims.

1. HISTORY OF TUBERCULOSIS.

Tuberculosis is the greatest human killer in history; taking only the past two centuries into account, TB was responsible for the deaths of approximately one billion human beings [2, 3]. It is presumed that an early progenitor of Mtb was probably contemporaneous and co-evolved with early hominids in East Africa, three million years ago [4]. Signs of the disease have also been found in Egyptian mummies dated between 3000 and 2400 BC and it appears that Akhenaten and his wife Nefertiti both died from TB [5]. Mycobacterial DNA was detected in some pathology skeletal lesions in Egyptian and Peruvian mummies dating back to 500-1500 BC, and also in a human skeleton from the Iron Age (400-230 BC) found in the United Kingdom [6].

TB has also been called *consumption*, because it seemed to consume people from within, with a bloody cough, fever, pallor, and a long relentless wasting. Hippocrates, around 460 BC, used the term “phthisis” (from the Greek *phthiein*, meaning “to waste away”) to describe the most widespread disease of the times [7]. Although Aristotle

believed that the disease might be contagious, many of his contemporaries believed it to be hereditary [8].

It is believed that Europe became the epicenter of many TB epidemics from the 16th and 17th century due to the growing population expansion, the industrialization and the development of large urban settlements. TB was supposed to be an incurable disease and it was called "*The Great White Plague*" or the "*White death*" because sufferers appear markedly pale. Death by TB was considered inevitable, being the principal cause of death in 1650. The high population density as well as the poor sanitary conditions that characterized most European and North American cities created a perfect environment for the propagation of the disease. The epidemic reached its peak in Europe in the first half of the 19th century, and it is estimated that as many as one quarter of Europeans died of TB at this time [7].

In 1854, Hermann Brehmer postulated that TB is a curable disease [5, 8]. He was a young student affected by TB when his physician advised him to seek a healthier climate, so he spent some time in the Himalayas and came back home cured. This experience moved him to build the first sanatorium, places where patients were exposed to fresh air and healthy nutrition. Sanatoriums, founded throughout Europe and the United States, provided a dual function: to isolate the sick people from the general population, and to force the patients to rest, thus assisting the healing process.

In 1865, Jean Antoine Villemin demonstrated that TB was transmitted from humans to cattle and from cattle to rabbits. In the light of this revolutionary evidence, he postulated that a specific microorganism caused the disease [8].

On March 24th 1882, Robert Koch made his famous presentation "The etiology of TB". He demonstrated the infectious nature of TB and described Mtb thanks to the new techniques developed by him, notably specific staining techniques and special solid culture media. The studies of Koch fulfilled in a paradigmatic manner the criteria named after him, the Koch's postulates. These comprise identification of the pathogen

in affected tissue, growth of single clones of the pathogen *in vitro*, and establishment of a similar disease in experimental animals by means of the pure culture [9].

Once Mtb had been identified Koch's next step was to find a cure for the disease. Eight years later Koch announced the discovery of a vaccine against TB consisting of glycerol extracts of pure cultures of tubercle bacilli. The vaccine candidate was assayed in a clinical trial with disastrous results but in 1908, Charles Mantoux found that it was an effective intradermic test for diagnosing TB [9].

With Edward Jenner's successful invention, showing that infection with cowpox confered immunity against small pox in humans, many doctors placed their hopes on the use of *Mycobacterium bovis* (the agent that causes bovine TB) for the development of a vaccine against human TB. In 1908 Albert Calmette and Camille Guérin started the development of a vaccine against TB. They isolated *M. bovis* from a dead cow and for the next 13 years, grew every fortnight a new batch of bacteria in a solution of beef bile and potato. After 230 serial passages, the bacteria lost their ability to cause disease, but were still capable of stimulating the immune system to protect mice, pigs, guinea pigs and monkeys from TB. The attenuated strain was called Bacille Calmette-Guérin or BCG and it was first administered to humans in 1921. A total of 8 million babies and nearly 14 million people were given the BCG vaccine in the International TB Campaign, which ran through 1951. Since then, more than a billion people have been vaccinated with BCG [10].

Then, in 1943 during the World War II, Selman A. Waksman who had been working for decades to find an effective antibiotic against TB, finally succeeded. Streptomycin, a compound with antibiotic activity, was purified from *Streptomyces griseus*. When this therapy was used in TB patients a considerable improvement was observed. A rapid succession of anti-TB drugs appeared in the following years: para-aminosalicylic acid (PAS, 1949), isoniazid (INH, 1952), pyrazinamide (PAZ, 1954), ethambutol (EMB, 1962) and rifampicin (RIF, 1963). Unfortunately, this initial optimism was soon tempered by the development of the first resistant strains to anti-TB drugs. However, it was soon

demonstrated that combined treatment with two or three drugs enabled to overcome this problem [8].

1.1. The return.

The general improvement in public health and success of chemotherapy resulted in a pronounced reduction of infection and death rates in Europe and in the United States. But the hopes that the disease could be completely eliminated were dashed in the 1980s with its dramatic resurgence, the rising prevalence of multidrug-resistant (MDR) and extensively drug-resistant (XDR) strains, and the deadly form of MDR/XDR associated with HIV/AIDS [11]. The WHO issued a declaration of a global health emergency in 1993 [12].

Every year, nearly half a million new cases of MDR-TB are estimated to occur worldwide. Even more alarming is the existence of at least 12 patients infected with TB that has become resistant to all the drugs used against the disease, called TDR (Totally Drug-Resistant). In other words, they are untreatable as far as it is known. The first cases of these TDR were reported in Iran in 2009 and Italy in 2007 [13, 14].

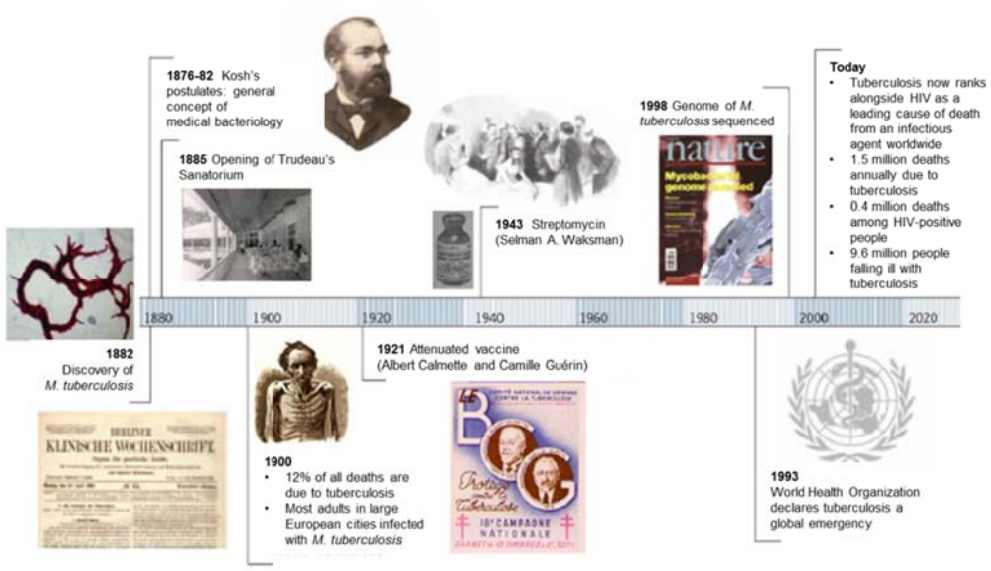

Figure 1. Timeline in TB research. It shows the most relevant highlights in the fight against this disease. Adapted from [9].

2. THE DISEASE: Diagnosis and Treatment.

The most common methods for TB diagnosis worldwide are sputum smear microscopy and the Mantoux tuberculin skin test. These methods are simple, inexpensive and quick, but their main drawbacks are low specificity and sensitivity. It is necessary to carry out more tests such as chest radiography, Interferon Gamma Release Assays (IGRAs), and culturing, to confirm the infection with Mtb [15]. Diagnosing TB using culture involves the identification of Mtb by biochemical tests [16], which is important to get successful treatment in drug-resistant TB patients.

Early identification of people with symptomatic TB not only allows therapy to be administered before serious lung damage occurs, but also helps to prevent the spread of the bacteria to other susceptible people. For this purpose, there are several new diagnostic technologies under development [17].

Drug treatment is the only effective therapy for TB. Drugs are classified into three groups based on evidence of efficacy, potency and experience of use [18].

- First-line anti-TB drugs are the most effective and widely used drugs for the treatment of drug-susceptible TB (which is not drug resistant).
- Second-line anti-TB drugs are reserved for resistant bacilli to first-line therapy. A drug may be classed as second-line instead of first-line for being less effective (e.g. *para*-aminosalicylic acid), having toxic side-effects (e.g. cycloserine) or being effective, but unavailable in many developing countries (e.g. fluoroquinolones).
- Third-line anti-TB drugs are characterized for not being very effective (e.g. clarithromycin) or because their efficacy has not been proven (e.g. clofazimine).

With appropriate antibiotic treatment, around 90% of HIV-negative patients with drug-susceptible TB can be cured in 6 months using a combination of RIF, INH, PAZ and EMB for 2 months, followed by a four-month continuation phase of RIF and INH. The main reason for prescribing this combination of medicines in the treatment of TB is because the likelihood of the emergence of MDR bacteria is virtually impossible [19], apart

from the fact that the distinct anti-TB drugs have different modes of action: INH is bactericidal against replicating bacteria; EMB is bacteriostatic at low doses, but is used in TB treatment at higher, bactericidal doses; RIF is bactericidal and has a sterilizing effect; and PAZ is only weakly bactericidal, but is very effective against bacteria located in acidic environments, inside macrophages, or in areas of acute inflammation.

3. BIOLOGY OF *M. tuberculosis.*

3.1. General characteristics of the bacillus.

Mtb is an acid-fast, rod-shape and aerobe bacterium belonging to the family *Mycobacteriaceae*, included into the suborder *Corynebacterineae*, order *Actinomycetales* [20].

Mtb is not classified as either Gram-positive or Gram-negative since it gives the appearance of "ghost" cells when it is Gram stained [21]. Phenotypically it is a catalase and nitrate reductase positive, non-motile and non-spore forming bacillus of 2-5μm in width. Mtb is a slow-growing mycobacteria with a generation time of approximately 15-20 hours. It takes 4 weeks to get visual colonies on solid medium. In smears made from *in vitro*-grown colonies, chains of cells often form distinctive serpentine cords, this phenomenon is called cording, and it is associated to virulent strains of the bacterium.

3.2. Genetics of *M. tuberculosis.*

The complete genome sequence of the best-characterized strain of Mtb, H37Rv [22], was obtained in 1998 [23] and it is in continuous revision since then [24]. The genomic sequence consists of 4.411.529 base pairs (bp), with an unusual G+C (guanine plus cytosine) content of 65.6%. Approximately 91% of the genome presents coding capacity; the last re-annotation identified 4,110 genes though to encode 4,018 proteins and 80 stable RNAs. It has the capacity to synthesize all the essential amino

acids, vitamins and co-factors, though some pathways that may differ from those found in other bacteria. It also comprise a complex repertoire of genes involved in lipid metabolism, and components for anaerobic respiration such as nitrate reductase and hemoglobin-like proteins that could compete with the lung for oxygen, indicating the capability of adapting to metabolic changes encountered in the granuloma (Figure 2).

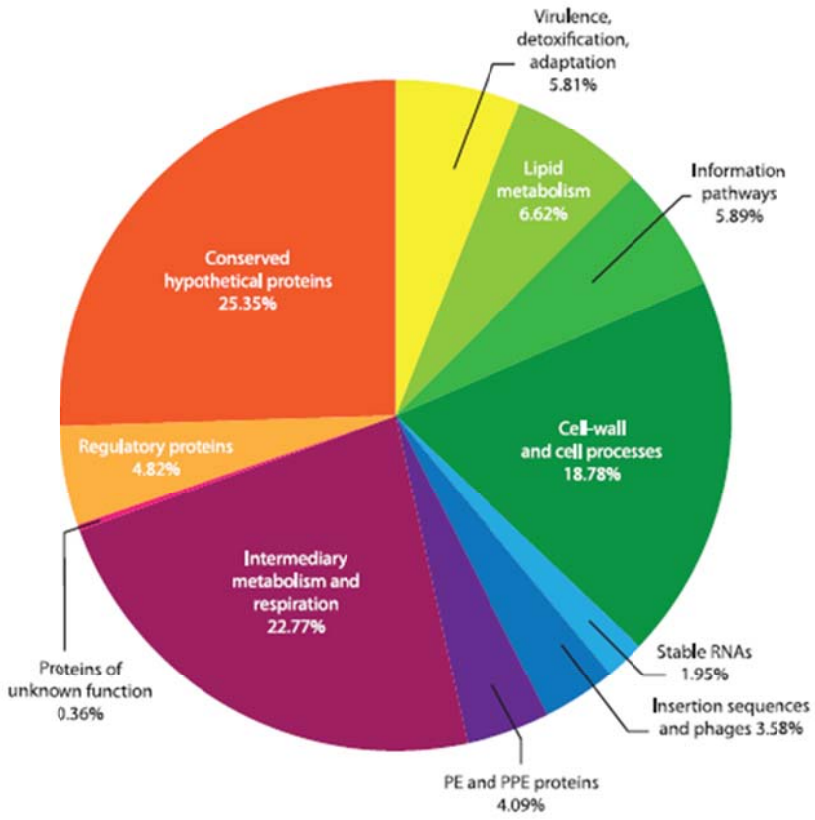

Figure 2. Functional distribution of *M. tuberculosis* genes. Adapted from [24, 25].

Genetic manipulation of DNA remains one of the most powerful approaches for understanding the molecular basis of survival, virulence, and pathogenicity of a bacterium. It should be noticed that genetic manipulation of slow-growing mycobacteria such as Mtb is complicated by its pathogenesis, slow growth rate, inefficient DNA uptake and high level of illegitimate recombination. Eventually, the discovery of mycobacteriophages and plasmids, the development of mycobacterial vectors and transposons, transformation by electroporation, and successful methods to generate knockout mutant strains allowed the study of gene function in mycobacteria.

3.3. The mycobacterial envelope.

The mycobacterial envelope is unique, both in molecular composition and in the architectural arrangement of its constituents. Its complex structure consists of a plasma membrane surrounded by a complex cell wall of peptidoglycan (PG) and arabinogalactan (AG) to which an outer membrane or mycomembrane is attached, which is in turn enveloped by an outer layer called “capsule”. Between the plasma membrane and the PG there is a periplasmic space. The plasma membrane does not seem to differ from other biological plasma membranes and it is composed mainly of anionic phospholipids in a bilayer arrangement with proteins [26]. The “cell wall skeleton” consists of covalently linked PG, AG and mycolic acids, and it defines the shape of the mycobacterial cell. The mycomembrane consist of an asymmetric lipid bilayer with its inner leaflet made of the long chain (C60-C90) mycolic acids residues covalently attached to the cell wall AG, and an outer leaflet constituted with non-covalently intercalating glycolipids, waxy components and proteins [27-29]. The capsule is mainly composed of polysaccharides, proteins and small amounts of lipids, and it is considered to have a different molecular composition in pathogenic and non-pathogenic species [30]. The outermost layer is visible in conventional electron microscopy preparations only when cultures have been grown in detergent- free medium (Figure 3) [31].

Non-covalently attached glycolipids are important components of the mycomembrane outer leaflet. Among them can be found trehalose dimycolates (TDM), often referred as cord factor, trehalose monomycolates (TMM), glucose monomycolates (GMM), glycerol monomycolates, diacyltrehaloses (DAT), triacyltrehaloses (TAT), polyacyltrehaloses (PAT), the recently characterized family of mannosyl-β-1-phosphomycoketides, sulpholipids (SLs), phenolic glycolipids (PGLs) and phthiocerol dimycocerosates (PDIM). Other major glycolipids are lipomannan (LM), lipoarabinomannan (LAM) and phosphatidylinositol mannosides (PIMs) (Figure 3).

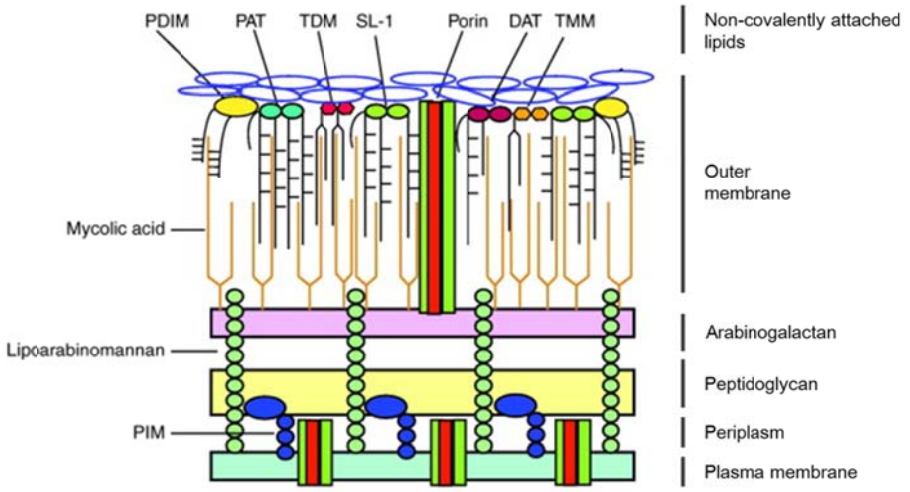

Figure 3. Schematic representation of cell envelope of *M. tuberculosis*. Adapted from [32].

The mycobacterial envelope is involved in important roles, such as defining the shape of the cell and providing mechanical and osmotic protection. This highly hydrophobic envelope decreases the permeability and susceptibility to degradation and makes the bacterium naturally resistant to most of the antibiotics and chemical agents and confers unique staining properties. During infection, cell-wall compounds have been shown to trigger a set of biological effects including adjuvanticity, toxicity, immune down-modulation, and arrest of phagosomal maturation [33].

4. PATHOGENESIS AND VIRULENCE.

TB is a contagious disease transmitted through inhalation of aerosols containing the bacteria which are spread by persons with active pulmonary TB. After inhalation, bacilli reach the alveoli, where Mtb is engulfed mainly by alveolar macrophages and also disseminated by the lymphatic circulation. The most common form of the disease is pulmonary TB, although TB-meningitis, miliary (disseminated) TB, lymphadenitis, osteomyelitis and Pott's disease (affecting bones) can also occur.

4.1. Life inside the macrophages.

Mtb is an obligate intracellular pathogen widely adapted to survive within the human macrophages. Phagocytosis provides an effective initial barrier against infection; mycobacterial entrance is mediated by specific macrophage receptors, and a pro-inflammatory response, that leads to recruitment of mononuclear cells from neighboring blood vessels, is induced [34], triggering granuloma formation [35]. The granuloma contains the infection but does not eliminate Mtb. Over time, the granuloma becomes a stratified lesion which includes blood-derived infected and uninfected macrophages, foamy macrophages, epithelioid cells (uniquely differentiated macrophages), and multinucleated giant cells (Langerhans cells), B and T lymphocytes, and fibroblasts [36]. In many lesions these cell populations are separated by a fibrous layer of extracellular matrix (Figure 4) [37].

The main function of the granuloma is to localize and contain Mtb while concentrating the immune response to a limited area. Thanks to this strategy 90% of infected individuals defeat the disease or are successful in controlling TB (latent TB) [35]. People with latent TB are still infected but are non-infectious and asymptomatic. However, in 10% of the cases, when the host immune status changes as consequence of aging, malnutrition, stress, cancer, immunosuppressive drugs or co-infection with HIV among other factors, this situation leads to active disease in which the centre of the granuloma becomes necrotic, liquefies (caseous necrosis), and viable bacilli can be released and spread to the lung, other parts of the body and the atmosphere (Figure 4) [36].

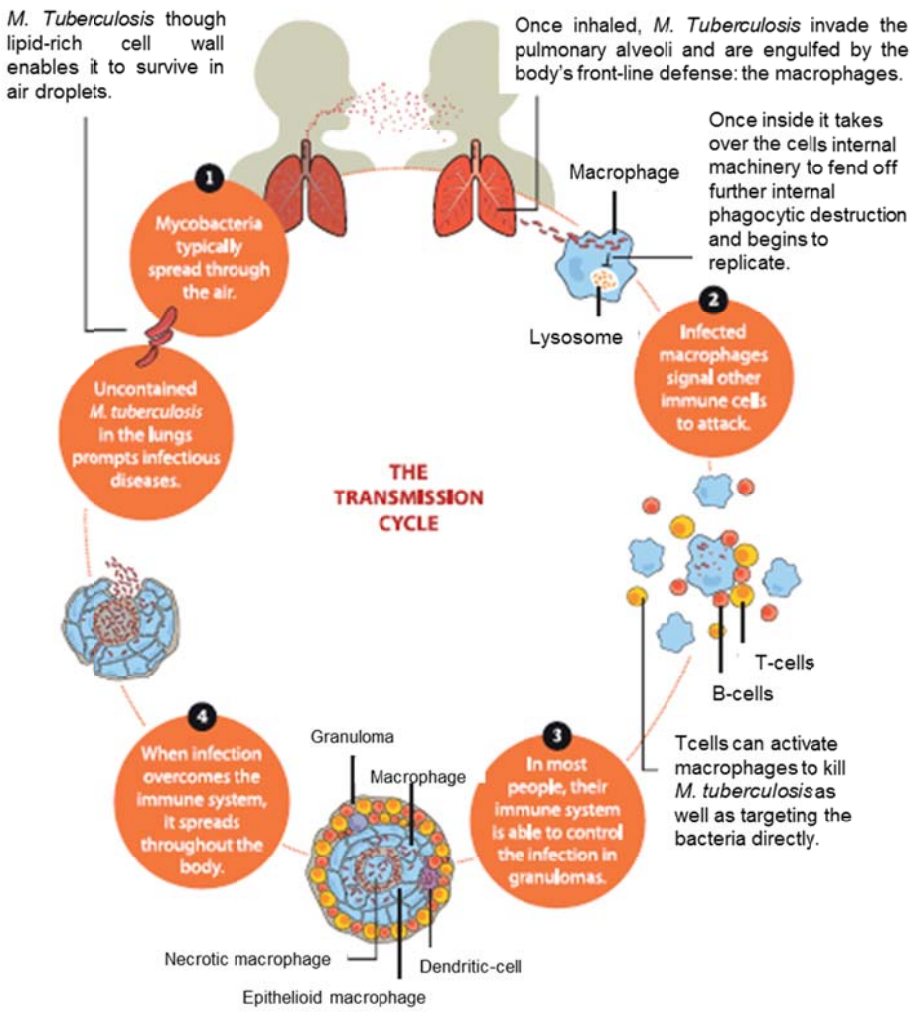

Figure 4. The transmission cycle of *M. tuberculosis* [3].

Once engulfed, ingested bacteria are contained within intracellular vesicles, or phagosomes. Under normal circumstances, activated macrophages promote phagosomal maturation by a process that finally involves fusion with lysosomes and formation of the phagolysosome. These vesicles provide a hostile environment for the bacilli including acid pH, reactive oxygen and nitrogen intermediates (ROI and RNI), lysosomal enzymes and toxic peptides (Figure 5). However, intracellular pathogens have developed strategies to overcome these defense mechanisms.

Mtb does not have classical virulence determinants like toxins produced by other pathogenic bacteria. The ability of Mtb to persist in the host involves a variety of factors at specific times during infection. Mainly it has evolved to survive within

macrophages by arresting the normal phagosomal maturation at an early stage, thereby restricting its acidification and limiting fusion with lysosomes. Modulating of the maturation seems to be mainly mediated by mycobacterial cell-wall lipids and other bacterial effectors.

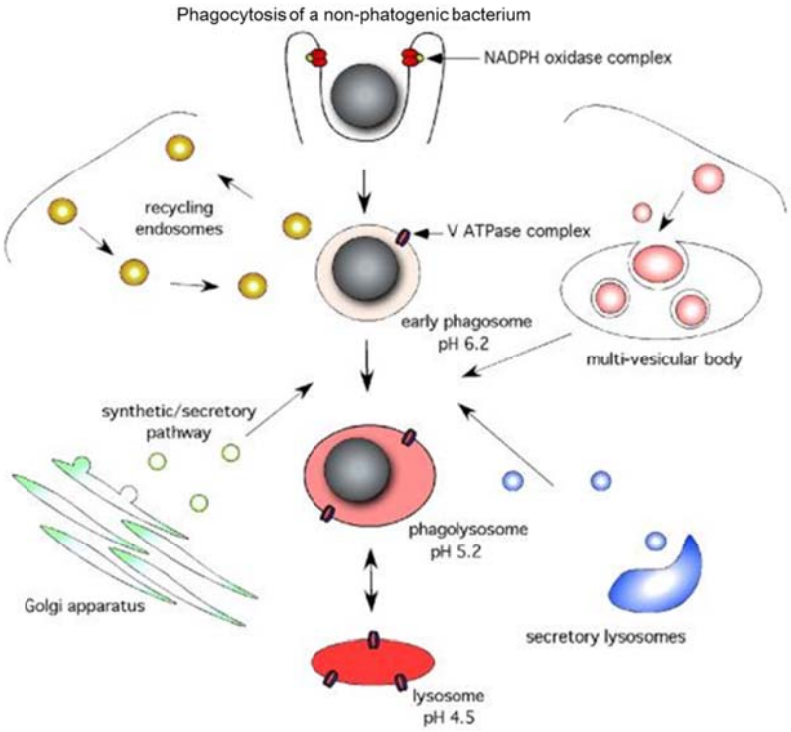

Figure 5. Phagosomal maturation refers to the process of phagosome remodeling through a series of independent events, following its formation at the surface of the phagocyte, and culminating in the complete fusion of the phagosome with the lysosome. Following engagement of phagocytic receptors, the phagosome becomes increasingly more acidic, through the accumulation of V-ATPases that pump protons into the compartment, and hydrolytically competent, through the acquisition of lysosomal enzymes. This process is marked by transient fusion events with multiple intracellular organelles including the recycling endosomal machinery, the synthetic-secretory apparatus including the endoplasmic reticulum, secretory lysosomes, and multi-vesicular bodies. Adapted from [38].

Phagosomes containing Mtb fail to acidify due to bacterial interference with the recruitment of the vesicular proton ATPase pump (V-ATPase) [39]. Another interference with host pathways is the fact that Mtb possesses at least 11 eukaryotic-like protein kinases which have been shown to regulate mycobacterial signal transduction pathways, morphology, and cell division [40, 41]; an example is PknG,

which has been shown to be released from pathogenic mycobacteria inside the macrophage cytosol where it prevents lysosomal delivery and degradation [42, 43]; it also has been proposed that Mtb interferes with phagolysosome biogenesis by a putative Zn^{2+}-dependent metalloproteinase (Zmp1) that prevents caspase-1 dependent activation and secretion of IL-1β [44, 45].

There is considerable evidence that Mtb cell wall lipids act as virulence factors during infection [46-50]. Mtb lipids have been observed to intercalate into host membranes leading to decreased membrane fluidity and increased passive permeability [51]. The ability of mycobacterial PDIM and TDMs to alter host membrane fluidity may influence the process of phagocytosis as well as subsequent trafficking. PDIM also constitute a potential candidate for modulating the initial step of entry into macrophages and for controlling the outcome of bacterial infection; it has been demonstrated that PDIM production in Mtb contributes to the initial growth of the bacillus in mice by protecting it from the nitric oxide-dependent killing of macrophages and modulating the production of key inflammatory cytokines such as TNFα [52]. The mycobacterial analog to the phosphatidylinositol 3-phosphate (PI3P), blocks the host PI3P altering the signal of late phagosome endosome fusion [53]; PIMs and mannose-capped lipoarabinomannan (Man-LAM) both interfere with phagosome maturation [54]. Purified SL has been described as modulating phagosome-lysosome fusion [55, 56] and the cytokine responses of human phagocytes [57]. DAT and PAT lipids also participate in early interactions between Mtb and phagocytes [52, 58].

The use of transposon mutant libraries in combination with different *in vivo* screening methods has allowed the identification of mycobacterial virulence genes, and factors, whose role in virulence is clear. For example, the nucleoside diphosphate kinase Ndk [59] and the phosphatase SapM [53] both affect the maturation of the mycobacterial containing phagosome; but also enzymes such as AhpC, SodC, KatG ant Tpx which contribute to the detoxification of ROI and RNI [60, 61]; or isocitrate lyase enzyme, essential for the metabolism of fatty acids [62]. It has also been demonstrated that many of these mutants present altered intracellular trafficking [56, 58, 63], which is consistent with all the facts mentioned before.

A great variety of secreted and cell wall-associated proteins has been demonstrated to play a key role in bacterial survival and immune modulation in the host. For example, ESAT-6 is secreted in the early stages of Mtb infection, induces strong cell mediated and humoral immune responses [64] and facilitates the access and/or translocation of Mtb into the macrophage cytoplasm from the phagosome [65-67]. ESAT-6, encoded in the region of difference-1 (RD1) gene cluster, plays a key role in this process [66, 68, 69]. The Ag85 complex (Ag85A, Ag85B and Ag85C) is the major secreted protein constituent of mycobacterial cell culture, and contributes to the biosynthesis of TMM and TDM [61]. Several *pks* genes along with *fadD26*, *fadD28*, *drrC* and *mmpL7*, take part in the biosynthesis or transport of PDIM, a major virulence factor of Mtb, in particular during the early step of infection when bacilli encounter host macrophages [61].

The bacterium also needs intermediate metabolism and nutrient uptake as it has to face hostile, nutrient-deprived environment during infection, like the biosynthesis of purines (*purC*) [70] and several amino acids (*leuD*, *lysA*, *glnA1*, *trpD*, *argF* and *proC*) [70-75] required for bacterial survival *in vivo.* However, adaptation to environmental stimuli in bacteria is mediated primarily through the expression of transcriptional regulators, including serine-threonine protein kinases; extracytoplasmic function sigma factors, and two-component signal transduction systems. These strategies allow Mtb to prevent elimination and survive during the initial stages of infection. The course of infection during later stages is mainly determined by the state of the host immune system.

4.2. Two-component signal transduction systems (TCSs).

The number of systems present in a given organism generally correlates with its genome size and the complexity of the environment(s) in which the bacterium typically resides. TCSs have been shown to regulate many physiological processes, including sporulation, competence, antibiotic resistance, transition into stationary phase,

virulence, and carbon, nitrogen, and phosphate utilization. The importance of TCSs in bacterial survival and the absence of them in higher eukaryotes also make these systems attractive targets for therapeutic development against pathogenic organisms. Consistent with this idea mutant strains that are defective in specific TCSs that lead to virulence attenuation are now being investigated as potential vaccine candidates [76].

TCSs as its name indicates are protein complexes based on a histidine sensor kinase (SK), placed in the membrane and a response regulator (RR), located in the cytoplasm. Both SK and RR can act as dimmers and some TCSs have shown more complexity presenting intermediate connectors that transfer the phosphate between the SK to RR (Figure 6) [76].

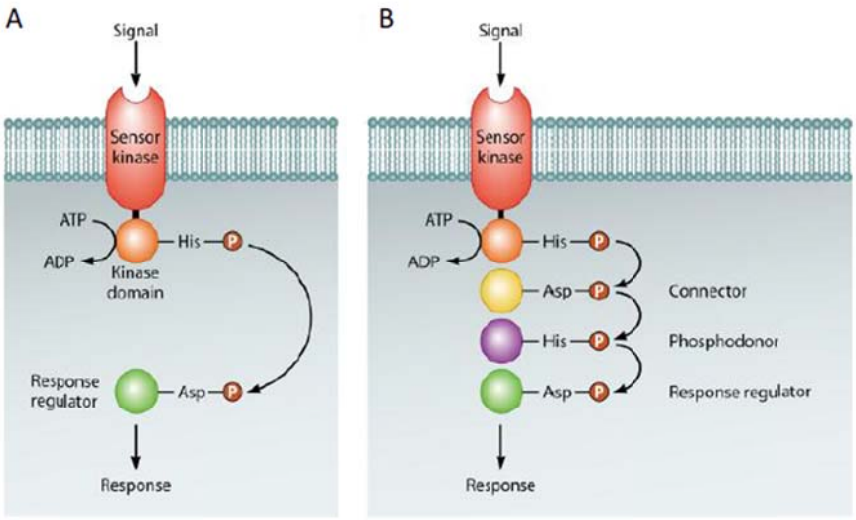

Figure 6. Scheme of TCS work flow. **A)** Canonical TCS. The sensor kinase senses an extracellular signal resulting in an activation of the kinase domain which autophosphorylates a conserved histidine residue in the domain. Once phosphorylated, the SK interacts with a RR, transferring the phosphate group to a conserved aspartate residue. Phosphorylation results in a conformational change of RR that allows DNA binding site to interact with DNA generating a response. **B)** Phosphorelay. This system comprised of a SK and a RR, there is also an intermediate regulator (connector) and a phosphodonor which interacts with the RR. In some phosphorelay SK, connector and phosphodonor are fused. Adapted from [76].

The mechanism by which a prototypical TCS acts includes two steps: the surface protein SK senses a specific signal outside the bacteria. As result of this stimulus the kinase domain present in the SK activates and autophosphorylates a histidine residue

conserved in the SKs. Once this residue is phosphorylated, it interacts with the receiver domain. Consequently, there is a conformational change in the RR which allows the DNA binding domain of the RR to interact with the DNA of the chromosome (Figure 6).

Mtb is an intracellular pathogen subjected to numerous stimuli and stresses once into eukaryotic cells. To face this particular environment, Mtb encodes approximately 11 genetically linked TCSs, five orphan RRs and two orphan SKs. The number of intact TCSs is lower than typically found in other bacteria of similar genome size, possibly reflecting the evolution if this bacterium as a strict human pathogen and its adaptation to a predominantly intracellular lifestyle [76].

4.2.1. TCS PhoP/PhoR.

One of the most studied TCS is PhoP/PhoR, essential in Mtb virulence [77]; this system is coded by the genes Rv0757 (*phoP*) and Rv0758 (*phoR*), these genes are transcribed in operon although the *phoR* gene may also be expressed under the influence on its own promoter [78]. DNA footprinting studies have demonstrated that PhoP binds upstream *phoP* gene controlling the operon expression [78] recognizing two direct repeats (DR) of 9bp upstream the transcription starting point [79, 80]. These DRs have also been found upstream several genes: *pks2*, *pks3*, *lipF* and *fadD21* [80] identifying it as a possible consensus sequence for PhoP binding to DNA. PhoP binding to DNA has been demonstrated to occur due to a conformational change upon phosphorylation of Asp-71 [9, 81, 82], that promotes the protein dimerization and DNA binding stability.

Structure of PhoP DNA binding domain has been resolved presenting typical fold of a winged helix-turn-helix DNA binding domain [83, 84]. PhoP of the attenuated, Mtb strain, H37Ra presents a point mutation in the DNA binding domain that inhibits most part of the affinity of the domain for the DR region affecting gene expression of PhoP regulated genes [85, 86]; this mutation can explain the attenuation of H37Ra due to a malfunction of PhoP regulation progress.

PhoP has been described to control expression of, approximately, 2% of the total genome of Mtb [87, 88] including many genes involved in lipid metabolism and respiration (Figure 7), some of them implicated in the synthesis of cell wall lipids like SL (*pks2*) and PAT and DAT (*pks3*). There are also genes involved in virulence in mice like *lipF* or the nitrite transporter *narK1*, required for anaerobic respiration [88]. *phoP* mutants, also present a lower level of expression of the transcription factor, *espR*, and the genes *dosRS*, that code for one of the HK and the RR of the TCS DosRST (Figure 7) [88], it is likely that genes affected by these regulatory genes will be affected downstream by a deficiency in PhoP action, due to an indirect effect of regulation.

DosRST is a TCS where DosR is the RR meanwhile DosS and DosT are HKs that interact with DosR and sense different external signals, DosS is sensing redox potential and DosT is sensing hypoxia signals [89]. DosRST regulon has been widely characterized using microarrays [90-92] and it has been related to adaptation to hypoxia and dormancy [90, 91]. PhoP-dependent expression of many genes of the DosR regulon as well as *dosR* and *dosS* themselves, might indicate an indirect regulation of hypoxia and dormancy mediated by PhoP in Mtb.

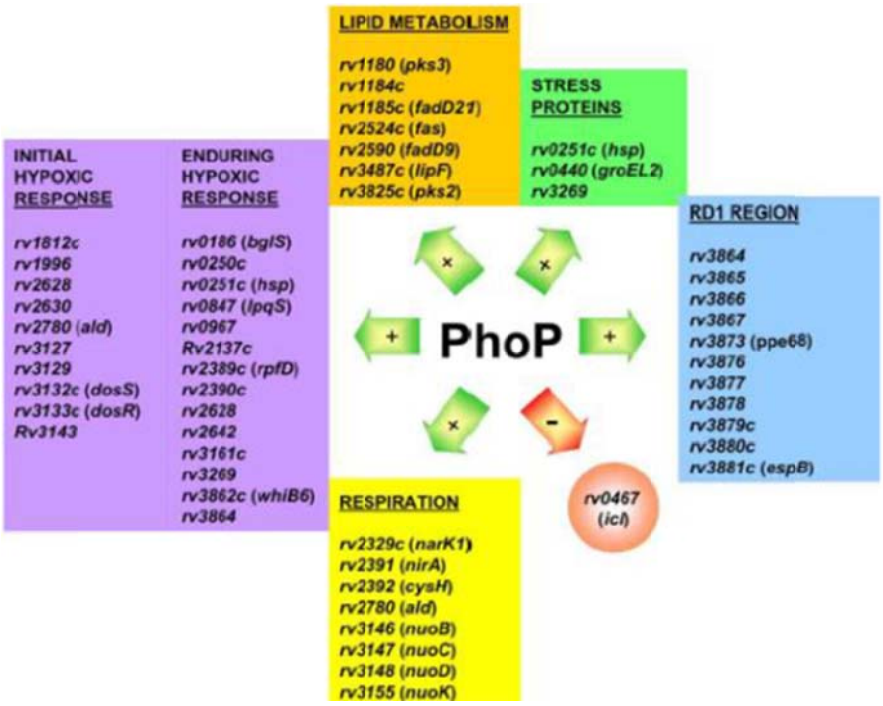

Figure 7. Microarray comparison between the transcriptomes of a wild type strain and a *phoP* mutant. Relevant genes with differential expression between the wild type strain Mt103 and the *phoP* mutant

SO2. Green arrows mean positive regulation, red arrow means negative regulation. PhoP is controlling the initial and the enduring hypoxic response (*phoP* is regulating the TCS *dosRS*), lipid metabolism pathways (PAT, DAT and SL synthesis pathways are controlled by *phoP* through regulation of *pks3* and *pks2* respectively), genes involved in respiration and genes responsible of ESAT-6 secretion by ESX-1 secretion system (RD1 region encoding the ESX-1 secretion system is deleted in the vaccine strain BCG). Adapted from [88].

There are also many genes of the ESX-1 secretion system (responsible for secretion of the major antigens ESAT-6 and CFP-10) affected by PhoP regulation (Figure 7) [88]; being EspR, the responsible for regulation of ESAT-6 secretion, itself PhoP-regulated [93]. A synergistic effect of both transcriptional regulators over the operon *espACD* in order to activate its expression and, ultimately essential for a correct secretion of ESAT-6 and CFP-10 has been recently described [94, 95]. It has also been shown that a *phoP* mutation impairs ESAT-6 secretion in the bacteria whereas it does not impair ESAT-6 production, the same phenotype has been observed in H37Ra [96].

PhoP implications in virulence have been demonstrated by several lines of evidence: i) A XDR *M. bovis* carrying an IS*6110* copy upstream *phoP* which acts as a strong promoter, caused a TB outbreak in Spain [97, 98], ii) a *phoP* insertion mutant presents attenuation in replication experiments within phagocytic cells [77, 87, 99] and it is also attenuated compared to the wild type strain in animal models, including mice, guinea pigs and macaques [100, 101]. Taken together all these evidences, PhoP virulence implications and *phoP* mutant attenuation, a new vaccine candidate, MTBVAC, based on a *phoP* deletion has been constructed at the University of Zaragoza [102].

5. VACCINES.

5.1. BCG, the current vaccine.

Currently, the only commercial vaccine licensed to use against TB is *M. bovis* Bacillus Calmette-Guérin (BCG). It is a live attenuated strain obtained in 1921 by subcultivation of a virulent strain of *M. bovis* during 13 years by 230 consecutive passages in the laboratory. This process resulted in the deletion of a number of regions (RD regions) implicated in many cellular process including virulence factors. BCG has lost more than 100 genes and chromosomal regions being an attenuated strain unable to induce disease but stimulating the immune response [103]. The most described deleted region implicated in virulence is RD1, containing the ESX-1 cluster, which includes the genes *esxA*(Rv3875) and *esxB* (Rv3874), encoding for the virulence factors ESAT-6 and CFP-10 respectively, as well as genes coding for proteins directly involved in their secretion [104]. A deletion of this region in H37Rv results in attenuation [105] of the strain, but complementation of RD1 in BCG Pasteur does not restore full virulence [106].

BCG is able to protect against the most severe forms of TB in children, like tuberculous meningitis and miliary TB but its efficacy against pulmonary TB, the transmissible form of the disease, is variable with protection ratios from 80% in developed countries to 0% in some developing countries [107]. The causes of the divergence in protection are still unknown; exposure to environmental mycobacteria has been proposed to explain it, pre-exposed mice with non-pathogenic mycobacteria inhibit BCG replication before the vaccination immune response is fully developed [108]. These evidences together with the fact that regions were BCG barely confers protection, such as Mali or Malawi, are those where there is more exposition to these environmental mycobacteria support this theory [108].

Since the first BCG strain was obtained in 1921, it has suffered numerous passages resulting in a number of different BCG substrains (Figure 8) that differ in gene expression, levels of production of surface proteins and immunodominant antigens

[103, 109] and immune response induction, BCG Japan induces higher levels of IFNγ, IL2 and higher proliferation of $CD4^+$ and $CD8^+$ cells than BCG Pasteur in neonates [110]. These differences between substrains may result in a difference in vaccine efficacy between zones depending on which strain is administrated (there are 3 different substrains licensed to human administration, Tokyo 17, Danish 1331 and Russian BCG-I) [111].

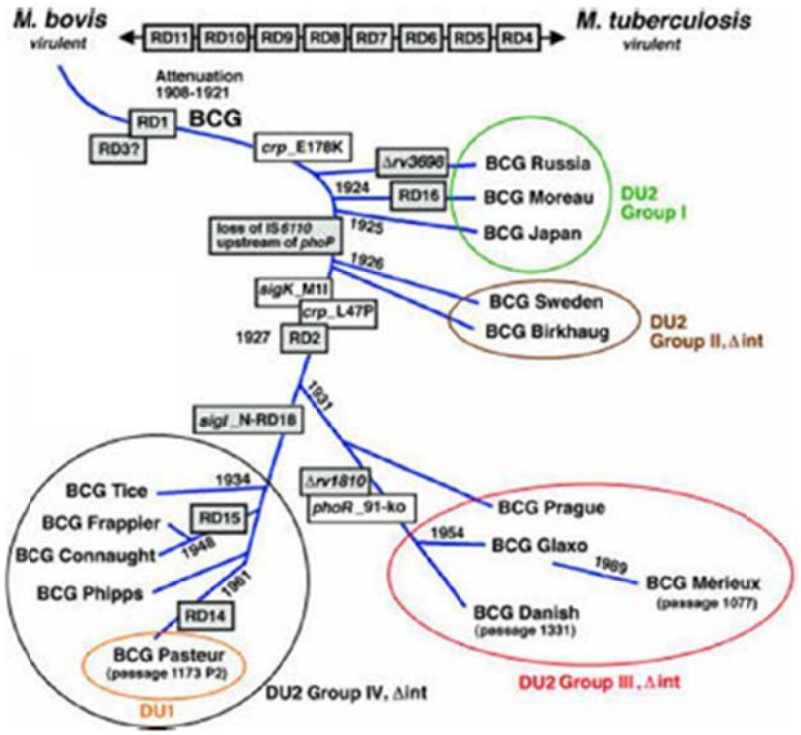

Figure 8. The phylogeny of BCG vaccines. Scheme represents positions referred to genetic markers, RD markers, strains specific deletions and group vaccine distribution. Taken from [103].

Despite all these considerations, the WHO still recommends vaccination with BCG in countries, where TB has a high incidence and remains as a prevalent disease, as this vaccine demonstrated to protect against Mtb. It is the most administrated vaccine worldwide, administrated in more than 167 countries to more than 2.5 billion people since 1948 [112].

On the other hand there is an effort to develop a new TB vaccine that improves protection and safety of BCG to replace it in the future. To that purpose there are different strategies being followed. One strategy is to improve BCG by boosting

immune response either with subunit vaccines or with viral vectors coding for antigens or epitopes [112]. Other strategy is based on construction recombinant strains of BCG (rBCG) that express antigens not present in BCG [112] to enhance immune recognition and its concomitant response. There is a third strategy based on a rationally attenuated live Mtb derivate [112].

5.2. MTBVAC.

In 1991, a MDR-TB outbreak was detected, killing over 100 people, most of them also infected with HIV [98]. Surprisingly, it was caused by a *M. bovis* strain, characterized for being capable to infect humans but not usually transmissible between them. This strain, called strain B, was initially described as MDR in 1997 but today is considered to be extremely resistant (XDR) [97] and therefore virtually untreatable. Genetic studies revealed that this strain carried a copy of a IS*6110* upstream *phoP* which acted as strong promoter of the gene increasing *phoP* expression [97], these data suggested the role of PhoP in Mtb virulence.

The SO2 strain is a *phoP* mutant generated by the insertion of a kanamycin-resistance cassette in a Mtb clinical isolate, Mt103 [77]. Primary mouse bone marrow macrophages infected with this *phoP* mutant showed an impairment of intracellular replication [77], same phenotype was observed in immunocompetent BALB/c mice [77].

SO2 was used as a prototype vaccine in several preclinical studies showing similar efficiency to BCG Pasteur in BALB/c mice protection studies, and higher immunity. SCID survival studies with SO2 showed high attenuation: the SCID mice inoculated by aerosol route with the *phoP* mutant survived until the end of the experiment (6 months) [100]. Protection studies performed in guinea pigs showed a decrease in bacterial load in lungs and spleen in animals vaccinated with SO2 when compared to BCG [100].

Experiments in non-human primates (Rhesus Macaques) showed that SO2 conferred induction of immune response and better protection against TB than BCG [101].

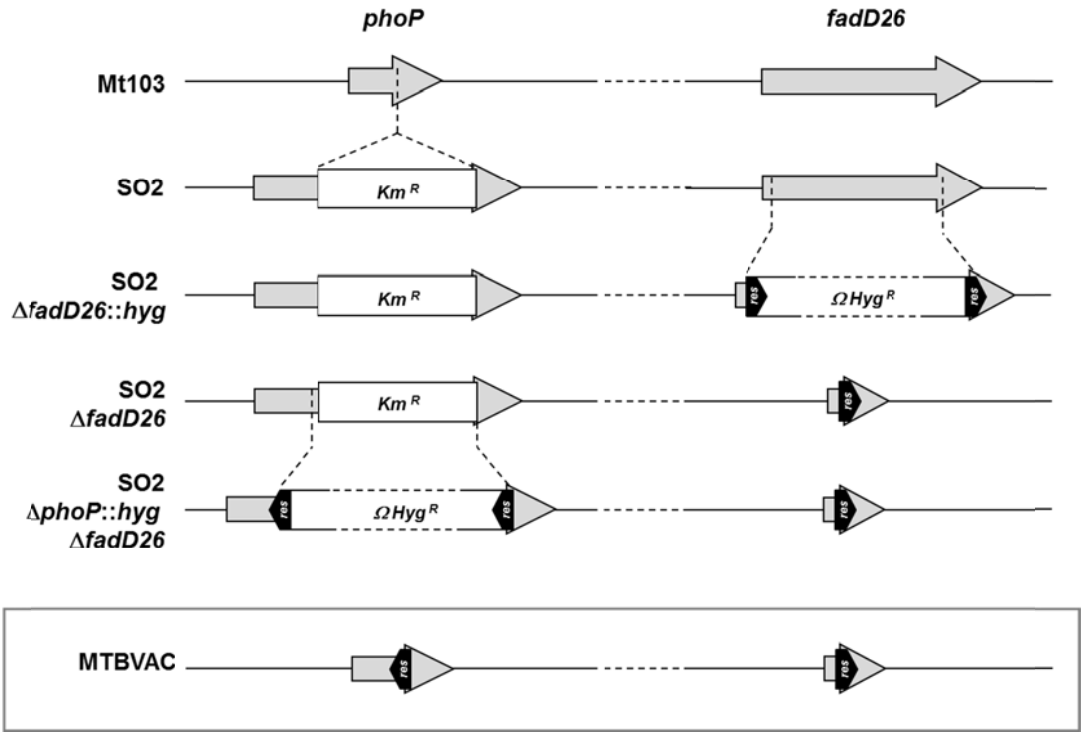

Figure 9. Diagram of MTBVAC construction. On the original strain SO2 deletions in *phoP* and *fadD26* were genetically engineered. Resistance markers were resolved using *res* sites flanking the antibiotic markers. *phoP* and *fadD26* genes are represented as grey arrows, white rectangles illustrate antibiotic-resistance markers and black arrow-heads depicts *res* sites. Vertical discontinuous lines indicate the position of restriction sites used for strain construction and horizontal discontinuous lines depict DNA regions that are not to scale. Adapted from [102].

The adoption of the Geneva consensus for new live TB vaccines, which recommends two non-reversible and independent mutations in the mycobacterial genome without antibiotic resistance markers [102, 113], required the addition of a second mutation in SO2 to enter into clinical trials. For that purpose a new strain was constructed based on the SO2 prototype, carrying no resistance markers and an additional mutation, in *fadD26*. *fadD26* is essential for PDIM synthesis, and a deficiency in PDIM has been described to result in an attenuation of the strain [114]. Resulting strain was called MBVAC [102] (Figure 9).

Bridging studies demonstrated that MTBVAC was functionally comparable to its prototype SO2, being possible to apply SO2 preclinical results to MTBVAC [102]. Compared to the licensed European vaccine, BCG Danish 1331, MTBVAC demonstrated similar safety characteristics in SCID mice, inoculated animals survived to endpoint of the experiment at 13 weeks post infection, but induced better protection in lungs and spleen of C57BL/6 mice, after TB challenge [102].

MTBVAC is the first Mtb live-attenuated vaccine that has entered into clinical trial evaluation in history (ClinicalTrial.gov identifier: NCT02013245), phase I has been already completed [115]. Currently MTBVAC has entered in clinical trial phase II with newborns in South Africa (NCT02729571).

REFERENCES

1. WHO, *Global Tuberculosis Report*. 2015, World Health Organization.
2. Ryan, F., *Tuberculosis: The greatest story never told.* 1992.
3. Paulson, T., *Epidemiology: A mortal foe.* Nature, 2013. **502**(7470): p. S2-3.
4. Gutierrez, M.C., et al., *Ancient origin and gene mosaicism of the progenitor of Mycobacterium tuberculosis.* PLoS Pathog, 2005. **1**(1): p. e5.
5. Daniel, T.M., *The history of tuberculosis.* Respir Med, 2006. **100**(11): p. 1862-70.
6. Taylor, G.M., D.B. Young, and S.A. Mays, *Genotypic analysis of the earliest known prehistoric case of tuberculosis in Britain.* J Clin Microbiol, 2005. **43**(5): p. 2236-40.
7. Smith, I., *Mycobacterium tuberculosis pathogenesis and molecular determinants of virulence.* Clin Microbiol Rev, 2003. **16**(3): p. 463-96.
8. Herzog, H., *History of tuberculosis.* Respiration, 1998. **65**(1): p. 5-15.
9. Kaufmann, S.H., *Robert Koch, the Nobel Prize, and the ongoing threat of tuberculosis.* N Engl J Med, 2005. **353**(23): p. 2423-6.
10. Behr, M.A., *BCG--different strains, different vaccines?* Lancet Infect Dis, 2002. **2**(2): p. 86-92.
11. Gandhi, N.R., et al., *Extensively drug-resistant tuberculosis as a cause of death in patients co-infected with tuberculosis and HIV in a rural area of South Africa.* Lancet, 2006. **368**(9547): p. 1575-80.
12. WHO, *TB: a global emergency. World Health Organization.* 1994.
13. Loewenberg, S., *India reports cases of totally drug-resistant tuberculosis.* Lancet, 2012. **379**(9812): p. 205.
14. Udwadia, Z.F., et al., *Totally drug-resistant tuberculosis in India.* Clin Infect Dis, 2012. **54**(4): p. 579-81.
15. CDC. *Diagnosis of Tuberculosis Disease. Centers forDisease Control and Prevention.* 2011.
16. Babady, N.E., et al., *Comparison of the Luminex xTAG RVP Fast assay and the Idaho Technology FilmArray RP assay for detection of respiratory viruses in pediatric patients at a cancer hospital.* J Clin Microbiol, 2012. **50**(7): p. 2282-8.
17. Clayden, P., et al., *Pipeline Report. HIV, Hepatitis C Virus (HCV), and Tuberculosis (TB) drugs, diagnostics, vaccines, preventive technologies, research toward a cure, and immune-based and gene therapies in development.* 2014.
18. Zumla, A., P. Nahid, and S.T. Cole, *Advances in the development of new tuberculosis drugs and treatment regimens.* Nat Rev Drug Discov, 2013. **12**(5): p. 388-404.
19. WHO/IUATLD, *Anti-tuberculosis drug resistance in the world. Report nº2. Prevalence and Trends*. 2000. p. 253.
20. Stackebrandt, E., F. A. Riney, and N.L. Ward-Rainey, *Proposal for a New Hierarchic classification System, Actinobacteria classis now.* International Journal of Systematic Bacteriology, 1997. **47**: p. 479-491
21. Trifiro, S., et al., *Ghost mycobacteria on Gram stain.* J Clin Microbiol, 1990. **28**(1): p. 146-7.
22. Bifani, P., et al., *Molecular characterization of Mycobacterium tuberculosis H37Rv/Ra variants: distinguishing the mycobacterial laboratory strain.* J Clin Microbiol, 2000. **38**(9): p. 3200-4.

23. Cole, S.T., et al., *Deciphering the biology of Mycobacterium tuberculosis from the complete genome sequence.* Nature, 1998. **393**(6685): p. 537-44.
24. Camus, J.C., et al., *Re-annotation of the genome sequence of Mycobacterium tuberculosis H37Rv.* Microbiology, 2002. **148**(Pt 10): p. 2967-73.
25. Lew, J.M., et al., *TubercuList--10 years after.* Tuberculosis (Edinb), 2011. **91**(1): p. 1-7.
26. Daffe, M., *The cell envelope of tubercle bacilli.* Tuberculosis (Edinb), 2015. **95 Suppl 1**: p. S155-8.
27. Hoffmann, C., et al., *Disclosure of the mycobacterial outer membrane: cryo-electron tomography and vitreous sections reveal the lipid bilayer structure.* Proc Natl Acad Sci U S A, 2008. **105**(10): p. 3963-7.
28. Zuber, B., et al., *Direct visualization of the outer membrane of mycobacteria and corynebacteria in their native state.* J Bacteriol, 2008. **190**(16): p. 5672-80.
29. Groenewald, W., et al., *Differential spontaneous folding of mycolic acids from Mycobacterium tuberculosis.* Chem Phys Lipids, 2014. **180**: p. 15-22.
30. Lemassu, A., et al., *Extracellular and surface-exposed polysaccharides of non-tuberculous mycobacteria.* Microbiology, 1996. **142 (Pt 6)**: p. 1513-20.
31. Sani, M., et al., *Direct visualization by cryo-EM of the mycobacterial capsular layer: a labile structure containing ESX-1-secreted proteins.* PLoS Pathog, 2010. **6**(3): p. e1000794.
32. Ouellet, H., J.B. Johnston, and P.R. de Montellano, *Cholesterol catabolism as a therapeutic target in Mycobacterium tuberculosis.* Trends Microbiol, 2011. **19**(11): p. 530-9.
33. Lopez-Marin, L.M., *Nonprotein structures from mycobacteria: emerging actors for tuberculosis control.* Clin Dev Immunol, 2012. **2012**: p. 917860.
34. Killick, K.E., et al., *Receptor-mediated recognition of mycobacterial pathogens.* Cell Microbiol, 2013. **15**(9): p. 1484-95.
35. Ehlers, S. and U.E. Schaible, *The granuloma in tuberculosis: dynamics of a host-pathogen collusion.* Front Immunol, 2012. **3**: p. 411.
36. Guirado, E. and L.S. Schlesinger, *Modeling the Mycobacterium tuberculosis Granuloma - the Critical Battlefield in Host Immunity and Disease.* Front Immunol, 2013. **4**: p. 98.
37. Russell, D.G., et al., *Mycobacterium tuberculosis wears what it eats.* Cell Host Microbe, 2010. **8**(1): p. 68-76.
38. Russell, D.G., *Mycobacterium tuberculosis and the intimate discourse of a chronic infection.* Immunol Rev, 2011. **240**(1): p. 252-68.
39. Dey, B. and W.R. Bishai, *Crosstalk between Mycobacterium tuberculosis and the host cell.* Semin Immunol, 2014. **26**(6): p. 486-96.
40. Han, G. and C.C. Zhang, *On the origin of Ser/Thr kinases in a prokaryote.* FEMS Microbiol Lett, 2001. **200**(1): p. 79-84.
41. Ponting, C.P., et al., *Eukaryotic signalling domain homologues in archaea and bacteria. Ancient ancestry and horizontal gene transfer.* J Mol Biol, 1999. **289**(4): p. 729-45.
42. Walburger, A., et al., *Protein kinase G from pathogenic mycobacteria promotes survival within macrophages.* Science, 2004. **304**(5678): p. 1800-4.

43. Scherr, N., et al., *Survival of pathogenic mycobacteria in macrophages is mediated through autophosphorylation of protein kinase G.* J Bacteriol, 2009. **191**(14): p. 4546-54.
44. Master, S.S., et al., *Mycobacterium tuberculosis prevents inflammasome activation.* Cell Host Microbe, 2008. **3**(4): p. 224-32.
45. Sander, P., et al., *Deletion of zmp1 improves Mycobacterium bovis BCG-mediated protection in a guinea pig model of tuberculosis.* Vaccine, 2015. **33**(11): p. 1353-9.
46. Camacho, L.R., et al., *Identification of a virulence gene cluster of Mycobacterium tuberculosis by signature-tagged transposon mutagenesis.* Mol Microbiol, 1999. **34**(2): p. 257-67.
47. Goren, M.B., O. Brokl, and W.B. Schaefer, *Lipids of putative relevance to virulence in Mycobacterium tuberculosis: phthiocerol dimycocerosate and the attenuation indicator lipid.* Infect Immun, 1974. **9**(1): p. 150-8.
48. Goren, M.B., O. Brokl, and W.B. Schaefer, *Lipids of putative relevance to virulence in Mycobacterium tuberculosis: correlation of virulence with elaboration of sulfatides and strongly acidic lipids.* Infect Immun, 1974. **9**(1): p. 142-9.
49. Cox, J.S., et al., *Complex lipid determines tissue-specific replication of Mycobacterium tuberculosis in mice.* Nature, 1999. **402**(6757): p. 79-83.
50. Stanley, S.A. and J.S. Cox, *Host-pathogen interactions during Mycobacterium tuberculosis infections.* Curr Top Microbiol Immunol, 2013. **374**: p. 211-41.
51. Rhoades, E.R. and H.J. Ullrich, *How to establish a lasting relationship with your host: lessons learned from Mycobacterium spp.* Immunol Cell Biol, 2000. **78**(4): p. 301-10.
52. Rousseau, C., et al., *Production of phthiocerol dimycocerosates protects Mycobacterium tuberculosis from the cidal activity of reactive nitrogen intermediates produced by macrophages and modulates the early immune response to infection.* Cell Microbiol, 2004. **6**(3): p. 277-87.
53. Vergne, I., et al., *Mechanism of phagolysosome biogenesis block by viable Mycobacterium tuberculosis.* Proc Natl Acad Sci U S A, 2005. **102**(11): p. 4033-8.
54. Mishra, A.K., et al., *Lipoarabinomannan and related glycoconjugates: structure, biogenesis and role in Mycobacterium tuberculosis physiology and host-pathogen interaction.* FEMS Microbiol Rev, 2011. **35**(6): p. 1126-57.
55. Goren, M.B., et al., *Prevention of phagosome-lysosome fusion in cultured macrophages by sulfatides of Mycobacterium tuberculosis.* Proc Natl Acad Sci U S A, 1976. **73**(7): p. 2510-4.
56. Brodin, P., et al., *High content phenotypic cell-based visual screen identifies Mycobacterium tuberculosis acyltrehalose-containing glycolipids involved in phagosome remodeling.* PLoS Pathog, 2010. **6**(9): p. e1001100.
57. Brozna, J.P., et al., *Monocyte responses to sulfatide from Mycobacterium tuberculosis: inhibition of priming for enhanced release of superoxide, associated with increased secretion of interleukin-1 and tumor necrosis factor alpha, and altered protein phosphorylation.* Infect Immun, 1991. **59**(8): p. 2542-8.

58. Astarie-Dequeker, C., et al., *Phthiocerol dimycocerosates of M. tuberculosis participate in macrophage invasion by inducing changes in the organization of plasma membrane lipids.* PLoS Pathog, 2009. **5**(2): p. e1000289.
59. Sun, J., et al., *Mycobacterial nucleoside diphosphate kinase blocks phagosome maturation in murine RAW 264.7 macrophages.* PLoS One, 2010. **5**(1): p. e8769.
60. Ehrt, S. and D. Schnappinger, *Mycobacterial survival strategies in the phagosome: defence against host stresses.* Cell Microbiol, 2009. **11**(8): p. 1170-8.
61. Forrellad, M.A., et al., *Virulence factors of the Mycobacterium tuberculosis complex.* Virulence, 2013. **4**(1): p. 3-66.
62. McKinney, J.D., et al., *Persistence of Mycobacterium tuberculosis in macrophages and mice requires the glyoxylate shunt enzyme isocitrate lyase.* Nature, 2000. **406**(6797): p. 735-8.
63. Ferrer, N.L., et al., *Interactions of attenuated Mycobacterium tuberculosis phoP mutant with human macrophages.* PLoS One, 2010. **5**(9): p. e12978.
64. Meher, A.K., et al., *Analysis of complex formation and immune response of CFP-10 and ESAT-6 mutants.* Vaccine, 2007. **25**(32): p. 6098-106.
65. van der Wel, N., et al., *M. tuberculosis and M. leprae translocate from the phagolysosome to the cytosol in myeloid cells.* Cell, 2007. **129**(7): p. 1287-98.
66. Stamm, L.M., et al., *Mycobacterium marinum escapes from phagosomes and is propelled by actin-based motility.* J Exp Med, 2003. **198**(9): p. 1361-8.
67. Smith, J., et al., *Evidence for pore formation in host cell membranes by ESX-1-secreted ESAT-6 and its role in Mycobacterium marinum escape from the vacuole.* Infect Immun, 2008. **76**(12): p. 5478-87.
68. Simeone, R., et al., *Phagosomal rupture by Mycobacterium tuberculosis results in toxicity and host cell death.* PLoS Pathog, 2012. **8**(2): p. e1002507.
69. Brodin, P., et al., *Dissection of ESAT-6 system 1 of Mycobacterium tuberculosis and impact on immunogenicity and virulence.* Infect Immun, 2006. **74**(1): p. 88-98.
70. Jackson, M., et al., *Persistence and protective efficacy of a Mycobacterium tuberculosis auxotroph vaccine.* Infect Immun, 1999. **67**(6): p. 2867-73.
71. Hondalus, M.K., et al., *Attenuation of and protection induced by a leucine auxotroph of Mycobacterium tuberculosis.* Infect Immun, 2000. **68**(5): p. 2888-98.
72. Gordhan, B.G., et al., *Construction and phenotypic characterization of an auxotrophic mutant of Mycobacterium tuberculosis defective in L-arginine biosynthesis.* Infect Immun, 2002. **70**(6): p. 3080-4.
73. Pavelka, M.S., Jr., et al., *Vaccine efficacy of a lysine auxotroph of Mycobacterium tuberculosis.* Infect Immun, 2003. **71**(7): p. 4190-2.
74. Smith, D.A., et al., *Characterization of auxotrophic mutants of Mycobacterium tuberculosis and their potential as vaccine candidates.* Infect Immun, 2001. **69**(2): p. 1142-50.
75. Tullius, M.V., G. Harth, and M.A. Horwitz, *Glutamine synthetase GlnA1 is essential for growth of Mycobacterium tuberculosis in human THP-1 macrophages and guinea pigs.* Infect Immun, 2003. **71**(7): p. 3927-36.

76. Bretl, D.J., C. Demetriadou, and T.C. Zahrt, *Adaptation to environmental stimuli within the host: two-component signal transduction systems of Mycobacterium tuberculosis.* Microbiol Mol Biol Rev, 2011. **75**(4): p. 566-82.
77. Perez, E., et al., *An essential role for phoP in Mycobacterium tuberculosis virulence.* Mol Microbiol, 2001. **41**(1): p. 179-87.
78. Gonzalo-Asensio, J., et al., *The Mycobacterium tuberculosis phoPR operon is positively autoregulated in the virulent strain H37Rv.* J Bacteriol, 2008. **190**(21): p. 7068-78.
79. Gupta, S., et al., *Mycobacterium tuberculosis PhoP recognizes two adjacent direct-repeat sequences to form head-to-head dimers.* J Bacteriol, 2009. **191**(24): p. 7466-76.
80. Cimino, M., et al., *Identification of DNA binding motifs of the Mycobacterium tuberculosis PhoP/PhoR two-component signal transduction system.* PLoS One, 2012. **7**(8): p. e42876.
81. Gupta, S., A. Sinha, and D. Sarkar, *Transcriptional autoregulation by Mycobacterium tuberculosis PhoP involves recognition of novel direct repeat sequences in the regulatory region of the promoter.* FEBS Lett, 2006. **580**(22): p. 5328-38.
82. Sinha, A., et al., *PhoP-PhoP interaction at adjacent PhoP binding sites is influenced by protein phosphorylation.* J Bacteriol, 2008. **190**(4): p. 1317-28.
83. Wang, S., J. Engohang-Ndong, and I. Smith, *Structure of the DNA-binding domain of the response regulator PhoP from Mycobacterium tuberculosis.* Biochemistry, 2007. **46**(51): p. 14751-61.
84. He, X., L. Wang, and S. Wang, *Structural basis of DNA sequence recognition by the response regulator PhoP in Mycobacterium tuberculosis.* Sci Rep, 2016. **6**: p. 24442.
85. Chesne-Seck, M.L., et al., *A point mutation in the two-component regulator PhoP-PhoR accounts for the absence of polyketide-derived acyltrehaloses but not that of phthiocerol dimycocerosates in Mycobacterium tuberculosis H37Ra.* J Bacteriol, 2008. **190**(4): p. 1329-34.
86. Lee, J.S., et al., *Mutation in the transcriptional regulator PhoP contributes to avirulence of Mycobacterium tuberculosis H37Ra strain.* Cell Host Microbe, 2008. **3**(2): p. 97-103.
87. Walters, S.B., et al., *The Mycobacterium tuberculosis PhoPR two-component system regulates genes essential for virulence and complex lipid biosynthesis.* Mol Microbiol, 2006. **60**(2): p. 312-30.
88. Gonzalo-Asensio, J., et al., *PhoP: a missing piece in the intricate puzzle of Mycobacterium tuberculosis virulence.* PLoS One, 2008. **3**(10): p. e3496.
89. Kumar, A., et al., *Mycobacterium tuberculosis DosS is a redox sensor and DosT is a hypoxia sensor.* Proc Natl Acad Sci U S A, 2007. **104**(28): p. 11568-73.
90. Voskuil, M.I., K.C. Visconti, and G.K. Schoolnik, *Mycobacterium tuberculosis gene expression during adaptation to stationary phase and low-oxygen dormancy.* Tuberculosis (Edinb), 2004. **84**(3-4): p. 218-27.
91. Park, H.D., et al., *Rv3133c/dosR is a transcription factor that mediates the hypoxic response of Mycobacterium tuberculosis.* Mol Microbiol, 2003. **48**(3): p. 833-43.

92. Kendall, S.L., et al., *The Mycobacterium tuberculosis dosRS two-component system is induced by multiple stresses.* Tuberculosis (Edinb), 2004. **84**(3-4): p. 247-55.
93. Solans, L., et al., *The PhoP-dependent ncRNA Mcr7 modulates the TAT secretion system in Mycobacterium tuberculosis.* PLoS Pathog, 2014. **10**(5): p. e1004183.
94. Blasco, B., et al., *Virulence regulator EspR of Mycobacterium tuberculosis is a nucleoid-associated protein.* PLoS Pathog, 2012. **8**(3): p. e1002621.
95. Anil Kumar, V., et al., *EspR-dependent ESAT-6 secretion of Mycobacterium tuberculosis requires the presence of virulence regulator PhoP.* J Biol Chem, 2016.
96. Frigui, W., et al., *Control of M. tuberculosis ESAT-6 secretion and specific T cell recognition by PhoP.* PLoS Pathog, 2008. **4**(2): p. e33.
97. Soto, C.Y., et al., *IS6110 mediates increased transcription of the phoP virulence gene in a multidrug-resistant clinical isolate responsible for tuberculosis outbreaks.* J Clin Microbiol, 2004. **42**(1): p. 212-9.
98. Samper, S., et al., *Transmission between HIV-infected patients of multidrug-resistant tuberculosis caused by Mycobacterium bovis.* AIDS, 1997. **11**(10): p. 1237-42.
99. Gonzalo Asensio, J., et al., *The virulence-associated two-component PhoP-PhoR system controls the biosynthesis of polyketide-derived lipids in Mycobacterium tuberculosis.* J Biol Chem, 2006. **281**(3): p. 1313-6.
100. Martin, C., et al., *The live Mycobacterium tuberculosis phoP mutant strain is more attenuated than BCG and confers protective immunity against tuberculosis in mice and guinea pigs.* Vaccine, 2006. **24**(17): p. 3408-19.
101. Verreck, F.A., et al., *MVA.85A boosting of BCG and an attenuated, phoP deficient M. tuberculosis vaccine both show protective efficacy against tuberculosis in rhesus macaques.* PLoS One, 2009. **4**(4): p. e5264.
102. Arbues, A., et al., *Construction, characterization and preclinical evaluation of MTBVAC, the first live-attenuated M. tuberculosis-based vaccine to enter clinical trials.* Vaccine, 2013. **31**(42): p. 4867-73.
103. Brosch, R., et al., *Genome plasticity of BCG and impact on vaccine efficacy.* Proc Natl Acad Sci U S A, 2007. **104**(13): p. 5596-601.
104. Hsu, T., et al., *The primary mechanism of attenuation of bacillus Calmette-Guerin is a loss of secreted lytic function required for invasion of lung interstitial tissue.* Proc Natl Acad Sci U S A, 2003. **100**(21): p. 12420-5.
105. Lewis, K.N., et al., *Deletion of RD1 from Mycobacterium tuberculosis mimics bacille Calmette-Guerin attenuation.* J Infect Dis, 2003. **187**(1): p. 117-23.
106. Pym, A.S., et al., *Loss of RD1 contributed to the attenuation of the live tuberculosis vaccines Mycobacterium bovis BCG and Mycobacterium microti.* Mol Microbiol, 2002. **46**(3): p. 709-17.
107. Fine, P.E., *Variation in protection by BCG: implications of and for heterologous immunity.* Lancet, 1995. **346**(8986): p. 1339-45.
108. Brandt, L., et al., *Failure of the Mycobacterium bovis BCG vaccine: some species of environmental mycobacteria block multiplication of BCG and induction of protective immunity to tuberculosis.* Infect Immun, 2002. **70**(2): p. 672-8.
109. Liu, J., et al., *BCG vaccines: their mechanisms of attenuation and impact on safety and protective efficacy.* Hum Vaccin, 2009. **5**(2): p. 70-8.

110. Hussey, G.D., et al., *Neonatal mycobacterial specific cytotoxic T-lymphocyte and cytokine profiles in response to distinct BCG vaccination strategies.* Immunology, 2002. **105**(3): p. 314-24.
111. WHO, *WHO global tuberculosis control report 2010. Summary.* Cent Eur J Public Health, 2010. **18**: p. 237.
112. Marinova, D., et al., *Recent developments in tuberculosis vaccines.* Expert Rev Vaccines, 2013. **12**(12): p. 1431-48.
113. Walker, K.B., et al., *The second Geneva Consensus: Recommendations for novel live TB vaccines.* Vaccine, 2010. **28**(11): p. 2259-70.
114. Infante, E., et al., *Immunogenicity and protective efficacy of the Mycobacterium tuberculosis fadD26 mutant.* Clin Exp Immunol, 2005. **141**(1): p. 21-8.
115. Spertini, F., et al., *Safety of human immunisation with a live-attenuated Mycobacterium tuberculosis vaccine: a randomised, double-blind, controlled phase I trial.* Lancet Respir Med, 2015. **3**(12): p. 953-62.

Objectives

The general objectives of this work are:

1. Comparative analysis of the secreted protein fractions from the vaccine candidate MTBVAC and its parental strain.

2. Characterization of MTBVAC intracellular trafficking and deciphering the individual contribution of *phoP* and *fadD26* deletions to the final phenotype.

3. In depth study of the signal that activates the major virulence Two Component System PhoPR.

4. Construction of a new stable and unmarked MTBVAC *zmp1*$^{-}$ strain, as an hyper-attenuated strain for use in immunocompromised population.

Chapter 1:

Contribution of single *phoP* and *fadD26* mutations to the lipid and protein composition of MTBVAC vaccine candidate and its interaction with the host.

INTRODUCTION

Protein secretion is one of the most important mechanisms that allows intracellular bacteria to interact with the host. Through action of these secreted proteins bacteria can adapt to intracellular conditions, such as the environment inside the phagosome, and/or escape from one compartment to another [1].

In Mtb, there are two highly conserved protein secretion systems the Sec and TAT export pathways. Mtb also possesses specialized protein export systems dedicated to the secretion of a more limited set of proteins: the accessory SecA2 export pathway and ESX pathways [1]. Evolutionary conserved secretion systems are present in all bacteria (SecA secretion system) or in a large number of families but not in all microorganisms (TAT secretion system). The specialized secretion systems are not conserved among species and play specific roles, like those implicated in pathogenesis of some important intracellular bacteria [1, 2].

Twin-arginine translocase (TAT) export systems exist in both Gram-negative and Gram-positive bacteria, but they are not present in all bacteria. When TAT export systems are found in bacterial pathogens, they are frequently responsible for exporting virulence factors, and thus contribute to pathogenesis. In Mtb, the TAT system plays a role in both virulence and drug resistance, and it is also essential for viability [2, 3].

ESX secretion systems, which are also referred to as Type VII are specialized protein export systems originally identified in mycobacteria. The first ESX system identified was ESX-1 of Mtb, which is responsible for exporting the ESAT-6 protein (early secreted antigenic target 6 kD). Mtb has five ESX systems (ESX-1-5), which export ESAT-6-like proteins with various functions in mycobacterial physiology and/or virulence [4, 5].

In a previous work proteomic analysis were done in order to compare the secretome of the Mtb H37Rv wild-type strain and its *phoP* mutant [3]. 37 proteins were found to be more secreted in the *phoP* mutant compared to the wild type strain, 16 of these

(43.24%) exhibited an RR motif within the first 50 aminoacids. On the other hand, 6 out of 35 proteins that were more abundant in the wild type, displayed the RR motif. This twin arginine motif (RR) is required to export proteins through the TAT secretory system [3]. The predicted TAT substrates (those with a RR motif) were significantly more present in the secreted fraction of the *phoP* mutant relative to wild type strain.

In addition, the relative secretion levels of ESAT-6, CFP-10, EspA and EspC were compared since these proteins are well-known PhoP-dependent ESX-1 secretion substrates [6] and as it was expected, the secretome of the *phoP* mutant contained very low amounts of ESAT-6, CFP-10, EspA and EspC, thus showing the opposite trend to TAT-dependent substrates [3].

A novel regulatory model was identified, where Mcr7, an ncRNA strictly regulated by PhoP is playing a key role in the *tatC* mRNA regulation, probably preventing its ribosome loading and, consequently translation of *tatC* mRNA. Thus the TAT secretory system regulation will be impaired [3].

This entire new regulatory model implies that the Mtb H37RvΔ*phoP* mutant presents diverse phenotypic divergences, beside the absence of production of SL, DAT and PAT [7], it has altered protein secretion. The *phoP* mutant displays absence of secretion of ESX-1 substrates, while TAT substrates are considerably increased in the secreted fraction [3].

Besides the secreted proteins, a significant contributor of Mtb pathogenicity during infection resides in its capacity to manage the hostile environment encountered within the host in order to survive and replicate. Mtb has evolved mechanisms of resistance to overcome the defense functions of macrophages; these involve the use of receptors for cell invasion [8], the modulation of normal progression of the phagosome into an acid and hydrolytically active phagolysosome, the regulation of local modulators of the immune response and the control of cell apoptosis [9].

One of the most important mechanisms that allow Mtb to persist and replicate inside the macrophage is the phagosomal maturation arrest [10]. It retains or eliminates some host molecules from the phagosome in order to prevent its maturation, it stops the compartment acidification which will remain at pH=6,5 approximately. To manage this, for instance, the mycobacteria block the presence of the vacuolar proton ATPase (V-ATPase) responsible of the phagosomal acidification; other mycobacterial enzymes also helps to keep the neutral pH of the phagosome through the production of $NH4^+$ ions, like the urease, the glutamine synthetase or the ureoamide lyase [11].

By inhibiting the formation of the phagolysosome, Mtb persists in a phagosome with markers typical from an early endosome like the mannose receptor or the small GTPase, but not with markers typical from late endosomes or phagolysosomes like the cathepsin D, the small GTPase protein Rab 7, the lysosomal-associated membrane protein 1 (LAMP-1) and the lysosomal-associated membrane protein 2 (LAMP-2) or the membrane protein CD63 [12] (Figure 1). Inside this mycobacterial-containing phagosome, the bacteria have sources of nutrients, can evade the immune system, avoid the acidic pH and the hydrolases contained in the phagolysosome.

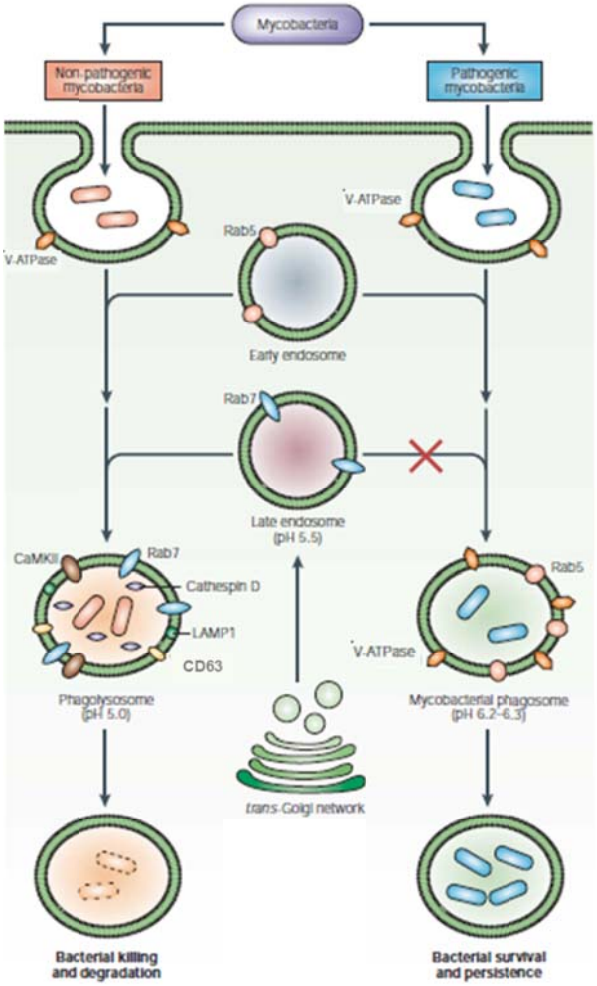

Figure 1. Lysosome mycobacterial evasion. Vacuoles containing non-pathogenic mycobacteria show early endosomal markers, such as Rab5 and the proton-ATPase pump (V-ATPase). These vacuoles fuse with late endosomal vesicles and acquire proteins such as the lysosome-associated membrane glycoprotein 1 (LAMP1) and the membrane protein CD63. Although vacuoles containing pathogenic mycobacteria do not fuse with lysosomes/late endosomes (represented by a red cross), and finally they are able to survive and replicate in the mycobacterial phagosome. Whereas non-pathogenic mycobacteria are readily killed in phagolysosomes with an extremely low pH, hydrolytic enzymes and bactericidal peptides. Adapted from [13].

There are a number of mechanisms involved in the phagosomal maturation arrest such as the inhibition of the intracellular Ca^{2+} which plays a key role in the immune activation [14], or the secretion by Mtb of a lipid phosphatase that blocks the phosphatidylinositol 3-phosphate (PI3P), a molecule involved in signaling phagosome fusion with late endosomes [15, 16].

Mycobacterial lipids also play an important role in the modulation of the host immune response. The outermost layer of the mycobacterial cell envelope contains unique cell-surface lipids and acts as an interface between the host and the pathogen. Passemar *et al.* established for SL, PDIM and DAT/PAT an essential role in the remodeling of the Mtb-containing phagosome and in preventing its acidification, and as a consequence in the survival in human macrophages [17].

PDIM constitute a potential candidate for modulating the initial step of entry into macrophages and for controlling the outcome of bacterial infection. Astarie *et al.* proposed a model in which contact of Mtb with phagocytes is followed by the insertion of PDIM into the plasma membrane of the host. This modification increases the efficiency of receptor-mediated phagocytosis and affects phagosome acidification thereby facilitating the access of the pathogen to its ecological niche. A mutant lacking PDIM was unable to prevent vacuole acidification, acquiring late endosomal markers [17, 18]. Purified SL has been described as modulating phagosome-lysosome fusion [19, 20], blocking monocyte priming [21], increased superoxide production by neutrophils [22], increased phagosome acidification [20] or growth restriction in human macrophages [23] among others. Concerning DAT and PAT, their role in downmodulation of IL2, IL10, IL12 and TNF-α responses in $CD4^+$ and $CD8^+$ human T cells has been demonstrated [24], DAT/PAT are potent inhibitors of leucocyte migration [25] and T cell proliferation [26] and participate in early interactions between Mtb and phagocytes [27]. It also has been reported that deficiency in some forms of DAT and PAT affects the surface properties of Mtb, resulting in enhanced interaction with host cells [18, 28].

The presence of PDIM is required but not sufficient to arrest the phagosome maturation since heat-killed bacteria that contain PDIM, accumulate in acidified compartment. All these results imply that modulation of phagosome maturation is likely a multifactorial process [18]. A study based on screening of mycobacterial mutants [29, 30] identified multiple genes required for phagosomal arrest, including

those involved in biosynthesis of surface lipids, transport of possible effector molecules, and production of isoprenoid compounds.

The SO2 vaccine candidate strain is a *phoP* mutant in the Mtb clinical isolate, Mt103, which is also naturally deficient in SL. Due to the *phoP* mutation, the strain also lacks DAT and PAT [31]. The ability of SO2 to arrest phagosome maturation was studied by colocalization analysis with the acido-trophic probe Lysotracker (for early stages of maturation), LAMP-1 and CD63 markers, two different lysosome-associated membrane glycoprotein characteristic of late-compartments of the phagocytic route (for late endosome-phagosome and phagolysosome stages, respectively). High colocalization of SO2 was observed with Lysotracker and LAMP-1, but it showed poor colocalization with CD63 [32]. Suggesting that SO2 does not escape phagosomal maturation, however it displays a persistence phenotype. SO2 attenuation could be due partially to its inability to inhibit phagosome maturation characteristic of the wild-type strain [32].

Beside the trafficking studies, rigorous preclinical testing of SO2 as a vaccine candidate provided robust data for its high degree of safety, improved immunogenicity and protective efficacy compared to BCG in relevant animal models of TB, from mice to non-human primates [31, 33]. Despite the promising results, the establishments of Geneva consensus for new live mycobacterial vaccines, requiring the presence of two stable independent mutations without antibiotic-resistance markers for Mtb-based candidates, in addition to a safety and efficacy profile at least comparable to BCG in the relevant animal models, rendered SO2 unsuitable for entry into clinical trials [34, 35].

Simultaneously to the preclinical testing, it was observed that the *phoP* mutant SO2 showed incomplete restoration of the wild-type virulence in immunocompetent mice when it was complemented with the *phoP* gene, suggesting that other genetic lesions might also be involved in the attenuated phenotype [36]. Lipid profile analysis of SO2 mutant revealed that, apart from being deficient in DAT and PAT as result of the *phoP* mutation, the strain is devoid of PDIM. Although the precise reason for the loss of

PDIM synthesis in SO2 is unknown, similar “spontaneous” losses of PDIM production have been reported in other allelic exchange mutants; PDIM deficiency is also a characteristic of attenuated mycobacteria strains generated by subculture, like H37Ra [37].

The *fadD26* gene is required for PDIM biosynthesis; it encodes an acyl-AMP ligase, the first gene in the PDIM biosynthesis operon. Thus, an Mtb mutant in this gene is completely devoid of this family of lipids, being attenuated in several mouse models. When tested as vaccine, this mutant protected mice infected with virulent Mtb [38, 39].

Based on these last results, a new vaccine candidate was constructed following a stepwise approach to genetically engineer two stable, unmarked deletions in *phoP* and *fadD26* genes in the SO2 strain, generating a novel vaccine candidate that was named MTBVAC. Results obtained in immunogenicity and protective efficacy bridging experiments provide evidence that MTBVAC is functionally comparable to its prototype SO2 [40].

This new vaccine candidate, even considering it is a *phoP* mutant and it is based on SO2, is a new strain. Accordingly, we considered necessary to analyze both the secretome and the trafficking of MTBVAC itself and to study the contribution of each single mutation (*phoP* and *fadD26* genes) to the intracellular trafficking in order to a better understanding the nature of host-vaccine interactions during infection.

1.1. Proteomic profiling of the vaccine candidate strain.

In vitro culture of Mtb results in the accumulation in the extracellular milieu of a complex set of proteins. A considerable number of the proteins secreted by Mtb are known to contribute to the immunology of TB and to possess enzymatic activities associated with pathogenicity. In previous studies it has been proved that culture filtrate is a major repository of antigens involved in the protective immune response and it has also been demonstrated the ability of these proteins to induce a protective T-cell response [41].

In order to verify the secretome profile of MTBVAC, we cultivated MTBVAC and its parental strain Mt103 until late stationary phase in standard culture medium without any detergent (tween) or albumin to avoid protein interferences. Comparative analysis between the wild type strain Mt103 and the vaccine candidate MTBVAC secreted protein were carried out by two methodologies, western blot and differential gel electrophoresis techniques.

The main objective of this part of the work was analyzing the secreted proteins through the fluorescence two-dimensional difference gel electrophoresis (2D-DiGE). DiGE is based on fluorescent cyanine dyes and allows comparisons between two protein samples, which are resolved on the same gel [42]. The principle involved in the DiGE technique is that different dyes provide different fluorescence wavelengths for detection, allowing two or more differentially labeled samples to be combined before being loaded onto isoelectric focusing (IEF)(first dimension). The strip is subsequently subjected to a SDS-PAGE (second dimension) and the gel is scanned with the excitation wavelength of each dye so we are able to resolve each sample separately. Frequently, three samples are labeled: two of them are experimental samples whereas the third sample is composed of a mixture of equal amounts of all experimental samples (pooled internal standard). This creates a standard for each protein during analysis. The protein samples are then visualized using fluorescence imaging, which enables the detection of differences between protein abundances in the samples [42]. The most

commonly used fluorescent protein labeling reagents for DiGE are synthetic N-hydroxysuccinimidyl (NHS) ester derivate of the cyanine dyes (Cy2, Cy3, Cy5). These fluorophore dyes are structurally similar and react with primary amine groups of lysine residues. The dyes are positively charged to offset the charge of lysine. At this point, the samples should be labeled in denaturing 2-D electrophoresis lysis buffer at pH values between 8 and 8,5 [42].

The different protein samples labeled can be visualized separately by exciting the different dyes at their specific excitation wavelengths. Therefore, from the images generated for each dye, the signals from labeled proteins spots are determined and the normalized intensities or spot volumes for each spot are compared in order to identify differentially expressed protein between samples.

For quantitative protein analysis, an internal standard is used, which is marked with a dye (generally Cy2) and applied to gel electrophoresis, along with two samples to be analyzed (labeled with Cy3 and Cy5) (Figure 2). The internal standard is prepared from a mixture of equal amounts of proteins from the two samples and therefore contains all proteins that are present in each sample. Thus, each protein has a single signal in the internal standard, which is used for a direct quantitative comparison within each gel and for normalizing the abundance values for each protein when comparing different gels. As a consequence, the abundance of each protein spot in a biological sample can be measured as a ratio (not a volume) to its corresponding spot present in the internal standard. In this way, as each sample spot is co-detected with a standard spot map, all spots are compared in the gel to the same standard. This enables accurate quantification and accurate spot statistics between gels and, most importantly, separation of experimental gel-to-gel variation from biological variation in studying protein spot abundance [42, 43].

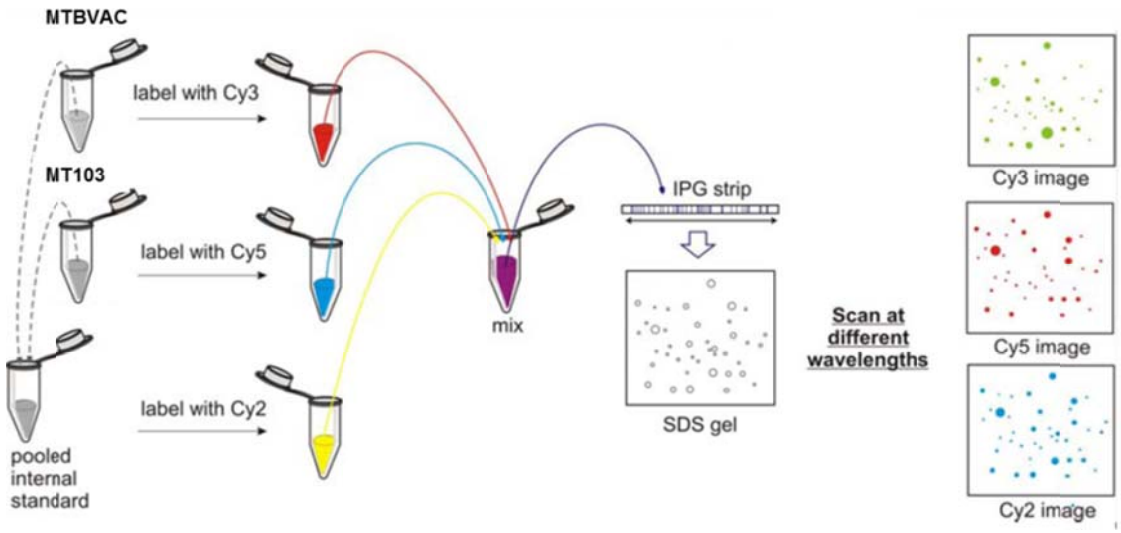

Figure 2. Diagram of the proteomic analysis by 2-D DiGE. Adapted from Ettan™ DIGE Basic Course of GE Healthcare.

1.1.1. Western-Blot.

Previous results demonstrated increased secretion of TAT substrates in MTBVAC and the absence of ESAT-6 secretion in this strain [3]. With the objective of validate these phenotypes in protein samples subsequently analyzed by DiGE, we carried out some Western-Blot experiments using antibodies against Antigen 85 complex (Ag85A, Ag85B and Ag85C) and the ESX-1 substrate ESAT-6 (Figure 3).

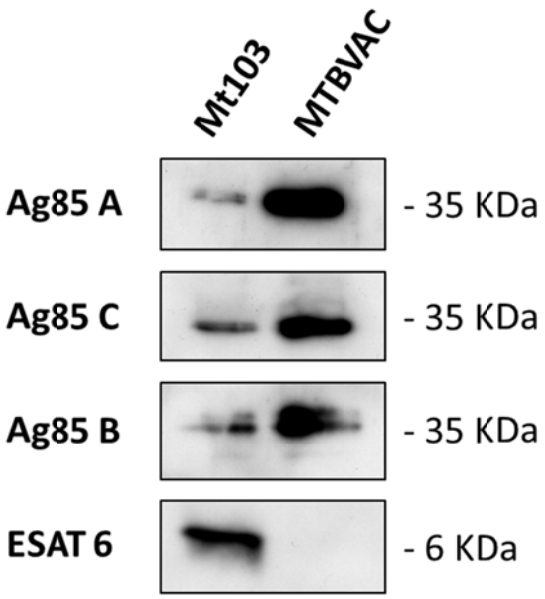

Figure 3. Western Blot image showing that components of the Antigen 85 complex are more abundant on the secreted fraction of MTBVAC compared to the parental strain. The ESX-1 substrate ESAT-6 has the opposite trend, being only secreted on Mt103. Same amounts of protein were loaded in each western blot assay.

We verified that Antigens 85 A, B and C showed increased secretion in MTBVAC compared to the parental strain Mt103. This effect is due to the absence of the ncRNA Mcr7, the strongest PhoP-regulated region, which has been proposed to be a TatC down regulator. Therefore the absence of Mcr7 is traduced on an increased secretion of TAT substrates, like the components of the Antigen 85 Complex.

We also corroborated that ESAT-6 is not secreted by the vaccine candidate strain. The ESAT-6 protein is a PhoP-dependent ESX-1 substrate and a key virulence factor, therefore is absent in the secretome of PhoP-mutant strains as MTBVAC.

1.1.2. Differential in Gel Electrophoresis (DiGE).

In order to compare the secretome of the vaccine candidate MTBVAC and its parental strain we performed the 2-D DiGE technique. First of all we carried out a regular two-dimensional electrophoresis (2-D) with one of the samples of MTBVAC secreted proteins, without fluorescent dying and using silver staining to visualize protein spots. For the IEF separation we used strips with pH range from 3 to 11. In this range proteins did not separate correctly since Mtb proteins are mainly acidic. However, we could observe that our protein extractions work fine for 2D-DiGE technique (Figure 4).

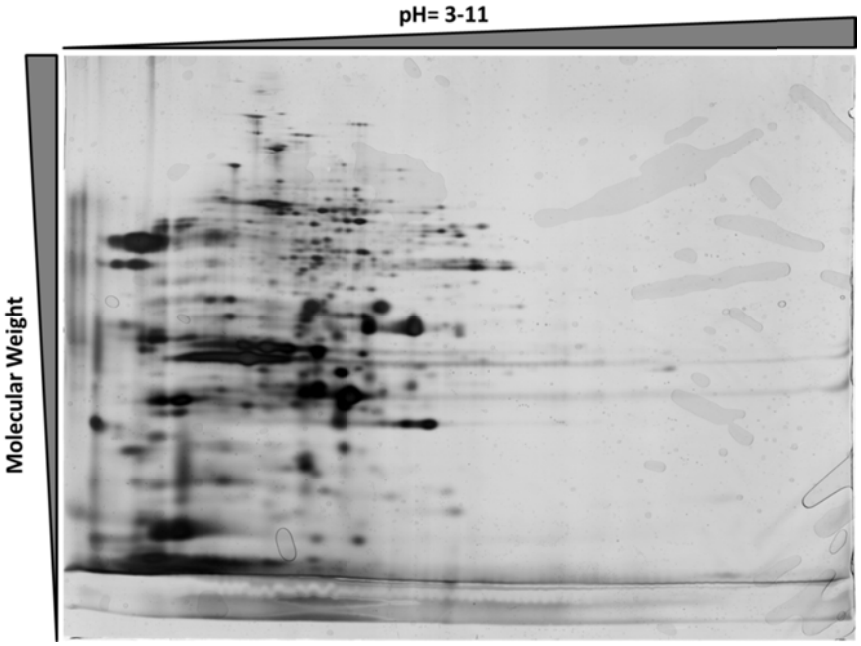

Figure 4. Two-dimensional electrophoresis of the MTBVAC secreted proteins with subsequent silver staining to visualize spots. During the first step, IEF using a strip with a pH range from 3 to 11 was used; considering that Mtb proteins are naturally acidic they did not separate correctly and are all grouped in the left side of the gel.

In the next step we confirmed that our secreted proteins interact properly with the DiGE fluorescent dyes Cy3 and Cy5. We run a standard polyacrylamide-SDS gel with the marked samples to corroborate that dying was correct for both extractions. We were able to observe some differences in the secreted proteins, the already predicted absence of ESAT-6 or the increased presence of antigens from the Antigen 85 Complex (Antigen 85 A and Antigen 85 C) in the vaccine candidate strain, both contributing to the efficacy of MTBVAC (Figure 5).

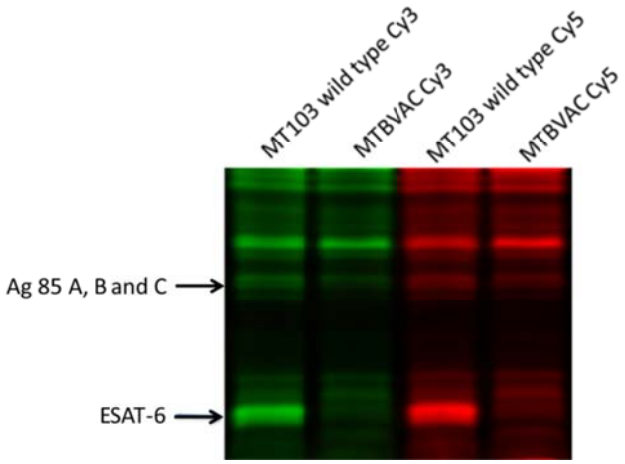

Figure 5. Regular SDS-PAGE with secreted proteins from MTBVAC vaccine candidate and its parental strain Mt103 marked with the fluorescent dyes Cy3 and Cy5. Note the absence of the band which putatively corresponds to ESAT-6 in MTBVAC. Differences in the bands corresponding to the Ag85 A, B and C are not as notable as in the western blot analysis.

After these tests we proceeded to carry out the 2-D DiGE technique, the secreted proteins from Mt103 were dyed with Cy3 (green) and the MTBVAC ones with Cy5 (red). This time, we used a strip with a pH range from 3 to 7 for IEF and proteins did separate properly across the entire gel (Figure 6). Below we can observe one representative gel to perform the technique. Red spots are proteins from MTBVAC strain, green spots are proteins from the Mt103 parental strain, while the yellow or orange spots are from proteins present in both strains (Figure 6). In the lower part of the gel we can observe a big exclusively green spot, considering the previous results obtained for Western Blot, we suggest that to correspond with ESAT-6 and ESAT-6-like proteins.

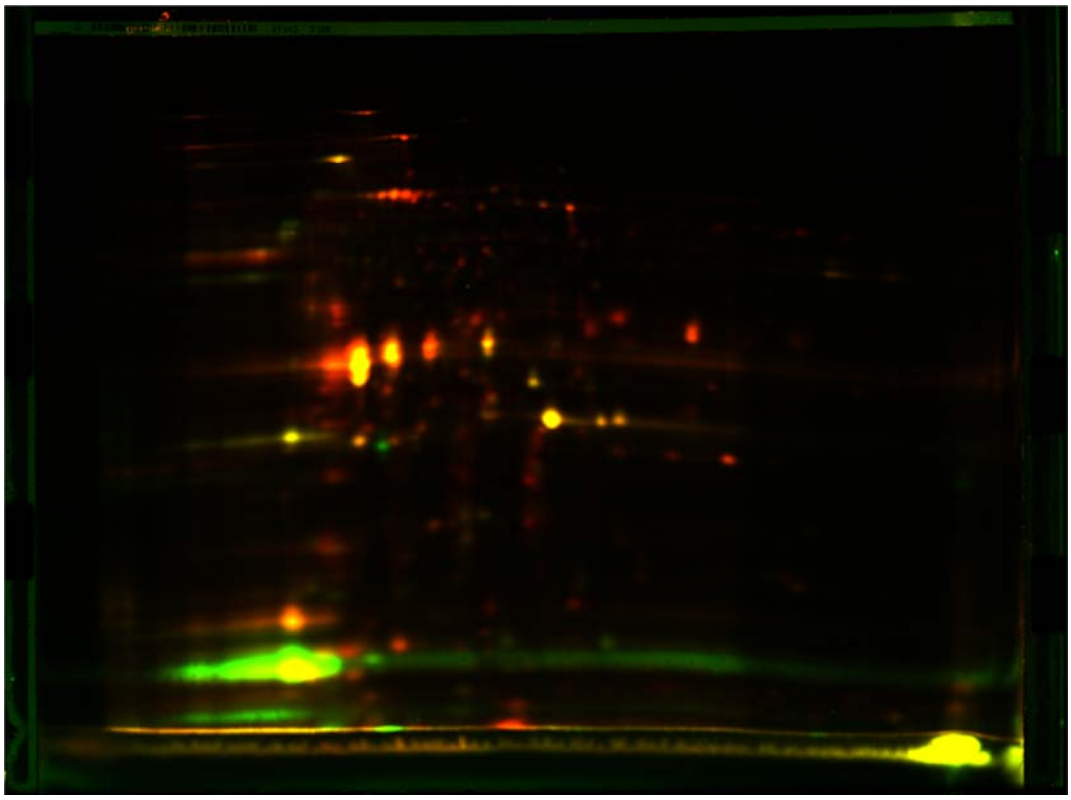

Figure 6. Mt103 (Cy3) versus MTBVAC (Cy5). The red spots are proteins from MTBVAC strain, the green spots are proteins from the Mt103 parental strain, and the yellow or orange spots are from proteins present in both strains.

After image analysis, spots were divided into two groups, major ones, those with higher density; and minor ones, those with lower intensity. The two groups were analyzed separately since it was necessary to use different exposition times in order to take the pictures for the subsequent image analysis; when long exposition times were used for detect the minor spots, the major protein spots appeared saturated and vice versa. Therefore short times of exposition were used to visualize major spots and long times of exposition for minor spots (Figure 7).

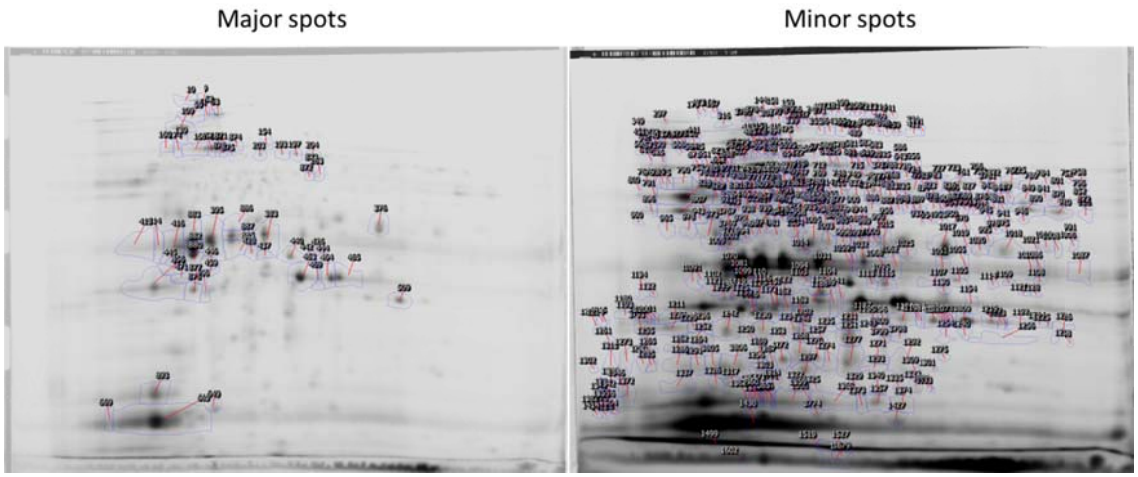

Figure 7. Different exposition times where used to obtain the images of the spots corresponding to secreted proteins. Short times of exposition allow us to obtain the image for major spots, while long times of exposition allow us to obtain the image for minor spots.

315 of them were selected to be picked and analyzed by MALDI-TOF mass spectrometry in order to identify the protein corresponding to each spot. The spots identified are listed in Figure 8 and Figure 9.

Mt103			
Rv	**gene**	**Product**	**Fold change**
Rv0350	*dnaK* or *hsp70*	HSP70, heat shock protein	1,78
Rv3310	*sapM*	Acid phosphatase	1,79
Rv1980c	*mpt64*	Mpt64, immunogenic protein	2,00
Rv3874	*esxB*	CFP10, culture filtrate antigen	7,92
Rv3874	*esxB*	CFP10, culture filtrate antigen	5,28
Rv1860	*apa* or *mpt32*	Apa, alanine and proline rich secreted protein	2,14
Rv1984c	*cfp21*	CFP21, probable cutinase precursor	2,65
Rv1910c		Probable exported protein. Predicted to be an outer membrane protein	2,06

Figure 8. The table lists the proteins identified by MALDI-TOF from the picked spots separated though DiGE technique that are more expressed in the parental strain Mt103 than in MTBVAC. Fold change expressed as the differential secretion between Mt103 and MTBVAC in $\log_2$.

MTBVAC			
Rv	**gene**	**Product**	**Fold change**
Rv1837c	*glcB*	GlcB, Malate synthaseG	1,89
Rv2220	*glnA1*	GlnA, glutamine synthetase	1,60
Rv0040c	*mtc28*	Mtc28, secreted proline rich protein	1,66
Rv1886c	*fbpB*	Ag85B, secreted antigen 85-B	1,46
Rv0315		Possible B-1,3-glucanase precursor	1,98
Rv2220	*glnA1*	GlnA, glutamine synthetase	2,18
Rv3248c	*sahH*	SahH, possible adenosylhomocysteinase	2,12
Rv1093	*glyA1*	GlyA1, serine hydroxymethyl transferase	1,73
Rv0242c	*fabG4*	FabG4, probable 3-ketoacyl-acylcarrier protein reductase	2,68
Rv0331		Possible dehydrogenase/reductase	2,09
Rv3587c		Probable conserved membrane protein	2,21
Rv2889c	*tsf*	Tsf, probable elongation factor	1,62
Rv0040c	*mtc28*	Mtc28, secreted proline rich protein	2,59
Rv0040c	*mtc28*	Mtc28, secreted proline rich protein	1,80
Rv2145c	*ag84* or *wag31*	Wag31, correspond to antigen 84 of *M. tuberculosis*	1,54
Rv0040c	*mtc28*	Mtc28, secreted proline rich protein	1,49

Figure 9. The table lists the proteins identified by MALDI-TOF from the picked spots separated though DiGE technique that are more expressed in the vaccine candidate strain MTBVAC than in Mt103. Fold change expressed as the differential secretion between Mt103 and MTBVAC in $\log_2$.

There are some proteins repeated on the list from different spots in the gels, they might correspond to different isoforms of the same protein which have been separated into different spots.

Once obtained the protein datasets, we proceeded to perform a cross identification with various proteins lists obtained from Comas *et al.* 2010 [44], Copin *et al*. 2014 [45] and Solans *et al.* 2014 [3]. From the Comas *et al*. and Copin *et al*., lists of human T cell

epitopes of Mtb and antigens absent or with epitope sequence variants in BCG were respectively obtained. Few proteins were in common with both MTBVAC and Mt103 protein lists. It is remarkable the presence of Rv1886c/*fbpB* for MTBVAC with both lists, it codifies for the Antigen 85 B, involved in bacterial attachment to the host; it is an immunodominant antigen and a TAT substrate. Also the Rv3874/*esxB* was in common for Mt103 with both lists, it codifies for the culture filtrate antigen EsxB or CFP10, an ESAT-6-like protein part of the region of difference 1 (RD1), it is involved in the phagosomal escape and secreted through the PhoP-dependent ESX system.

Since Ag85B is a common antigen between all lists and MTBVAC and Ag85B is also a TAT secretion system substrate, we decided to elaborate a list of TAT substrates from an "In-depth proteomic analysis of the secretome of H37Rv wild type, *phoP* mutant and the complemented strains" from Solans *et al.* [3]. To elaborate the list of TAT substrates we considered those proteins with an expression ratio higher than 2 for the *phoP* mutant compared to the wild type and those with an expression ratio lower that 0.5 for the wild type and complemented strain compared with the *phoP* mutant; that is, proteins that are more secreted in the *phoP* mutant than in the wild type or the complemented strain. The cross identification with these lists turn out in a list of 10 common proteins with MTBVAC (Figure 10), ergo only 2 of the 12 spots identify as secreted proteins for MTBVAC in our DIGE experiment are not secreted by the TAT secretion system.

MTBVAC Tat substrates

Rv	gene	Product	Fold change Δ*phoP* vs. WT	Fold change ::*phoP* vs. Δ*phoP*
Rv1837c	*glcB*	GlcB, Malate synthaseG		-0,0774367
Rv2220	*glnA1*	GlnA, glutamine synthetase		0,490262
Rv0040c	*mtc28*	Mtc28, secreted proline rich protein	2,09185	-1,73908
Rv1886c	*fbpB*	Ag85B, secreted antigen 85-B		-1,33865
Rv0315		Possible β-1,3-glucanase precursor		-1,72628
Rv2220	*glnA1*	GlnA, glutamine synthetase		0,490262
Rv1093	*glyA1*	GlyA1, serine hydroxymethyl transferase		-0,428682
Rv0242c	*fabG4*	FabG4, probable 3-ketoacyl-acylcarrier protein reductase	2,33825	-0,456365
Rv0331		Possible dehydrogenase/reductase		-0,0167455
Rv3587c		Probable conserved membrane protein		-1,32829
Rv2889c	*tsf*	Tsf, probable elongation factor	3,06431	-0,802663
Rv0040c	*mtc28*	Mtc28, secreted proline rich protein	2,09185	-1,73908
Rv0040c	*mtc28*	Mtc28, secreted proline rich protein	2,09185	-1,73908
Rv0040c	*mtc28*	Mtc28, secreted proline rich protein	2,09185	-1,73908

Figure 10. The table lists the MTBVAC proteins identified by MALDI-TOF from the picked spots separated though DiGE technique that are TAT substrates. From proteins from Solans *et al.*, proteins with a secreted ratio Δ*phoP* vs. WT higher than 2 and/or a secreted ratio of the *phoP* complemented strain (::*phoP*) vs. Δ*phoP* lower than 0.5 were considered; all those are more secreted on the *phoP* mutant strain than in the parental strain one. . Fold change expressed as the differential secretion between H37Rv (WT), H37RvΔ*phoP* (Δ*phoP*) and H37RvΔ*phoP-phoP* complemented (::*phoP*) in $\log_2$.

It is remarkable the absence of ESAT-6, part of the RD1, in the obtained protein lists. Nevertheless we did verify its presence in the protein samples through the western blot analysis. Although, in the image obtained of the DiGE gel (Figure 6), we can observe in the down-left part of the gel a big green spot that might correspond to the ESAT-6 and ESAT-6-like proteins. These proteins are exported through the ESX secretion system which is PhoP-dependent, therefore they are absent in MTBVAC and consequently we visualize them in green. On the other hand, the CFP-10 protein, which is part of the ESX system and is secreted together with ESAT-6, was identified from the picked spots of the gel. It presence corroborates our assumption.

1.2. Analysis of the mycobacterial cell envelope lipid composition.

One of the aims of this chapter was to characterize the intracellular trafficking of the vaccine candidate MTBVAC. The vaccine candidate is the product of two independent and non-reversible deletions in *phoP* and *fadD26* genes. In addition to characterize the MTBVAC trafficking, we also wanted to study the individual contribution of these mutations to the vaccine trafficking since, as it has been previously described, some Mtb single mutants present defects in phagosome maturation arrest and in their intracellular trafficking [29, 30].

To carry out the trafficking characterization, we designed the experiments using GFP-fluorescent strains. An integrative plasmid with the *gfp* gene under the control of a strong promoter was introduced by electroporation in each strain.

On the other hand it has been described the spontaneous loss of the lipid PDIM during *in vitro* subculturing [37]. The "spontaneous" loss of PDIM is probably an energy saving process since the biosynthesis and transport of this lipid have a high energetic cost due to the high size and abundance of this compound. Consequently, mutants that are no longer synthesizing PDIM have a competitive growth advantage within a heterogeneous population. This study was performed in H37Rv laboratory reference strain, but the loss of PDIM has also been noted for the clinical isolate Mt103 [46].

To perform our study with Mt103 and its derivative strains, the first step was to characterize the lipid profile of the strains in order to verify that PDIM were not spontaneously lost. Cultures of the wild type strain Mt103, the single mutants Mt103Δ*phoP* and Mt103Δ*fadD26* and the double mutant MTBVAC vaccine candidate were incubated with ^{14}C-propionate. ^{14}C-propionate integrates in the lipid synthesis pathway of the mycobacteria because it is the precursor of the malonyl-CoA molecule and it is integrated in the methyl-branched fatty acids which will form part of the cell wall complex lipids; thus mycobacterial lipids are radio labeled. We extracted lipids from liquid cultures and analyzed them by thin layer chromatography (TLC) using

different combinations of solvents to separate the different types of lipids. Besides the presence of PDIM in *phoP* mutants (or its absence in *fadD26* mutants), we also wanted to observe the absence of SL and DAT and PAT.

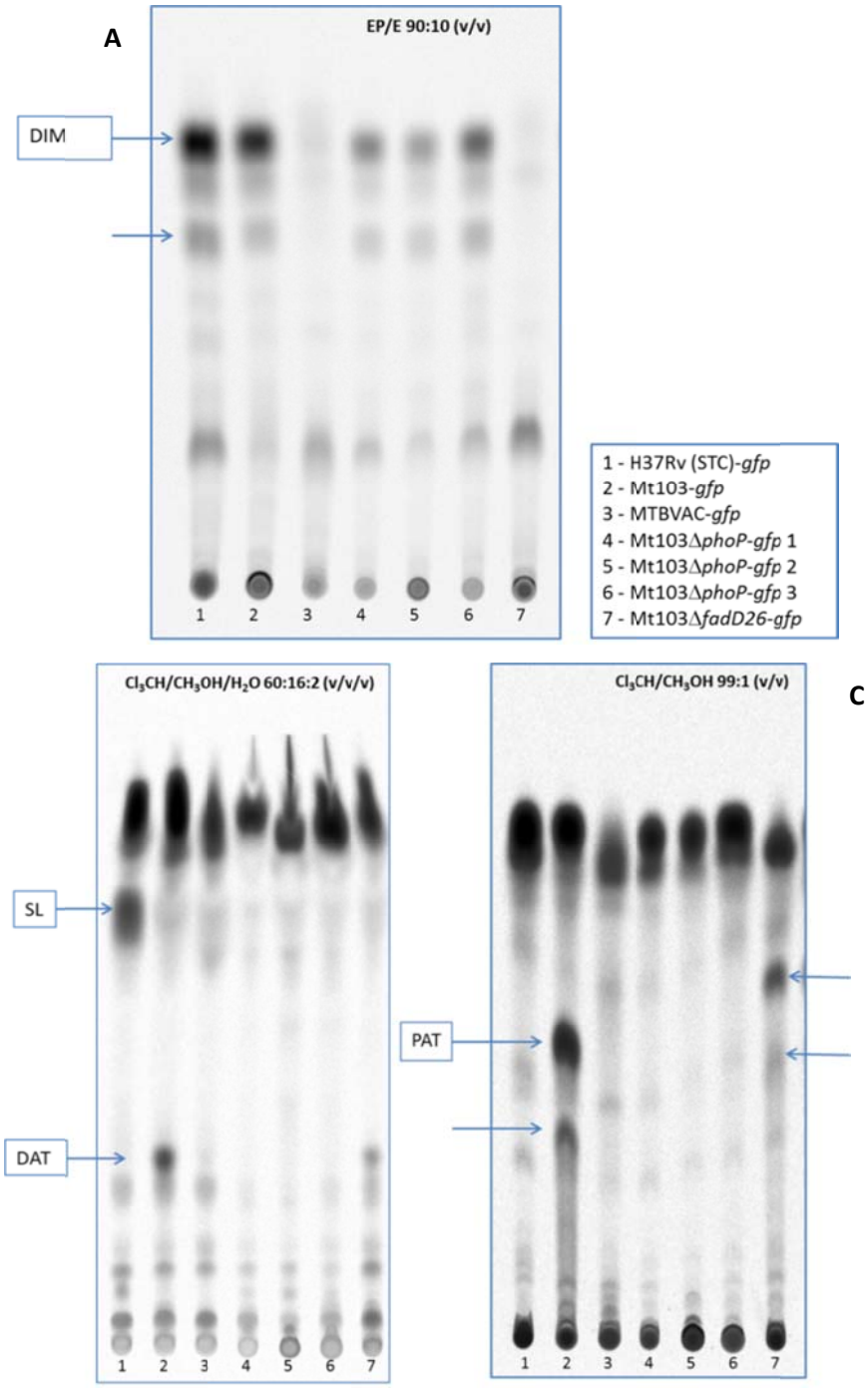

Figure 11. TLC of Mt103, MTBVAC and *phoP* and *fadD26* single mutants. In all cases, sample 1 H37Rv (STC) is a positive control which has been previously analyzed for the presence of PDIM and SL. **A.** Presence of PDIM was verified in samples 1, 2 and 4-6; the absence of PDIM in samples 3 and 7 is natural since these are *fadD26* mutant. **B.** The absence of SL was verified for in Mt103 strains and

mutants (lanes 2-7), since the wild type strain is naturally defective in SL synthesis. Presence of DAT is only observed in the strains were the *phoP* gene has not been deleted, lanes 2 and 7. **C.** Presence of PAT is only observed in the strains were the *phoP* gene has not been deleted, lanes 2 and 7.

For the present study we used the strain H37Rv (STR)-*gfp*, which is known to be devoid of DAT/PAT, as positive control for PDIM presence. On the other hand we previously know that the clinical isolate Mt103 is naturally defective in SL synthesis, thus neither the wild type strain nor its mutants synthesize SL molecule. For Mt103Δ*phoP-gfp* strain we analyzed three different clones.

TLC results confirm the presence of PDIM in the wild type strain Mt103-*gfp* and in the three Mt103Δ*phoP-gfp* selected clones; the absence of PDIM was confirmed in the *fadD26*$^{-}$ strains, MTBVAC-*gfp* and Mt103Δ*fadD26-gfp* as it was expected. SL absence in Mt103 and its mutants was confirmed in all cases. And finally DAT and PAT presence was confirmed for Mt103-*gfp* and Mt103Δ*fadD26-gfp*; *phoP*$^{-}$ strains are not able to synthesize these lipids as it has been previously described [7], it can be observed for the Mt103Δ*phoP-gfp* selected clones and for the vaccine candidate MTBVAC (Figure 11).

1.3. Determination of the individual contribution of the single *phoP* and *fadD26* gene deletions to the intracellular trafficking of the vaccine candidate.

Once inside the organism, Mtb reaches the alveolar macrophages that phagocyte the bacterium in order to contain the infection. Mycobacteria-containing phagosomes will evolve to a more hostile environment whose final aim is to harm and kill intracellular bacteria. Mtb has developed strategies to arrest the phagosomal maturation and to be able to replicate inside the macrophages so it can survive [10].

The vaccine candidate SO2 strain is a *phoP* insertion mutant in a Mtb clinical isolate, Mt103 [47]. Despite the promising results in preclinical studies [31, 33, 48], SO2 does not fulfill the establishment of the Geneva consensus for new live mycobacterial vaccines [34, 35]. Therefore it was necessary to construction of a new strain based on the prototype SO2. The novel vaccine candidate MTBVAC was constructed by genetically engineer two stable, unmarked deletions in *phoP* and *fadD26* genes in the SO2 strain [40].

Defective arrest of the phagosomal maturation was previously observed for SO2 [32, 49]. MTBVAC, even though is based on SO2, is a new strain with an additional mutation which alters its lipid profile and hence its intracellular trafficking. Consequently, we wanted to characterize the intracellular trafficking of the new vaccine candidate in two different cellular models, the murine alveolar macrophage (MHS) cell line and primary human macrophages (hMDM). Additionally we wanted to study the individual contribution of each mutation in the trafficking of MTBVAC using *phoP* and *fadD26* single mutants.

1.3.1. Colocalization studies at early phagosomal maturation stage in MHS mouse macrophages cell line.

We decided to analyze the trafficking of the vaccine candidate MTBVAC, its parental strain Mt103 and the single mutants Mt103Δ*phoP* and Mt103Δ*fadD26*; we also

included in the study the present vaccine BCG Pasteur and a PDIM$^-$ BCG Pasteur strain [18] in order to compare the effect of the absence of PDIM in both strains. All these strains carried a GFP expression plasmid. We chose a murine cell line of alveolar macrophages (MHS) for the study, which were infected with the strains mentioned below and processed after 48 hours of infection.

The infection was performed over cover glasses in order to analyze results with the confocal microscope. Before fixing the cells, we incubated them with the acidotropic probe Lysotracker, which will dye in red those compartments with a pH lower than 6. After that, the cell nuclei were dyed in blue with the nucleic acid stain Hoechst. Since the bacterial strains were GFP positive, we were able to observe them in green through the microscope. When the bacteria is in an acidified compartment, hence the maturation has not been arrested, we will observe it in orange/yellow due to the superposition of both colors, green for the bacteria and red for the Lysotracker acid compartments.

The quantification of the colocalization of bacteria with acidic compartments was performed by counting a representative number of total bacteria in different fields of each cover glasses. We determined the % of colocalization with Lysotracker by dividing the number of bacteria colocalizing by the number of total bacteria counted.

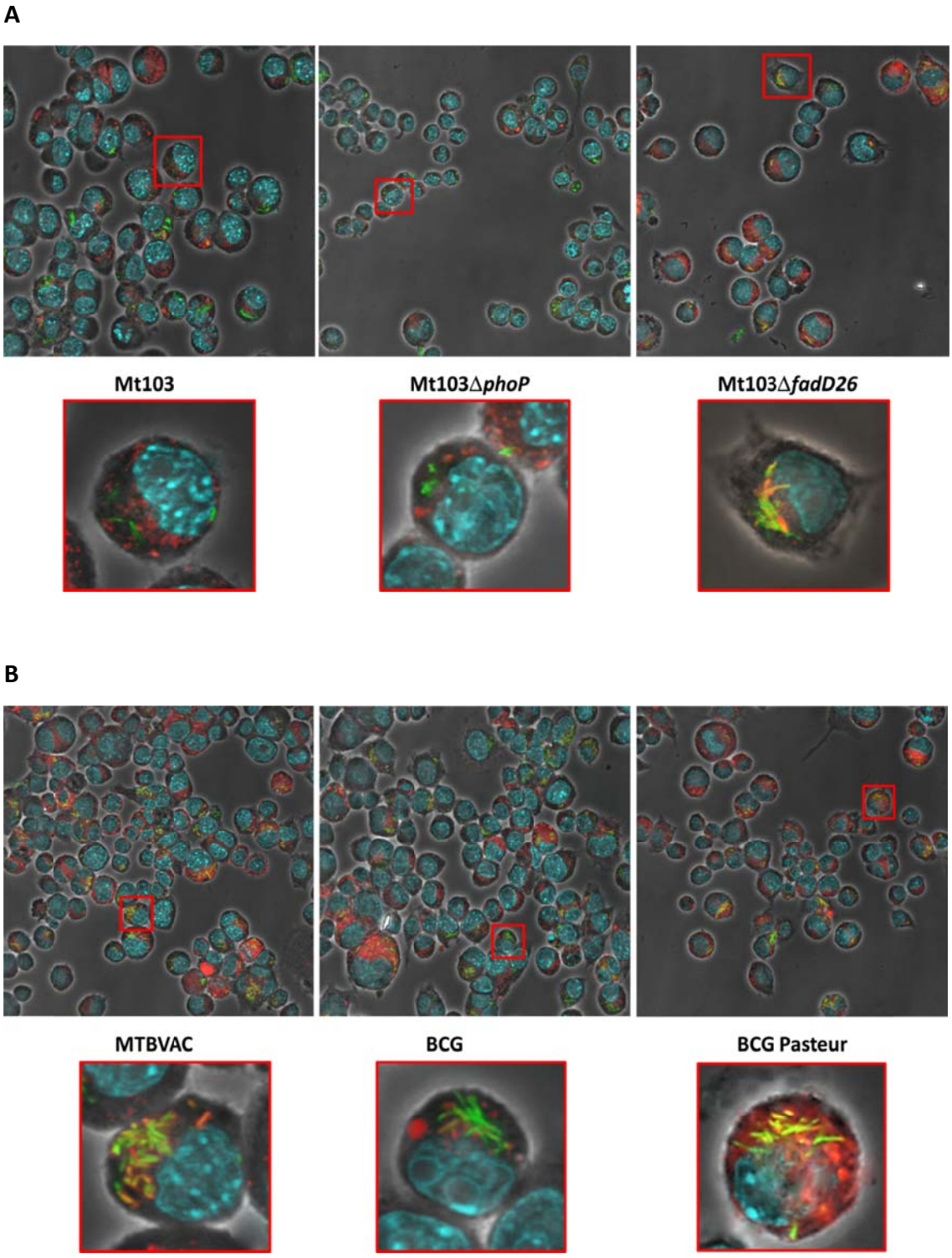

Figure 12. Confocal images obtained from the infection of MHS cells with the corresponding GFP^+ strains. The image is a merge between four different images, green fluorescence (bacteria), blue fluorescence (nucleus), red fluorescence (acidic compartments) and phase contrast (cells contour). **A.** When a bacterium is not located inside an acidified compartment we can visualize it as a green bacillus, e.g. in the Mt103 expanded image. **B.** A bacterium located in an acidified compartment (red) is

visualized with both green and red fluorescence filter, and so, in the merged image we will see it in yellow/orange, e.g. in the MTBVAC expanded image.

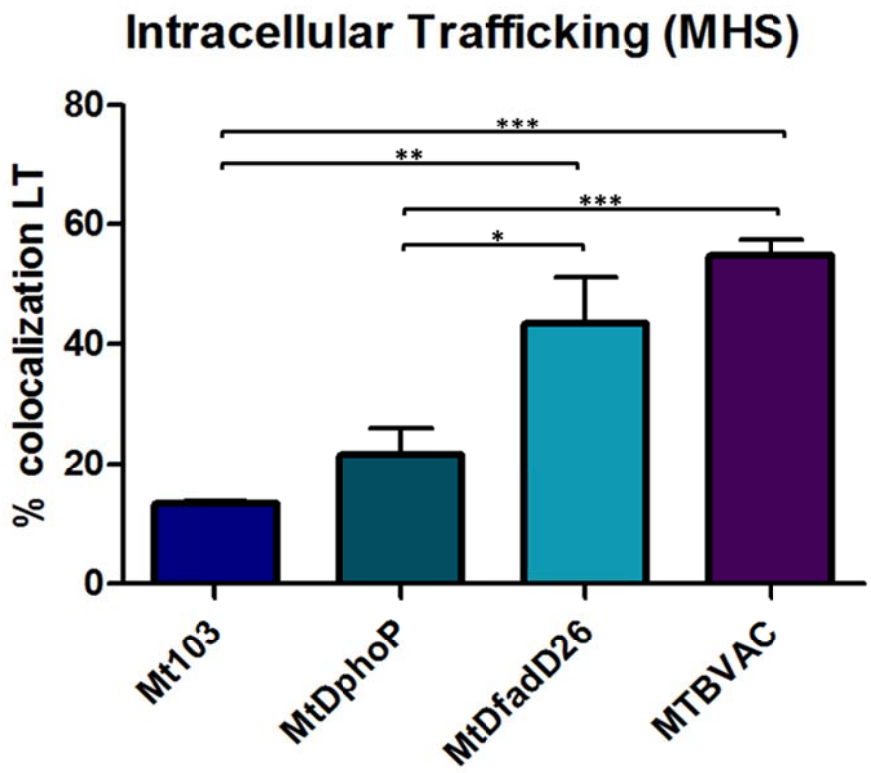

Figure 13. Percentage of colocalization of the GFP^{+} strains with Lysotracker in MHS. Higher percentage of colocalization means the bacteria are residing in acidified compartments, and thus they are not able to arrest phagosomal maturation. MTBVAC presents much higher colocalization percentages with Lysotracker than its parental strain Mt103. Mt103Δ*fadD26* single mutant present a phenotype very similar to MTBVAC. Mt103Δ*phoP* presents low colocalization percentages, similar to the parental strain. (*p<0.005, **p<0.001, ***p<0.0001).

The vaccine candidate MTBVAC presents the highest percentage of colocalization with Lysotracker compared with the rest of the strains of the study. As it was expected, the parental strain Mt103 shows poor colocalization with compartments marked with Lysotracker. Concerning the single mutants, the *phoP* mutant shows poor colocalization with Lysotracker, presenting a phenotype more similar to the parental strain; meanwhile the *fadD26* mutant shows higher colocalization with compartments marked with Lysotracker, more likely the vaccine candidate MTBVAC phenotype (Figure 13).

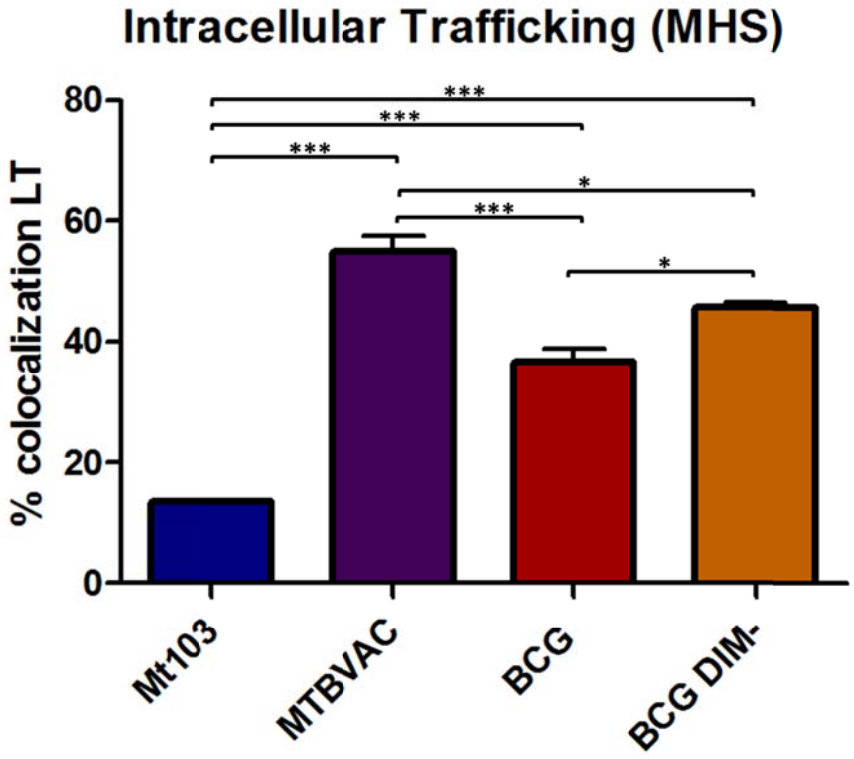

Figure 14. Percentage of colocalization of the GFP^{+} strains with Lysotracker in MHS. Higher percentage of colocalization means the bacteria are residing in acidified compartments, and thus they are not able to arrest phagosomal maturation. BCG presents an intermediate colocalization percentage between MBTVAC and Mt103. The colocalization for the strain of BCG without PDIM is higher than the registered for BCG but still slightly lower then the MTBVAC one. (*p<0.005, **p<0.001, ***p<0.0001).

Comparing the vaccine candidate MTBVAC with the current vaccine BCG, there is a significant difference in the Lysotracker colocalization. The BCG Pasteur DIM^{-} strain [18] colocalizes more frequently with Lysotracker than the parental BCG strain, but still its colocalization is lower than the one presented by MTBVAC stain. BCG besides being a *phoP* mutant has many other deficiencies compared with a wild-type strain, so the absence of PDIM does not have to have the same effects for Mt103 strain than for BCG (Figure 14).

1.3.2. Colocalization studies at different phagosomal maturation stages in primary human macrophages (hMDM).

After having performed the trafficking study in a mouse cell line, we decided to move to a more physiological model and to carry out the infections on human macrophages derived from monocytes (hMDM) obtained from peripheral blood. The bacterial strains used for the infections were the double mutant and vaccine candidate MTBVAC, its parental strain Mt103 and the single mutants Mt103Δ*phoP* and Mt103Δ*fadD26*.

We decided to broaden the tracking of the intracellular pathway to more mature stages of the phagosomal maturation. In order to do this, three markers of different phases of maturation of the phagosome were selected. Lysotracker, LAMP-1 is a lysosome-associated membrane protein and CD63 is also a membrane glycoprotein characteristic of the phagolysosome.

The infections were performed following the same protocol as in the previous assays with MHS cell line.

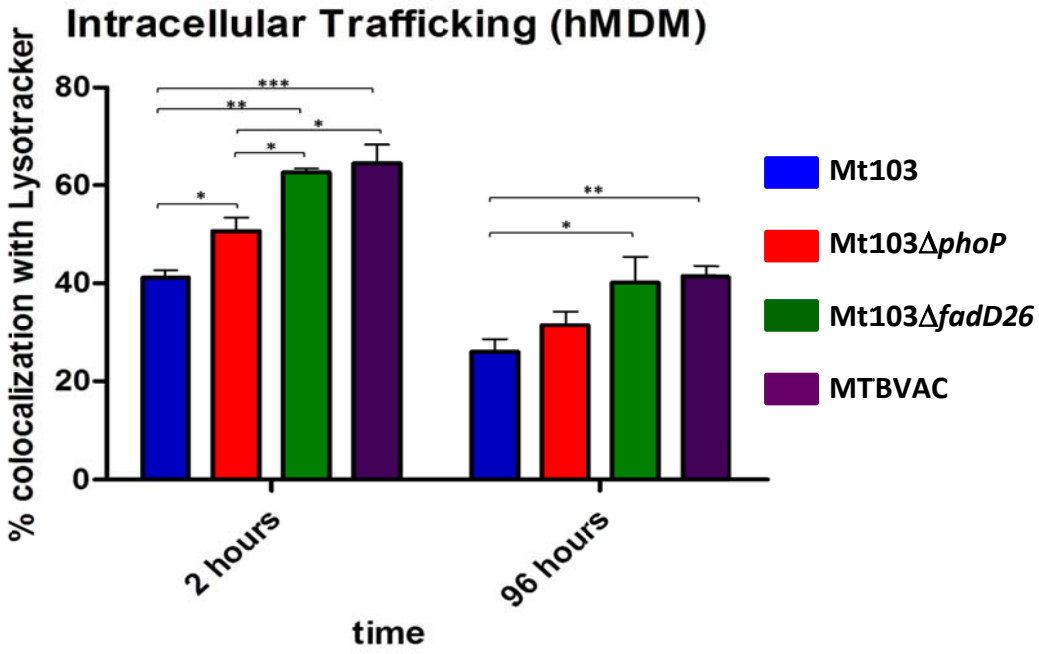

Figure 15. Colocalization percentages of the four GFP^{+} strains with Lysotracker in hMDM. Colocalization means the bacteria are residing in acidified compartments, where maturation has not been arrested.

MTBVAC and the single mutant Mt103Δ*fadD26* present the highest colocalization percentages compared with the parental strain Mt103 and the single mutant Mt103Δ*phoP*. (*p<0.005, **p<0.001, ***p<0.0001).

At two hours post-infection the vaccine candidate MTBVAC presents the highest percentage of colocalization with Lysotracker compared with the rest of the strains of the study. As it was expected the parental strain Mt103 shows significantly less colocalization with compartments marked with Lysotracker. Concerning the single mutants, the *phoP* mutant shows poor colocalization with Lysotracker, presenting a phenotype more similar to the parental strain; meanwhile the *fadD26* mutant shows higher colocalization with compartments marked with Lysotracker, more likely the vaccine candidate MTBVAC phenotype (Figure 15). Differences are less marked after 96 hours post-infection. Results obtained for Lysotracker in hMDM are comparable with those obtained with MHS cell line for the same marker.

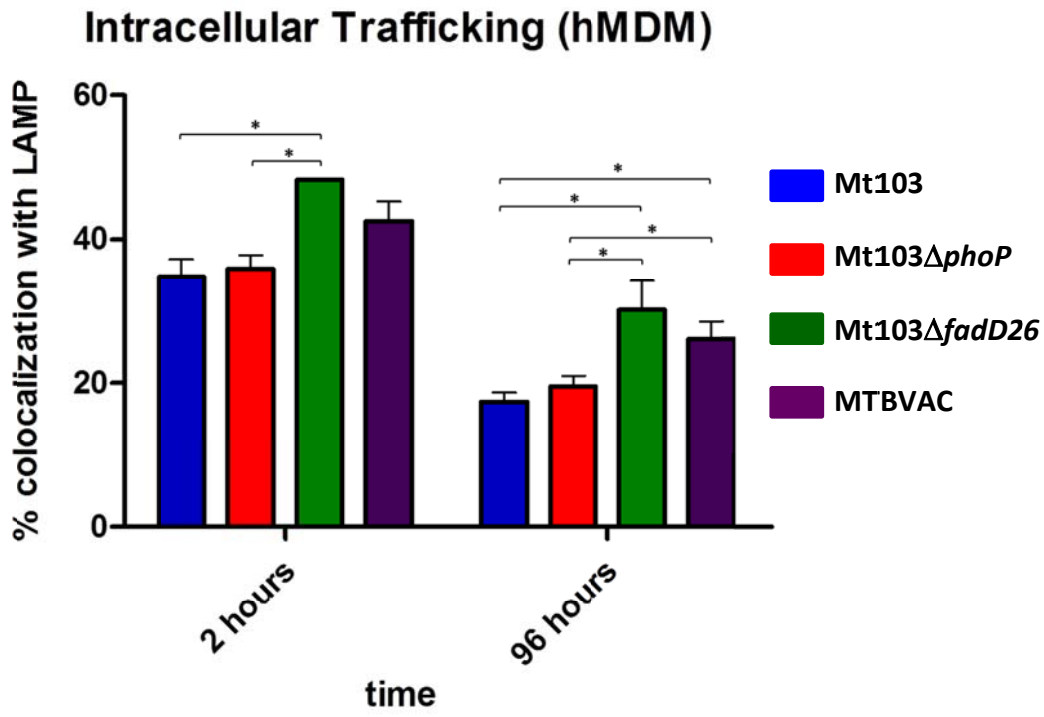

Figure 16. Colocalization percentages of the four GFP$^+$ strains with late endosomal marker, LAMP-1 in hMDM. Colocalization means the bacteria are residing in compartments where maturation has not been arrested. MTBVAC and the single mutant Mt103Δ*fadD26* present higher colocalization percentages compared with the parental strain Mt103 and the single mutant Mt103Δ*phoP*. (*p<0.005, **p<0.001, ***p<0.0001).

For both time points 2 and 96 hours post-infection the vaccine candidate MTBVAC and the single mutant Mt103D*fadD26* show more colocalization with the late endosomal marker LAMP-1 than the parental strain Mt103 and the *phoP* single mutant but differences are not as significant as the ones for the early endosome marker Lysotracker (Figure 16).

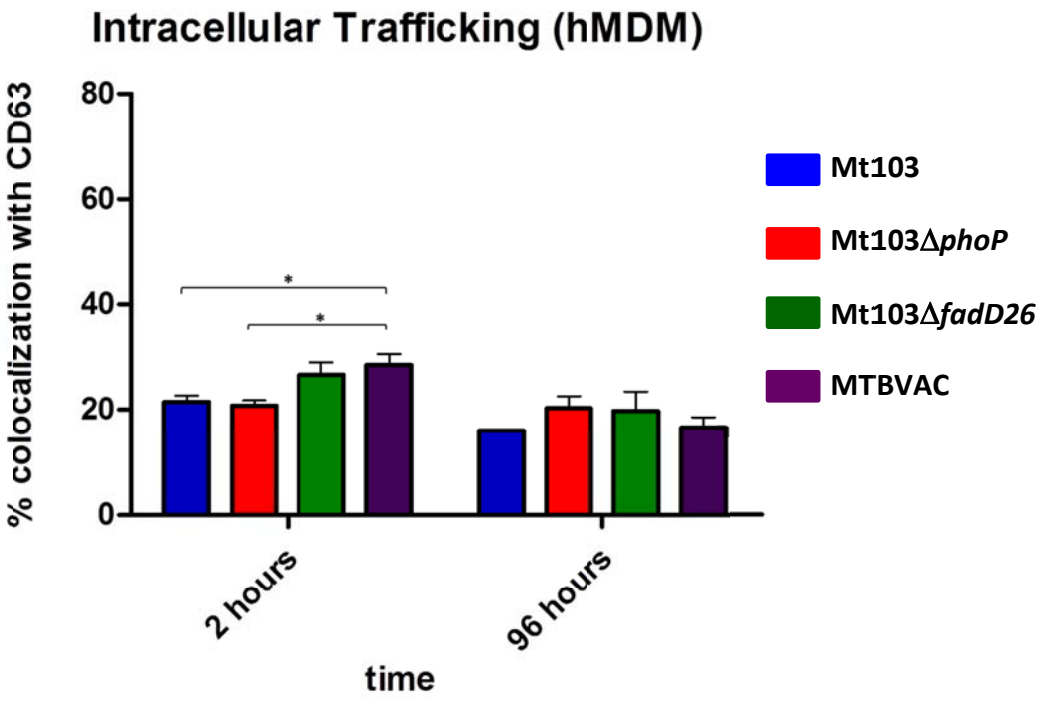

Figure 17. Colocalization percentages of the four GFP$^+$ strains with the phagolysosomal marker, CD63 in hMDM. Colocalization means the bacteria are residing in compartments where maturation has not been arrested. MTBVAC and the single mutant Mt103Δ*fadD26* present slightly higher colocalization percentages compared with the parental strain Mt103 and the single mutant Mt103Δ*phoP* at 2 hours post-infection. (*p<0.005, **p<0.001, ***p<0.0001).

Lower percentages of colocalization are observed for the phagolysosome marker CD63 for all the strains of study compared with early maturation markers. At 2 hours post-infection, the colocalization of the vaccine candidate MTBVAC and the single mutant Mt103Δ*fadD26* are slightly higher than the colocalization registered for the parental strain Mt103 and its *phoP* mutant. However at 96 hours post-infection, non-significantly differences in colocalization are observed. These results suggest that the attenuated strains, the single mutants and the vaccine candidate, arrest the

phagosome maturation at some intermediate stage before the formation of the phagolysosome (Figure 17).

For vaccine candidate MTBVAC infection, we observed more percentage of colocalization with Lysotracker and LAMP-1 markers which mean that phagosomal maturation is able to progress to more advanced stages. However, the lower colocalization percentage with the phagolysosome marker CD63 points that MTBVAC is still able to arrest the phagosomal maturation at some intermediate stage.

DISCUSSION

The aim of this chapter was to perform a finest characterization of MTBVAC vaccine candidate in some aspects that had not been studied before, like the secretome analysis compared with the parental strain or the study of the intracellular trafficking.

We studied the comparative secretome of MTBVAC vaccine candidate and its parentl strain Mt103 though Western-Blot and DiGE techniques. Finally we obtained a list of proteins identified. The list is quite small compared with the high number of spots that were marked and picked. There were a high number of unidentified spots, this could be due to the detection limit of the technique used, as a result of the fact that it could be a low concentration of protein in some spots.

The list obtained was divided in two, the proteins that were more expressed in MTBVAC and the ones which expression was higher in the parental strain Mt103. Both lists were compared with different antigen lists as the Epitope list that compiles all the human T cell epitopes of Mtb eliciting a positive immune response in humans reported in the literature from the work of Comas *et al.* 2010 [44]; or the classification of Mtb T cell antigens absent from BCG strains and the classification of Mtb proteins with epitope sequence variants in BCG strains obtained from the work of Copin *et al.* 2014 [45].

The Rv1886c/*fbpB* gene, encodes for the Ag85B, part of the Antigen 85 complex (Ag85A-C), it is mainly expressed in MTBVAC strain and it was common with the two protein lists compared. These proteins are TAT secretory system substrates and based on the work of Solans *et al.* 2014, their secretion is indirectly and negative regulated by PhoP through the ncRNA *mcr7* thus in a PhoP mutant as MTBVAC, secretion of TAT substrates like Ag85B is upregulated [3]. From the work of Solans *et al.* we obtained a list of TAT substrates [3]. The cross identification turn out in a list of 10 common proteins with MTBVAC, ergo only 2 of the 12 spots identified as secreted proteins for MTBVAC in our DIGE experiment are not secreted by the TAT secretion system,

demonstrating therefore the importance of TAT substrates in the secretome of the vaccine candidate strain.

Some of the TAT secreted proteins are involved in the interaction with the host cell wall, like the Rv0315 which possible encodes for a β-1,3-glucanase-precursor that could have lytic activity against cell walls [50]. Also the Ag85B, part of the Ag85 complex (Ag85A-C) which is a family of proteins all with enzymatic mycolyl-transferase activity involved in the generation of trehalose dimycolates (TDM) or cord factor, an envelope lipid essential in Mtb virulence; these proteins are also known for their capacity to bind to the extracellular matrix proteins fibronectin and elastin, and to induce strong Th1-type immune responses. Members of the Ag85 complex are immunodominant mycobacterial antigens and because of their role in cell wall integrity and synthesis of the cord factor, they have long been considered as virulence factors [51-53]. Components of the antigen 85 complex, Ag85A and Ag85B mainly, are largely used in development of new vaccine candidates as subunits protein transported in viral vectors with the objective of increase and improve the immunological response of BCG as vaccine [54].

Through the DiGE analysis only the Ag85B was identified, but in the previous western-blot analysis with the same culture filtrate we were able to verify the more abundant presence of the three Ag85A, Ag85B and Ag85C in MTBVAC strain compared to the parental strain Mt103. This upregulation of the Ag85 complex in the attenuated vaccine candidate MTBVAC is a highlight since it is going be really helpful in order to generate a better immunological response to Mtb infection itself without the need of introduce any external vector as boosting strategy.

On the other hand, from the Mt103 identified proteins it is remarkable the Rv3874/*esxB* gene, coding for the Culture filtrate antigen CFP10. This protein is encoded in the region of difference 1 (RD1), which contains part of the genes encoding the ESX-1 secretion system structural components and substrates, like the early secretion antigenic target ESAT-6. Both ESAT-6 and CFP-10 proteins are co-secreted

and are key virulence factors implicated in the phagovacuole escape of the mycobacteria in infected cells [4, 6, 55]. The secretion system ESX-1 is PhoP-regulated, and in consequence these proteins are more secreted in the parental strain Mt103. The ESAT6 protein was not identified in the DiGE, but it was identified through the western-blot techniques with the same culture filtrate and we can clearly visualize it in the DiGE image, a big green spot in the low molecular weight zone corresponding to a secretion due to Mt103 exclusively as we verify also with the western-blot.

The RD1 region is deleted or truncated in several attenuated strains, such as the actual vaccine *M. bovis* BCG. The absence of this region implies the attenuation of BCG with impaired cell-to-cell spread, apoptosis and autophagy induction, inflammasome activation or induction of type I interferon or CD8 T cell responses [56]. Additionally, ESAT-6 and CFP-10 contain a high percentage of the human T cell epitopes of Mtb [44]. The fact that MTBVAC does not secrete CFP-10 or ESAT-6, key virulence factors, is an advantage for its attenuation since it will not be able to escape from the phagosome [57], and consequently its trafficking will be also altered. However, even if MTBVAC does not secrete them, it does synthesize ESAT-6 and CFP-10 so they will accumulate inside the bacteria, and when it eventually reaches the lysosome MTBVAC will be degraded and the protein epitopes exposed to the immune system conferring an advantage since it will induce a proper immunological response.

Concerning the intracellular trafficking study, we decided to use fluorescent GFP^+ bacteria in order to simplify the post-infection treatment before the microscope analysis of the infected cells. Since the construction of GFP-expressing strains was necessary for the study, and considering the spontaneous loss of PDIM lipid that could occur during the electroporation process or the subculture process [37], we needed to analyze the lipid profile of the new GFP^+ strain in order to confirm the presence of PDIM. Once we assured that PDIM was still present in our GFP^+ derived strains, we could proceed to the trafficking study.

For both cellular models in which we performed the infection, MHS and hMDM, we can observe the marked differential phenotype between MTBVAC and Mt103 at early stages of maturation. The parental strain presents a low colocalization rate with Lysotracker, which means it resides in non-acidificated phagosomes; therefore it is arresting the phagosomal maturation. The vaccine candidate, as it was expected, presents high colocalization percentage with Lysotracker, it is not arresting the phagosomal maturation at this early stages and it remains in acidificated phagosomes.

More advanced stages of phagosomal maturation were only studied in hMDM. Mt103 presents low percentage of colocalization with late phagosomal and phagolysosomal markers, LAMP-1 and CD63 respectively; indicates that as being a fully virulent strain, Mt103 is arresting the maturation of the phagosome at early stages creating a favorable environment in which it could be able to persist and replicate. The vaccine candidate MTBVAC, as attenuated strain, is not able to arrest the phagosomal maturation at early stages, as we can observe through the colocalization with the late phagosomal marker LAMP-1; but the poor colocalization with the phagolysosome marker CD63 suggests it do arrest the maturation in some intermediate point during the maturation process, presenting a persistence phenotype.

Concerning to the single mutants, the Mt103Δ*phoP* strain presents a phenotype more similar to the Mt103 wild type, for both types of cells and all the different maturation markers, and so the bacteria is arresting the phagosomal maturation at an early stage. Nevertheless the Mt103Δ*fadD26* single mutant phenotype is remarkably alike to the MTBVAC one, for both type cells and all the different maturation markers; this strain is not able to arrest phagosomal maturation at early stages, but it do not colocalize with the phagolysosome marker CD63, suggesting indeed that the single mutant also arrest the maturation in some intermediate point before the phagolysosome stage presenting the same persistence phenotype as MTBVAC (Figure 18).

The *fadD26* gene product is an acyl-AMP ligase which is required for the biosynthesis of PDIM. Thus, an Mtb mutant in this gene is completely devoid of this family of lipids.

The phthiocerol dimycocerosates (PDIM) constitute potential candidates for modulating the initial step of entry into macrophages and for controlling the outcome of bacterial infection [18, 27]. Therefore considering the literature data and our results it is consistent a model where the absence of PDIM might make the bacteria more sensitive to the stresses generated by the phagosome.

The phenotypes of the single mutant strains suggest that the *phoP* contribution to intracellular trafficking is considerably lower than the *fadD26* contribution. However, taking into consideration previous studies carried out in the study of the virulence of these two single mutants [36], we propose a model in which both mutations have a synergistic effect contributing to the altered trafficking of MTBVAC.

Regarding the trafficking of BCG Pasteur, it was only analyzed for early stages of maturation and its colocalization with Lysotracker was significantly lower compared with MTBVAC. Its percentage of colocalization it is intermediate between the parental strain Mt103 and the vaccine candidate, meaning it is more able to stop phagosomal acidification than MTBVAC (Figure 18). The BCG strain lacking of PDIM shows a higher percentage of colocalization than BCG but lower than MTBVAC.

BCG was obtained through the long-term subculture of a virulent strain, during this process the bacteria got attenuated but it was not a controlled event. Genomic analyses have been carried out and several regions have been identified as deleted from BCG, resulting in the loss of more than 100 genes compared with Mtb [58]. Thus we cannot reach any conclusion here, because even observing an improvement in the BCG-PDIM^{-} colocalization with Lysotracker, BCG has so many genes deleted compared to an Mtb strain [45] that the analysis of the differences observed when PDIM is absent are much wider and not comparable with the mentioned for the Mt103 strain.

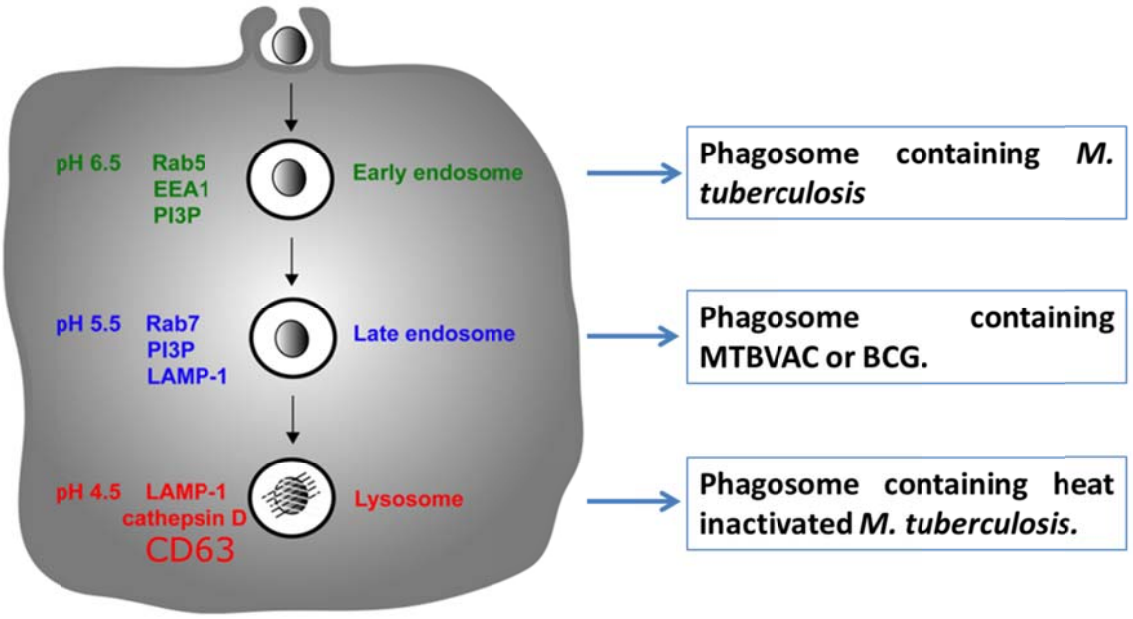

Figure 18. Intracellular trafficking schema. When the bacteria enter inside the macrophage a mechanism of fusion and fission events happen in a process called phagosomal maturation which finality is to degrade the intruder. A virulent strain of Mtb has the ability to arrest phagosomal maturation at early stages; an inactivated bacterium of Mtb will not arrest maturation, reaching the lysosome and being finally degrade and expose to the immune system; attenuated strains like BCG or MTBVAC, do not arrest the maturation at early stages but however, they do no reach the lysosome.

Besides the absence of more than 100 genes including the RD1, the original BCG strain was distributed to laboratories worldwide where its subculture continued, this event had led to the appearance of different variants of BCG vaccines, with different immunological properties. Comparison of the genome sequences has demonstrated that differences in immunogenicity are related to genomic diversity. An important consideration in the use of BCG-based vaccines is that five of the six immunodominant antigens of *M. bovis* are either deleted or downregulated in some or all BCG strains (ESAT-6, CFP10, Ag85, MPB64, MPB70 or MPB83) [45, 58].

Many of these immunodominant antigens are being used in the development new vaccines against TB through the BCG boosting strategies in which BCG is given at birth and then boosting is administered with antigens specific for Mtb. These subunit vaccines are based on one or a few Mtb-specific protein antigens using viral vector or

adjuvants as delivery system; these antigens include the mycolyltransferase Ag85A and Ag85B, ESAT-6 or the low molecular weight protein antigen 7 (10KDa) EsxH [59]. There is a dominance of vaccines that express containing Ag85 proteins, with six of the eight subunit vaccines in development containing an Ag85 protein (Ag85A or Ag85B) [54]: MVA85A employs MVA to deliver Ag85A, Ad5Ag85A is a recombinant human-type AdHu5 expressing Ag85A, Ad35/AERAS-402 uses human Ad35 to express a fusion protein of the three common antigens Ag85A, Ag85B and EsxH, Hybrid 1 (H1) is a recombinant fusion protein of Ag85B and ESAT-6, H56-IC31:H56 is another recombinant protein expressing Ag85B and ESAT-6 or Hyvac 4-IC31 is a recombinant fusion protein of Ag85B and TB10.4 [59]. All the mentioned vaccine candidates are currently in different stages of clinical trials.

In contrast MTBVAC, as we have described before in the secretome analysis, has improved secretion of important immunodominant antigens part of the Antigen 85 complex and it is deficient in secretion of ESX-1 substrates, like ESAT-6 or CFP-10 proteins which are key virulence factors, absent in BCG strains [4, 5, 57]. The lack of ESAT-6 secretion makes the strain unable to escape from the phagosome, so even if it is able to arrest the phagosomal maturation before reaching the phagolysosome, it will get trapped inside the macrophage and will be eventually degraded; its components, including ESAT-6 and CFP-10 epitopes which will accumulate inside the bacteria, will be exposed to the major histocompatibility complex in order to develop an immunological response to the infection [60].

The absence of the genetic decay in important genes that happens for BCG but do not occur for MTBVAC since it comes from a clinical isolate rationally attenuated; the improvement secretion of immunodominant antigens; the impaired trafficking, that finally permit its degradation and presentation to the immunological system point at the vaccine candidate MTBVAC as better option in generating the proper immunological response to face the infection with Mtb than BCG.

REFERENCES

1. Ligon, L.S., J.D. Hayden, and M. Braunstein, *The ins and outs of Mycobacterium tuberculosis protein export.* Tuberculosis (Edinb), 2012. **92**(2): p. 121-32.
2. Feltcher, M.E., J.T. Sullivan, and M. Braunstein, *Protein export systems of Mycobacterium tuberculosis: novel targets for drug development?* Future Microbiol, 2010. **5**(10): p. 1581-97.
3. Solans, L., et al., *The PhoP-dependent ncRNA Mcr7 modulates the TAT secretion system in Mycobacterium tuberculosis.* PLoS Pathog, 2014. **10**(5): p. e1004183.
4. Simeone, R., et al., *Cytosolic access of Mycobacterium tuberculosis: critical impact of phagosomal acidification control and demonstration of occurrence in vivo.* PLoS Pathog, 2015. **11**(2): p. e1004650.
5. Simeone, R., D. Bottai, and R. Brosch, *ESX/type VII secretion systems and their role in host-pathogen interaction.* Curr Opin Microbiol, 2009. **12**(1): p. 4-10.
6. Frigui, W., et al., *Control of M. tuberculosis ESAT-6 secretion and specific T cell recognition by PhoP.* PLoS Pathog, 2008. **4**(2): p. e33.
7. Gonzalo Asensio, J., et al., *The virulence-associated two-component PhoP-PhoR system controls the biosynthesis of polyketide-derived lipids in Mycobacterium tuberculosis.* J Biol Chem, 2006. **281**(3): p. 1313-6.
8. Killick, K.E., et al., *Receptor-mediated recognition of mycobacterial pathogens.* Cell Microbiol, 2013. **15**(9): p. 1484-95.
9. Ehrt, S. and D. Schnappinger, *Mycobacterial survival strategies in the phagosome: defence against host stresses.* Cell Microbiol, 2009. **11**(8): p. 1170-8.
10. Dey, B. and W.R. Bishai, *Crosstalk between Mycobacterium tuberculosis and the host cell.* Semin Immunol, 2014. **26**(6): p. 486-96.
11. Stanley, S.A. and J.S. Cox, *Host-pathogen interactions during Mycobacterium tuberculosis infections.* Curr Top Microbiol Immunol, 2013. **374**: p. 211-41.
12. Via, L.E., et al., *Arrest of mycobacterial phagosome maturation is caused by a block in vesicle fusion between stages controlled by rab5 and rab7.* J Biol Chem, 1997. **272**(20): p. 13326-31.
13. Koul, A., et al., *Interplay between mycobacteria and host signalling pathways.* Nat Rev Microbiol, 2004. **2**(3): p. 189-202.
14. Malik, Z.A., G.M. Denning, and D.J. Kusner, *Inhibition of Ca(2+) signaling by Mycobacterium tuberculosis is associated with reduced phagosome-lysosome fusion and increased survival within human macrophages.* J Exp Med, 2000. **191**(2): p. 287-302.
15. Vergne, I., et al., *Mechanism of phagolysosome biogenesis block by viable Mycobacterium tuberculosis.* Proc Natl Acad Sci U S A, 2005. **102**(11): p. 4033-8.
16. Flannagan, R.S., G. Cosio, and S. Grinstein, *Antimicrobial mechanisms of phagocytes and bacterial evasion strategies.* Nat Rev Microbiol, 2009. **7**(5): p. 355-66.
17. Passemar, C., et al., *Multiple deletions in the polyketide synthase gene repertoire of Mycobacterium tuberculosis reveal functional overlap of cell envelope lipids in host-pathogen interactions.* Cell Microbiol, 2014. **16**(2): p. 195-213.

18. Astarie-Dequeker, C., et al., *Phthiocerol dimycocerosates of M. tuberculosis participate in macrophage invasion by inducing changes in the organization of plasma membrane lipids.* PLoS Pathog, 2009. **5**(2): p. e1000289.
19. Goren, M.B., et al., *Prevention of phagosome-lysosome fusion in cultured macrophages by sulfatides of Mycobacterium tuberculosis.* Proc Natl Acad Sci U S A, 1976. **73**(7): p. 2510-4.
20. Brodin, P., et al., *High content phenotypic cell-based visual screen identifies Mycobacterium tuberculosis acyltrehalose-containing glycolipids involved in phagosome remodeling.* PLoS Pathog, 2010. **6**(9): p. e1001100.
21. Pabst, M.J., et al., *Inhibition of macrophage priming by sulfatide from Mycobacterium tuberculosis.* J Immunol, 1988. **140**(2): p. 634-40.
22. Zhang, L., et al., *Effect of Mycobacterium tuberculosis-derived sulfolipid I on human phagocytic cells.* Infect Immun, 1988. **56**(11): p. 2876-83.
23. Gilmore, S.A., et al., *Sulfolipid-1 biosynthesis restricts Mycobacterium tuberculosis growth in human macrophages.* ACS Chem Biol, 2012. **7**(5): p. 863-70.
24. Saavedra, R., et al., *Mycobacterial trehalose-containing glycolipid with immunomodulatory activity on human CD4+ and CD8+ T-cells.* Microbes Infect, 2006. **8**(2): p. 533-40.
25. Husseini, H. and S. Elberg, *Cellular reactions to phthienoic acid and related branch ed-chain acids.* Am Rev Tuberc, 1952. **65**(6): p. 655-72.
26. Saavedra, R., et al., *Mycobacterial di-O-acyl-trehalose inhibits mitogen- and antigen-induced proliferation of murine T cells in vitro.* Clin Diagn Lab Immunol, 2001. **8**(6): p. 1081-8.
27. Rousseau, C., et al., *Production of phthiocerol dimycocerosates protects Mycobacterium tuberculosis from the cidal activity of reactive nitrogen intermediates produced by macrophages and modulates the early immune response to infection.* Cell Microbiol, 2004. **6**(3): p. 277-87.
28. Chesne-Seck, M.L., et al., *A point mutation in the two-component regulator PhoP-PhoR accounts for the absence of polyketide-derived acyltrehaloses but not that of phthiocerol dimycocerosates in Mycobacterium tuberculosis H37Ra.* J Bacteriol, 2008. **190**(4): p. 1329-34.
29. Pethe, K., et al., *Isolation of Mycobacterium tuberculosis mutants defective in the arrest of phagosome maturation.* Proc Natl Acad Sci U S A, 2004. **101**(37): p. 13642-7.
30. Stewart, G.R., et al., *Mycobacterial mutants with defective control of phagosomal acidification.* PLoS Pathog, 2005. **1**(3): p. 269-78.
31. Martin, C., et al., *The live Mycobacterium tuberculosis phoP mutant strain is more attenuated than BCG and confers protective immunity against tuberculosis in mice and guinea pigs.* Vaccine, 2006. **24**(17): p. 3408-19.
32. Ferrer, N.L., et al., *Interactions of attenuated Mycobacterium tuberculosis phoP mutant with human macrophages.* PLoS One, 2010. **5**(9): p. e12978.
33. Cardona, P.J., et al., *Extended safety studies of the attenuated live tuberculosis vaccine SO2 based on phoP mutant.* Vaccine, 2009. **27**(18): p. 2499-505.
34. Kamath, A.T., et al., *New live mycobacterial vaccines: the Geneva consensus on essential steps towards clinical development.* Vaccine, 2005. **23**(29): p. 3753-61.

35. Walker, K.B., et al., *The second Geneva Consensus: Recommendations for novel live TB vaccines.* Vaccine, 2010. **28**(11): p. 2259-70.
36. Arbues, A., *Construction and characterization of a new generation of phoP-based vaccines agains tuberculosis.*, in *Microbiology, Preventive Medicine and Public Health Department*. 2010, University of Zaragoza.
37. Domenech, P. and M.B. Reed, *Rapid and spontaneous loss of phthiocerol dimycocerosate (PDIM) from Mycobacterium tuberculosis grown in vitro: implications for virulence studies.* Microbiology, 2009. **155**(Pt 11): p. 3532-43.
38. Infante, E., et al., *Immunogenicity and protective efficacy of the Mycobacterium tuberculosis fadD26 mutant.* Clin Exp Immunol, 2005. **141**(1): p. 21-8.
39. Camacho, L.R., et al., *Identification of a virulence gene cluster of Mycobacterium tuberculosis by signature-tagged transposon mutagenesis.* Mol Microbiol, 1999. **34**(2): p. 257-67.
40. Arbues, A., et al., *Construction, characterization and preclinical evaluation of MTBVAC, the first live-attenuated M. tuberculosis-based vaccine to enter clinical trials.* Vaccine, 2013. **31**(42): p. 4867-73.
41. Sonnenberg, M.G. and J.T. Belisle, *Definition of Mycobacterium tuberculosis culture filtrate proteins by two-dimensional polyacrylamide gel electrophoresis, N-terminal amino acid sequencing, and electrospray mass spectrometry.* Infect Immun, 1997. **65**(11): p. 4515-24.
42. Arruda, S.C., et al., *Two-dimensional difference gel electrophoresis applied for analytical proteomics: fundamentals and applications to the study of plant proteomics.* Analyst, 2011. **136**(20): p. 4119-26.
43. McNamara, L.E., et al., *Fluorescence two-dimensional difference gel electrophoresis for biomaterial applications.* J R Soc Interface, 2010. **7 Suppl 1**: p. S107-18.
44. Comas, I., et al., *Human T cell epitopes of Mycobacterium tuberculosis are evolutionarily hyperconserved.* Nat Genet, 2010. **42**(6): p. 498-503.
45. Copin, R., et al., *Impact of in vitro evolution on antigenic diversity of Mycobacterium bovis bacillus Calmette-Guerin (BCG).* Vaccine, 2014. **32**(45): p. 5998-6004.
46. Cardona, P.J., et al., *Neutral-red reaction is related to virulence and cell wall methyl-branched lipids in Mycobacterium tuberculosis.* Microbes Infect, 2006. **8**(1): p. 183-90.
47. Perez, E., et al., *An essential role for phoP in Mycobacterium tuberculosis virulence.* Mol Microbiol, 2001. **41**(1): p. 179-87.
48. Aguilar, D., et al., *Immunological responses and protective immunity against tuberculosis conferred by vaccination of Balb/C mice with the attenuated Mycobacterium tuberculosis (phoP) SO2 strain.* Clin Exp Immunol, 2007. **147**(2): p. 330-8.
49. Ferrer, N.L., et al., *Intracellular replication of attenuated Mycobacterium tuberculosis phoP mutant in the absence of host cell cytotoxicity.* Microbes Infect, 2009. **11**(1): p. 115-22.
50. Malen, H., et al., *Definition of novel cell envelope associated proteins in Triton X-114 extracts of Mycobacterium tuberculosis H37Rv.* BMC Microbiol, 2010. **10**: p. 132.

51. Daffe, M., *The mycobacterial antigens 85 complex - from structure to function and beyond.* Trends Microbiol, 2000. **8**(10): p. 438-40.
52. Kruh-Garcia, N.A., et al., *Antigen 85 variation across lineages of Mycobacterium tuberculosis-implications for vaccine and biomarker success.* J Proteomics, 2014. **97**: p. 141-50.
53. Huygen, K., *The Immunodominant T-Cell Epitopes of the Mycolyl-Transferases of the Antigen 85 Complex of M. tuberculosis.* Front Immunol, 2014. **5**: p. 321.
54. Fletcher, H.A. and L. Schrager, *TB vaccine development and the End TB Strategy: importance and current status.* Trans R Soc Trop Med Hyg, 2016. **110**(4): p. 212-8.
55. Tharad, M., et al., *A three-hybrid system to probe in vivo protein-protein interactions: application to the essential proteins of the RD1 complex of M. tuberculosis.* PLoS One, 2011. **6**(11): p. e27503.
56. Brosch, R., et al., *Genome plasticity of BCG and impact on vaccine efficacy.* Proc Natl Acad Sci U S A, 2007. **104**(13): p. 5596-601.
57. Simeone, R., et al., *Phagosomal rupture by Mycobacterium tuberculosis results in toxicity and host cell death.* PLoS Pathog, 2012. **8**(2): p. e1002507.
58. Asensio, J.A., et al., *Live tuberculosis vaccines based on phoP mutants: a step towards clinical trials.* Expert Opin Biol Ther, 2008. **8**(2): p. 201-11.
59. Marinova, D., et al., *Recent developments in tuberculosis vaccines.* Expert Rev Vaccines, 2013. **12**(12): p. 1431-48.
60. Coscolla, M., et al., *M. tuberculosis T Cell Epitope Analysis Reveals Paucity of Antigenic Variation and Identifies Rare Variable TB Antigens.* Cell Host Microbe, 2015. **18**(5): p. 538-48.

Chapter 2:
In-deep study of the PhoP regulon.

INTRODUCTION

Two-component systems (TCSs) are highly conserved prokaryotic signal-transduction pathways, consisting in a sensor histidine kinase (HK) and an effector response regulator (RR). The HK, often membrane-associated, is responsible for detection of extracellular stimuli. In response to signal sensing, the HK auto-phosphorylates itself and then transfers its phosphate to the RR, which alters its conformation and modulates gene expression, usually through DNA binding. Overall, this mechanism enables bacteria to detect and respond to a wide range of environmental stimuli [1]. Intracellular pathogens usually use TCSs to respond to host defenses being often essential for virulence.

Compared with environmental bacteria, *M. tuberculosis* (Mtb) possesses a few TCSs, 11 operons among the genome [1]; this relatively small number of TCSs might reflect the adaptation of Mtb to the intracellular lifestyle. One of the most widely studied TCS is PhoPR virulence system [2]. To study the essential role of PhoPR in Mtb virulence, a *phoP* mutant was constructed in the clinical isolate Mt103, it was unable to replicate in mouse bone marrow-derived macrophages and showed marked attenuation in intravenously inoculated BALB/c mice [3]. It was also observed altered colony morphology, diminished cording formation and smaller bacillary size compared to the wild type. These phenotypes are related to the cell-wall composition, studies of lipid composition of different *phoP* and *phoPR* mutants demonstrate that PhoP controls the biosynthesis of SL and DAT and PAT [4, 5]. In addition to the impaired synthesis of acyltrehalose-based lipids, PhoP controls secretion of ESAT-6 by regulating the *espACD* gene cluster [6]; ESAT-6 is considered one of the major Mtb secreted virulence factors [7], promoting phagosome escape [8, 9] and mediating in the induced macrophage apoptosis [10, 11]. This latter phenotype is involved in the cell-to-cell spread of pathogenic strains and consequently in propagation of Mtb [12]. Additionally, an Mtb *phoP* mutant displays increased immunogenicity and enhanced generation of memory T-cells [13]; a recent work has demonstrated an increased secretion of substrates (including immunodominant antigens) from the Twin Arginine Translocation (TAT) export pathway, depending on a PhoP-regulated non-coding RNA [14], as it was

described in chapter 1 for MTBVAC secreted protein fraction which is enriched in TAT substrates.

In an attempt to decipher the entire PhoP regulon, transcriptomes of wild type and *phoP* mutant strains were compared using microarrays [4, 15]. Comparisons started to delineate the molecular mechanism by which PhoP controls the synthesis of SL and DAT/PAT or the secretion of ESAT-6. Although microarray analyses are useful to obtain a global landscape of gene expression, they fail to answer some basic biological questions such as whether a given gene is directly or indirectly regulated by transcription factors or if there are transcripts in non-coding regions.

A recent study has applied two next-generation sequencing (NGS) techniques to study the PhoP regulatory network [14]; ChIP-seq made possible to detect all PhoP binding region throughout the Mtb H37Rv chromosome and consequently to dissect those genes directly regulated by PhoP, and using RNA-seq, it was possible to obtain a detailed transcriptome and to identify PhoP-dependent transcription across the entire genome including intergenic and non-coding regions. The combination of all data together made possible to obtain a fine portrait of transcriptional regulation and allowed to discriminate between those genes regulated by PhoP in all conditions, the "core" PhoP regulon, and those genes whose transcriptional profile varies across conditions [16].

A total number of 35 regions were found to be significantly enriched in PhoP-DNA binding compared to *phoP* mutant (ChIP-seq); among them, 12 genes were found to keep the expression trend in all conditions tested by RNA-seq [16]. These twelve genes were proposed to be the PhoP "core" regulon. Among these genes some are involved in lipid metabolism, like the *pks2* gene which codifies for a polyketide synthase involved in the synthesis of SL [17], which has been reported to play a highly significant role in the interaction of the mycobacteria with its host [18]; *pks3*, which has a role in the synthesis of DAT/PAT [19]; *lipF* codifies for an esterase implicated on modifing the mycobacterial cell wall to render the bacteria more resistant to acidic stress, is known to be upregulated in the presence of acidic media and another possible function could

be to regulate the intracellular pH during acidic stress [20, 21]; or *fadD21* which is involved in lipid degradation and codifies for a probable fatty-acid-AMP synthetase [19]. The *nark1* gene is implicated in nitrite extrusion and respiration, codifies for a probable nitrite extrusion protein and it is involved in excretion of nitrite produced by the dissimilatory reduction of nitrate, process that allows the bacteria to face the respiratory stress once inside the macrophages [22]. Among the PhoP ChIP-seq peaks, the most prominent interaction was detected within an intergenic region and subsequent inspection of the adjacent RNA-seq profiles led to propose that a non-conding RNA (ncRNA) named *mcr7* is one of the most PhoP-regulated regions [14]. The characterization of *mcr7* demonstrated that this ncRNA modulates post-transcriptionally translation of the *tatC* mRNA, an essential gene and a constituent of the TAT secretion system, involved in the secretion of proteins with a twin arginine motif such as the Ag85 complex [23].

In-depth exploration of NGS data has allowed to propose PhoP as a master regulator of different genetic networks, there were also 6 other regions in where PhoP bound upstream of transcription factors indicating the presence of a complex regulatory network controlled by PhoP [16] where different responses like hypoxia adaptation and dormancy response (*dosR*) [24, 25], stress sensing (*whiB1*, *whiB3* and *whiB6*) [26] or activation of ESX-1 secretion system (*espR*) [27], are induced indirectly through action over these response regulators. Regarding PhoP control of ESAT-6 secretion, PhoP binds to the promoter region of *espR* and regulates the expression of this gene [14, 28] which has been proposed to transcriptionally regulate the *espACD* operon [29, 30]. PhoP is also able to interact with the *espA* promoter [31]. Taken together these facts and considering the essential role of EspA in ESAT-6 secretion [6, 32], PhoP is on the axis of the PhoP-EspR-EspA regulatory loop. On the other hand, recently it was reported that PhoP regulates expression of *whiB6* by interacting with its promoter region [33], it is located adjacent to the ESX-1 region that codes for the ESAT-6 secretory apparatus, pointing at WhiB6 as a putative regulator of this region. It has been demonstrated that WhiB6 interacts with the promoter regions of *espA* as well as with the ESX-1 genes *pe35* and *espB* [34], required for ESAT-6 secretion [35, 36]. Thus, a second regulatory network involving PhoP as the master regulator and WhiB6 as

secondary player is proposed to regulate ESAT-6 secretion and consequently *whiB6* is included within the ESX-1 system. Among the few genes negatively regulated there is *icl*, which allows mycobacteria to grow using fatty acids as sole carbon source and it is required for intracellular persistence [37, 38].

Despite the *phoP* gene and its implication in virulence have been extensively studied, the signal sensed by the PhoR component remains still unknown. Several works have attempted to identify the PhoPR stimulating signal and given the intracellular life cycle fitness of Mtb and the *in vitro* and *in vivo* attenuation showed by *phoPR* mutants [3, 39]; it is plausible to link the PhoR sensor kinase with intracellular signals. Thus, one could speculate that following phagocytosis of Mtb by resident macrophages, PhoR sensing some of the changes occurring during phagosomal maturation would likely result in phosphorylation of PhoP. Upon phosphorylation, PhoP is expected to modulate transcription of its regulon, which could result in positive regulation of SL and DAT/PAT synthesis and ESAT-6 secretion and in promoting immunomodulation of T cells and phagosome escape.

Taking in consideration all these facts we carried out a series of experiments, first through a reporter system and later directly measuring gene expression through qRT-PCR, in which we tried different extra- and intracellular conditions and analyzed the activity of different PhoP-regulated genes in H37Rv and its *phoP* mutant. The aim was to found any condition in which the PhoP regulon was upregulated compared to standard growth conditions and no changes in its expression were detected in the *phoP* mutant; consequently the upregulation would be due to a PhoP-dependent activation, which otherwise would be related to the PhoR activating stimulus.

2.1. Construction and characterization of a reporter system based on GFP expression to study the PhoP regulon.

With the aim to determine the signal modulating the PhoP regulon, we decided to evaluate the gene expression pattern of five PhoP-regulated genes by measuring the expression of a reporter gene, *gfp* (green fluorescent protein) [40]. Integrative plasmids containing the promoter regions of some of the genes inside the PhoP regulon (*dosR, icl, phoP, pks2* and *lipF*) upstream the *gfp* gene were generated by amplification of the mycobacterial DNA regions containing the gene promoter and cloning them into the pFPV27 plasmid [41]. These constructions were then transformed in H37Rv and its mutant H37RvΔ*phoP*.

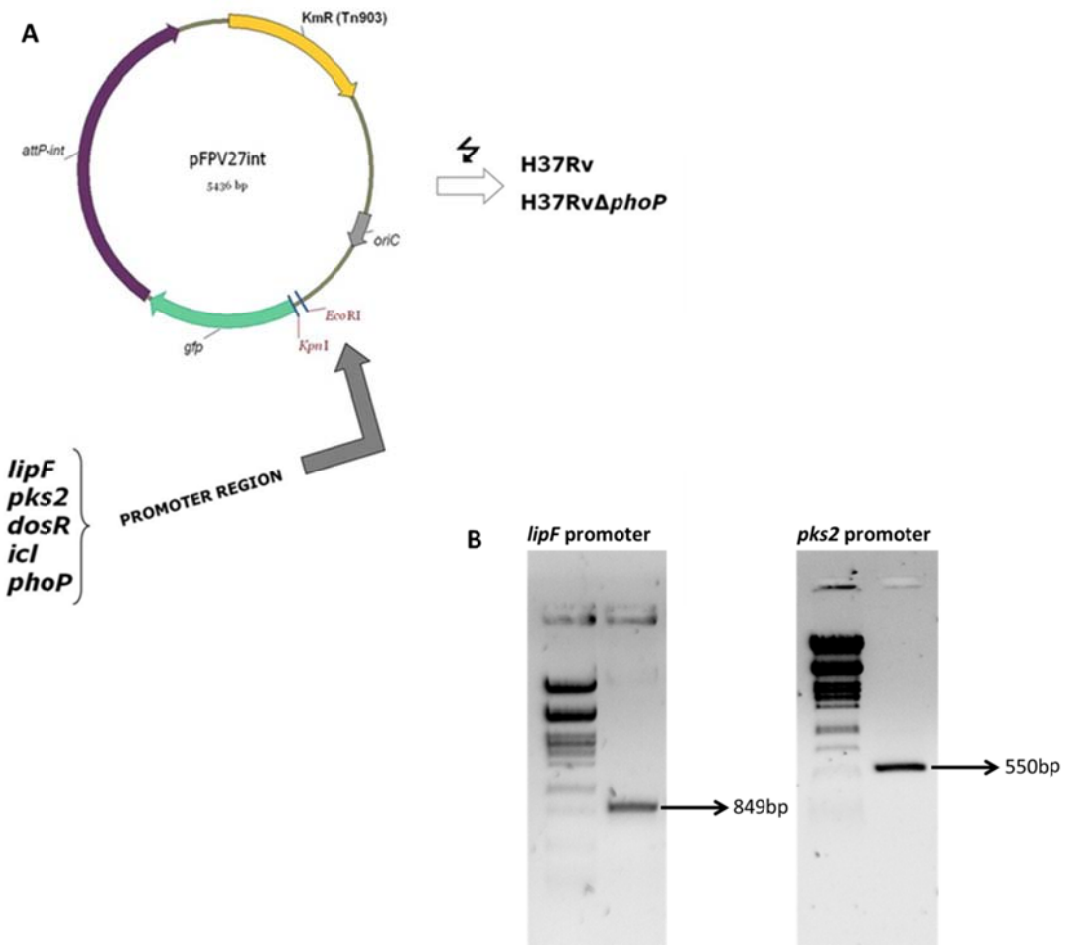

Figure 1. A. Map of the integrative plasmid pFPV27 with the *attP*-integrative region, the Kanamicine resistance cassette, and a replication origin for *E. coli* and the cloning site between *EcoRI* and *KpnI* upstream the *gfp* reporter gene. The promoters of five PhoP-regulated genes were cloned directionally

in the mentioned cloning site upstream the reporter gene and the final constructions were cloned in H37Rv Mtb reference strain and its *phoP* mutant. **B.** Representative images of agarose gels with the amplified region containing the promoters of two of the selected genes, this regions were cloned in the pFPV27 plasmid.

Once constructed, we tested the strains under *in vitro* standard growth conditions. The growths curves did not have any altered profile (Figure 2). We also measured the fluorescence of all the cultures and, we normalized the fluorescence registered data (GFP) with the optical density (OD) and graphically represented as GFP/OD (Figure 3).

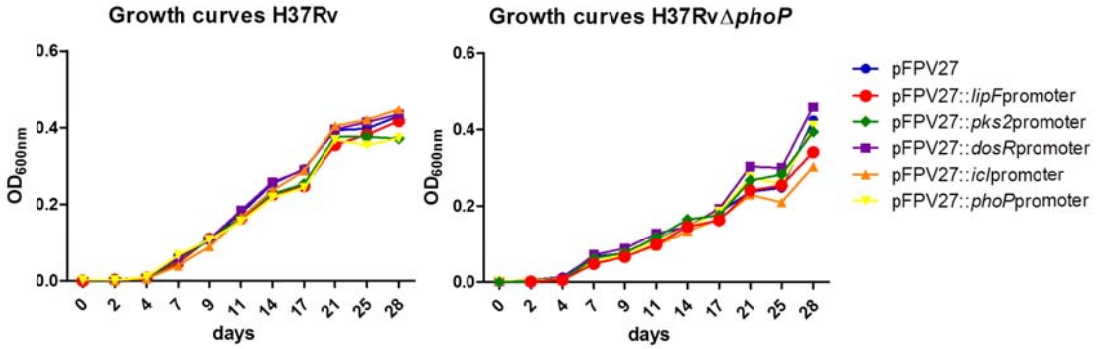

Figure 2. Graphical representation of the optical density (OD) at 600nm vs. days of the strains containing the pFPV27 plasmid and the pFPV27 plasmid with the PhoP-regulated gene promoter with *gfp* protein fusions. The curves did not show any altered profile. Representative graphs of a triplicate experiment.

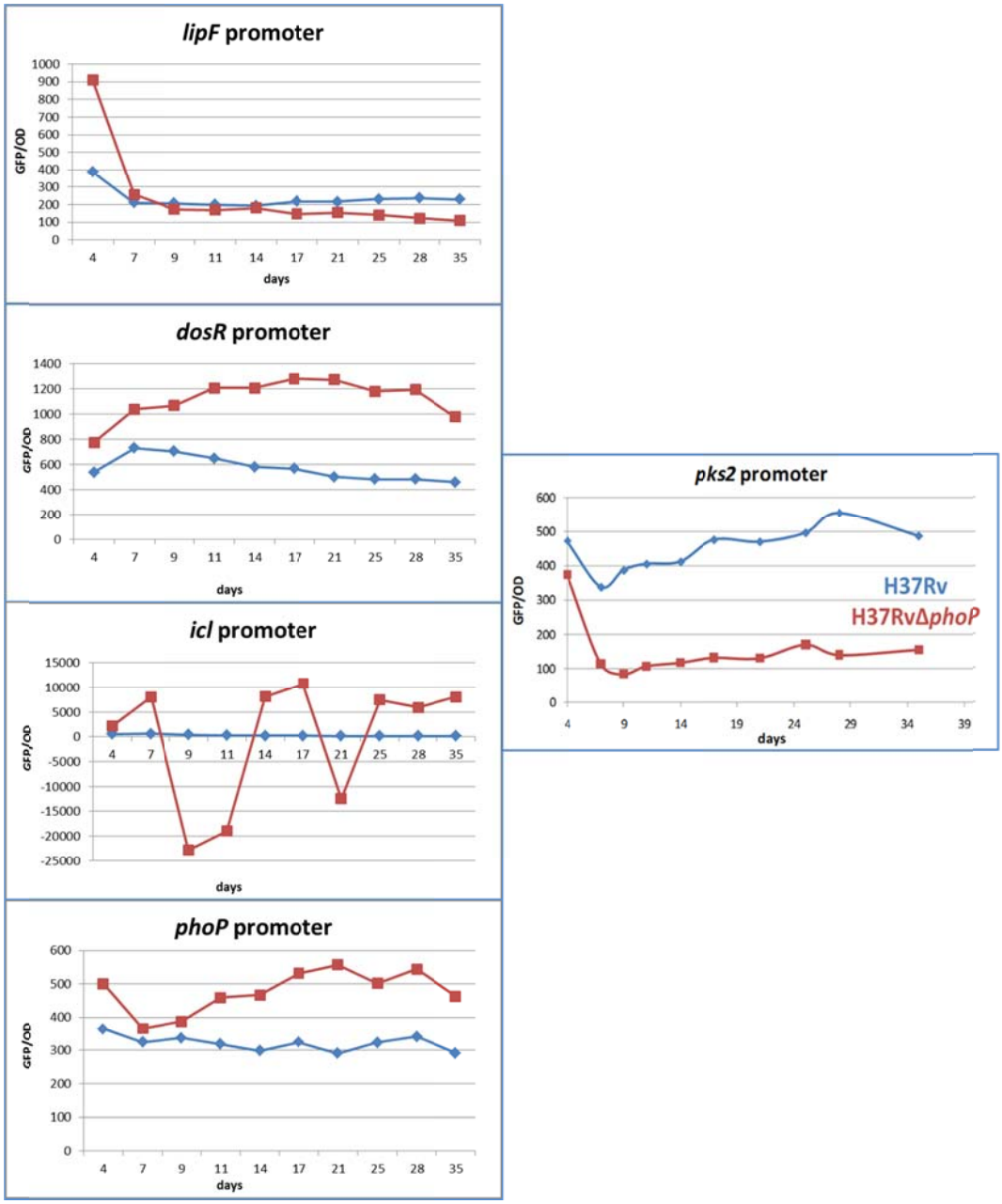

Figure 3. Graphical representation of normalized fluorescence GFP/OD vs. days for the activity of *dosR*, *icl*, *phoP*, *lipF* and *pks2* promoters in both strains H37Rv and its *phoP* mutant in standard growth conditions. The fluorescence of the culture is an indirect measure of the promoter activity. In response to stimuli the promoter will activate the transcription and translation of the GFP protein. Thus, the fluorescence registered will be proportional to the promoter activity. We can observe that PhoP absence leads to lower levels of *lipF, pks2* mediated GFP fluorescence since they are strongly regulated by PhoP when compared with wild type strain fluorescence levels. Representative graphs of a triplicate experiment.

We can observe that *dosR*, *icl* and *phoP* promoters present an expression profile that is not suitable for our purpose; *lipF* promoter has very low levels of expression. However

we found *pks2* promoter region to be strongly regulated by PhoP under the experimental conditions tested, thus it is going to be the best reporter of PhoP regulon response.

We choose the pFPV27::*pks2*promoter strain to study indirectly the activity of the PhoP regulon. The aim of the reporter system is to analyze the effect of different culture conditions on the expression of the PhoP regulon.

2.1.1. Expression of the PhoP regulon under acidic conditions.

Since Mtb is an intracellular pathogen and it has been already observed the importance of acidic pH inside the macrophage phagosome [42], we decided to study the pH effect on the Mtb reporter strains. The pH assay was performed with the strains containing the constructions of both *pks2* and *lipF* promoters because it has been previously reported the PhoP-independent pH-induced activation of *lipF* gene [20, 43].

Initially, we used in our constructions a region of 550bp upstream of *lipF* gene were the promoter was supposed to be. However, when we performed the assays in acidic pH, the *lipF* promoter did not show transcriptional activation which was incongruent with previously described experiments [43]. Recent results obtained in our laboratory from ChIP-seq and RNA-seq technologies, show that the distance between the PhoP peak and the ORF start site is in the majority of the cases (83%) between 0 and 200bp (Figure 4). Nevertheless there were two PhoP binding sites considerably far away from the closer ORF as was the case of *lipF*, with PhoP-binding region located at 525bp from the start site (Figure 5).

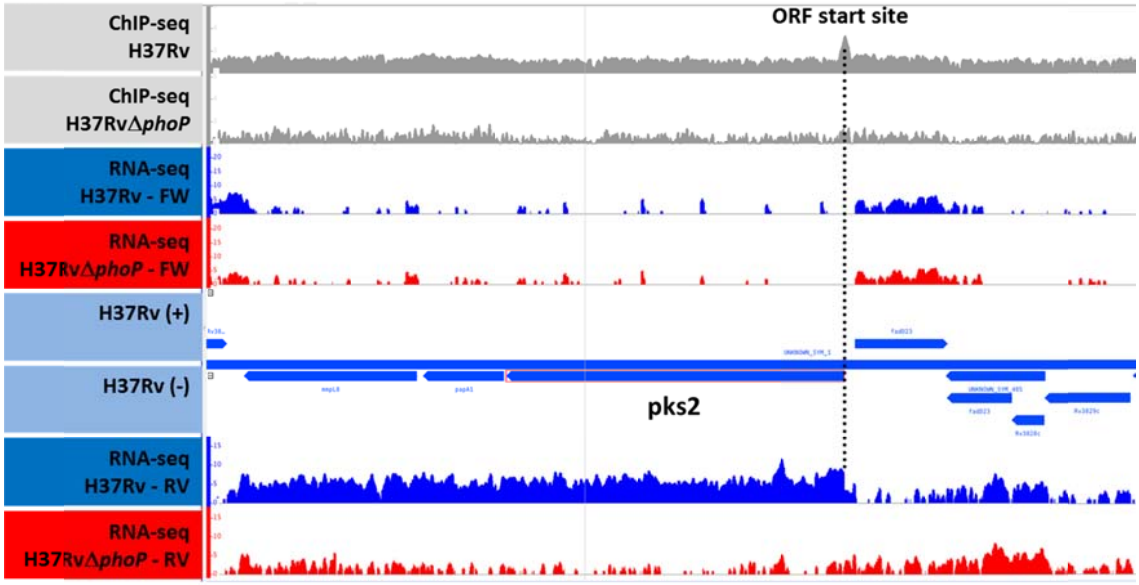

Figure 4. Image obtained from the ChIP-seq analysis. It is possible to observe how the ORF start site of *pks2* gene is immediately before the ATG start codon of the gene. This situation is a common feature sor 83% of the core PhoP regulon.

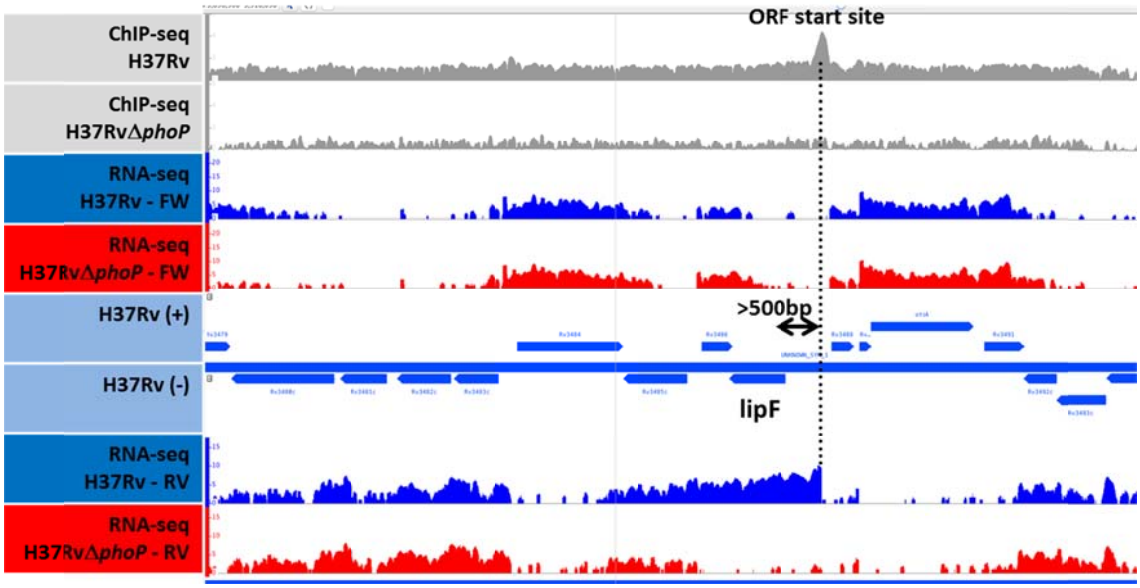

Figure 5. Image obtained from the ChIP-seq analysis. The *lipF* ORF start site is placed at 525bp from the codon start of the gene. Is one of the two exceptions registered in the ChIP-seq and RNA-seq analysis, where the majority of PhoP-regulated genes has a PhoP-binding region located between 0 and 200bp upstream the gene start codon.

Taking into consideration this result, we constructed a new plasmid with a longer region (849bp) upstream the *lipF* gene, to include promoter region of the gene. The

construction was transformed in the reference strain H37Rv and its *phoP* mutant as it has been previously described.

When we performed the acidic pH assay with the strains containing the *pks2* promoter and the new *lipF* promoter construction, results in both cases show an increase in the promoter expression at acidic pH when compared with pH 7. However in the case of the *pks2* promoter, increase of expression was observed in the wild-type strain but not for the *phoP* mutant strain. This profile, where a condition activate the expression of a given PhoP-regulated gene in the H37Rv strain, but not in the *phoP* mutant, indicates that this upregulation is exclusively dependent on PhoPR.

We represented the obtained data as the difference between the normalized fluorescence obtained at an acidic pH and the one obtained at neutral pH, to remark the differences between the activation in the wild type strain and the *phoP* mutant (Figure 6).

A

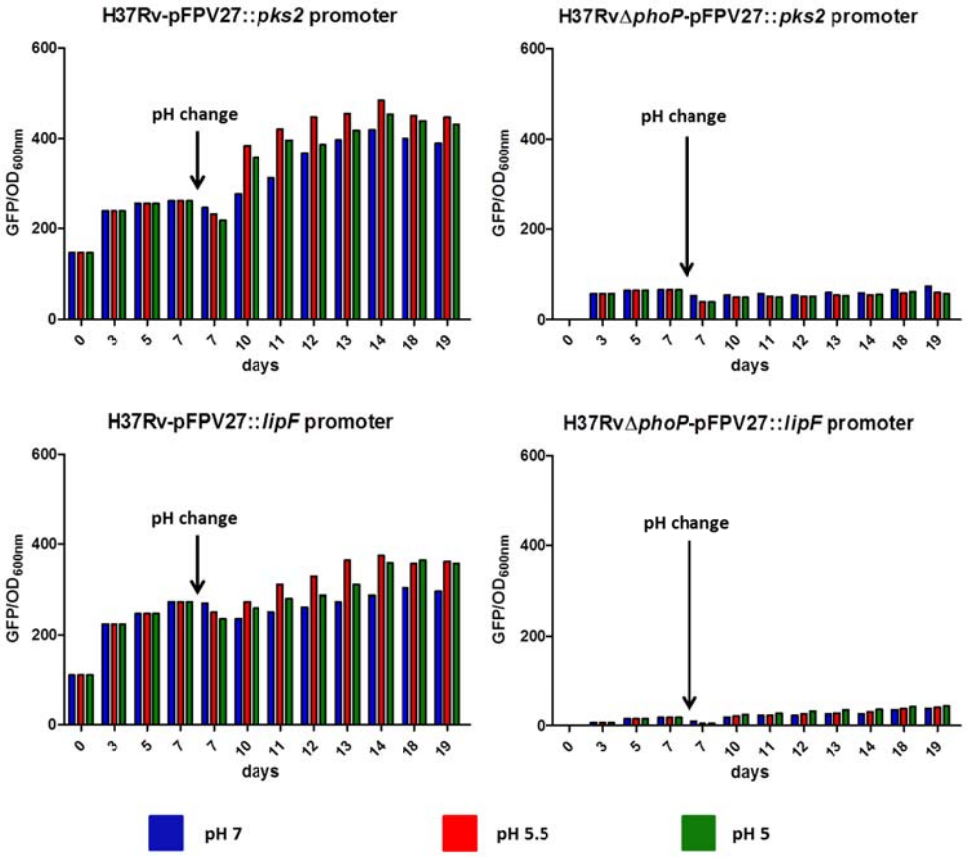

B

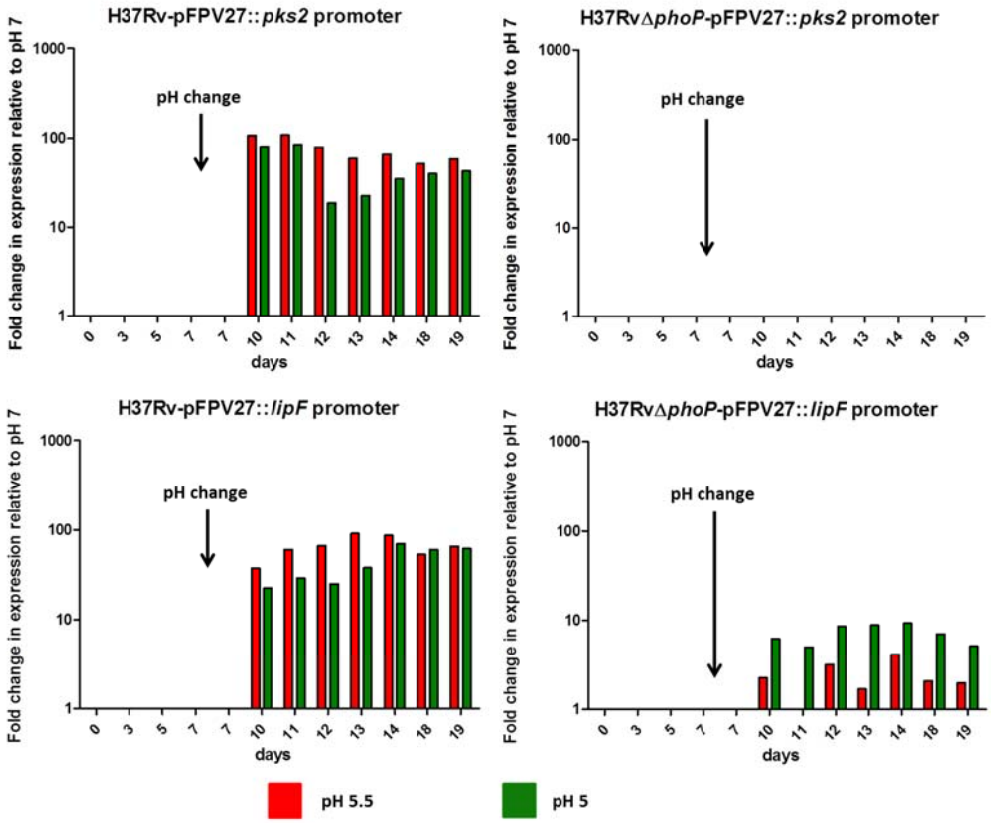

Figure 6. Induction of *pks2* and *lipF* expression after pH treatment. Cultures were grown for seven days before change the culture medium for the pH modified ones. Before and after the medium change, optical density and GFP fluorescence were measured. **A.** Normalized fluorescence (GFP fluorescence intensity divided by the optical density at 600nm of the culture in each point) is represented. We can observe an increase in the activity of *pks2* and *lipF* promoters at acidic pH. In the case of *pks2* promoter, the increase in its activity is shown for the wild type stain but not for the *phoP* mutant, demonstrating that it is a PhoP-dependent event. In the *lipF* promoter activity it is possible to observe some acidic pH response also in the *phoP* mutant strain. **B.** Here we represent the ratio between adjusted fluorescence (GFP/OD) at acidic pH and the neutral pH. For the *pks2* promoter, we can see an activation of the expression after exposure to acidic pH in the wild type strain H37Rv, but no activity for the *phoP* mutant strain. For the *lipF* promoter we can see activation of the expression at acidic pH for both strains demonstrating that *lipF* response to pH is PhoP-independent. Representative graphs from a triplicate experiment.

In the expression profile of the *lipF* promoter, even if it is a highly PhoP dependent event and the activity of the promoter decreases dramatically in the *phoP* mutant, there is some response to acidic pH, demonstrating that *lipF* response to low pH is a PhoP-independent event as it has been described in other works (Figure 6B) [43]. The

observed profile of expression of *pks2* promoter was a strictly PhoP dependent phenotype, we can observe an increase in the activity of the promoter at acidic pH for the wild type strain, but not in the *phoP* mutant (Figure 6A). This result could be explained if the activation of *pks2* promoter is regulated by PhoP under acidic conditions.

2.1.2. Expression of the PhoP regulon under culture conditions mimicking the intracellular environment.

Besides the acidic pH, we assayed the strains containing the GFP::promoter constructions under different conditions based on experiments previously described in the literature or under some stresses that mycobacteria face inside the phagosome.

We assayed not only the *pks2* promoter, but also other promoters from the PhoP regulon. The assays were performed in different conditions in *in vitro* culture:

- Different sources of Carbon in the culture medium: Glucose, Acetate or Propionate. The PhoP-regulated isocitrate lyase (Icl) is a metabolic enzyme used by bacteria to sustain growth on even-chain fatty acids through an anaplerotic pathway called the glyoxilate shunt. It also serves a parallel pathway involved in the metabolism of propionyl CoA generated by β-oxidation of oddchain fatty acids, called the methylcitrate cycle [38, 44]. This assay was performed in order to verify the activation of the *icl* promoter in presence of propionate, which allows us to verify the accurate functioning of the reporter system constructions.

- Hypoxia conditions: in order to mimic the anaerobic environment inside the granuloma during latent infection. Several studies have suggested that the PhoP-regulated DosR regulon plays a role in latent infection and in persistence in animal models [24, 25].

- Various concentrations of different ions in culture medium: the role of salts and ions in balancing the proton and electron gradients that accompany phagosome acidification and oxidative burst has been extensively studied, demonstrating the importance of the phagosomal lumen content in the antimicrobial mechanisms [45]. We designed assays considering broad range of Zn^{2+}, Cu^{2+}, Ca^{2+} and Mg^{2+} concentrations in order to analyze the response of the PhoP-regulated genes [46, 47].

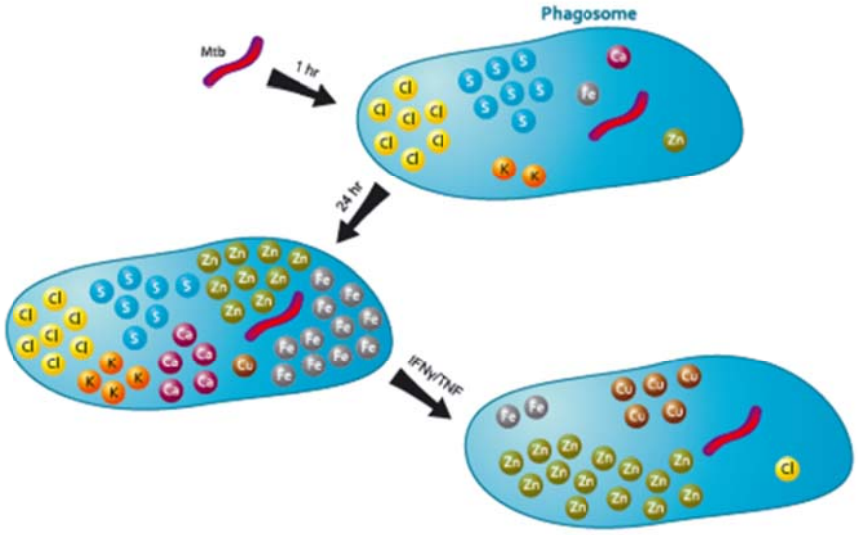

Figure 7. The phagosome ionome during mycobacterial Infection and macrophage activation. Wagner and colleages [48] have quantified the content of the mycobacterial phagosome in a number of elements during infection and upon host cell activation. The early phagosome was found enriched in sulphur and chloride, and depleted in calcium, as compared to extracellular bacteria. Later during infection, the vacuole was found replenished in calcium, zinc and iron. Activation of infected macrophages with inflammatory cytokines led to a marked depletion of the vacuole in chloride and iron, and to an increase in zinc and copper concentration. Adapted from [45].

- Oxidative stress: Another major arm of the phagocyte anti-microbial arsenal is the production of toxic reactive oxygen and nitrogen intermediates (ROI and RNI). A growing number of studies link the production of ROI, its effects on the phagosomal milieu and an indirect impact on bacterial killing [45, 49]. We decided to add different concentration of H_2O_2 to the culture medium to mimic the oxidative stress and analyze the response of the PhoP-regulon.

- Different Temperatures: even being 37^{o}C the physiological temperature the regular culture temperature, we decided to incubate cultures at 42^{o}C and room temperature trying to mimic different situations, like fever, that could stress the bacteria and analyze the response of the PhoP-regulon.

- Fatty acids: It has been shown that Mtb uses host lipids, in particular, fatty acids and cholesterol, as energy sources during intracellular growth and persistence [50]. In order to study the response of PhoP-regulon to fatty acids, we incubated cultures of Mtb with culture medium in presence of oleic, palmitic and estearic acids.

However, we could not find, in none of these assays, any expression profile corresponding to a PhoP regulon activation signal. Results detailed in the Appendix.

2.2. Direct quantification of the PhoP regulon by qRT-PCR.

Once we obtained an expression profile through the GFP reporter system that led us to think that PhoP is regulating the pH response or, in other words, that the acidic pH could be the signal activating the PhoP-regulon, the next step was to directly quantify the expression of *pks2* gene by RNA extraction and qRT-PCR, and confirm the induction of *pks2* expression as the PhoP activity reporter. We will also analyze some other genes of the PhoP core regulon.

Assays performed before were through a GFP reporter system, in which it is necessary *pks2* promoter to be activated so *gfp* gene started to be expressed. To be able to detect the fluorescence due to GFP expression the protein have to accumulate inside the bacterium, so the time course of the assay it is slower than the real response. In order to obtain a direct measure of the response of the PhoP-regulon to acidic pH, we decided to perform the study at different time points, starting from very short times to long times of exposure to acidic pH.

2.2.1. Expression of PhoP-regulated genes after short times of acid pH exposure.

In a first approach we performed the assay as it was done for the reporter system, were the acidic response was registered three days after introducing the stimulus in the culture medium, but no response was detected. Taking into consideration the time lapse due to the accumulation of GFP, we decided to perform a kinetic assay at short times after exposure to acidic pH.

RNA was extracted at 30 minutes, 1 and 6 hours after changing the growth medium to the acidified one in exponential growth cultures. We obtained cDNA in order to carry out the qRT-PCR and directly analyze the expression of the PhoP regulated genes.

We also wanted to check the pH of the culture supernatant to confirm that pH was maintained during the time course of the experiment. After centrifugation of the bacterial pellet, supernatant was filtered and the pH was measured.

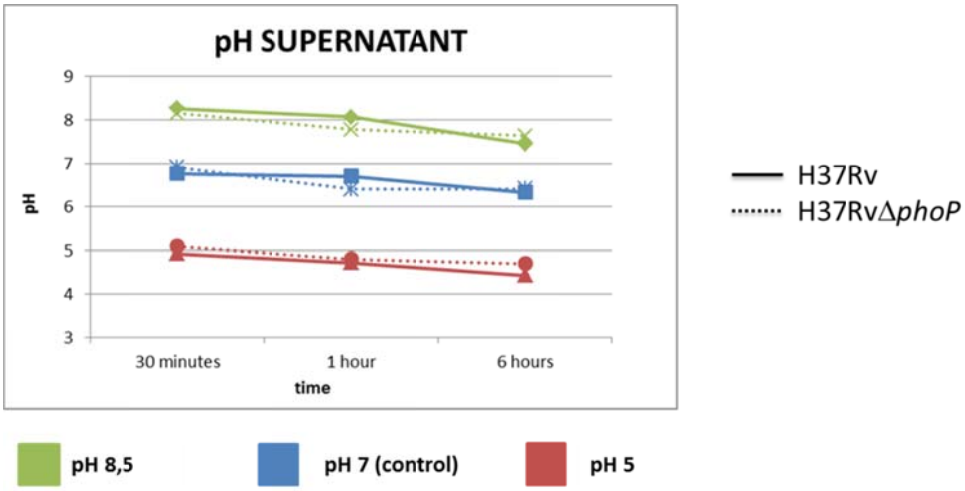

Figure 8. The culture supernatant obtained in the first centrifugation step of the protocol to extract bacterial RNA was filtered and pH was measured with a pHmeter for each sample. pH was maintained during the experiment since it acidifies slightly in a non-significant way.

Supernatant pH acidifies slightly during the experiment since the growth media was not buffered, but the change was not significant, the pH still remains in the range expected (Figure 8).

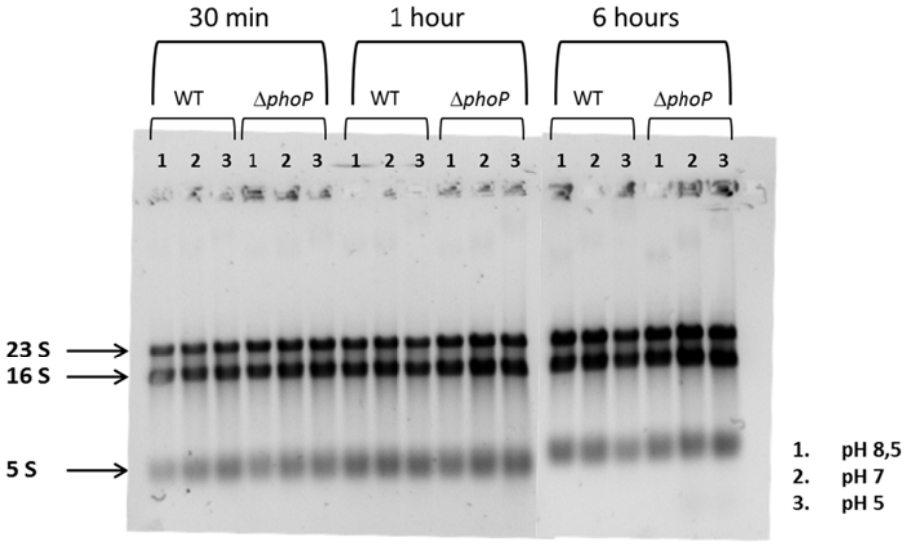

Figure9. Image of an agarose gel with the RNA extracted for each sample at each point loaded in the indicated lane. We can observe the three types of mycobacterial RNA, the 23S, the 16S and the 5S in good conditions and quantity.

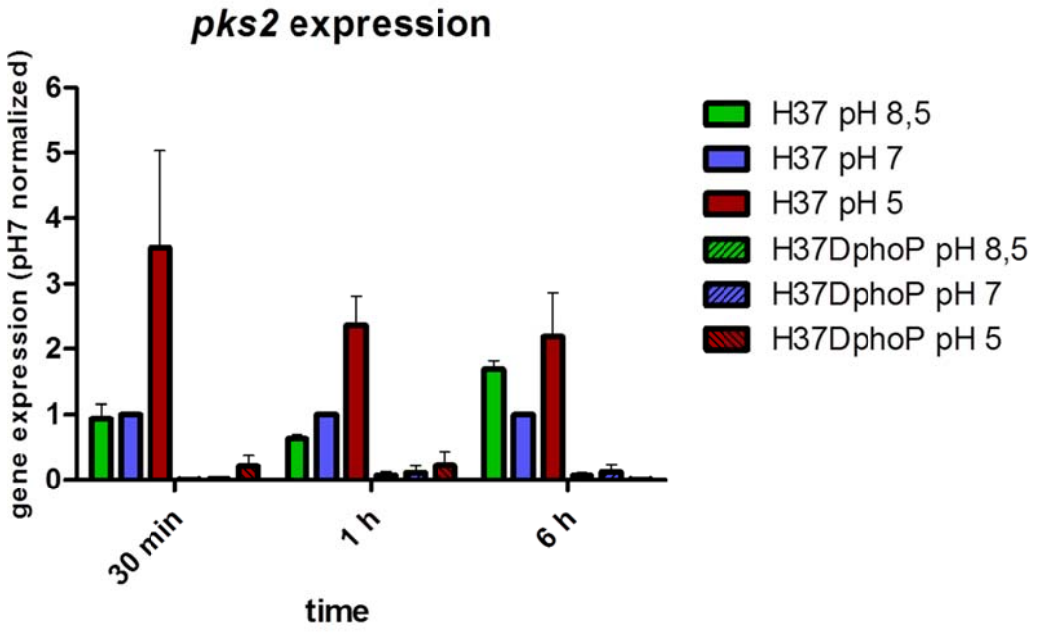

Figure 10. Expression kinetics of *pks2* gene in response to acidic pH normalized versus the expression at pH 7 in the H37Rv strain. There was barely expression for the *phoP* mutant strain. Meanwhile there is an upregulated expression of *pks2* gene when exposed to acidic pH 5 after 30 minutes exposure in the wild type strain H37Rv. The upregulation is maintained until 6 hours post exposure at pH 5. Average graph from a triplicate experiment.

For *pks2* expression, we found the response to the acidic pH to be faster than the response detected though the GFP readout. The gene expression is activated at very short time after acidic pH exposure. *pks2* gene is highly overexpressed up to 30 minutes of acidic pH exposure compared to neutral pH in H37Rv, but it did not happen in the *phoP* mutant strains (Figure 10), supporting the idea that this response is mediated by PhoP and confirming the profile previously observed with the GFP reporter system.

Besides *pks2* gene, which we have chosen for being strongly regulated by PhoP as good reporter of the regulator activity, there are some other genes considered to belong to the PhoP "core" regulon. We decided to analyze some of those genes in the RNA obtained.

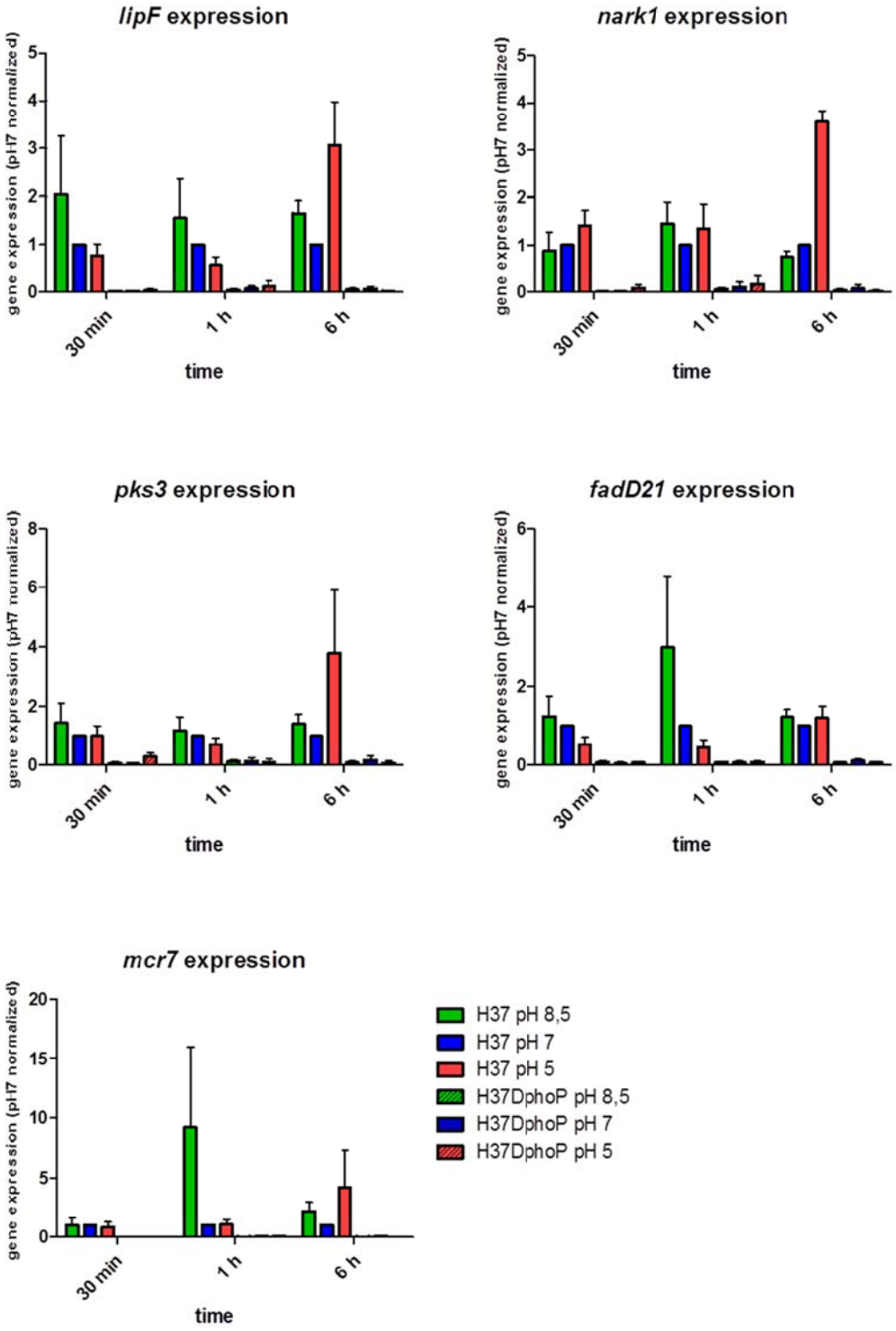

Figure 11. Kinetics of PhoP-regulated genes expression in response to acidic pH normalized versus the expression at pH 7 in the H37Rv strain. *lipF, nark1, pks3, fadD21* and *mcr7* are part of the considered PhoP "core" regulon, they are genes regulated by PhoP directly. We can observe an upregulation PhoP dependent at acidic pH for *lipF*, *nark1* and *pks3* at short times of exposure. Average graphs from triplicate experiments.

We can observe an increase in the expression of *lipF*, *nark1* and *pks3* at pH 5 at 6 hours after acid pH treatment. This is a fast response albeit not as immediate as the *pks2* promoter. Nevertheless we could not detect any remarkable increase in the expression of the PhoP most regulated region *mcr7* at acidic pH (Figure 11).

There are some other PhoP-regulated genes not considered to belong to the "core" regulon, like the transcriptional regulators *espR* or *whiB6*, where the direct action of PhoP might indicate the presence of a complex regulatory network controlled by PhoP. Different responses might be induced indirectly through action over these response regulators [16]. However, we were not able to observe specific expression profiles in response to acidic pH (Figure 12).

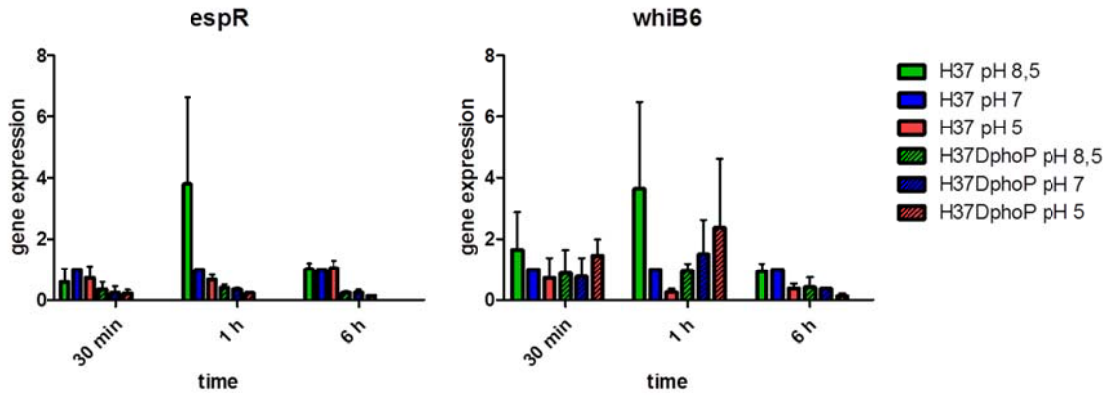

Figure 12. Kinetics of *espR* and *whiB6* genes expression in different pH conditions at short times of exposure, data are normalized against the expression at pH 7 in the H37Rv strain. These are transcriptional regulators regulated by PhoP. Average graphs from triplicate experiments.

2.2.2. Expression of PhoP-regulated genes after long times of acid pH exposure.

After analyzing the expression of the chosen PhoP-reporter gene *pks2* and some of the genes in the PhoP "core" regulon at short times of acidic pH exposure, the next step was studying the expression of those genes in a long time exposure kinetic.

On the other hand, in a recent study a region named *aprABC* locus was studied and described as a pH-driven adaptation and also regulated by PhoP [51]; however in this work it was only studied the acidic-response of this *aprABC* region. Considering the conditions of the assays described in the paper, we performed a long time of acid exposure assay reproducing those conditions and expanded the analysis of the results to some genes of the PhoP-regulon.

Besides the RNA extractions, we measured the pH of the culture supernatants. We had seen that pH slightly acidifies during the previous short-term experiment, and since this experiment was a long time kinetic, we buffered the 7H9 culture medium with MOPS and MES for pH 7.0 and pH 6-5.5 respectively to ensure that pH was maintained stable during the assay (Figure 13).

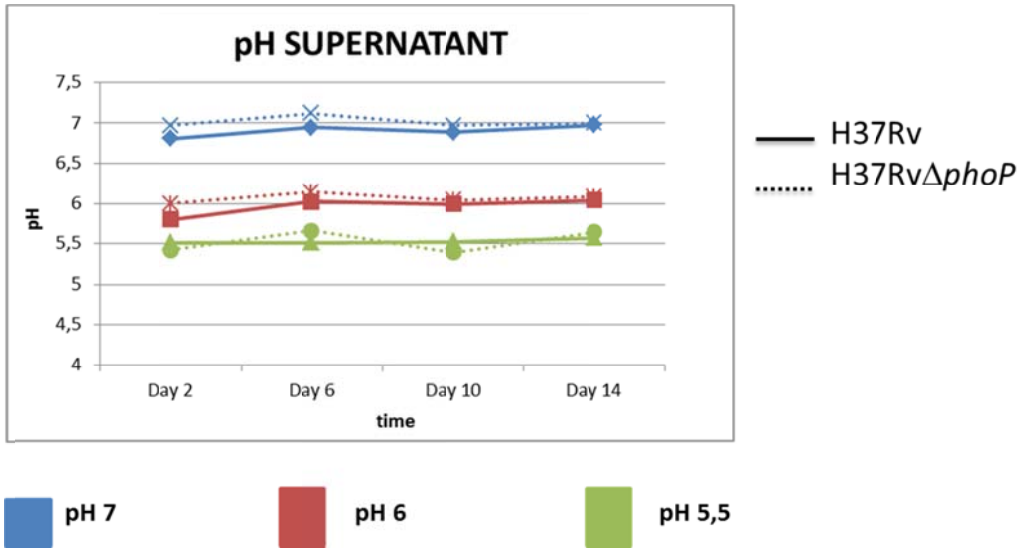

Figure 13. The culture supernatant obtained in the first centrifugation step of the protocol to extract bacterial RNA was filtered and pH was measured with a pHmeter for each sample. For this assay we added MOPS and MES in order to buffer the culture medium and we can assure pH was maintained during the experiment.

During the assay, we also controlled the OD_{600nm} of the cultures in order to assure the optimal growth of the strains under the diverse pH of the study (Figure 14). For these experiments we grew cultures up to an optical density of 0.5 before changing the medium to an acidified one. In this study we also introduced a new *phoP* mutant strain complemented with the *phoP* gene under the control of its own promoter, and a *phoP*

mutant strain complemented with the *mcr7* gene under the control of the 16S rRNA promoter, known to be independently regulated by PhoP.

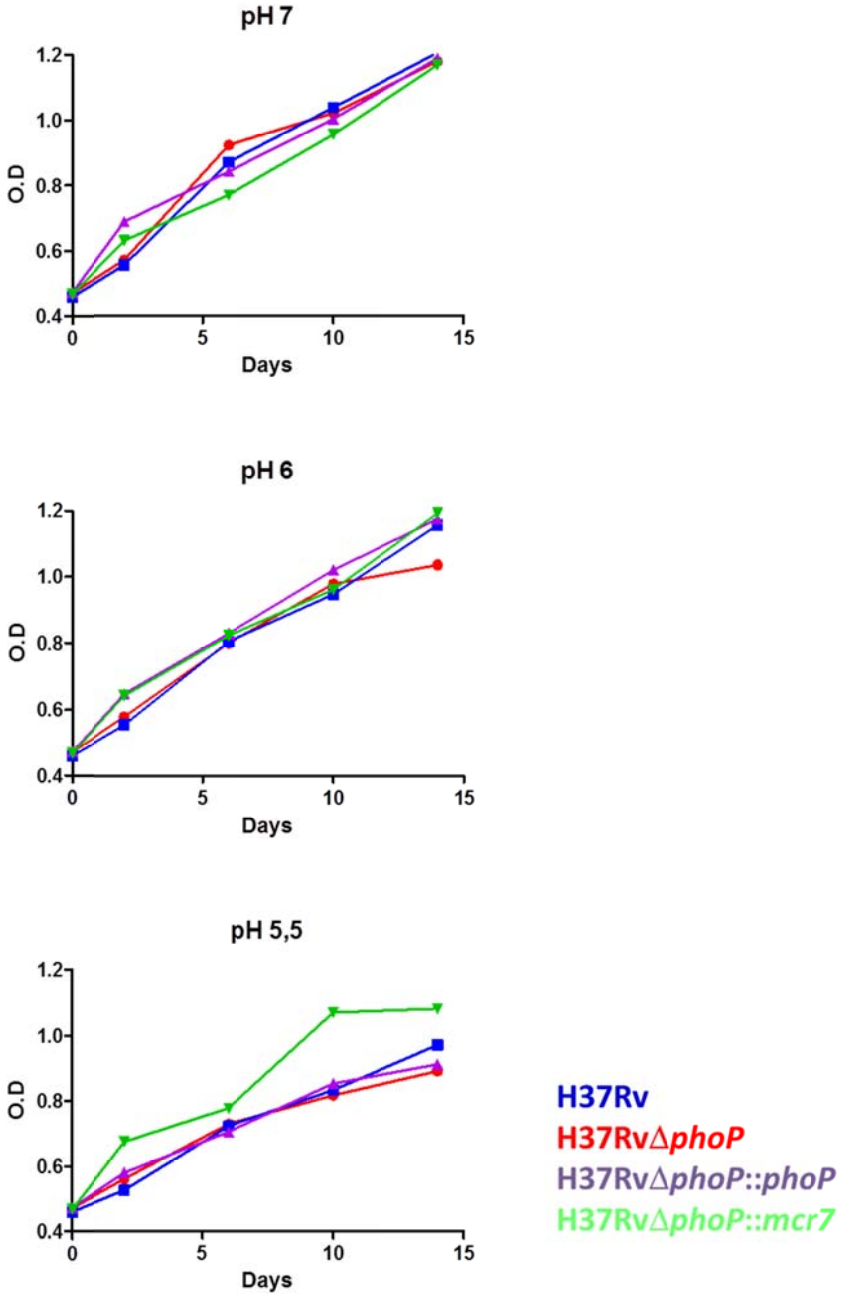

Figure 14. Optical density of the cultures at each time point was measured in order to confirm the optimal growth of the strains during the experiments at different pHs. For these experiments we grew the cultures up to an optical density of 0.5 before changing the medium to an acidified one.

We extracted RNA at the established time points to obtain cDNA and to measure expression of some genes of the PhoP "core" by qRT-PCR.

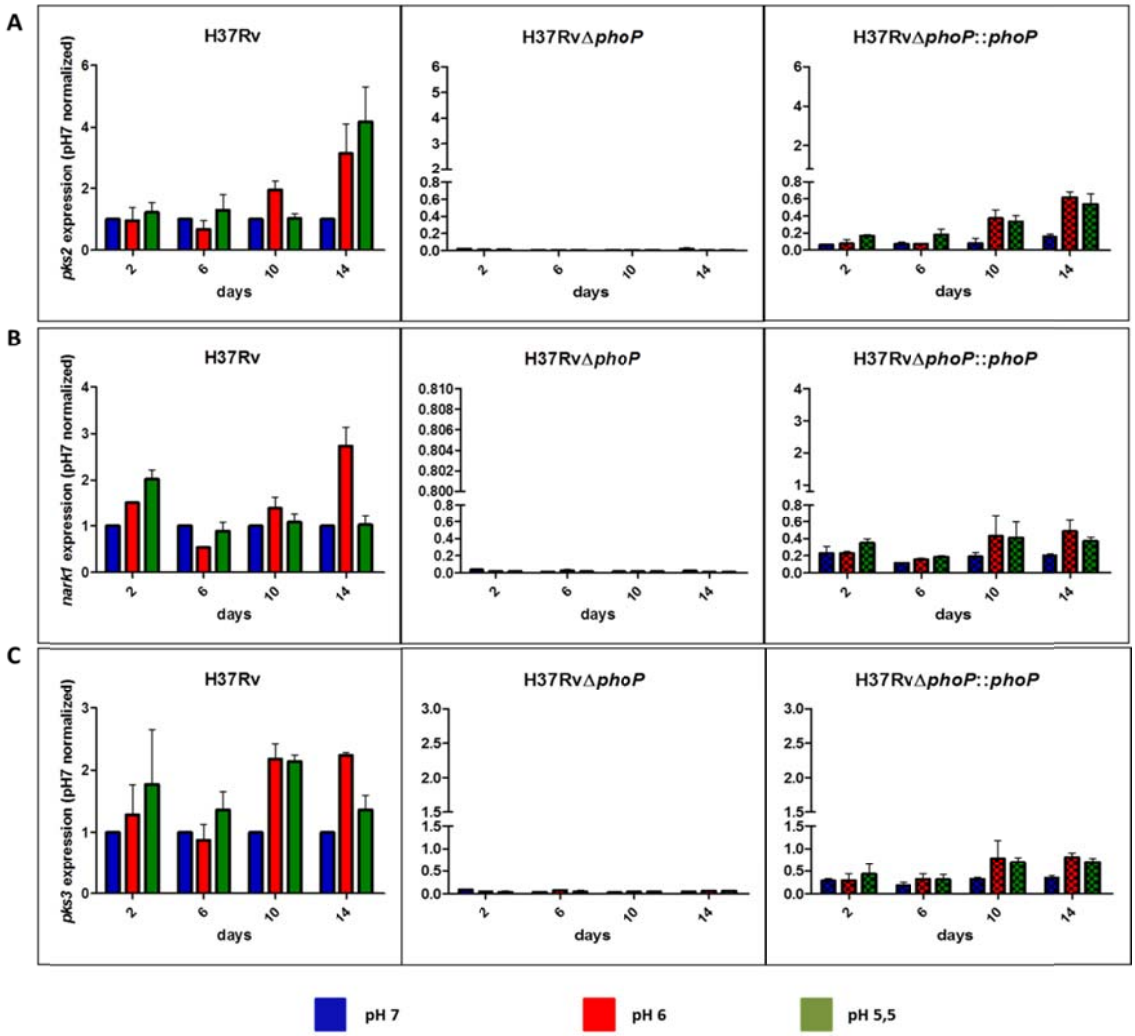

Figure 15. Gene expression in response to long time of acidic pH exposure. RNA was extracted at established time points and gene expression was analyzed by qRT-PCR and normalized against the expression at pH 7 in the H37Rv strain. **A.** For *pks2* gene we can observe no upregulation of the gene until 14 days of exposure for the wild-type stain. **B.** For *nark1* gene, we can observe the upregulation of the gene at 2 days post-exposure for the wild-type stain. **C.** *pks3* gene expression is upregulated at acidic pH during the entire assay for the wild-type stain. In all cases, the *phoP* mutant strain levels of expression were barely detectable and for the *phoP* complemented strain, the expression was restored following the same expression profile as for the wild-type. Average graphs from triplicate experiments.

For *pks2* gene we did not obtained a response at long times (days) of acidic exposure, the results of the short-time exposure experiment (hours) suggest that the response to acidic conditions occurs immediately after exposure. In all the three cases *pks2*, *nark1*

and *pks3* the general trend is to increase the expression of the gene at acidic pH after long times of exposure. When compared the increase of expression at acidic pH of the H37Rv strain with the *phoP* mutant one, it remains clear that is a PhoP-dependent event since the profile is not reproduced in the mutant strain; when we studied the expression in the *phoP* complemented strain, expression was not completely restored at wild-type levels, but we can observe the same expression profile (Figure 15).

For the study of *mcr7*, the most PhoP-regulated region, we also constructed a *phoP* mutant strain complemented with the *mcr7* gene under the control of a ribosomal promoter in order to confirm that the effects observed in the wild-type strain are exclusively due to PhoP effect.

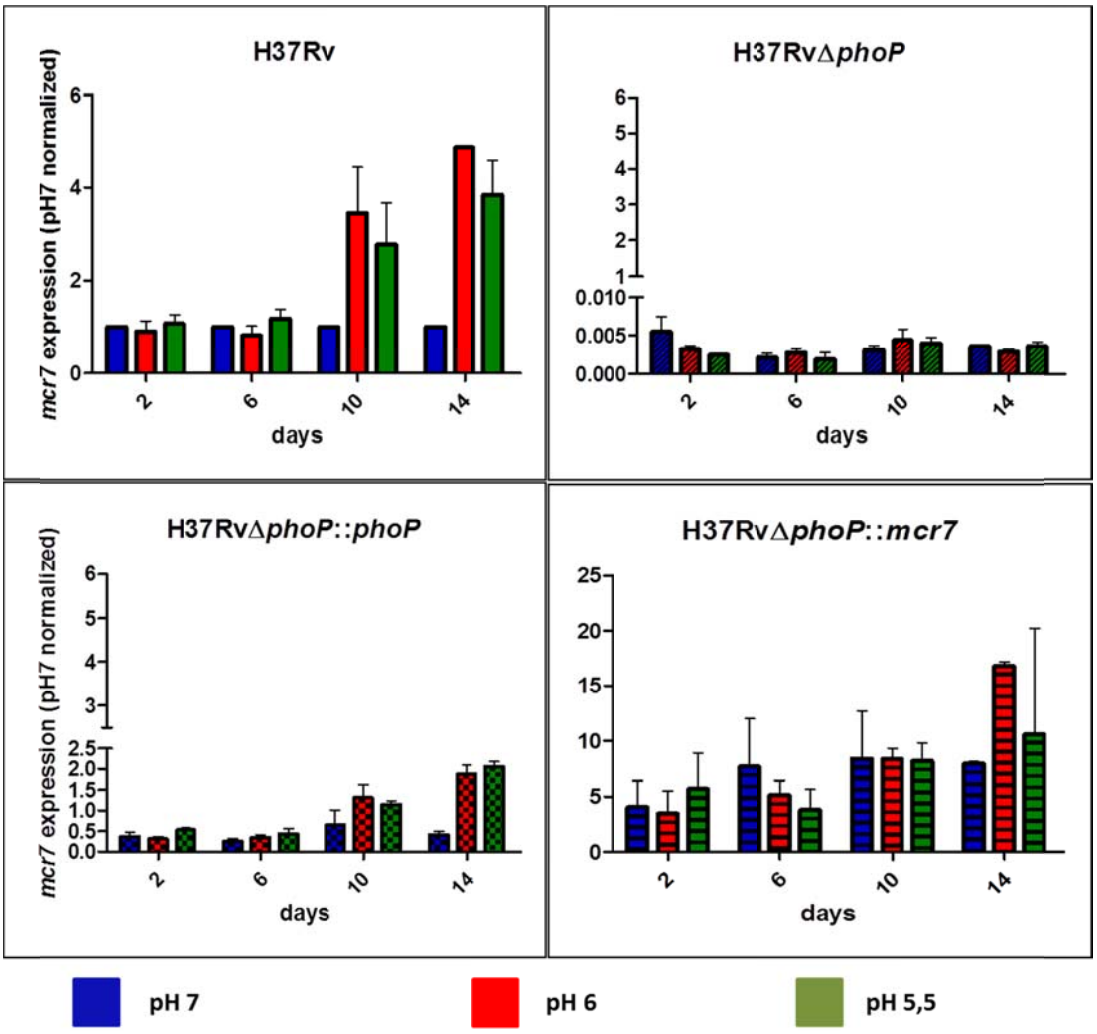

Figure 16. *mcr7* region expression in response to long time of acidic pH exposure. RNA was extracted at established time points; gene expression was analyzed by qRT-PCR and normalized against the

expression at pH 7 in the H37Rv strain. We can observe a strong upregulation of the region up to day 6 of acidic exposure for the wild-type stain. In the *phoP* mutant strain the levels of expression are very low and the expression profile was not repeated; in the *phoP* complemented strain the expression was partially restored following the same profile as for the wild-type Meanwhile for the *mcr7* complemented strain, there is a considerably higher expression of the region and the expression profile is different compared with the wild-type or the *phoP* complemented strains. Average graphs from triplicate experiments.

We found *mcr7* to be highly overexpressed in acidic pH after 5-6 days of exposure for the wild type strain, but not in the *phoP* mutant, meaning that response to acidic pH is activated by PhoP. When *phoP* is complemented, response to pH is restored, confirming the PhoP-mediated phenotype (Figure 16). Mcr7 has been recently described as an ncRNA, in fact is the first report of an ncRNA controlled by a 2CS in Mtb [14]. This ncRNA was identified by ChIP-seq and RNA-seq (placed between Rv2395 and PE-PGRS41) as the most PhoP-regulated region. Surprisingly, in the *aprABC* study previously cited [51], the locus, placed in Rv2392-Rv2397, was described to be upregulated by acidic pH and PhoP-dependent, however the biochemical function of its products was unknown. *mcr7* matches with the region and the phenotype described for the *aprABC* locus in the work of Abramovitch *et al.*.

2.3. Intracellular expression of the PhoP regulon in different cell types.

Mtb is known to be an intracellular pathogen, it infects and multiplies in phagocytic cells like macrophages; it can also infect non-phagocytic cells like fibroblasts or epithelial cells, and proliferate inside them [52]. Macrophages are the first line of defense for the host, presenting a high number of vacuoles containing acidic pH, hydrolases and lytic enzymes that leads to an oxidative response producing H_2O_2 and NO, toxic for the bacilli [53]. On the other hand, mycobacteria has an important role blocking or retarding acidification of the phagolysosome and avoiding lysosomal fusion through the manipulation of host signal transduction pathways.

One of the first signals encountered when the mycobacteria enter into the phagosome hostile environment, is the acidic pH. Since we have already studied the expression in *in-vitro* assays, we decided to confirm the pH driven phenotype in *ex vivo* conditions.

2.3.1. Comparative expression studies between phagocytic and non-phagocytic cells using a GFP reporter system.

We wanted to compare PhoP-regulon expression inside two different cellular models, phagocytic and non-phagocytic cells, through the reporter system based on the fusion of the *pks2* promoter with the GFP protein as representative gene from the PhoP regulon.

As phagocytic cells, mouse alveolar macrophage MHS cell line was chosen; and mouse embryonic fibroblast MEF cell line was used as non-phagocytic cells. We infected the correspondent cells with the strains H37Rv and its *phoP* mutant both containing the described reporter. The cells were processed and fixed at different times post infection and fluorescence was measured using a flow cytometer (FACS); the registered fluorescence was normalized taking into consideration the auto-fluorescence of the cells. The intensity of the normalized fluorescence would be proportional to the

promoter activity and GFP production and accumulation, and consequently to the PhoP regulation.

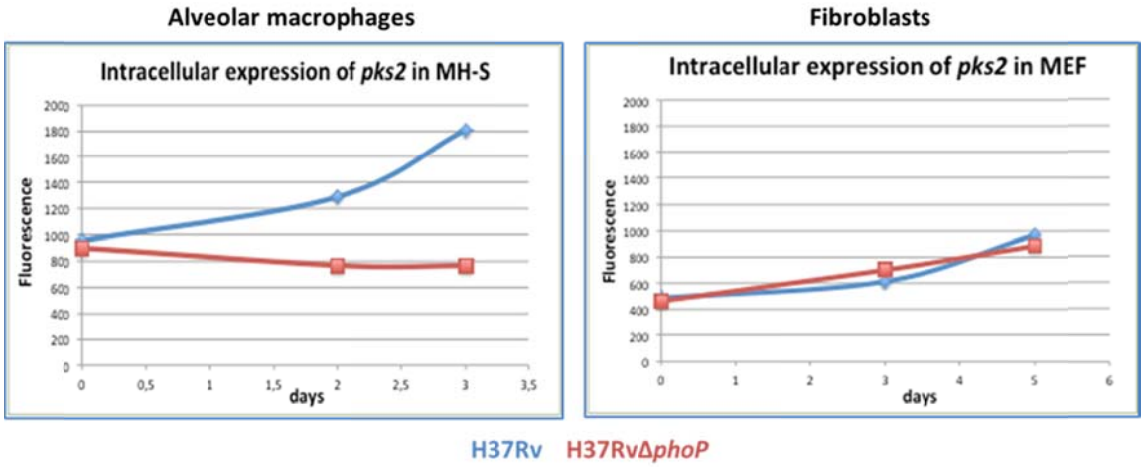

Figure 17. Mouse alveolar macrophages (MHS) and mouse fibroblast (MEF) were infected with a multiplicity of infection (MOI) of 10 for the MHS and 30 for the MEF, bacteria per cell with the H37Rv and its *phoP* mutant strains. Cells were analyzed by flow cytometry and data were normalized against the auto-fluorescence of the cells itself. In the wild-type strain there is an increase in the *pks2* promoter activity when it is infecting MHS cells, non-observed in the *phoP* mutant strain or when infecting MEF cells. Representative graphs from triplicate experiments.

We can observe how *pks2* induction is abolished in the *phoP* mutant in macrophages, but not in fibroblasts (Figure 17), suggesting that PhoP respond to intraphagosomal conditions. Below we can observe dot plots images obtained from cytometry analysis of one MHS representative infection experiment, where the population cells R2 moves to the right as its fluorescence increase, meaning they are infected with GFP^{+}-strains (Figure 18).

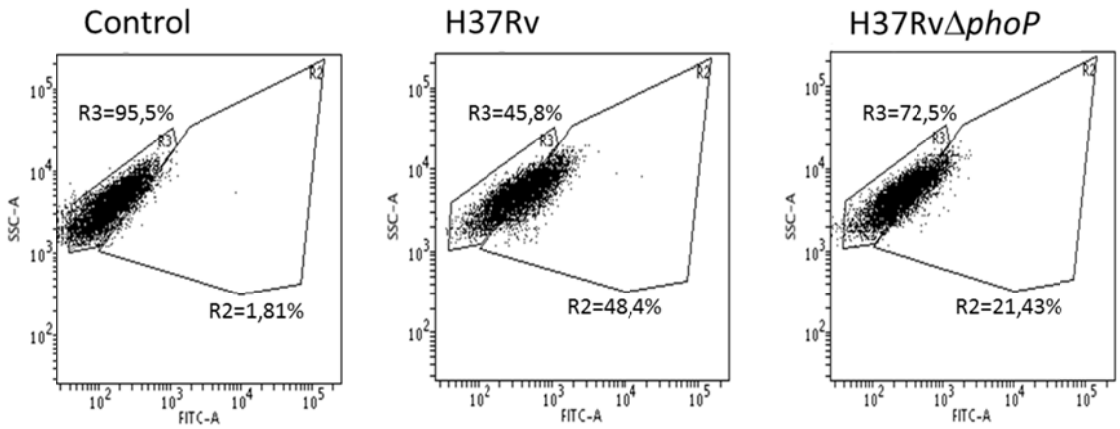

Figure 18. Cytometry dot plots of a representative experiment of MHS cell line infection. Here we are able to observe the cells taking into consideration their shape (SSC-A) and their green fluorescence (FITC-A). Control represents non-infected cells, and their autofluorescence (R3) was used to normalize the fluorescence obtained for the infected cells (R2). The population of cells moves to the right as its fluorescence increase, which is the case of the cells infected with the H37Rv strain. In the cells infected with the *phoP* mutant strain we barely can observe any increased in the fluorescence detected.

We also performed the experiment with another phagocytic cell line J774, fluorescence of the cells was measured by flow cytometry, and also colony forming units (CFU) were enumerated. We wanted to confirm that the effect observed was not due to wild-type replication inside macrophages, where the *phoP* mutant in unable to replicate. So the measured and normalized fluorescence (as described for MHS cells) was also normalized with the CFU per milliliter (CFU/ml) of mycobacteria contained in the infected cells.

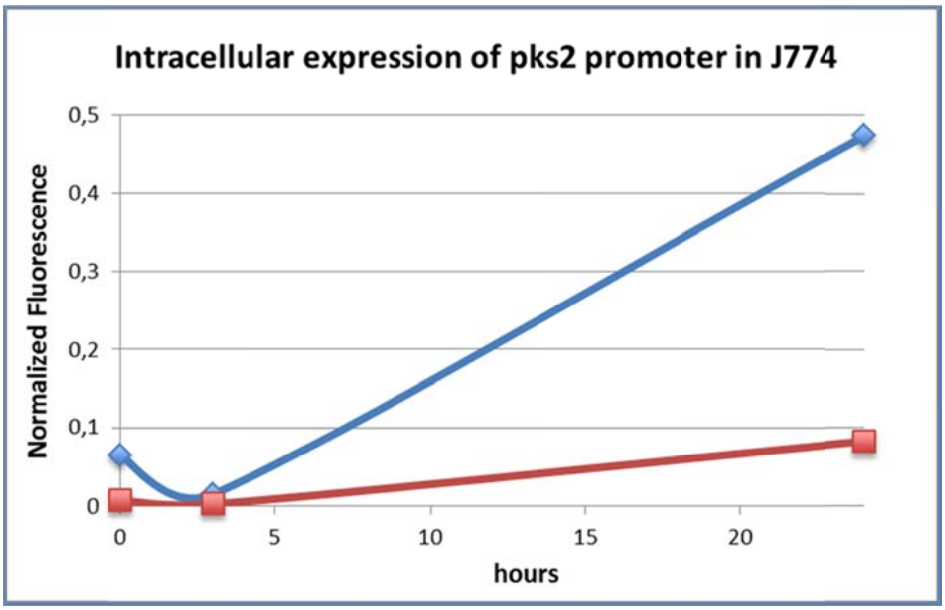

Figure 19. Phagocytic cell line J774 was infected with H37Rv and its *phoP* mutant containing the *pks2*::GFP construction with a MOI of 10 bacteria per cell. Cells were processed and analyzed by flow cytometry and also growing of the intracellular bacteria in solid media to CFU counting. Fluorescence registered was normalized versus the CFU counting. There is an increase in *pks2* promoter activity when the wild-type strain is infecting the cells that was not observed in the *phoP* mutant strain infection. Representative graph from a triplicate experiment.

In this experiment, time course was shorter than the one for MHS cells; cells were infected 24 hours before processing, in order to minimize bacterial replication. The activity of *pks2* promoter at 24 hour in the wild-type strain compared to the *phoP* mutant strain was considerably increased when the fluorescence registered was normalized with the number of intracellular bacteria (CFUs/ml). We can observe a significant increase in the expression of *pks2* promoter in the wild-type strain, not observed in the mutant one (Figure 19). This result in J774 cell line is consistent with the previous results obtained with the MHS macrophages cell line. In addition artifacts due to replication inside host cells can be discarded.

2.3.2. Direct measurement of gene expression profiles in activated and non-activated phagocytic cells.

We have already checked the correspondence between the GFP reporter system and the direct quantification by qRT-PCR of the *pks2* gene to study the activity of PhoP regulon in *in-vitro* conditions. Therefore we decided to verify the upregulation of *pks2* inside phagocytic cells compared to extracellular conditions, in both wild-type and *phoP* mutant strains.

For this assay we use bone marrow derived macrophages (BMDM) from C56BL/6 mice, some of them were activated with INFγ and LPS as it occurs *in vivo*. Cells were infected with H37Rv and its *phoP* mutant strain and processed to extract intracellular mycobacterial RNA after 24 hours post-infection. We performed qRT-PCR for direct quantification of *pks2* gene.

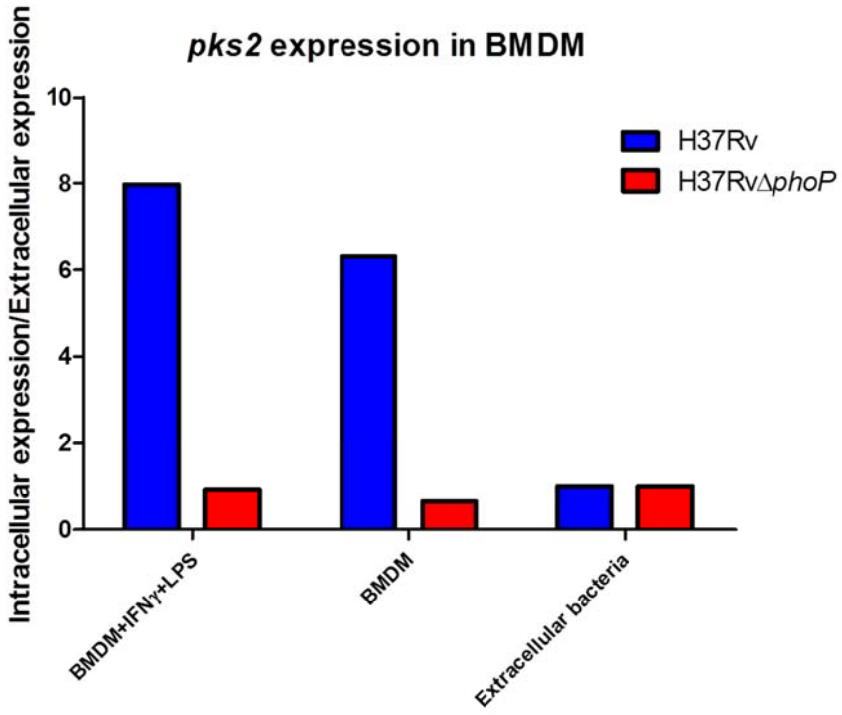

Figure 20. BMDM cells were infected with H37Rv and its *phoP* mutant with a MOI of 10 bacteria per cell. RNA of intracellular bacteria was extracted and *pks2* gene expression was directly quantified by qRT-PCR. Here we represent the *pks2* gene expression after 24 hours of infecting BMDM activated and non-activated cells and from extracellular bacterial culture, the expression was normalized against gene expression in extracellular bacteria. Representative graph from a duplicate experiment.

High expression levels were registered for *pks2* in intracellular conditions. This expression was higher for activated macrophages compared to resting cells, when compared with the expression of this gene in bacterial culture (Figure 20). These results are consistent with those obtained through the GFP reporter system in different cell lines; consequently we can conclude that the GFP reporter system is also a representative model for the PhoP regulon in intracellular expression study.

2.3.3. Time-dependent expression of the PhoP regulon in mouse bone marrow derived macrophages (BMDM).

Once we checked the correspondence between the signals obtained by the GFP reporter system and the direct study of the gene expression, in infected cells we wanted to study the *pks2* promoter expression kinetics at short times post-infection in phagocytic cells (BMDM). For this experiment we infected BMDM with H37Rv and its *phoP* mutant containing the GFP::*pks2* promoter-reporter system, cells were processed at 2, 8 and 20 hours post-infection and analyzed by flow cytometry.

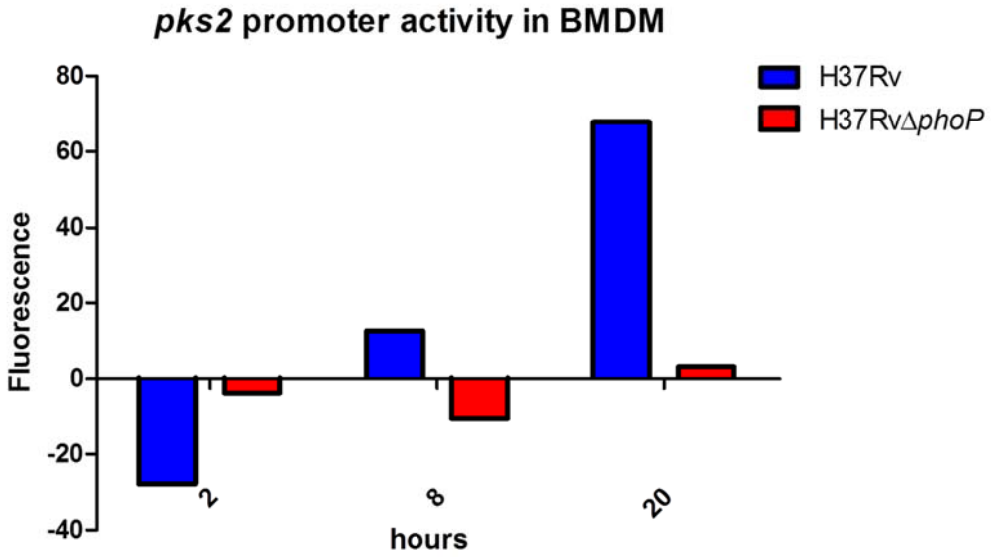

Figure 21. BMDM cells were infected with H37Rv and its *phoP* mutant strains containing the *pks2* promoter::GFP construction with a MOI of 10 bacteria per cell, and analyzed at short times post infection by flow cytometry. There is an increase in the activity of *pks2* promoter in the wild-type strain non-observed in the *phoP* mutant strain. Representative graph from a duplicate experiment.

pks2 promoter is activated in the wild-type strain at 8h post-infection and expression continues increasing up to 20h, which was the final time point of the experiment (Figure 21).

Simultaneously, cells were infected on cover glasses in order to analyze the expression kinetic with confocal microscopy. GFP fluorescence intensity observed is related with Mtb *pks2* promoter activity (green) inside the cells (red).

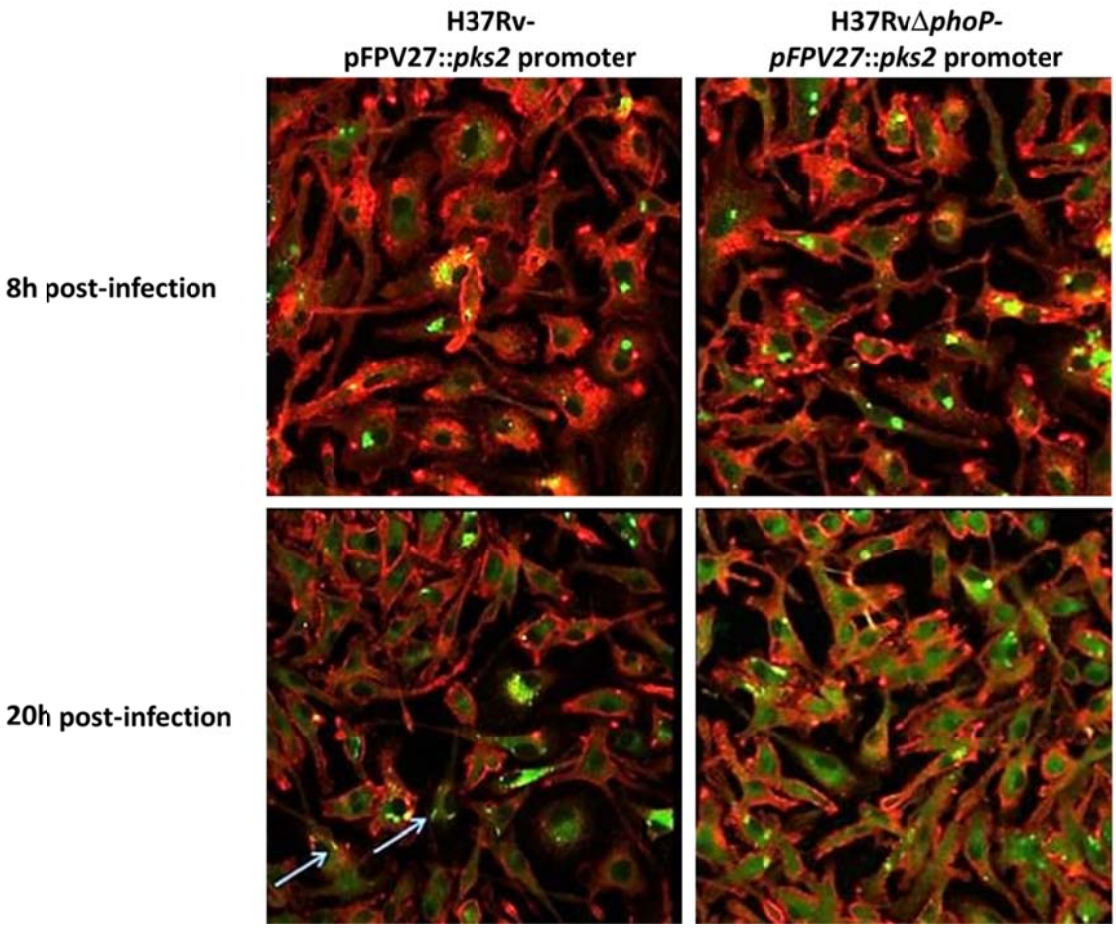

Figure 22. Infection of BMDM cells with H37Rv and its *phoP* mutant containing the *pks2* promoter::GFP construction was performed in coved glasses. After 8 and 20 hours of infection cells were fixed and analyzed by confocal microscopy. Well defined-green bacteria are observed in the infection with the wild-type strain at 20h post-infection due to the accumulation of GFP inside the bacteria, which is correlated with the *pks2* promoter activity. Residual fluorescence instead of defined bacteria is observed when infecting with the *phoP* mutant strain or at 8h post-infection point due to a low rate of GFP production.

Accordingly to flow cytometry results, for the wild-type strain, bacilli are well defined (pointed in figure) inside cells at 20h post-infection, meanwhile for the *phoP* mutant strain we can barely observe residual fluorescence due to GFP low expression levels (Figure 22).

2.3.4. Effects of phagosomal acidification over the PhoP regulon activity during cell infection.

One of the first hostile signals the mycobacteria find once inside the phagosome is the acidic environment. In this assay we want to study the impact on the PhoP regulon activity of bafilomycin, an H^+- ATPase inhibitor, whose effect is translated on an inhibition of the phagosomal acidification. We carried out the infection with Bafilomycin pre-treated cells on cover glasses that were processed at 20 hours post-infection. Cells were marked with Lysotracker (to verify the efficacy of the bafilomycin treatment) and fixed to be analyzed by microscopy.

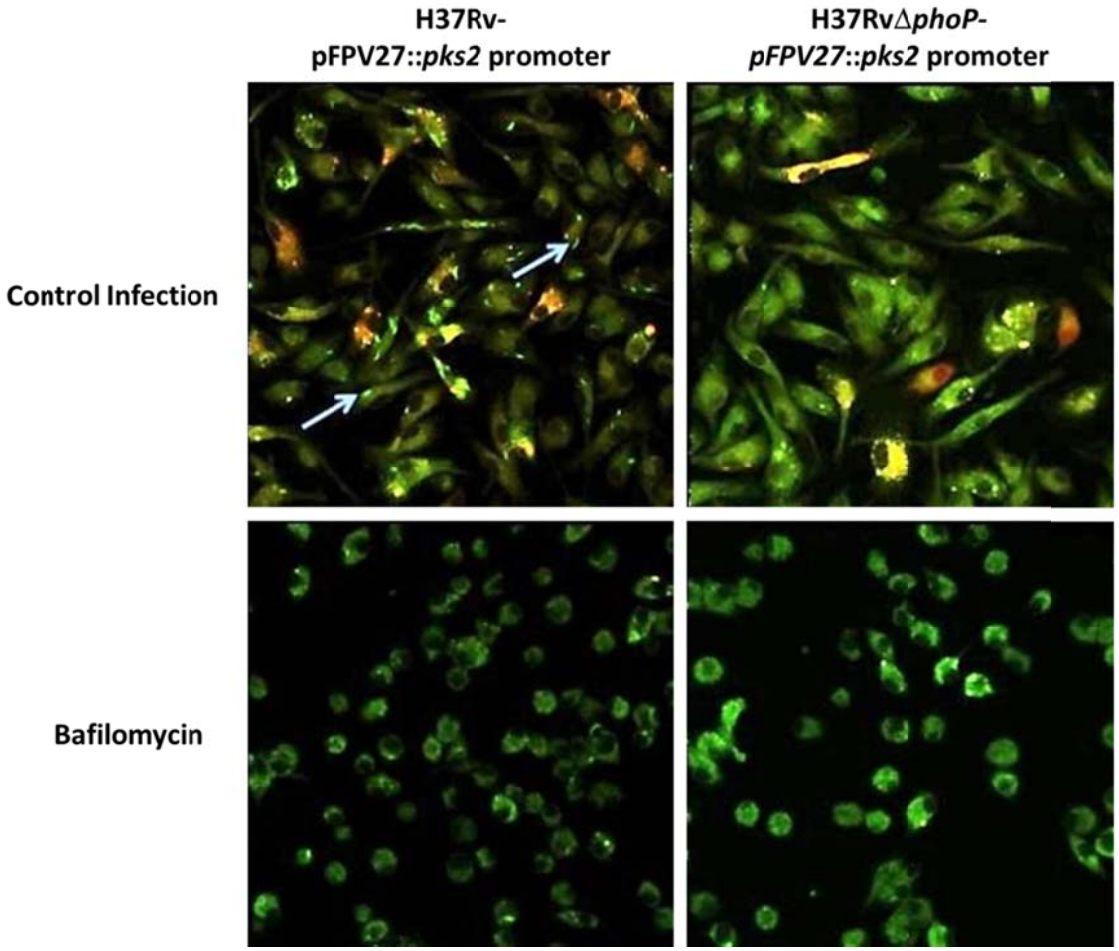

Figure 23. Infection of control and Bafilomycin pre-treated BMDM cells with H37Rv and its *phoP* mutant containing the *pks2* promoter::GFP construction was performed on coved glasses. After 8 and 20 hours of infection cells were processed, marked with Lysotracker probe and analyzed by confocal microscopy. Well defined-green bacteria are observed in the infection of non-treated cells with the wild-type strain at 20h post-infection due to the accumulation of GFP inside the bacteria, which is correlated with the

pks2 promoter activity. When BMDM are pre-treated with Bafilomycin, acidification of the phagosome is inhibited, and we can only observe residual fluorescence instead of defined bacteria. The same residual fluorescence is observed when infecting with the *phoP* mutant strain.

In non-treated cells (control), bacilli (green) colocalize with Lysotracker (red) marked compartments inside the cells, registered by an overlapping in both markers (yellow). Well defined mycobacteria are observed in cells infected with the wild-type strain but not in cells infected with the *phoP* mutant strain, where we can only observe residual fluorescence due to the low expression levels of the *pks2* promoter in this strain. In the case of Bafilomycin-treated cells, we were not able to observe Lysotracker marked compartments since phagosomal acidification was inhibited, and consequently, no GFP activity was observed due to absence of *pks2* promoter expression (Figure 23).

Infected cells were also processed (fixed) at 20h post infection and analyzed by flow citometry. Results from microscopy and by flow cytometry are both in concordance. The difference in fluorescence correspondent to H37Rv infected cells treated and untreated with Bafilomycin is significantly higher than the difference obtained for *phoP* mutant infected cells; meaning that the effect of the Bafilomycin dramatically decreases the levels of GFP fluorescence registered and in consequence, the expression of *pks2* gene in the case of wild-type infection, while in the *phoP* mutant infections the effect is considerably minor since the GFP fluorescence levels registered are much lower in a regular infection (Figure 24).

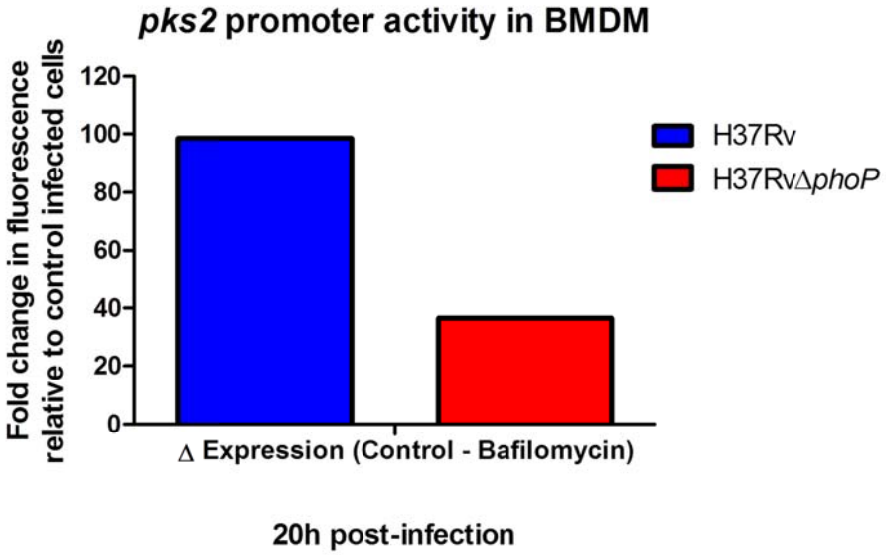

Figure 24. Infection of control and Bafilomycin pre-treated BMDM cells with H37Rv and its *phoP* mutant containing the *pks2* promoter::GFP construction. After 20 hours of infection cells were processed, and analyzed by FACS. Here is represented the difference in the fluorescence registered for untreated BMDM cells (Control) and Bafilomycin-treaded BMDM cells (Bafilomycin). The Δ-Expression is significantly higher for cells infected with the wild-type strain than for cells infected with the *phoP* mutant. Representative graph from a duplicate experiment.

DISCUSSION

Mtb is a known intracellular pathogen which preferentially infects alveolar macrophages. Once inside the cells the mycobacteria are rapidly engulfed in the phagosome, trying to contain the infection. Meanwhile, Mtb senses the host signals and activates its virulence network in order to protect itself and to avoid lysosomal fusion of the phagosome through the manipulation of host signal transduction pathways, this ability gives it the capacity to persist and replicate within macrophages [42].

In the present study we wanted to analyze the host signal(s) that activates the PhoPR TCS of Mtb. In a first approach we used a gene activity reporter system based on the fusion of some PhoP-regulated genes promoter region with *gfp* (green fluorescent protein) gene to perform a wider study of different stress conditions. But GFP has a limitation since it is necessary to accumulate enough protein amounts to be detected by the fluorimeter. Consequently the response we register is slower than the real one. Finally we carried out a deeper gene expression study through RNA extraction and semi-quantitative qRT-PCR where expression of the genes is detected in a much direct and reliable way.

Based on our results studying the effect of several extracellular stimuli, PhoP system might respond to acidic pH and it triggers the expression of the PhoP "core" regulon. The acidic pH is one of the first stresses that mycobacteria have to face inside the macrophage phagosome. Besides these extracellular assays, we validated our hypothesis *ex-vivo*, where we were able to observe a response in the activity of *pks2*, chosen as PhoP regulon reporter gene, under intracellular conditions. There was a notably increase in the expression of *pks2* when Mtb is infecting phagocytic cells, meanwhile no changes are detected when is infecting non-phagocytic cells or when the infection is carried out with the *phoP* mutant strain, demonstrating once again that it is a PhoP-dependent phenotype. Additionally, the expression is repressed when we used a phagosomal acidification inhibitor during the infection of phagocytic cells, reinforcing the suggested role of the pH in activating PhoPR.

We propose that the acidic environment initiates a specific kinetic mechanism activating PhoPR-regulated genes depending on the lifecycle of Mtb during infection.

One of the first genes expressed when the bacteria are exposed to acidic conditions are those implicated in lipid metabolism, like *pks2*, which is highly overexpressed at very short times of acidic exposure. There is also overexpression of *lipF* and *pks3* genes. It is possible that, to face the acidic environment, the bacteria activates the production of SL, DAT and PAT which have an important role in the host-mycobacteria interaction and mainly modifies components of the cell wall to protect itself [54]. These responses were only registered for the wild type strain, but not for the *phoP* mutant one, demonstrating that is a PhoP-mediated response.

Genes involved in oxidative stress like *nark1* are also overexpressed at short times after exposure to acidic pH; its product is implicated in the excretion of nitrite, helping the bacteria to face the respiratory stress [45, 49]. Likewise the acidic stress, the oxidative stress is a mechanism of phagosomal defense against bacteria, so it could be possible that in response to acidic stress, PhoP also activates the genes to help the bacteria to survive inside the macrophage.

Meanwhile *mcr7* which is the most PhoP-regulated region, it is not responding to acidic pH at short times of exposure. A highly marked overexpression started up to day 6 of exposure. Mcr7 was predicted to highly interact with ribosome binding site of the *tatC* gene, Mcr7 probably prevents ribosome loading and consequently translation of *tatC* mRNA. TatC gene encodes a transmembrane protein part of the TatABC secretory apparatus required for export of proteins with a twin arginine motif such as the Ag85 complex, immunodominant antigens involved in binding to human fibronectin important for cell adhesion and invasion [14]. Consequently, activation of *mcr7* at long time post-infection would result in decreased export of Ag85 complex.

According to the results, we propose a model of virulence where Mtb needs to interact with the host once it is engulfed by the macrophage in order to stimulate the innate immune response [42]. Inside the macrophage, bacteria are rapidly absorbed by the phagosome where it will find a hostile environment with acidic pH and oxidative stress mainly [53]. Acidic pH might activate the PhoPR TCS, starting the regulatory cascade. In this early phase of the infection it is important the presence of immunodominant agents as the Ag85 complex [55] or the sulfolipids present in the envelope [54], for these to occur it would be a reforming process of the cell wall in order to protect the bacteria and to stimulate host interactions. The first genes activated by the PhoP transcriptional regulator and, consequently expressed, are those implicated in the lipid metabolism as *pks2*, *pks3* and *lipF*; *nark1* gene is also expressed in this early response to help facing the oxidative stress. The PhoP-regulated region, *mcr7* increase its expression levels at long post-infection times. Since *mcr7* regulates the post-translational inhibition of the TAT secretory system, low levels of *mcr7* at early times post-infection suggest us the importance of having this secretory system actively working in order to allow immunodominant TAT-substrates (Ag85 complex) to be secreted by mycobacteria to interact with the host and to stimulate the immune system [23, 56]. In this regard it is important to remember that mycobacterial antigens are evolutionarily hyperconserved (Figure 25). This highlight the importance of immune recognition of Mtb [57].

On the other hand, the ESX-1 secretory system, where EsxA (ESAT-6) [32], EsxB (CFP-10), EspA and EspC are well known to be also PhoP-dependent, is going to play a key role [27] in inducing the phagosomal rupture and in consequence Mtb will escape to the cytosol [9]. This will happen up to 3-5 days post infection (Figure 25), being ESAT-6 and CFP-10 the key effector molecules of the ESX-1 system, generating pores in the phagosomal membrane and inducing the escape to the cytosol of Mtb [27]. Phagosomal escape allows the mycobacteria to overcome the immune control and favor bacterial dissemination [36], reported ESX-1 related effects in tubercle bacilli include the suppression of pro-inflammatory responses, necrosis, apoptosis, membrane-lysis and cytolysis [27].

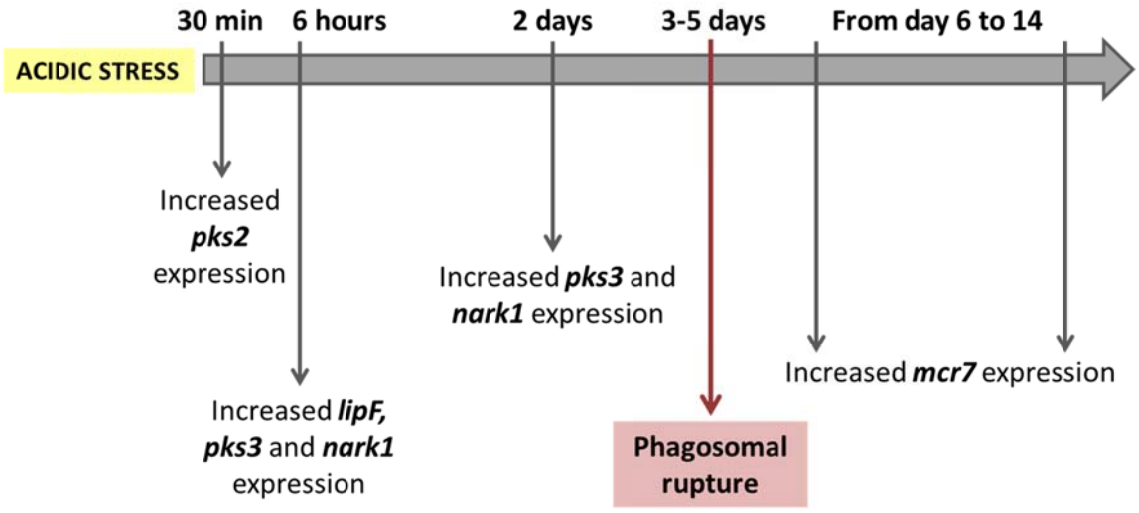

Figure 25. Time course of the activation of PhoP-regulated genes in response to acidic stress. The expression of those genes involved in lipid metabolism is induced at early times, like *pks2* which upregulation is registered up to 30min after inducing acidic stress. Genes involved in oxidative stress are induced at early times and its upregulation last longer, up to 2 days. Meanwhile the ncRNA *mcr7,* implicated in the negative regulation of Tat secretory system, is induced up to 6 day post acidic stress until the end point of the assays at 14 days.

At this time of the infection, the levels of expression of the genes highly activated described before, like *pks2*, *lipF* or *nark1*, are considerably lower. Since the environment has changed to the gentle cytosol and bacteria are no longer inside the phagosome. On the contrary, the expression of *mcr7* is highly increased, which means the TatC protein it is not going to be synthesized, and in consequence the components from the Ag85 complex are not going to be exported. The inhibition of the secretion of these immunodominant antigens is coherent with a model in which, once in the cytosol, bacteria need to be "discrete" for antigen presentation in order to escape the immune system and survive.

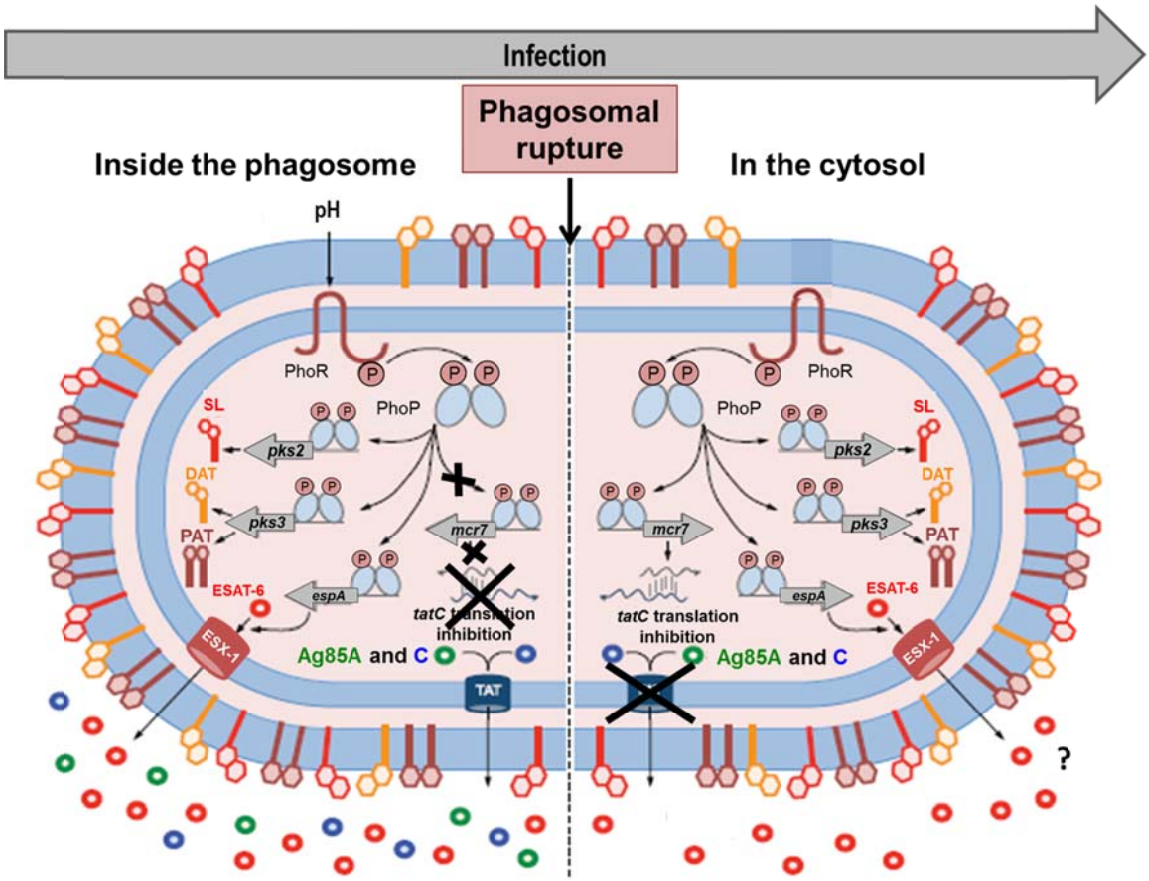

Figure 26. Illustration of the PhoPR-regulated phenotype in Mtb. Mtb is able to sense its cognate stimulus (pH) and subsequently phosphorylate PhoP. Phosphorylated PhoP regulates three well-known phenotypes, including synthesis of SL and DAT/PAT (via *pks2* and *pks3* regulation), secretion of ESAT-6 (through *espA* regulation), and posttranscriptional regulation of *tatC* (mediated by the *mcr7* ncRNA). These three events follow a time course depending on the lifecycle of Mtb where firstly genes involved in lipid metabolism are PhoP-activated in order to protect the bacteria from the acidic and hostile phagosomal environment, antigens from Ag85 Complex are secreted through TAT system favoring the interactions with the host immune system; secretion of ESAT-6 and CFP-10 are PhoP and EspR-activated through ESX-1 secretory system in order to facilitate the phagosomal escape of the bacteria; and finally, in more advanced stages of the infection, PhoP activates the transcription of Mcr7, which would initiate the post-translational regulation of TatC gene and subsequently the inhibition of TAT secretory system substates (Ag85 complex) . Adapted from [58].

The pathogenic potential of Mtb is intimately linked to the interplay between the host defense and the persistence of the mycobacteria. The intracellular localization and cytosolic access of the bacterium has substantial consequences on the recognition of mycobacteria-associated patterns by the cytosolic receptors of the innate immunity

that determine innate and adaptive immune responses and ultimately the face of the host cell and the bacterium [59]. Subsequent to phagocytosis, in order to avoid the acidified environment generated by the phagosome-lysosome fusion, some specialized intracellular bacteria, such as *Shigella flexneri*, *Lysteria monocytogenes* or *Francisella tularensis*, evolved to rapidly escape from phagosomes into the cytosol [60-62]. In contrast, Mtb has been described as a bacterium that resists degradation in the phagosome by inhibiting the fusion with lysosomes, a characteristic feature that seems to protect the bacilli from bactericidal mechanisms of the phagocytes and allows intracellular survival and multiplication; at later stages of infection ESX-1-dependent vacuolar breakage might be an important requirement for the pathogenic potential of Mtb [63]. In addition, recent studies have demonstrated how the partial inhibition of phagosome acidification emerges as a prerequisite to mycobacterial phagosomal rupture, plausible only when phagosome acidification is partially inhibited, mycobacteria may survive; use their virulence factors and induce phagosomal membrane disruption [63].

Concluding, our results strongly suggest the key role of the acidic stress in the activation of the key TCS PhoPR, which not only initiates the mycobacterial mechanism of virulence but also carry out its function as transcriptional regulator during infection depending on the lifecycle of Mtb and its needs (Figure 26).

REFERENCES

1. Bretl, D.J., C. Demetriadou, and T.C. Zahrt, *Adaptation to environmental stimuli within the host: two-component signal transduction systems of Mycobacterium tuberculosis.* Microbiol Mol Biol Rev, 2011. **75**(4): p. 566-82.
2. Salzberg, L.I., et al., *Genome-wide analysis of phosphorylated PhoP binding to chromosomal DNA reveals several novel features of the PhoPR-mediated phosphate limitation response in Bacillus subtilis.* J Bacteriol, 2015. **197**(8): p. 1492-506.
3. Perez, E., et al., *An essential role for phoP in Mycobacterium tuberculosis virulence.* Mol Microbiol, 2001. **41**(1): p. 179-87.
4. Walters, S.B., et al., *The Mycobacterium tuberculosis PhoPR two-component system regulates genes essential for virulence and complex lipid biosynthesis.* Mol Microbiol, 2006. **60**(2): p. 312-30.
5. Gonzalo Asensio, J., et al., *The virulence-associated two-component PhoP-PhoR system controls the biosynthesis of polyketide-derived lipids in Mycobacterium tuberculosis.* J Biol Chem, 2006. **281**(3): p. 1313-6.
6. Frigui, W., et al., *Control of M. tuberculosis ESAT-6 secretion and specific T cell recognition by PhoP.* PLoS Pathog, 2008. **4**(2): p. e33.
7. Pym, A.S., et al., *Loss of RD1 contributed to the attenuation of the live tuberculosis vaccines Mycobacterium bovis BCG and Mycobacterium microti.* Mol Microbiol, 2002. **46**(3): p. 709-17.
8. Houben, D., et al., *ESX-1-mediated translocation to the cytosol controls virulence of mycobacteria.* Cell Microbiol, 2012. **14**(8): p. 1287-98.
9. Simeone, R., et al., *Phagosomal rupture by Mycobacterium tuberculosis results in toxicity and host cell death.* PLoS Pathog, 2012. **8**(2): p. e1002507.
10. Derrick, S.C. and S.L. Morris, *The ESAT6 protein of Mycobacterium tuberculosis induces apoptosis of macrophages by activating caspase expression.* Cell Microbiol, 2007. **9**(6): p. 1547-55.
11. Aguilo, N., et al., *Bim is a crucial regulator of apoptosis induced by Mycobacterium tuberculosis.* Cell Death Dis, 2014. **5**: p. e1343.
12. Aguilo, J.I., et al., *ESX-1-induced apoptosis is involved in cell-to-cell spread of Mycobacterium tuberculosis.* Cell Microbiol, 2013. **15**(12): p. 1994-2005.
13. Nambiar, J.K., et al., *Protective immunity afforded by attenuated, PhoP-deficient Mycobacterium tuberculosis is associated with sustained generation of CD4+ T-cell memory.* Eur J Immunol, 2012. **42**(2): p. 385-92.
14. Solans, L., et al., *The PhoP-dependent ncRNA Mcr7 modulates the TAT secretion system in Mycobacterium tuberculosis.* PLoS Pathog, 2014. **10**(5): p. e1004183.
15. Gonzalo-Asensio, J., et al., *PhoP: a missing piece in the intricate puzzle of Mycobacterium tuberculosis virulence.* PLoS One, 2008. **3**(10): p. e3496.
16. Solans, L., *PhoP regulon characterization and its implication in protein secretion in Mycobacterium tuberculosis. New vaccine construction based on PhoP mutant.* , in *Microbiology, Preventive Medicine and Public Health Department*. 2014, Universidad de Zaragoza: Zaragoza.
17. Sirakova, T.D., et al., *The Mycobacterium tuberculosis pks2 gene encodes the synthase for the hepta- and octamethyl-branched fatty acids required for sulfolipid synthesis.* J Biol Chem, 2001. **276**(20): p. 16833-9.

18. Goyal, R., et al., *Phosphorylation of PhoP protein plays direct regulatory role in lipid biosynthesis of Mycobacterium tuberculosis.* J Biol Chem, 2011. **286**(52): p. 45197-208.
19. Belardinelli, J.M., et al., *Biosynthesis and translocation of unsulfated acyltrehaloses in Mycobacterium tuberculosis.* J Biol Chem, 2014. **289**(40): p. 27952-65.
20. Richter, L., et al., *Determination of the minimal acid-inducible promoter region of the lipF gene from Mycobacterium tuberculosis.* Gene, 2007. **395**(1-2): p. 22-8.
21. Zhang, M., et al., *Expression and characterization of the carboxyl esterase Rv3487c from Mycobacterium tuberculosis.* Protein Expr Purif, 2005. **42**(1): p. 59-66.
22. Cole, S.T., et al., *Deciphering the biology of Mycobacterium tuberculosis from the complete genome sequence.* Nature, 1998. **393**(6685): p. 537-44.
23. Huygen, K., *The Immunodominant T-Cell Epitopes of the Mycolyl-Transferases of the Antigen 85 Complex of M. tuberculosis.* Front Immunol, 2014. **5**: p. 321.
24. Kendall, S.L., et al., *The Mycobacterium tuberculosis dosRS two-component system is induced by multiple stresses.* Tuberculosis (Edinb), 2004. **84**(3-4): p. 247-55.
25. Leistikow, R.L., et al., *The Mycobacterium tuberculosis DosR regulon assists in metabolic homeostasis and enables rapid recovery from nonrespiring dormancy.* J Bacteriol, 2010. **192**(6): p. 1662-70.
26. Larsson, C., et al., *Gene expression of Mycobacterium tuberculosis putative transcription factors whiB1-7 in redox environments.* PLoS One, 2012. **7**(7): p. e37516.
27. Simeone, R., D. Bottai, and R. Brosch, *ESX/type VII secretion systems and their role in host-pathogen interaction.* Curr Opin Microbiol, 2009. **12**(1): p. 4-10.
28. Cao, G., et al., *EspR, a regulator of the ESX-1 secretion system in Mycobacterium tuberculosis, is directly regulated by the two-component systems MprAB and PhoPR.* Microbiology, 2015. **161**(Pt 3): p. 477-89.
29. Rosenberg, O.S., et al., *EspR, a key regulator of Mycobacterium tuberculosis virulence, adopts a unique dimeric structure among helix-turn-helix proteins.* Proc Natl Acad Sci U S A, 2011. **108**(33): p. 13450-5.
30. Blasco, B., et al., *Virulence regulator EspR of Mycobacterium tuberculosis is a nucleoid-associated protein.* PLoS Pathog, 2012. **8**(3): p. e1002621.
31. He, X. and S. Wang, *DNA consensus sequence motif for binding response regulator PhoP, a virulence regulator of Mycobacterium tuberculosis.* Biochemistry, 2014. **53**(51): p. 8008-20.
32. Garces, A., et al., *EspA acts as a critical mediator of ESX1-dependent virulence in Mycobacterium tuberculosis by affecting bacterial cell wall integrity.* PLoS Pathog, 2010. **6**(6): p. e1000957.
33. Solans, L., et al., *A specific polymorphism in Mycobacterium tuberculosis H37Rv causes differential ESAT-6 expression and identifies WhiB6 as a novel ESX-1 component.* Infect Immun, 2014. **82**(8): p. 3446-56.
34. Minch, K.J., et al., *The DNA-binding network of Mycobacterium tuberculosis.* Nat Commun, 2015. **6**: p. 5829.

35. Brodin, P., et al., *Dissection of ESAT-6 system 1 of Mycobacterium tuberculosis and impact on immunogenicity and virulence.* Infect Immun, 2006. **74**(1): p. 88-98.
36. Xu, J., et al., *A unique Mycobacterium ESX-1 protein co-secretes with CFP-10/ESAT-6 and is necessary for inhibiting phagosome maturation.* Mol Microbiol, 2007. **66**(3): p. 787-800.
37. Munoz-Elias, E.J. and J.D. McKinney, *Mycobacterium tuberculosis isocitrate lyases 1 and 2 are jointly required for in vivo growth and virulence.* Nat Med, 2005. **11**(6): p. 638-44.
38. Eoh, H. and K.Y. Rhee, *Methylcitrate cycle defines the bactericidal essentiality of isocitrate lyase for survival of Mycobacterium tuberculosis on fatty acids.* Proc Natl Acad Sci U S A, 2014. **111**(13): p. 4976-81.
39. Martin, C., et al., *The live Mycobacterium tuberculosis phoP mutant strain is more attenuated than BCG and confers protective immunity against tuberculosis in mice and guinea pigs.* Vaccine, 2006. **24**(17): p. 3408-19.
40. Kremer, L., et al., *Green fluorescent protein as a new expression marker in mycobacteria.* Mol Microbiol, 1995. **17**(5): p. 913-22.
41. Barker, L.P., D.M. Brooks, and P.L. Small, *The identification of Mycobacterium marinum genes differentially expressed in macrophage phagosomes using promoter fusions to green fluorescent protein.* Mol Microbiol, 1998. **29**(5): p. 1167-77.
42. Russell, D.G., *Who puts the tubercle in tuberculosis?* Nat Rev Microbiol, 2007. **5**(1): p. 39-47.
43. Richter, L. and B. Saviola, *The lipF promoter of Mycobacterium tuberculosis is upregulated specifically by acidic pH but not by other stress conditions.* Microbiol Res, 2009. **164**(2): p. 228-32.
44. Munoz-Elias, E.J., et al., *Role of the methylcitrate cycle in Mycobacterium tuberculosis metabolism, intracellular growth, and virulence.* Mol Microbiol, 2006. **60**(5): p. 1109-22.
45. Soldati, T. and O. Neyrolles, *Mycobacteria and the intraphagosomal environment: take it with a pinch of salt(s)!* Traffic, 2012. **13**(8): p. 1042-52.
46. Botella, H., et al., *Mycobacterial p(1)-type ATPases mediate resistance to zinc poisoning in human macrophages.* Cell Host Microbe, 2011. **10**(3): p. 248-59.
47. Botella, H., et al., *Metallobiology of host-pathogen interactions: an intoxicating new insight.* Trends Microbiol, 2012. **20**(3): p. 106-12.
48. Wagner, D., et al., *Elemental analysis of Mycobacterium avium-, Mycobacterium tuberculosis-, and Mycobacterium smegmatis-containing phagosomes indicates pathogen-induced microenvironments within the host cell's endosomal system.* J Immunol, 2005. **174**(3): p. 1491-500.
49. Aussel, L., et al., *Salmonella detoxifying enzymes are sufficient to cope with the host oxidative burst.* Mol Microbiol, 2011. **80**(3): p. 628-40.
50. Rodriguez, J.G., et al., *Global adaptation to a lipid environment triggers the dormancy-related phenotype of Mycobacterium tuberculosis.* MBio, 2014. **5**(3): p. e01125-14.
51. Abramovitch, R.B., et al., *aprABC: a Mycobacterium tuberculosis complex-specific locus that modulates pH-driven adaptation to the macrophage phagosome.* Mol Microbiol, 2011. **80**(3): p. 678-94.

52. Ferrer, N.L., et al., *Intracellular replication of attenuated Mycobacterium tuberculosis phoP mutant in the absence of host cell cytotoxicity.* Microbes Infect, 2009. **11**(1): p. 115-22.
53. Dey, B. and W.R. Bishai, *Crosstalk between Mycobacterium tuberculosis and the host cell.* Semin Immunol, 2014. **26**(6): p. 486-96.
54. Passemar, C., et al., *Multiple deletions in the polyketide synthase gene repertoire of Mycobacterium tuberculosis reveal functional overlap of cell envelope lipids in host-pathogen interactions.* Cell Microbiol, 2014. **16**(2): p. 195-213.
55. Daffe, M., *The mycobacterial antigens 85 complex - from structure to function and beyond.* Trends Microbiol, 2000. **8**(10): p. 438-40.
56. Coscolla, M., et al., *M. tuberculosis T Cell Epitope Analysis Reveals Paucity of Antigenic Variation and Identifies Rare Variable TB Antigens.* Cell Host Microbe, 2015. **18**(5): p. 538-48.
57. Comas, I., et al., *Human T cell epitopes of Mycobacterium tuberculosis are evolutionarily hyperconserved.* Nat Genet, 2010. **42**(6): p. 498-503.
58. Broset, E., C. Martin, and J. Gonzalo-Asensio, *Evolutionary landscape of the Mycobacterium tuberculosis complex from the viewpoint of PhoPR: implications for virulence regulation and application to vaccine development.* MBio, 2015. **6**(5): p. e01289-15.
59. Behar, S.M., M. Divangahi, and H.G. Remold, *Evasion of innate immunity by Mycobacterium tuberculosis: is death an exit strategy?* Nat Rev Microbiol, 2010. **8**(9): p. 668-74.
60. Ray, K., et al., *Tracking the dynamic interplay between bacterial and host factors during pathogen-induced vacuole rupture in real time.* Cell Microbiol, 2010. **12**(4): p. 545-56.
61. Barel, M. and A. Charbit, *Francisella tularensis intracellular survival: To eat or to die.* Microbes Infect, 2013.
62. Cossart, P., *Illuminating the landscape of host-pathogen interactions with the bacterium Listeria monocytogenes.* Proc Natl Acad Sci U S A, 2011. **108**(49): p. 19484-91.
63. Simeone, R., et al., *Cytosolic access of Mycobacterium tuberculosis: critical impact of phagosomal acidification control and demonstration of occurrence in vivo.* PLoS Pathog, 2015. **11**(2): p. e1004650.

Chapter 3:
Study of a new vaccine generation based on MTBVAC *zmp1*$^{-}$.

INTRODUCTION

The only existing licensed vaccine against tuberculosis (TB) is an attenuated strain of *M. bovis* Bacille Calmette-Guerin (BCG) which has been used worldwide since 1921 when it was first administrated to a newborn with a household contact of TB. BCG confers protection against severe forms of TB (meningitis and miliary TB) in children but lacks consistency preventing the pulmonary disease, the most common transmissible form [1]. Even though BCG is considered very safe, serious immunodeficiency states have been associated with increased risk of systemic BCG dissemination post-vaccination [2]. The risk groups, for which vaccination with BCG is contraindicated, include patients with primary and secondary immunodeficiency and HIV-infected people, including HIV-infected newborn infants [1]. There has been particular concern in HIV implications into BCG vaccination safety [3]. A recent retrospective study documented a high frequency of BCG infection with complications in HIV-infected infants [4]. Current WHO vaccination policy includes a recommendation not to vaccinate with BCG infants known to be HIV-infected, with or without infection symptoms [1].

Very substantial efforts have been made over the past decade to develop vaccines against TB, including vaccines targeting individuals in risk of immune suppression [5]. Various preventive strategies in the current Global TB vaccine Portfolio include recombinant BCG strains, boost subunit vaccines for use in BCG-immunized individuals or live attenuated *M. tuberculosis* (Mtb) strains at different stages of clinical and preclinical trial development [6].

MTBVAC, a live attenuated Mtb vaccine based on two independent stable deletion mutations, without antibiotic resistance markers, in the virulence genes *phoP* and *fadD26*, is currently the first and only vaccine to fulfill the Geneva consensus criteria for progressing new live mycobacterial vaccines to clinical evaluation [7, 8]. MTBVAC has been the first vaccine based on Mtb attenuation to enter and complete clinical

phase I trials (NCT02013245) [9], and currently has entered in clinical trials phase II with newborns in South Africa (NCT02729571).

Considering individuals in risk of immune suppression as a possible target population for MTBVAC, here we describe the hyperattenuated profile of a vaccine based on MTBVAC with an additional inactivation in the *zmp1* gene. This gene encodes a putative Zn^{2+} metalloprotease implicated in intracellular survival of mycobacteria [10]. The *zmp1* gene plays a critical role in preventing the inflammasome activation. The inflammasome is a multiprotein complex composed by members of the cytosolic sensor proteins family called nucleotide binding oligomerization domain which, once activated upon recognition of pathogen-associated molecules in the extracellular or the intracellular compartments, drives the activation of pro-caspase-1. Activated caspase-1, proteolitically activates pro-IL-1β in to IL-1β, which once secreted, in an autocrine and paracrine fashion triggers the phagosome fusion with intracellular lysosomes and the early inflammatory response [11].

Phagolysosomes are equipped with the machinery to generate peptide-MHC class II complexes, and inhibition of phagosome-lysosome fusion is one proposed mechanism by which Mtb may escape efficient MHC class II antigen presentation [12]. Arrest of phagosome maturation may also affect cross-presentation of mycobacterial peptides via the putative phagosome-to-cytosol MHC class II antigen presentation pathway or via MHC class I presentation that occurs by fusion and fission of phagosomes with endoplasmic reticulum-derived vesicles containing newly synthesized MHC class I molecules [13].

Consequently an Mtb strain, with *zmp1* disrupted, during mice infection might allow the inflammasome activation and an increased IL-1β secretion, which is traduced in an enhanced maturation of mycobacterial-containing phagosomes, in a better MHC I antigen cross-presentation, and in an improved mycobacterial clearance by macrophages and lower bacterial burden in the lungs of infected mice [10].

Here we describe the construction and preclinical characterization of a live-attenuated vaccine based on Mtb (*phoP*$^{-}$, *fadD26*$^{-}$ and *zmp1*$^{-}$) conceived to be administrated to patients in risk of immune suppression.

This work was done in collaboration with Peter Sander group, from the University of Zurich.

3.1. *zmp1* inactivation in MTBVAC.

Different *zmp1* mutants were obtained by using the classic double recombination system [14]. A suicide vector (called pZmp1) carrying a *sacB* gene (lethal in mycobacteria in presence of sucrose), Hyg^r (confers resistance to hygromycin), Km^r (confers resistance to kanamycin) and a *zmp1* gene with 777 bp deleted and 3 stop codons inserted instead (Figure 1). The vector has no resistance marker inside the gene in order to make easier the final selection of double recombinants, however it is a huge advantage since it is no necessary to eliminate it after the double recombination. The vector was provided by Peter Sander group, from the University of Zurich.

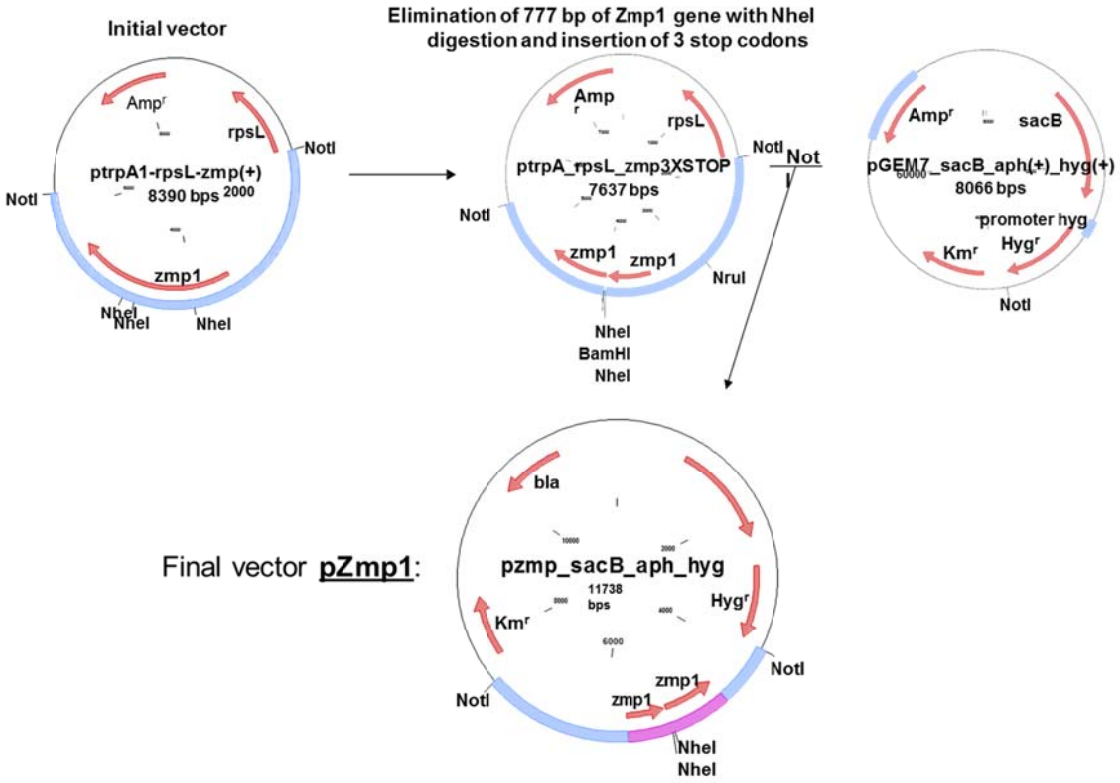

Figure 1. Shematic representation of pZmp1 construction. pZmp1 was constructed by Peter Sander team in Zurich University, Switzerland.

pZmp1 was transformed into Mt103 and MTBVAC and allelic exchange events were selected in two differentiated steps. In the first step (positive selection), single recombinant mutants were selected onto plates containing hygromycin and kanamycin

and were unable to grow in presence of sucrose (*sacB* is lethal in mycobacteria in presence of sucrose) (Figure 2).

In a second step (negative selection), single recombinant mutants were propagated in liquid media containing kanamycin and then plated in sucrose-supplemented plates to force a second recombination. Double recombinant mutants were selected onto plates containing sucrose, but they were unable to grow in plates containing hygromycin or kanamycin, indicating they had lost the Hyg^r and Km^r markers and the *sacB* gene (Figure 2). In this step either double recombination or reverting to wild type genotype could have happened with the same probability since there is no resistance marker inside the deleted gene that allows us an easier selection.

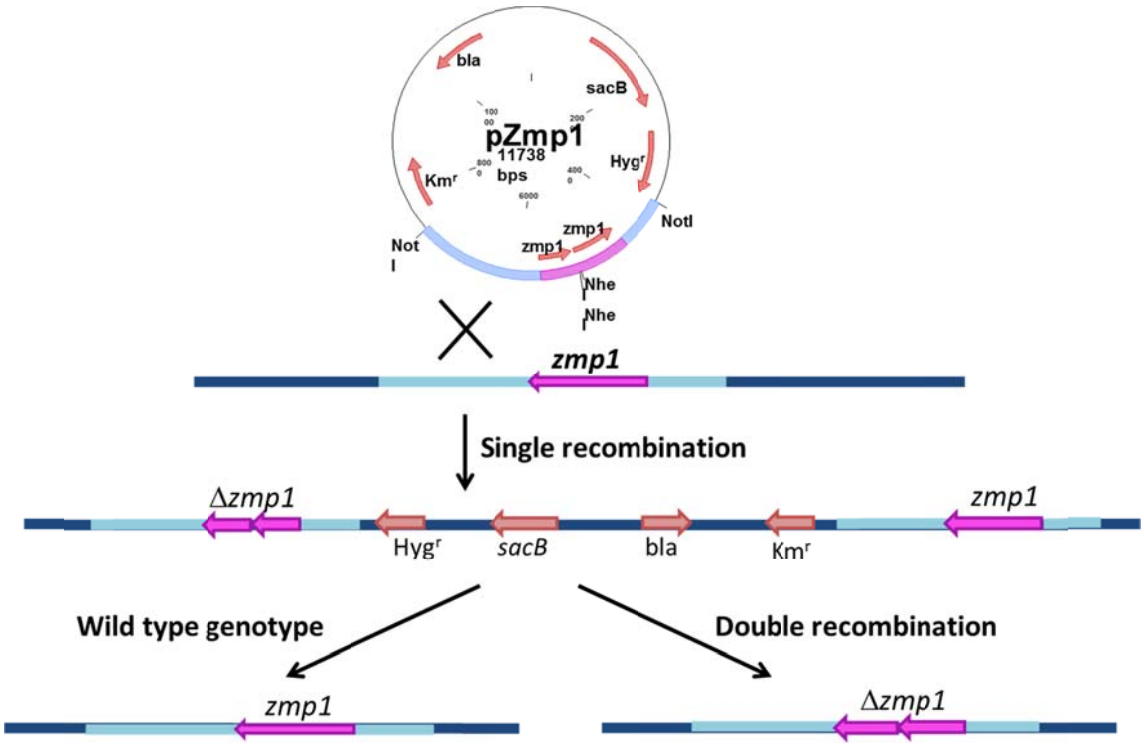

Figure 2. Schematic representation of double recombination in two steps. Positive-negative strategy for selection and isolation of double recombinant colonies. Single recombinant mutants were Km resistant, Hyg resistant and were sensitive to sucrose. Double recombinant mutants were sensitive to both Km and Hyg antibiotics and were resistant to sucrose.

Proper double recombination was analyzed by PCR using primers positioned flanking the deleted region inside the *zmp1* gene, Delzmp1-Fw and Delzmp1-Rv; and with two pairs of primers flanking the cloned region, in each pair one primer will be placed in the cloned region of the vector and the other one will be placed in the flanking genome region. These last pairs UPzmp1-Fw/UPzmp1-Rv and DOWNzmp1-Fw/DOWNzmp1-Rv were designed in order to confirm that the double recombination had placed in the right *zmp1* genome site (Figure 3).

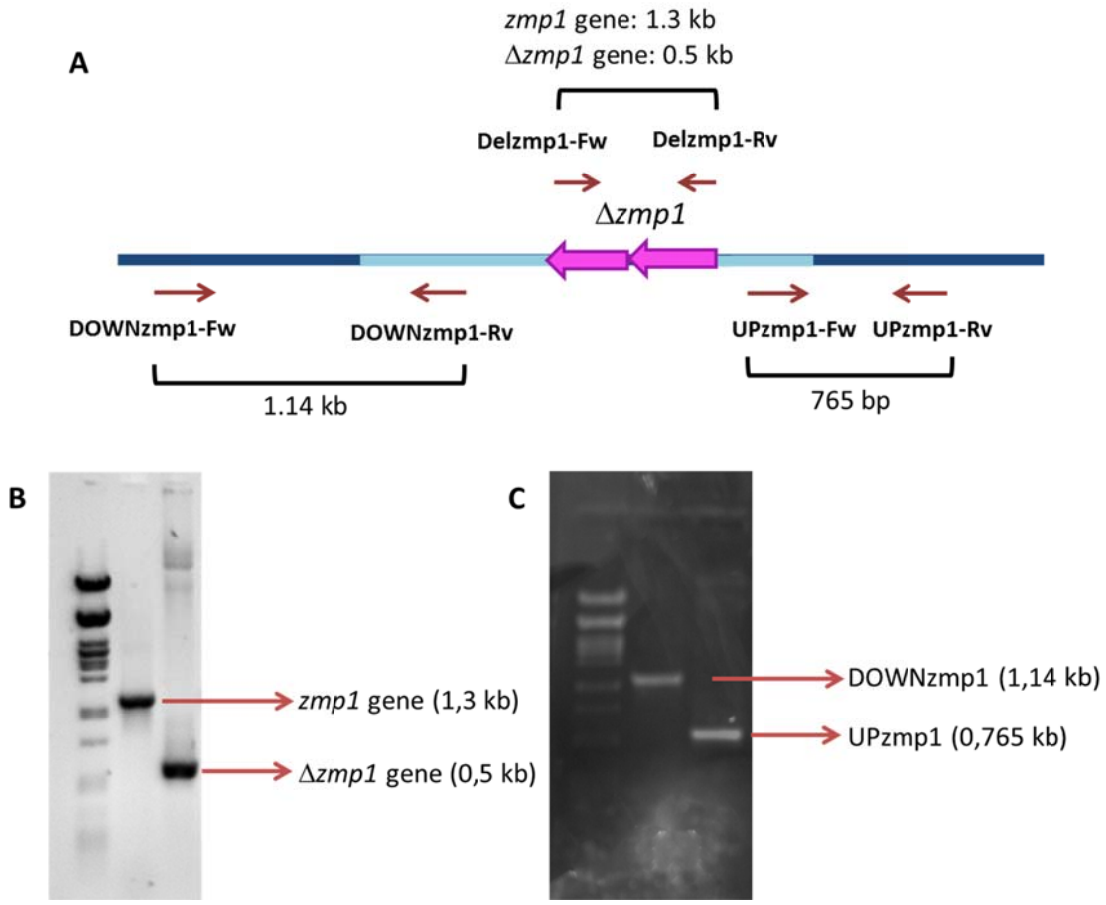

Figure 3. Characterization of *zmp1* deletion mutants. A. DNA was amplified using three pairs of primers, the delzmp1 pair allows us to differentiate the double recombinants from the wild type gene; the UPzmp1 and DOWNzmp1 pairs permit us to assure that the double recombination events had taken place in the right genome site. Double recombinants with *zmp1* gene deleted were obtained and PCR checked for Mt103 and MTBVAC strains. **B.** Agarose gel image allow us to differentiate the double recombinant mutants (Δ*zmp1*) from those whose genome has reverted to the wild type genotype (*zmp1*). **C.** Agarose gel image allow us to visualize the flanking fragments to confirm that the double recombination had placed in the right genome site.

3.2. Characterization of the triple mutant (*phoP*⁻, *fadD26*⁻ and *zmp1*⁻) strain.

3.2.1. Replication of MTBVAC *zmp1*⁻ in phagocytic and non-phagocytic cells.

First, we studied in a cellular model whether *zmp1* inactivation conferred additional attenuation to MTBVAC. Thus, murine cell line MHS was used as model of alveolar macrophages for replication experiments comparing Mt103, MTBVAC and MTBVAC *zmp1*⁻. At 72 hours post infection Mt103 replicated within MH-S cells 2 $\log_{10}$ orders, reaching 3 $\log_{10}$ orders after seven days post infection, MTBVAC and MTBVAC *zmp1*⁻ exhibited very similar impaired replication capacity with less than one $\log_{10}$ increase in seven days. We also performed the replication experiment in non-phagocytic cells using the murine cell line MEF, comparing MTBVAC and MTBVAC *zmp1*⁻. After seven days post infection MTBVAC *zmp1*⁻ replicates 1 $\log_{10}$ order less than MTBVAC (Figure 4).

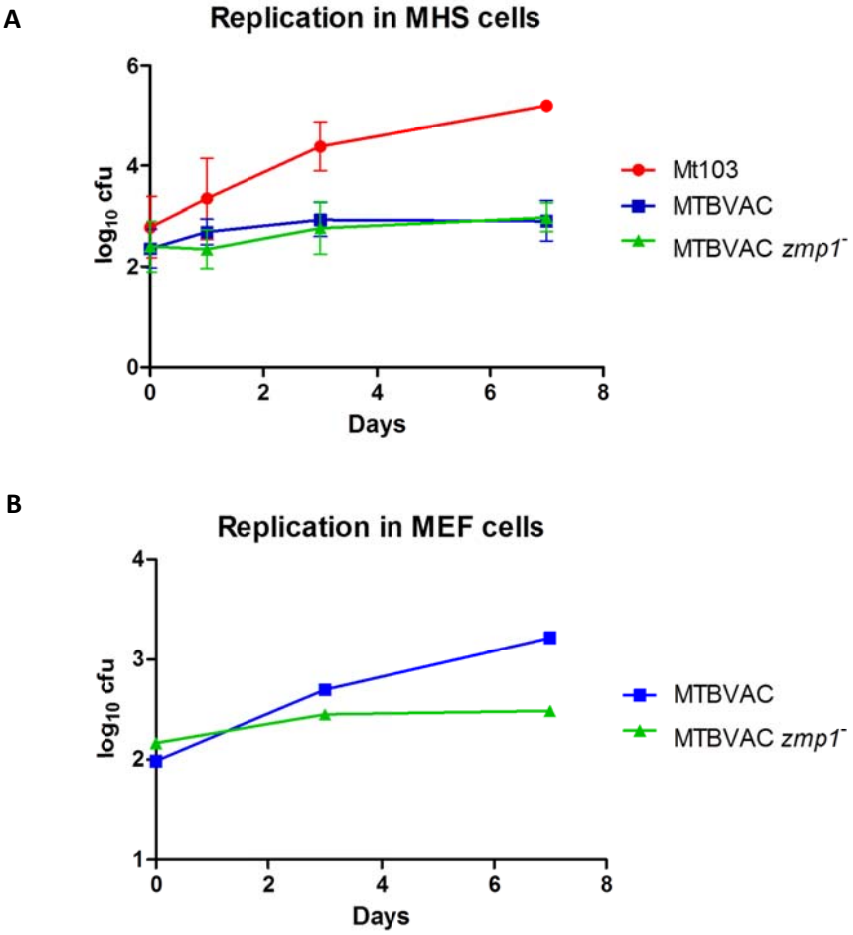

Figure 4. A. Intracellular replication in MH-S cell line. Average graph from a triplicate experiment. **B.** Intracellular replication in MEF non-phagocytic cell line.

3.2.2. Hyperattenuation studies in SCID mice

Next, we studied MTBVAC *zmp1*$^-$ attenuation in CB17 severe combined immunodeficiency (SCID) mouse, in comparison with Mt103, BCG Pasteur and MTBVAC following intraperitoneal administration. SCID mice are used for these kind of experiments since they are very susceptible to TB due to their lack in adaptive immune responses (T and B cells). SCID mice inoculated with MTBVAC *zmp1*$^-$ survived 134 days. When analyzed survival of the groups inoculated with MTBVAC and MTBVAC *zmp1*$^-$, data revealed no significant differences in their attenuation profile. Both vaccine candidates MTBVAC and MTBVAC *zmp1*$^-$ were significantly safer than BCG Pasteur in this model (Figure 5).

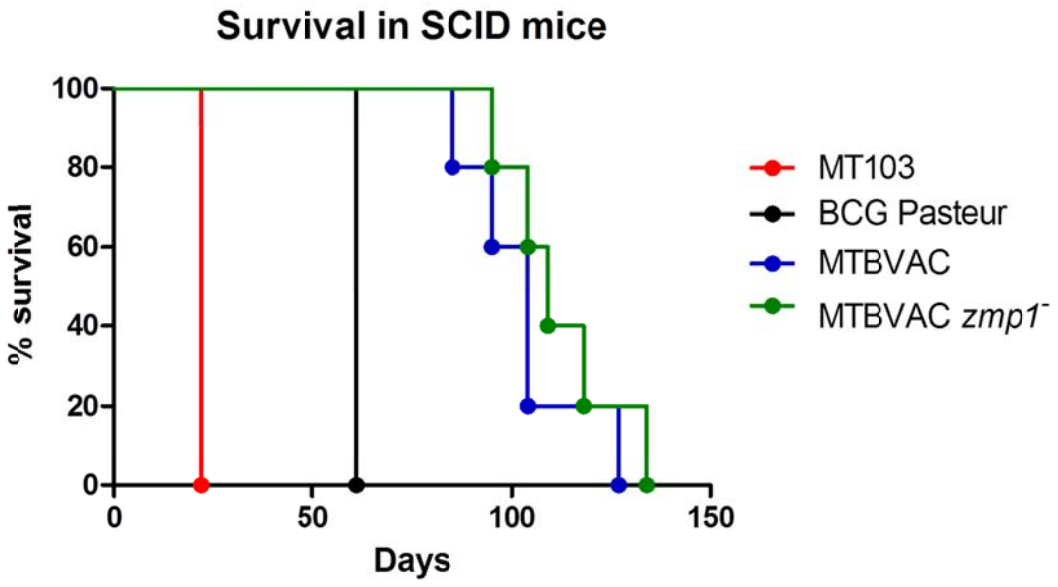

Figure 5. Survival experiment in SCID mice.

3.2.3. MTBVAC *zmp1*⁻ protective efficacy against TB in immunocompetent mice.

Since the deletion of the third gene may result in a decrease of the protective efficacy, it was tested protection efficacy conferred by MTBVAC *zmp1*⁻ compared to BCG and MTBVAC following challenge with H37Rv in C57BL/6 mice. Both BCG and MTBVAC *zmp1*⁻ showed similar protective efficacy in lungs, whereas MTBVAC showed a significantly improved protection. However, no significant differences were observed between any of the vaccine strains BCG, MTBVAC or MTBVAC *zmp1*⁻ in the spleen (Figure 6).

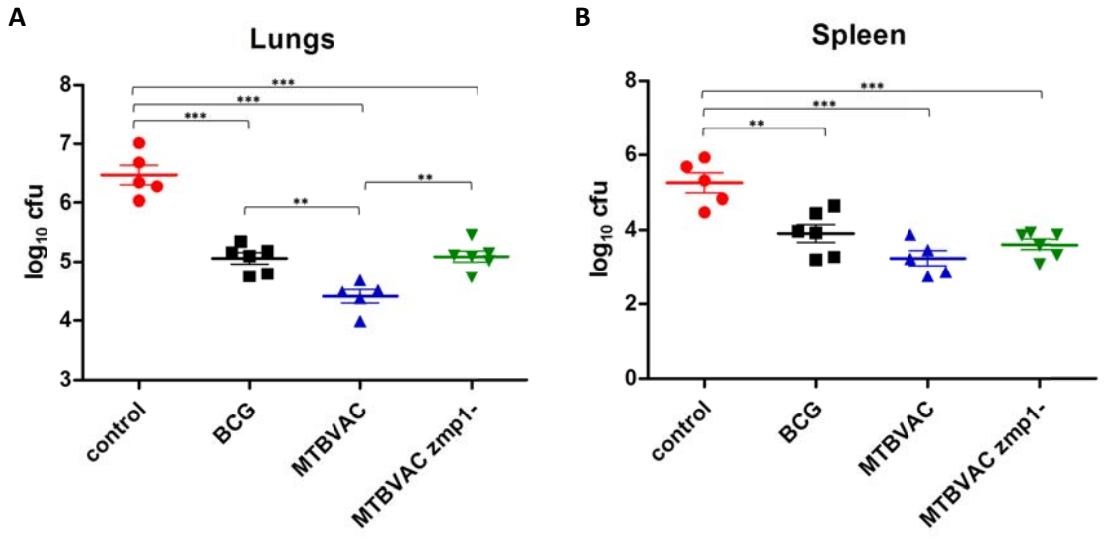

Figure 6. MTBVAC *zmp1*⁻ protects against TB disease. **A.** Protection induced in lungs at 4 weeks post challenge. **B.** Protection induced in spleen at 4 weeks post challenge. Total cfu were seeded in 7H11 plates supplemented with 0.5% glycerol, 10% albumin-dextrose-catalase (ADC, Middlebrook), polymixin B 50/ml, trimetroprim 0.02 mg/ml and amphotericin B 0.01 mg/ml. Representative graphs from a duplicate experiment, in groups of five mice per sample. (*p<0.005, **p<0.001, ***p<0.0001).

3.2.4. Immunogenicity of the vaccine candidate MTBVAC *zmp1*⁻.

In order to analyze immunogenicity of MTBVAC *zmp1*⁻, $CD4^+/INF\gamma^+$ and $CD8^+/INF\gamma^+$ cell activation were measured following 4 week of vaccination with *M. bovis* BCG, MTBVAC and MTBVAC *zmp1*⁻. An increase of $CD4^+/INF\gamma^+$ and $CD8^+/INF\gamma^+$ cells was observed in all vaccinated groups. The percentage of both $CD4^+/INF\gamma^+$ and $CD8^+/INF\gamma^+$ was very similar for BCG and MTBVAC *zmp1*⁻, no statistical difference was found between any of the strains of analysis neither in lungs nor spleen (Figure 7).

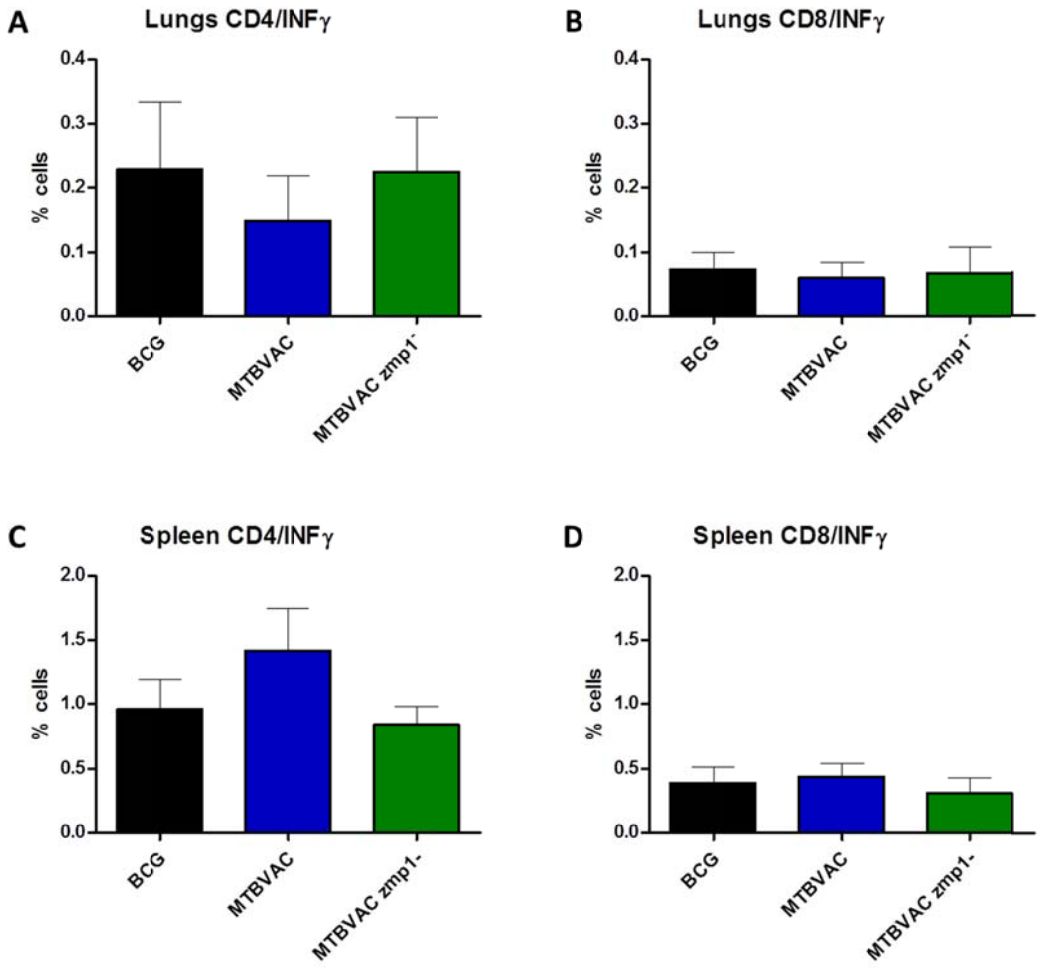

Figure 7. Immunogenicity induced in c57BL mice. A. $CD4^+/INF\gamma^+$ cell activation levels in lungs at four weeks post vaccination. **B.** $CD8^+/INF\gamma^+$ cell activation levels in lungs at four weeks post vaccination. **C.** $CD4^+/INF\gamma^+$ cell activation levels in spleen at four weeks post vaccination. **D.** $CD8^+/INF\gamma^+$ cell activation levels in spleen at four weeks post vaccination. Cells were stimulated with PPD for 18h and cell populations were measured by flow cytometry. Representative graphs for duplicate experiment, in groups of five mice per sample.

DISCUSSION

Although BCG administration has many benefits for TB prevention against the most severe forms of the disease common mainly in children in the developing world; the failure of BCG to protect against pulmonary TB, the transmissible form of the disease, makes this vaccine incapable to stop the global TB pandemia, mainly striking the poorest countries where TB is prevalent among population [1]. As a result there is urgent need for effective vaccines that could arrest the social and medical problem caused by TB. One of the advantages of using live attenuated Mtb vaccines is that major antigens lost during BCG attenuation would still be retained [15, 16], thus providing a rational solution for replacing BCG. Moreover BCG vaccination is contraindicated in patients with primary and secondary immunodeficiencies including HIV-infected people [1]. As a result, development of effective TB vaccines safer than BCG that could be used in this population is also urgently needed.

The main challenge in the development of live vaccines is achieving a satisfactory level of safety (attenuation) without severely compromising vaccine immunogenicity and protectiveness. There are examples in the existing literature in the field of invention of live-attenuated Mtb mutants as vaccine candidates that even though attenuated, confer protection levels, against infection, comparable to BCG. The single auxotroph mutant of Mtb deficient in the biosynthesis of leucine (H37RvΔ*leu*) exhibits attenuation *in vitro* and *in vivo* but is characterized by poor protective efficacy relative to BCG [17]. Whereas the lysine auxotroph of Mtb was only able to induce similar protection as BCG against TB challenge when two doses were administrated [18].

Pantothenate auxotroph (H37RvΔ*panCD*), which exhibits higher degree of attenuation, can induce protection comparable to BCG in a single dose of administration [19]. When combining the auxotrophic mutations to generate a safer double auxotroph of Mtb based on leucine and pantothenate (H37RvΔ*leu*Δ*panCD*) [20] or lysine and pantothenate [21], the resulting candidates are highly attenuated but does not increase the protection induced by the pantothenate auxotroph strain [19, 20]. These

evidences strongly suggest a non-additive effect of the second mutation either in protection or attenuation.

M. bovis BCG *zmp1* mutant has been studied and it presents a phenotype with an increase in presentation of MHC class II-restricted antigens. Deletion of the *zmp1* gene reestablished the activation of the inflammasome and consequently the full maturation of the phagosome into phagolysosome, leading to the clearance of the pathogen [11]. Results suggest that phagosome maturation and lysosomal delivery of BCG facilitate mycobacterial antigen presentation and enhance immunogenicity [12]. Safety of BCG *zmp1* mutant strains was studied in a recent work; safety profile of BCG Denmark *zmp1*$^{-}$and BCG Pasteur *zmp1*$^{-}$mutants was tested in immunocompromised CB17 SCID mice in parallel with their parental strains, showing that the median survival was prolonged for 50-150 days for each mutant strain, indicating that they are attenuated when compared to their BCG parental strains [22]. Furthermore *zmp1* deletion mutants of BCG provided enhanced protection by reducing the bacterial load of tubercle bacilli in the lungs of infected guinea pigs, making BCGΔ*zmp1*mutants promising candidates for further vaccine development [22].

Based on these last results on BCG *zmp1*$^{-}$, here we present the triple mutant MTBVAC *zmp1*$^{-}$ as a vaccine candidate with protective capacity against TB infection holding potential use for patients in risk of immune suppression. However no special hyper-attenuated phenotype was observed when compared with MTBVAC in the survival study with SCID mice, the immunocompromised mice infected with MTBVAC *zmp1*$^{-}$ survive 134 days and the ones infected with MTBVAC 127 days; on the other hand, they do survive longer than BCG Pasteur infected mice. The *zmp1* mutation introduced in MTBVAC (*phoP*$^{-}$ and *fadD26*$^{-}$) does not seem to present any effect in attenuation and it does not affect the protection ability of the vaccine against TB infection either when compared to MTBVAC vaccine candidate, which is coherent with the first studies performed in mice with BCG *zmp1*$^{-}$, where no difference in attenuation were registered [12]. When compared to BCG, protection conferred in this model has no

significant differences; however the BCG *zmp1*$^{-}$ vaccine candidate did not show any improvement in protection in the mouse model, only in guinea pigs [22].

This work was done in parallel with the development of the triple mutant MTBVAC *erp*$^{-}$ in our group. Nevertheless our triple mutant MTBVAC *zmp1*$^{-}$ does not present the attenuated profile but, MTBVAC *erp*$^{-}$ presented a hyper-attenuation phenotype in SCID mice. In this case, the *erp* mutation introduced in MTBVAC (*phoP*$^{-}$ and *fadD26*$^{-}$) likely presents a synergic effect in attenuation that not affects the protection ability of the vaccine against TB infection [23].

The absence of hyper attenuation in SCID mice for the triple mutant MTBVAC *zmp1*$^{-}$ drives it out of consideration for a future prophylactic strategy development for use in individuals at risk of immune suppression. Nevertheless, further studies are needed in other animal models in order to establish any conclusions in the protective capacity of our candidate MTBVAC *zmp1*$^{-}$.

REFERENCES

1. WHO. *Information Sheet: observed rate of vaccine reactions Bacille Calmette-Ghérin (BCG) vaccine.* . Global VAccine Safety, Immunization and Biologicals. 2012.
2. Murphy, D., L.A. Corner, and E. Gormley, *Adverse reactions to Mycobacterium bovis bacille Calmette-Guerin (BCG) vaccination against TB in humans, veterinary animals and wildlife species.* TB (Edinb), 2008. **88**(4): p. 344-57.
3. Mak, T.K., et al., *Making BCG vaccination programmes safer in the HIV era.* Lancet, 2008. **372**(9641): p. 786-7.
4. Hesseling, A.C., et al., *The risk of disseminated Bacille Calmette-Guerin (BCG) disease in HIV-infected children.* Vaccine, 2007. **25**(1): p. 14-8.
5. Marinova, D., et al., *Recent developments in TB vaccines.* Expert Rev Vaccines, 2013. **12**(12): p. 1431-48.
6. van der Wel, N., et al., Mtb *and M. leprae translocate from the phagolysosome to the cytosol in myeloid cells.* Cell, 2007. **129**(7): p. 1287-98.
7. Kamath, A.T., et al., *New live mycobacterial vaccines: the Geneva consensus on essential steps towards clinical development.* Vaccine, 2005. **23**(29): p. 3753-61.
8. Walker, K.B., et al., *The second Geneva Consensus: Recommendations for novel live TB vaccines.* Vaccine, 2010. **28**(11): p. 2259-70.
9. Spertini, F., et al., *Safety of human immunisation with a live-attenuated Mycobacterium TB vaccine: a randomised, double-blind, controlled phase I trial.* Lancet Respir Med, 2015. **3**(12): p. 953-62.
10. Master, S.S., et al., *Mycobacterium TB prevents inflammasome activation.* Cell Host Microbe, 2008. **3**(4): p. 224-32.
11. Ferraris, D.M., et al., *Crystal structure of Mycobacterium TB zinc-dependent metalloprotease-1 (Zmp1), a metalloprotease involved in pathogenicity.* J Biol Chem, 2011. **286**(37): p. 32475-82.
12. Johansen, P., et al., *Relief from Zmp1-mediated arrest of phagosome maturation is associated with facilitated presentation and enhanced immunogenicity of mycobacterial antigens.* Clin Vaccine Immunol, 2011. **18**(6): p. 907-13.
13. Raghavan, M., et al., *MHC class I assembly: out and about.* Trends Immunol, 2008. **29**(9): p. 436-43.
14. Lamrabet, O. and M. Drancourt, *Genetic engineering of Mycobacterium TB: a review.* TB (Edinb), 2012. **92**(5): p. 365-76.
15. Arbues, A., et al., *Construction, characterization and preclinical evaluation of MTBVAC, the first live-attenuated* Mtb-*based vaccine to enter clinical trials.* Vaccine, 2013. **31**(42): p. 4867-73.
16. Brosch, R., et al., *Genome plasticity of BCG and impact on vaccine efficacy.* Proc Natl Acad Sci U S A, 2007. **104**(13): p. 5596-601.
17. Hondalus, M.K., et al., *Attenuation of and protection induced by a leucine auxotroph of Mycobacterium TB.* Infect Immun, 2000. **68**(5): p. 2888-98.
18. Pavelka, M.S., Jr., et al., *Vaccine efficacy of a lysine auxotroph of Mycobacterium TB.* Infect Immun, 2003. **71**(7): p. 4190-2.

19. Sambandamurthy, V.K., et al., *A pantothenate auxotroph of Mycobacterium TB is highly attenuated and protects mice against TB.* Nat Med, 2002. **8**(10): p. 1171-4.
20. Sampson, S.L., et al., *Protection elicited by a double leucine and pantothenate auxotroph of Mycobacterium TB in guinea pigs.* Infect Immun, 2004. **72**(5): p. 3031-7.
21. Sambandamurthy, V.K., et al., *Long-term protection against TB following vaccination with a severely attenuated double lysine and pantothenate auxotroph of Mycobacterium TB.* Infect Immun, 2005. **73**(2): p. 1196-203.
22. Sander, P., et al., *Deletion of zmp1 improves Mycobacterium bovis BCG-mediated protection in a guinea pig model of TB.* Vaccine, 2015. **33**(11): p. 1353-9.
23. Solans, L., et al., *Hyper-attenuated MTBVAC erp mutant protects against TB in mice.* Vaccine, 2014. **32**(40): p. 5192-7.

General Conclusions

1. MTBVAC presents an increased secretion of immunodominant antigens, like the components of the Antigen 85 complex, through the upregulation of TAT secretion system. Also presents an impaired phenotype for ESX-1 secretion system substrates, like the key virulence factor ESAT-6; although it does not secrete it, MTBVAC does produce and accumulate it inside the bacteria, allowing the presentation of ESAT-6 epitopes to the immune system once the bacteria are degraded. These two facts suggest that the vaccine candidate MTBVAC is going to generate a better immune response and protection than the actual vaccine BCG.

2. MTBVAC presents an altered intracellular trafficking phenotype where it is not able to arrest phagosomal maturation at early stage but it does not reach the lysosome, suggesting that it arrest the maturation in some intermediate point between the late endosome and the lysosome phases.

3. The single mutations *phoP* and *fadD26* of MTBVAC have a synergistic effect on the intracellular trafficking phenotype of the vaccine candidate.

4. Acid pH might activate the Mtb TCS PhoPR, starting a cascade of events where lipid metabolism and defense against oxidative stress are upregulated at short times; and where the TAT secretory system works normally secreting the immunodominant components of the Antigen 85 complex in order to stimulate the host interactions. After 3-5 days, the components of the RD1, ESAT-6 and CFP-10 induce phagosomal rupture and bacteria will reside in the cell cytosol; at this time an upregulation of Mcr7 ncRNA is registered and consequently, Antigen 85 complex secretion through the TAT secretory system will be interrupted in order to “hide” from the host immune system.

5. No improvements in attenuation or immunogenicity were registered for the new strain MTBVAC *zmp1*$^{-}$ compared with MTBVAC in mouse model.

Conclusiones Generales

1. MTBVAC presenta un aumento en la secreción de antígenos inmunodominantes, como los componentes del complejo Antígeno 85, a través del incremento en la actividad del sistema de secreción TAT. Así mismo presenta un defecto en la secreción de algunos sustratos del sistema de secreción ESX-1, como el factor de virulencia ESAT-6; a pesar de no secretarlo, MTBVAC sí que lo sintetiza y acumula en el interior de la bacteria, permitiendo la presentación de los epítopos de ESAT-6 al sistema inmune del hospedador una vez que la bacteria ha sido degradada. Estos dos hechos sugieren que el candidato a vacuna MTBVAC será capaz de generar una mejor respuesta inmune y protección contra la TB que la actual vacuna BCG.

2. MTBVAC presenta un fenotipo de tráfico intracelular alterado, en el que no es capaz de detener la maduración del fagosoma en etapas tempranas, sin embargo, el fagosoma no alcanza la fase lisosomal, sugiriendo que la bacteria sí es capaz de detener la maduración en algún punto intermedio entre la fase de endosoma tardío y lisosoma.

3. Las mutaciones individuales en *phoP* y *fadD26* de MTBVAC tienen un efecto sinérgico sobre el tráfico intracelular del candidato a vacuna.

4. Es posible que el pH ácido active el sistema de dos components PhoPR en Mtb, iniciando una cascada de eventos que evoluciona conforme avanza el curso de la infección y las necesidades de la bacteria, primeramente hay un incremento en la actividad de genes relacionados con el metabolismo lipídico y con la defensa frente al estrés oxidativo; en este estadío el sistema de secreción TAT funciona normalmente secretando los componentes inmunodominantes del complejo Antígeno 85 con el objetivo de estimular las interacciones con la célula hospedadora. Tras 3-5 días, los componentes de la región de diferencia 1

(RD1), ESAT-6 y CFP-10 inducen la ruptura fagosomal y la bacteria escapa al citosol de la célula; es a partir de este momento cuando tiene lugar un gran incremento en la actividad del ncRNA Mcr7 y consecuentemente, los componentes del complejo Antígeno 85 verán interrumpida su secreción a través del sistema TAT con el objetivo de "esconderse" del sistema inmune del hospedador.

5. No se registró ninguna mejora en cuanto a la atenuación o inmunogenicidad de la nueva cepa MTBVAC *zmp1*$^{-}$ comparada con MTBVAC en modelo de ratón.

Materials and Methods

1. Basic procedures.

1.1. Bacterial strains and culture conditions.

E. coli XL1-Blue and DH5α strains were used for cloning experiments. Strains were grown at 37°C in Luria-Bertani (LB) broth or LB agar supplemented with ampicillin (Amp; 100μg/ml), kanamycin (Km; 20 μg/ml) or hygromycin (Hyg; 50 μg/ml) when necessary. Liquid cultures were grown in glass tubes in a shaker.

M. bovis BCG strains were grown at 37°C in Middlebrook 7H9 medium supplemented with ADC (0.5% bovine serum albumin, 0.2% dextrose, 0.085% NaCl, 0.0003% beef catalase) (Difco) and 0.05% Tween80 (7H9-T-ADC), or on solid Middlebrook 7H10 medium supplemented with 10% ADC (7H10-ADC). Km (20 μg/ml) or Hyg (50 μg/ml) were added if appropriate. Liquid cultures were done in cell culture flasks without shaking.

For the intracellular trafficking study the Mt103 strain [1] and its *phoP* and *fadD26* mutants were used, also the vaccine candidate MTBVAC [2] and the current vaccine BCG Pasteur [3] and BCG Pasteur PDIM^{-} [4] were used. All strains containing an integrative plasmid with the *gfp* gene preceded by a strong promoter. Mt103 and the vaccine candidate MTBVAC were used in the comparative analysis of the secreted proteins. Mt103 and its *zmp1* mutant, MTBVAC *zmp1*$^{-}$ and BCG Pasteur were used in the study of a new hyper attenuated vaccine generation. All *M. tuberculosis* (Mtb) strains were grown at 37°C in Middlebrook 7H9 supplemented with ADC (Difco). In order to keep the culture clump-free, Tween-80 was added to a final concentration of 0.05% (7H9-T-ADC). Solid medium was Middlebrook 7H10 supplemented with ADC (7H10-ADC), 2% sucrose was added if appropriate. Km (20 μg/ml) or Hyg (50 μg/ml) were added if appropriate. Liquid cultures were done in cell culture flask without shaking.

In order to study the PhoP-regulon expression under different conditions, wild type Mtb H37Rv [5] and its isogenic *phoP* mutant both containing the integrative plasmids pFPV27-GFP::*lipF* promoter, pFPV27-GFP::*pks2* promoter, pFPV27-GFP::*dosR*

promoter, pFPV27-GFP::*icl* promoter and pFPV27-GFP::*phoP* promoter were used. For the study of the promoter expression under acidic conditions, the pH of the 7H9-T medium was modified with HCl 6N or KOH 1N until the wanted pH, then supplemented with ADC; using different sources of carbon, strains were grown in 7H9-T medium supplemented with AS (0.5% BSA, 0.085% NaCl) and 0.2% of D-glucose ($C_6H_{12}O_6$), Na-acetate ($C_2H_3NaO_2$) or Na-propionate ($C_3H_5O_2Na$); under hypoxic conditions, 1.5μg/ml of blue methylene was added to the 7H9-T-ADC in control samples in order to know when the O_2 of the medium has been consumed; using a concentration range of different ions, for $ZnSO_4$ or $CuSO_4$ from 450μM to 0 μM and $CaCl_2$ from 8mM to 0mM or 8μM to 0μM modified Sauton medium (0.5g KH_2PO_4, 0.5mM $MgSO_4$, 2g Citric acid, 0.05g Ferric ammonium citrate, 0.05% Tween-80, 4g L-Asparagine) with ADC was used, for $MgSO_4$ from 8mM to 0mM modified Sauton without magnesium with ADC was used; under oxidative stress, 0mM, 10mM or 15mM H_2O_2 was added to 7H9-T supplemented with ADS (0.5% BSA, 0.2% dextrose, 0.085% NaCl); under different temperatures, strains were grown in 7H9-T-ADC and incubated at room temperature, 37°C and 42°C; using different fatty acids, 0.001% palmitic acid, 0.001% stearic acid and 0.001% oleic acid were added to 7H9-T-ADC. All the culture media used were supplemented with Km (20 μg/ml).

Storage of strains was done at -80°C in 7H9-T-ADC supplemented with 15% glycerol.

Mtb manipulation was carried out in a biosafety level 3 (BSL3) laboratory.

1.2. Neutral-red staining.

This method was adapted from Soto *el al*. [6] mycobacterial strains were grown on 7H10 ADC medium for 3 to 4 weeks. Cells were placed and gently disaggregated in 15ml Falcon tubes containing 4ml of 50% aqueous methanol, and incubated for 1h at 37°C. Cells were pelleted by centrifugation (4000rpm, 5min), and methanol removed. Then, 4ml barbital buffer (1% sodium barbital in 5% NaCl, pH=9.8) were added. Subsequently, 150μl of a solution of 0.05% aqueous neutral red were added. Results were evaluated after 1h incubation at 37°C.

2. Nucleic acid and genetic engineering techniques.

2.1. DNA extraction.

2.1.1. Extraction of genomic DNA from mycobacteria.

Genomic DNA of mycobacterial strains was isolated using CTAB method [7]. Briefly, mycobacteria were resuspended in 400µl TE (100mM Tris/HCl, 10mM EDTA, pH=8) and heated for 10min at 85^{o}C. Samples were slightly cooled at RT before adding 50µl of 10mg/ml lysozyme and were then incubated for at least 1h at 37^{o}C. Subsequently, 75µl of a solution containing 72.5µl of 10% SDS and 2.5µl of 20mg/ml proteinase K were added and the suspension warmed for 10min at 65^{o}C. Hereafter, 100µl 5M NaCl and 100µl CTAB/NaCl (10% CTAB in 0.7 NaCl) pre-warmed at 65^{o}C were added and samples incubated for further 10min at 65^{o}C. Genomic DNA was extracted by adding 750µl of chloroform:isoamyl alcohol 24:1. Samples were mixed by vortexing for 10s before centrifugation (13000rpm for 5min). The upper (aqueous) phase was transferred to a fresh tube containing 450µl isopropanol and samples incubated overnight at -20^{o}C. Precipitated nucleic acids were collected by centrifugation (13000rpm for 10min at 4^{o}C). The pellets were dissolved in 50µl double-distilled water and treated with RNAse. DNA was quantified by Abs_{260nm} readings using a ND-1000 spectrophotometer (NanoDrop Technologies).

2.1.2. Plasmid DNA extraction from *E. coli*.

2.1.2.1. Mini preparation (Mini-prep).

1.5ml of a liquid culture grown overnight were centrifuged (10000rpm for 3min) and the pellet resuspended in 100µl of Solution I (50mM glucose, 10mM EDTA, 2mM Tris HCl pH=8). 200µl of freshly made Solution II (0.2M NaOH, 1% SDS) were added, and the content mixed by inverting the tube several times, until it becomes transparent and viscous. After incubation on ice for 5min, 150µl of cold Solution III (5M KAc, 11.5% glacial HAc) were added and the tubes were mixed by inversion; as a result, a white pellet is formed. This mix was incubated on ice for 5min, followed by centrifugation

(12000rpm for 10min). Supernatants (400µl approx.) were then transferred to a fresh tube and mixed with the same volume of chloroform:isoamyl alcohol 24:1. After centrifugation, the aqueous phase was transferred to a tube containing 900µl EtOH and 50µl 3M NaAc and incubated at -20°C for 30min. By centrifugation (12000rpm for 5min) small nucleic acids (plasmids and RNA) were pelleted, and then washed with 100µl 70% EtOH. Finally, the pellet was dried in a vacuum drier and resuspended in 30µl of double distilled water. RNA, which co-purifies with plasmidic DNA, was removed by adding 1µl of RNAse 1mg/ml and incubating for 15min at 37°C. Plasmidic DNA was kept at -20°C.

2.1.2.2. Maxi-preparation (Maxi-prep).

This method was used to obtain large quantities of plasmid. The process is the same as the mini-preparation, but starting with 100ml of liquid culture. Larger volumes of solutions are needed: 5ml Solution I, 10ml Solution II and 7.5ml Solution II. Besides, precipitation of plasmid DNA is done by adding 0.7 volumes of isopropanol instead of ethanol. Finally, nucleic acids are dissolved in 350µl of double distilled water and treated with 10µl RNAse 1mg/ml for 15min at 37°C.

2.2. Mycobacterial RNA isolation.

2.2.1. RNA isolation in extracellular conditions.

Mtb cultures were grown in 7H9-T-ADC or the correspondent modified culture medium at 37°C until different times depending the corresponding experiment. Cells from 10ml of culture were harvested (4000 rpm for 5min at 37°C). To minimize RNA degradation, cells were resuspended in 1ml of RNA protect reactive (Qiagen). Cellular suspensions were incubated for 5min at RT and were centrifuged (14000rpm for 5min at RT). Pellets were resuspended in 400µl of lysis buffer (0.5% SDS, 20mM NaAc, 0.1 EDTA) and 1ml of acid-phenol:chloroform (5:1, pH=4.5) was added. Bacterial suspensions were transferred to tubes containing glass beads (Qbiogene) and were lysed by mechanical traction (Fast-prep instrument) in two cycles (45s at speed 6.5m/s) cooling the samples on ice for 5min between the pulses. Samples were

centrifuged (14000rpm for 5min at 4^{o}C). The upper (aqueous) phase was then transferred to a fresh tube containing 90μl of 0.3M NaAc (pH=5.5) and 900μl of isopropanol and samples were incubated overnight at -20^{o}C. Precipitated nucleic acids were collected by centrifugation (14000rpm for 1 hour at 4^{o}C). The pellets were rinsed with 70% ethanol and air dried before being re-dissolved in RNAse-free water. DNA was removed from RNA samples using Turbo DNA free (Ambion) by incubation at RT for 1hour 30min. Then RNA was purified with acid-phenol:chloroform (5:1, pH=4.5) and the same steps to precipitate, collect and dry were repeated to dissolve RNA in RNAse-free water. The concentration and purity of the extracted RNA was estimated from the Abs_{260nm}/Abs_{280nm} readings using ND-1000 spectrophotometer. RNA integrity was assessed by agarose gel electrophoresis. RNA samples were stored at -80^{o}C.

2.2.2. RNA isolation in intracellular conditions.

Intracellular mycobacteria RNA extraction was performed with a modified protocol based on the one described by Fontan *el al.* [8]. After the infection, at the established times, cells were lysed and homogeneized during 5min adding 10ml of GTC buffer (25mM sodium citrate, 4M guanidine thiocyanate, 0.5% N-lauryl sarcosine, 0.125M 2-mercaptoethanol and 0.5% Tween-80, pH=7). Next, samples were collected in 15ml centrifuge tubes and centrifuged at 4000rpm 1 hour. Bacterial pellets were washed with GTC buffer and centrifuged again 4000rpm 1hour. After that, dry bacterial pellets were treated as described above to extract mycobacterial RNA.

2.3. Construction of plasmids.

DNA fragments for cloning purposes were amplified by PCR using the Pwo high fidelity DNA polymerase (Roche) or the PrimeSTAR HS DNA polymerase (Takara Bio) for larger fragments, and gel-purified by using QIAquick Gel Extraction Kit (Qiagen). Ligations were done using T4 DNA ligase (Invitrogen).

2.3.1. Construction of the integrative plasmid pFPV27-GFP::*pks2*promoter.

A 580bp DNA fragment containing the promoter of *pks2* (Rv3825c) gene from Mtb was amplified by PCR with oligonucleotides pks2-Fw2 and pks2-Rv.

The previous PCR fragment was digested with the restriction enzymes EcoRI and KpnI and inserted into pFPV27 integrative vector [9] digested with EcoRI and KpnI. To confirm the absence of PCR-induced mutations in the final plasmid pFPV27-GFP::*pks2* promoter, it was validated by PCR and sequenced using the oligonucleotides described in Table 1.

Oligonucleotide	Sequence 5' ⟶ 3'	Use	Tm
pks2-Fw2	CATGAATTCTCAGAACGACATTGGGTTTCGCGTC	PCR, validation	72.42
pks2-Rv	CCTGGTACCCTGACGCCGCCGACCCCAAG	PCR, validation	79.24
Km903A	CTCGTGAAGAAGGTGTTGCT	Validation	62
Km903B	CCGACCATCAAGCATTTTAT	Validation	61

2.3.2. Construction of the integrative plasmid pFPV27-GFP::*lipF*promoter.

A 550 bp DNA fragment containing the promoter of *lipF* (Rv3487c) gene from Mtb was amplified by PCR with oligonucleotides lipF-Fw3 and lipF-Rv.

The obtained PCR fragment was digested with the restriction enzymes MfeI and KpnI and inserted into pFPV27 integrative vector [9] digested with EcoRI and KpnI. To confirm the absence of PCR-induced mutations in the final plasmid pFPV27-GFP::*lipF* promoter, it was validated by PCR and sequenced using the oligonucleotides described in Table 2.

Oligonucleotide	Sequence 5' 3'	Use	Tm
lipF-Fw3	CCTCAATTGCTGAAACTCCCGCATAGAACACCTC	PCR, validation	73.65
lipF-Rv	CCTGGTACCCACAGTCATAAGTGGCTTGATCGTC	PCR, validation	74.88
Km903A	CTCGTGAAGAAGGTGTTGCT	Validation	62
Km903B	CCGACCATCAAGCATTTTAT	Validation	61

A new construction was needed for this vector, with a larger fragment of DNA containing the complete sequence of the *lipF* promoter, in order to do this an 849bp fragment upstream the *lipF* promoter was amplified by PCR with oligonucleotides lipF-Fw4 and lipF-Rv2.

The same procedure was used to insert the new fragment into the pFPV27 vector. The final plasmid pFPV27-GFP::new*lipF*promoter was validated by PCR and sequenced using the oligonucleotides described in Table 3.

Oligonucleotide	Sequence 5' ⟶ 3'	Use	Tm
lipF-Fw4	CTTCAATTGGCGATCCTCGGTCAGTGCTGC	PCR, validation	73.66
lipF-Rv2	CCTGGTACCTGCATGCGAAGTCGACGAACC	PCR, validation	72.68
Km903A	CTCGTGAAGAAGGTGTTGCT	Validation	62
Km903B	CCGACCATCAAGCATTTTAT	Validation	61

2.4. Electrotransformation of *E.coli* and mycobacteria.

To prepare *E. coli* electrocompetent cells, bacteria were grown to an OD_{600nm} of 0.4 to 0.6. Then, the growth was stopped for 30min on ice, and bacteria were washed twice in chilled-cold water, and one in chilled-cold 10% glycerol. Cells are finally resuspended in 1ml chilled-cold 10% glycerol. Aliquots of 40µl were directly used or stored at -80°C for further use. Aliquots of 40µl were electroporated with 20-30ng of purified plasmid DNA in 0.2cm gap cuvettes (Bio-Rad) with a single pulse (2.5kV, 25µF, 200Ω) in a GenePulser Xcell™ (Bio-Rad). Cells were resuspended in LB to a final volume of 1ml and incubated for 1h at 37°C if required before plating several dilutions on plates containing the needed antibiotic. Colonies appeared after incubation overnight.

M. bovis and Mtb electrocompetent cells were prepared as described by Wards *et al.* [10]. Bacteria were grown until an OD_{600nm} of 0.6 to 0.8. Glycine was added to the cells to a final concentration of 0.2M and incubated at 37°C for 24 hours more. All the process was performed at RT. Bacterial pellet was washed twice with water 0.05% Tween-80 and one with 10% glycerol 0.05% Tween-80, and finally resuspended in 2ml of 10% glycerol 0.05% Tween-80. Aliquots of 200-400µl were electroporated with 100-

200ng of replicative or integrative plasmid DNA (previously purified), using 0.2cm gap cuvettes with a single pulse (2.5kV, 25μF, 1000Ω) in a GenePulser Xcell™. Cells were recovered with 1ml of 7H9-T-ADC and incubated for 24h at 37°C, to allow expression of the antibiotic resistance genes, before plating serial decimal dilutions on plates containing the relevant antibiotic. Colonies typically appeared in 3-4 weeks.

3. Methods for phenotypic characterization.

3.1. Gene expression under different conditions.

3.1.1. Acidic conditions.

3.1.1.1. Through the GFP reporter system.

Mtb strains were grown in 7H9-T-ADC at 37°C until an OD_{600nm} of 0.3-0.5. Cultures were centrifuged at 4000rpm for 10min, the supernatant discarded, the pellet washed in PBS with 0.05% Tween-80 and finally resuspended in the correspondent medium 7H9-T-ADC with modified pH 7, 5.5 or 5. Aliquots of 200μl of bacterial suspension were transferred into wells of a 96-well plate. Optical density (OD_{600nm}) and relative fluorescence was acquired during the established days (until 3 weeks) in a Synergy™ HT Detection Microplate Reader (Biotek® Instruments), using 485/35nm and 516/35nm as excitation and detection wavelengths, respectively.

3.1.1.2. Short kinetic.

Mtb strains were grown in 7H9-T-ADC at 37°C until an OD_{600nm} of 0.3-0.5. Cultures were centrifuged at 4000rpm for 10min, the supernatant discarded, the pellet washed in PBS with 0.05% Tween-80 and finally resuspended in the correspondent medium with modified pH 8.5, 7 or 5. Aliquots of 5ml of bacterial suspension were transferred to falcon tubes in order to proceed to bacterial RNA extraction after 30min, 1 and 6 hours post medium change. Gene expression was analyzed by qRT-PCR.

3.1.1.3. Long kinetic.

Mtb strains were grown in 7H9-T-ADC at 37ºC until an OD_{600nm} of 0.5. Cultures were centrifuged at 4000rpm for 10min, the supernatant discarded, the pellet washed in PBS with 0.05% Tween-80 and finally resuspended in the correspondent medium with modified pH 7 buffered with 100mM MOPS or pH 6 or 5.5 buffered with 100mM MES. Aliquots of 5ml of bacterial suspension were transferred to falcon tubes in order to proceed to bacterial RNA extraction after 2, 6, 10 and 14 days post medium change. Gene expression was analyzed by qRT-PCR.

3.1.2. Sources of Carbon.

Liquid cultures of Mtb strains in logarithmic phase were adjusted to $2x10^5$CFU/ml in 7H9-T-AS with 0.2% of glucose, acetate or propionate. 200µl of bacterial suspension were transferred into wells of a 96-well plate. Optical density (OD_{600nm}) and relative fluorescence was acquired during the established days (until 7 days) in a Synergy™ HT Detection Microplate Reader (Biotek® Instruments), using 485/35nm and 516/35nm as excitation and detection wavelengths, respectively.

3.1.3. Hypoxia.

Liquid cultures of MTB strains in logarithmic phase were adjusted to $2x10^5$CFU/ml in 7H9-T-ADC, growth until OD_{600nm} of 0.3-0.5 and distributed 13ml of culture in falcon tubes. One of them was the hypoxia control tube; 1.5µg/ml of blue methylene was added to the 7H9-T-ADC in order to know when the O_2 of the medium has been consumed and hypoxia starts. All tubes are sealed with Parafilm M Laboratory Film and cultured at 37ºC. Once the control tube turns white, 200µl of bacterial suspension of each tube were transferred into wells of 96-well plate. Optical density (OD_{600nm}) and relative fluorescence was acquired during the established days (until 4 weeks) in a Synergy™ HT Detection Microplate Reader (Biotek® Instruments), using 485/35nm and 516/35nm as excitation and detection wavelengths, respectively.

3.1.4. Ions.

3.1.4.1. Zn^{2+} and Cu^{2+}.

Serial two-fold dilutions of $ZnSO_4$ and $CuSO_4$ were performed in modified Sauton medium supplemented with ADC from 450μM to 0μM, in 96-well microtiter plates, with a final volume of 100μl per well.

Mtb strains were grown in modified Sauton+ADC at 37ºC until an OD_{600nm} of 0.4-0.7. 100 μl of culture were added to each well. Optical density (OD_{600nm}) and relative fluorescence was acquired during the established times (until 7 days) in a Synergy™ HT Detection Microplate Reader (Biotek® Instruments), using 485/35nm and 516/35nm as excitation and detection wavelengths, respectively.

3.1.4.2. Mg^{2+}.

Serial two-fold dilutions of $MgSO_4$ were performed in modified Sauton medium without magnesium supplemented with ADC from 4mM to 0mM, in 96-well microtiter plates, with a final volume of 100μl per well.

The rest of the procedure was identical to the Zn^{2+} and Cu^{2+} ones.

3.1.4.3. Ca^{2+}.

Serial two-fold dilutions of $CaCl_2$ were performed in modified Sauton medium supplemented with ADC from 4mM to 0mM and from 8μM to 0μM, in 96-well microtiter plates, with a final volume of 100μl per well.

The rest of the procedure was identical to the Zn^{2+}, Cu^{2+} and Mg^{2+}.

3.1.5. Oxidative stress.

Mtb strains were grown in 7H9-T-ADC at 37ºC until an OD_{600nm} of 0.4-0.6. Cultures were centrifuged at 4000rpm for 10min, the supernatant discarded, the pellet washed in PBS with 0.05% Tween-80 and finally resuspended in the correspondent medium

7H9-T-ADS with 15mM, 10mM or 0mM of H_2O_2. Aliquots of 200µl of bacterial suspension were transferred into wells of a 96-well plate. Optical density (OD_{600nm}) and relative fluorescence was acquired during the established days (until 2 weeks) in a Synergy™ HT Detection Microplate Reader (Biotek® Instruments), using 485/35nm and 516/35nm as excitation and detection wavelengths, respectively.

3.1.6. Different temperatures.

Mtb strains were grown in 7H9-T-ADC at 37ºC until an OD_{600nm} of 0.4-0.6. Aliquots of 500µl of each culture were dispensed in eppendorf tubes and incubated at 42ºC, 37ºC or RT. 200µl of bacterial suspension was transferred into wells of a 96-well plate. Optical density (OD_{600nm}) and relative fluorescence was acquired during the established times (until 7 days) in a Synergy™ HT Detection Microplate Reader (Biotek® Instruments), using 485/35nm and 516/35nm as excitation and detection wavelengths, respectively.

3.1.7. Fatty Acids.

Mtb strains were grown in 7H9-T-ADC at 37ºC until an OD_{600nm} of 0.3-0.5. Cultures were centrifuged at 4000rpm for 10min, the supernatant discarded, the pellet washed in PBS with 0.05% Tween-80 and finally resuspended in the modified medium 7H9-T-ADC with 0.001% palmitic acid, 0.001% oleic acid and 0.001% stearic acid. Aliquots of 7ml of bacterial suspension were transferred to falcon tubes in order to proceed to bacterial RNA extraction during the established times (until 24 hours) post medium change. Gene expression was analyzed by qRT-PCR.

3.2. Infection assays.

3.2.1. Isolation of mouse bone marrow derived macrophages.

Bone marrow derived macrophages (BMDM) were flushed out from 7- to 8-week-old C57/BL10 mice femurs with Dulbecco's modified Eagle's medium (DMEM) (Pan Biotech) enriched with 10% heat-inactivated fetal bovine serum (FBS) (Biological

Industries). Cellular suspensions were passed through a 40μm cell strainer (BD Falcon) to eliminate the aggregates, centrifuged and resuspended in DMEM supplemented with 10% FBS and 20ng/ml of differentiation factor to macrophages (M-CSF), seeded at the quantity needed ant let to differentiate for 7 days at 37^{o}C in a 5% CO_2 atmosphere. Medium was replaced after 3-4 days of culture with fresh complete medium with 10% fetal bovine serum (FBS).

3.2.2. Isolation of human macrophages derived from monocytes.

Peripheral blood monocytes from human blood samples (PBMCs) were isolated by dextran sedimentation and centrifugation through Pancoll tubes (PAN Biotech), after cells were counted, they were resuspended in FBS + 10% DMSO, distributed 10^8cells per vial and frozen at -80^{o}C. To obtain macrophages derived from monocytes (hMDM) from PBMCs, cells were seeded at the quantity established and let to differenciate for 7 days in complete Roswell Park Memorial Institute (RPMI) 1640 medium supplemented with 4mM L-glutamine and 7% human serum (FBS).

3.2.3. Intracellular trafficking.

3.2.3.1. In MHS.

Intracellular trafficking of mycobacterial strains was analyzed in MHS cell line. MHS cells were grown in Dulbecco's modified Eagle medium (DMEM) supplemented with 10% FBS and 4mM L-glutamine ("complete DMEM" from now) and seeded 1.5x10^5 cells per well in 24-well plates above cover glasses.

Bacterial liquid cultures in logarithmic phase were centrifuged at 4000rpm 8min, the supernatant discard and glass beads added to pellet, then vortex for 1min. Bacteria were resuspended in 6ml of 7H9-T-ADC and left 10min in order to allow the bacteria to settle down. From the bacterial suspension 5ml were collected and centrifuged during 5min at 1400rpm. OD_{600nm} of the supernatant were measured to adjust the volumes for the infection procedure. This protocol was followed in order to eliminate bacterial clumps in infection.

Infections were performed at MOI 10:1 bacterium per macrophage; plates were centrifuged for 2min at 1400rpm. After 2h, infection was stopped by removing bacterial suspensions and cells were washed three times with 0.5ml PBS, and finally cultured in 1ml complete DMEM per well.

Cover glasses with cells were collected at 0 and 24 hours post-infection, labeled with 500µl of 1/2000 diluted Lysotracker in complete DMEM for 1h at 37^{o}C, then fixed with 4% paraformaldehyde (4% PFA) and labeled with Hoechst reagent 500µl of 1/1000 dilution in PBS. Cover glasses were washed with PBS and water, finally fixed over 5µl of Fluorescent Mounting Medium (Dako) glue to a microscope slide and dried at 4^{o}C overnight before confocal microscope (Compact Confocal Microscope Olympus FV10-I Oil Type, IACS Aragón) analysis.

3.2.3.2. In Human macrophages derived from monocytes (hMDM).

Intracellular trafficking of mycobacterial strains was analyzed in hMDM cells. hMDM cells were cultured in RPMI supplemented 4mM L-glutamine ("RPMI+G" from now) and seeded 5x10^{6} cells per well in 24-well plates above cover glasses one week before the infection procedure. Medium was replaced after 3-4 days of culture with fresh RPMI+G supplemented with 7% human serum.

Liquid cultures of Mtb strains in logarithmic phase were prepared for infection following identical protocol as described above for trafficking in MHS cells.

Infections were performed at MOI 10:1 bacteria per macrophage for the plates processed at short times after infection, or MOI 2:1 bacterium per macrophage for the plates processed at long time post-infection. After 1h, infection was stopped by removing bacterial suspensions and cells were washed three times with 0.5ml RPMI+G at 37^{o}C, and finally cultured in 1ml complete RPMI per well.

Cover glasses with cells were collected at 2, 48 and 96h post-infection. Some of them were labeled with 500µl of 1/2000 diluted Lysotracker in complete RPMI for 1h at

37^{o}C. All cover glasses were fixed with 4% PFA and washed with PBS. Incubation with 500µl NH_4Cl for 5min neutralize the effect of the PFA, improving the fluorescence of the cells and incubation with 300µl PBS-1% bovine serum albumin (PBS-1%BSA) for 20min is useful to avoid unspecific labeling. Cells were incubated with 300µl PBS-0.3% Triton X-100 during 5min at RT, then some of them were labeled antibodies either with 300µl 1/100 anti-LAMP-1 (mouse monoclonal IgG_1, Santa Cruz Biotech) or with 300µl 1/100 anti-CD63 both in PBS-1%BSA during 1h at RT and washed 3 times with PBS. Secondary antibody for both labeling was a goat-anti-mouse-Red, 300µl of 1/1000 in PBS-1%BSA were incubated with cells during 1h at RT, then washed with PBS. Cover glasses were washed with water and fixed to a microscope slide with 5µl of Fluorescent Mounting Medium (Dako) glue, then dried overnight at 4^{o}C before the analysis in a wild-field microscope (WF LEICA DMLA).

3.2.4. Gene expression in intracellular conditions.

3.2.4.1. GFP expression in MHS cells.

Intracellular expression of PhoP-regulon was tested through the GFP reporter system in MHS (murine alveolar macrophages) cells. MHS cells were grown in complete DMEM.

Infections were performed at a multiplicity of infection (MOI) of 10:1 bacteria per macrophage, with 10^5 MHS cells per well. After 4h, infection was stopped by removing bacterial suspension and cells were washed three times with 1ml PBS, and finally cultured in 1ml complete DMEM per well. Medium was replaced when needed (typically every 1-2 days) by removing 0.5 ml of overlaying DMEM and adding the same volume of fresh complete DMEM.

Cells were collected at 0, 48 and 72 hours post-infection. Cells were labeled with annexin V-APC during 15min at RT to discern between live and dead cells, then washed with PBS and fixed with 4% PFA in calcium-containing buffer (“4% PFA + Ca” from now). Infected cells were analyzed by Fluorescence activated cell sorting (FACS), the

cytometer used in this work was a FACSaria (BDBiosciences) and the analysis was performed with the software Weasel.

3.2.4.2. GFP expression in J774 cells.

Intracellular expression of PhoP-regulon was tested through the GFP reporter system in J774 (mouse BALB/c monocyte macrophages cell line) cells. J774 cells were grown in complete DMEM and 10^5 J774 cells were seeded per well in duplicate 24-well plates.

Infections were performed at a MOI 10:1 bacteria per macrophage. After 2h, infection was stopped and cells were washed as described below.

For FACS analysis cells were collected at 0, 3 and 24 hours post-infection and processed as described for the MH-S. In order to know the number of intracellular bacteria at the end of time of infection (2h) and during the posterior 24h, DMEM medium was removed and 300μl 0.1% triton X-100 were added to each well in order to lyse the cells. 700μl of PBS were added per well and the solution carefully mixed. Several dilutions of this lysate were plated on 7H10-ADC plates and viable bacteria numbers was estimated after 2-3 weeks by counting the number of colonies.

3.2.4.3. GFP expression in MEF cells.

Intracellular expression of PhoP-regulon was tested through the GFP reporter system in MEF (mouse embryo fibroblasts cell line) cells. MEF cells were grown in complete DMEM and $6x10^4$ MEF cells were seeded per well in 6-well plates.

Infections were performed at a MOI 30:1 bacteria per fibroblast. After 4h, infection was stopped by removing bacterial suspension and cells were washed three times with 5ml PBS, and finally cultured in 5ml complete DMEM per well. Medium was replaced when needed (typically every 1-2 days) by removing 3ml of overlaying DMEM and adding the same volume of fresh complete DMEM.

Cells were collected at 0h, 3 and 5 days post-infection. Cells were labeled with annexin V-PE during 15min at RT to discern between live and dead cells, then washed with PBS

and fixed with 4% PFA + Ca. Infected cells were analyzed by FACS as described for MH-S and J774 cells.

3.2.4.4. GFP expression in BMDM.

Intracellular expression of PhoP-regulon was tested through the GFP reporter system in bone marrow derived macrophages (BMDM). BMDM were cultivated in complete DMEM and $2.5x10^5$ cells were seeded per well in duplicates 24-well plates. In some of the plates cells were seeded above cover glasses. If required, cells were pre-treated with 100nM Bafilomycin 1h before the infection.

Infections were performed at MOI 10:1 bacteria per macrophage. After 4h, infection was stopped and cells were washed as described below.

For FACS analysis cells were collected at 2, 8 and 20 hours post-infection, washed and fixed with 4% PFA. For microscopy analysis cover glasses were collected, washed, labeled with 500μl 1/2000 Lysotracker for 1 hour at 37°C and fixed with 4% PFA.

3.2.4.5. Direct measure of gene expression.

Intracellular expression of PhoP-regulon was analyzed by RNA extraction and qRT-PCR analysis of the genes. BMDM cells were cultivated in complete DMEM and 10^8 BMDM cells were seeded in $150cm^2$ flasks. Some flasks were treated with 0.5μg/ml of lipopolysaccharide (LPS) and 100U/ml of Interferon gamma (IFNγ) 24 hours before the infection.

Infections were performed at MOI 10:1 bacteria per macrophage. After 4h, infection was stopped by removing bacterial suspension and cells were washed three times with 10ml of PBS and finally cultured in 15ml complete medium.

Cells were treated to extract mycobacterial RNA from intracellular bacteria as described previously.

3.2.5. Intracellular replication.

3.2.5.1. In MHS cells.

Intracellular replication of Mtb strains was tested in MHS cells. MHS cells were grown complete DMEM and $2x10^4$ cell per well were seeded in 24-well plates. Infections were performed at MOI 1:1 bacteria per macrophage. After 4h, infection was stopped and cells treated as described previously in infection protocols.

In order to know the number of intracellular bacteria at the end of time of infection (4h) and days 1, 3 and 7 post-infection, DMEM medium was removed, and 300μl 0.1% Triton X-100 were added to each well in order to lyse the cells. 700μl of PBS were added per well and the solution carefully mixed. Several dilutions of this lysate were plated on 7H10-ADC plates and viable bacteria numbers was estimated after 2-3 weeks by counting the number of colonies.

3.2.5.2. In MEF cells.

Intracellular replication of Mtb strains were tested in MEF cells grown in complete DMEM and 10^4 fibroblasts per well were seeded in 6-well plates. Infections were performed at MOI 10:1 bacteria per fibroblast. After 4h, infection was stopped and cells treated as described previously.

In order to know the number of intracellular bacteria at the end of time of infection (4h) and 3 and 7 days post-infection, same protocol as for MH-S cells was followed.

3.2.6. Infection and survival experiment in SCID mice.

Groups of five 8-weeks-old CB17 SCID mice were infected intraperitoneally with 10^6 appropiate mycobacteria strain: Mt103, *M. bovis* BCG Pasteur, MTBVAC and MTBVAC *zmp1*$^-$. Endpoint of the experiment were determined by survival of mice, loss of weight lower than 17g was established to determine the point of euthanize. Statistical analysis was performed using GraphPad Prism Software.

3.2.7. Vaccination and protection efficacy in mice.

Groups of six C57BL/6JRj mice were vaccinated with 10^5 appropiate viable bacteria using an intradermal way. Four weeks post infection; mice were challenged with approximately 10^3 cfu of Mtb H37Rv strain via intratracheal inoculation. 8 weeks post challenge mice were sacrificed and viable mycobacteria present in spleen and lungs were measured by plating the appropriate dilutions in 7H11 plates. Statistical analysis was performed using GraphPad Prism software.

3.2.8. Immunogenicity test in mice.

C57BL/6 mice were immunized subcutaneously with 10^5 of appropriate viable bacteria. Mice were maintained in groups of five individuals for four weeks, and then were euthanized and spleen and lungs were extracted. Spleens were grinded and cells suspensions were treated with Red Blood Cell Lysing Buffer (Sigma) to eliminate erythrocytes. Lungs were homogenized in 10mM HEPES-NaOH pH=7.4, 150mM NaCl, 5mM KCl, 1mM $MgCl_2$ and 1.8mM $CaCl_2$ buffer, and smashed in gentleMACS dissociator (MACS) and incubated with Red Blood Cell Lysing Buffer (Sigma). 10^6 splenocytes or lungs cells were seeded in 96 well plate (TPP) and incubated in RPMI media supplemented with 10% FBS, glutamine 2mM, penicillin 100U/ml, streptomycin 100μg/ml and β-mercaptoethanol 50μM; in presence of PPD (SSI) 1μg/ml at 37°C in 5% CO_2 atmosphere. After 18h of incubation, cells were marked with α-IFN-APC (BD) and α-CD4-FITC (BD) using BD Cytofix/Cytoperm Fixation/Permeabilization kit according to manufacturer recommendations. Cells were analyzed by flow cytometry using FACsAria (BD). Statistical analysis was performed using GraphPad Prism software.

3.3. Real-Time Quantitative PCR (qRT-PCR).

Reverser transcription was done from 1μg of RNA using 0.5μg of Random Hexamers (Integrated DNA Technologies) and the SuperScript III (Invitrogen – Life Technologies), performing the reaction at 25°C for 5min, 50°C for 2 hours and 70°C for 15min. Actinomycin D (Sigma) was added to each sample in order to prevent second-strand

cDNA synthesis during reverse transcription. cDNA prepared in this way was diluted 1:10 prior to use it to Real Time PCR amplification in the StepOne Plus Real Time PCR System (Applied Biosystems) using Master Mix containing Syber Green (Roche), and the suitable set of primers (Table 3), which were designed using the Primer Express Software (Applied Biosystems). A melting curve was performed for every pair of primers to verify that they produce a single product. PCR amplification was carried out as recommended for the manufacturer (95^{o}C for 10min; and 40 cycles of 95^{o}C for 15s, 60^{o}C for 1min). All the reactions were performed in triplicate, and the levels of mRNA were calculated relative to *sigA* mRNA and the reference strain H37Rv by the $\Delta\Delta C_t$ method.

Oligonucleotide	Sequence
RT-sigA-fw	CCGATGACGACGAGGAGATC
RT-sigA-rv	CGGAGGCCTTGTCCTTTTC
RTpks3 fw	GACGCTCGCTGAATCACAAA
RTpks3 rv	TCGCCGTGTGTCAGTCCTAC
RTpks2 fw	GCATCGGTGAAGACCAACTTC
RTpks2 rv	GATTACGTGGAACCACACCATGT
RTlipF fw	GCAGGCCCGAAGACCTCTAT
RTlipF rv	GGCGGCAAGCTGGATTC
RT mcr7 fw	ACGCCGCGAGGACATG
RT mcr7 rv	AGGGAGCTGCTTGGACAGAA
RT whiB6 Fw	CGCGGCAGAGGCTACAAC
RT whiB6 Rv	GGCGGTTACTGTCATGTCTACGT
RT espR fw	ATGTCGGCTCCCTACCTATCAC
RT espR rv	CCCCCGATGGGTTCGTA
RT nark1 Fw	CGACGCAATCTGCTTTGGT
RT nark1 Rv	AGCGTCCACACCGAGTAACC
RT fadD21 Fw	CATTGGACTTGACCGGGAAT
RT fadD21 Rv	GGCGCTTGGCAGATCCTT

Table 3. Oligonucleotids used for qRT-PCR assays in this work.

3.4. Extraction and analysis of lipids of mycobacteria.

Methyl-branched fatty acid-containing lipids of Mtb strains were radiolabeled by adding 7μCi (55mCi/mmol; MP Biomedicals, Illkirch, France) of ^{14}C-propionate to 16ml cultures in 7H9-T-ADC grown for 10 days, and were incubated for 24 hours at 37^{o}C with continuous agitation. After incubation with the radioactive propionate, lipids were extracted adding 2 volumes of methanol and one volume of chloroform for each

0.8 culture volume, giving a homogeneous mixture of one single phase. Mixture was incubated at least for 24h at room temperature before adding chloroform/water (1:1 v/v) to separate in two phases. The organic phase was recovered and the process was repeated after a new addition of chloroform. Extracts were concentrated under vacuum, washed thrice with distilled water and dried. The different extracts were resuspended in 200μl of chloroform and were separated by thin layer chromatography (TLC) in silica gel G60 plates (20x20cm; Merk). Different solvents were used: petroleum ether/diethylether (90:10 v/v) for PDIM analysis, chloroform/methanol/water (60:16:2 v/v) for DAT and SL, and chloroform/methanol (99:1 v/v) to analyze PAT. The radiolabeled compounds were visualized using a PhosphorImager Typhoon scanner (GE Healthcare).

3.5. Secreted Protein extraction from mycobacteria and preparation of protein samples.

In order to avoid albumin contamination in the secreted protein fraction, cultures were grown in 7H9 0.05% Tween 80 supplemented with 0.2% dextrose, 0.085% NaCl. After 3-4 weeks incubation at 37^{o}C, cultures were pelleted by centrifugation 10min at 4000rpm. The supernatant containing secreted proteins was incubated with 10% trichloroacetic acid (TCA) for one hour at 4^{o}C and then centrifuged 1h 30min at 4000rpm/4^{o}C. Pelleted proteins were incubated with cold acetone for 2h at -20^{o}C and centrifuged during 30min at 4000rpm/4^{o}C, process was repeated then the pellet was air-dried for 15min in ice. Finally resuspended in 200 μl DiGE labeling buffer (7M Urea, 2M Thiourea, 4% CHAPS, 30mM Tris, MilliQ water).

Protein sample pH was checked and adjusted to 9.5 with KOH 1N, quantified with the RC DC Protein Assay Kit (BioRad) and protein integrity and absence of albumin contamination was checked by SDS-PAGE and Coomassie staining.

Secreted proteins were analyzed through fluorescence two-dimensional difference gel electrophoresis (2D-DiGE) in the Proteomics Service of the IACS-Aragon.

3.6. Western Blotting.

Protein samples were quantified using the RC DC Protein Assay (BioRad) and equal amounts of protein preparations were loaded per well. Proteins were separated on SDS-PAGE 12-15% gels and transferred onto PVDF membranes using a semidry electrophoresis transfer apparatus (BioRad). Membranes were incubated in TBS-T blocking buffer (25mM Tris pH 7.5, 150mM NaCl, 0.05% Tween 20) with 5% w/v skimmed milk powder for 30min prior to overnight incubation with primary antibodies at the dilution indicated below. Membranes were washed in TBS-T three times, and then incubated with secondary antibodies for 1h before washing. Antibodies were used at the following dilutions. Antibodies were used at the following dilutions: 1/2000 for anti-ESAT-6 (EsxA), 1/5000 for anti-Ag85A, 1/1000 for anti-Ag85B, 1/10000 for anti-Ag85C. Horseradish peroxidase (HRP) conjugated IgG secondary antibodies (Sigma-Aldrich) were used at a 1/10000 dilution. Signals were detected using chemiluminescent substrates (GE Healthcare).

REFERENCES

1. Gonzalo-Asensio, J., et al., *The Mycobacterium tuberculosis phoPR operon is positively autoregulated in the virulent strain H37Rv.* J Bacteriol, 2008. **190**(21): p. 7068-78.
2. Arbues, A., et al., *Construction, characterization and preclinical evaluation of MTBVAC, the first live-attenuated M. tuberculosis-based vaccine to enter clinical trials.* Vaccine, 2013. **31**(42): p. 4867-73.
3. Liu, J., et al., *BCG vaccines: their mechanisms of attenuation and impact on safety and protective efficacy.* Hum Vaccin, 2009. **5**(2): p. 70-8.
4. Astarie-Dequeker, C., et al., *Phthiocerol dimycocerosates of M. tuberculosis participate in macrophage invasion by inducing changes in the organization of plasma membrane lipids.* PLoS Pathog, 2009. **5**(2): p. e1000289.
5. Cole, S.T. and B.G. Barrell, *Analysis of the genome of Mycobacterium tuberculosis H37Rv.* Novartis Found Symp, 1998. **217**: p. 160-72; discussion 172-7.
6. Soto, C.Y., et al., *Simple and rapid differentiation of Mycobacterium tuberculosis H37Ra from M. tuberculosis clinical isolates through two cytochemical tests using neutral red and nile blue stains.* J Clin Microbiol, 2002. **40**(8): p. 3021-4.
7. van Soolingen, D., et al., *DNA fingerprinting of Mycobacterium tuberculosis.* Methods Enzymol, 1994. **235**: p. 196-205.
8. Fontan, P., et al., *Global transcriptional profile of Mycobacterium tuberculosis during THP-1 human macrophage infection.* Infect Immun, 2008. **76**(2): p. 717-25.
9. Barker, L.P., D.M. Brooks, and P.L. Small, *The identification of Mycobacterium marinum genes differentially expressed in macrophage phagosomes using promoter fusions to green fluorescent protein.* Mol Microbiol, 1998. **29**(5): p. 1167-77.
10. Wards, B.J. and D.M. Collins, *Electroporation at elevated temperatures substantially improves transformation efficiency of slow-growing mycobacteria.* FEMS Microbiol Lett, 1996. **145**(1): p. 101-5.

Appendix

Results of the different extracellular culture conditions tested in order to search a condition activating the PhoP-regulon through the reporter system based on GFP fusions with promoters of PhoP-regulated genes (*dosR*, *lipF*, *pks2*, *icl* and *phoP*).

The culture conditions assayed are registered in Table 1.

CULTURE CONDITIONS	
Sources of Carbon	Glucose
	Acetate
	Propionate
Hypoxia	
Ions	Zinc
	Cupper
	Calcium
	Magnesium
Oxidative Stress	
Different Temperatures	
Fatty Acids	Oleic
	Palmitic
	Esteraric

Table 1. List of different culture conditions assayed with the GFP fusions with the promoters of PhoP-regulated genes.

Different sources of carbon.

Different sources of Carbon were added to the culture medium: Glucose, Acetate or Propionate. The PhoP-regulated isocitrate lyase (Icl) is a metabolic enzyme used by bacteria to sustain growth on even-chain fatty acids through an anaplerotic pathway called the glyoxilate shunt. It also serves a parallel pathway involved in the metabolism of propionyl-Coa generated by β-oxidation of oddchain fatty acids, called the methylcitrate cycle [1, 2]. We performed this assay with the intention of verify the response of the *icl* promoter to the presence of propionate as it has been described, and ergo, the proper response of the GFP::promoter reporter system.

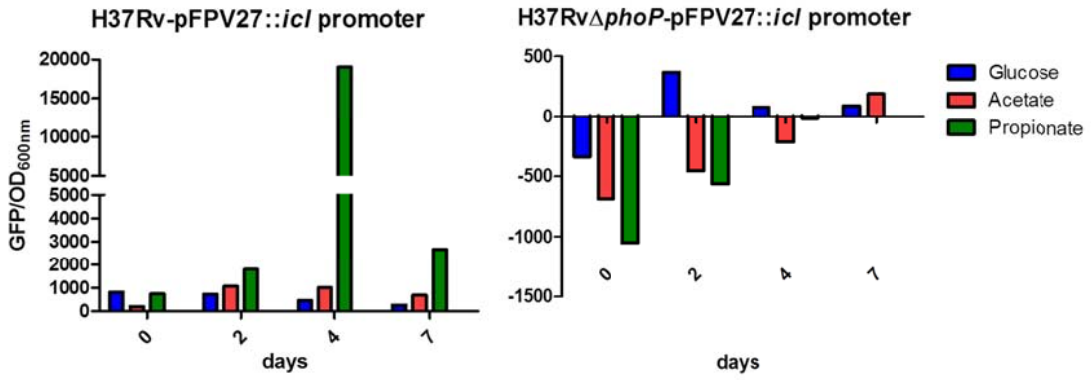

Figure 1. Graphical representation of the effect of different sources of carbon in the culture medium (glucose, acetate or propionate). The fluorescence registered is proportional to the activation of the *icl* promoter and it is normalized against the OD_{600nm} of the cultures at each point. The Icl gene has been described to activate in the presence of propionate in a PhoP-independent pathway, and the results corroborates that, allowing us to verify our GFP fusion reporter system is working properly. This is a representative graph from a triplicate experiment.

Hypoxia.

In order to mimic anaerobic environments those are developed inside the granuloma during latent infection. Several studies have suggested that the PhoP-regulated DosR regulon plays a role in latent infection and in persistence in animal models [3, 4]. In this assay both *dosR* and *pks2* promoters were chosen to be analyzed; DosR has been reported to response to hypoxia and Pks2 was chosen as a reporter for the activity of the PhoP-regulon. We did not find any remarkable differences in the activity of *pks2* promoter since the profile of the fluorescence registered was the same for both wild type and *phoP* mutant strains.

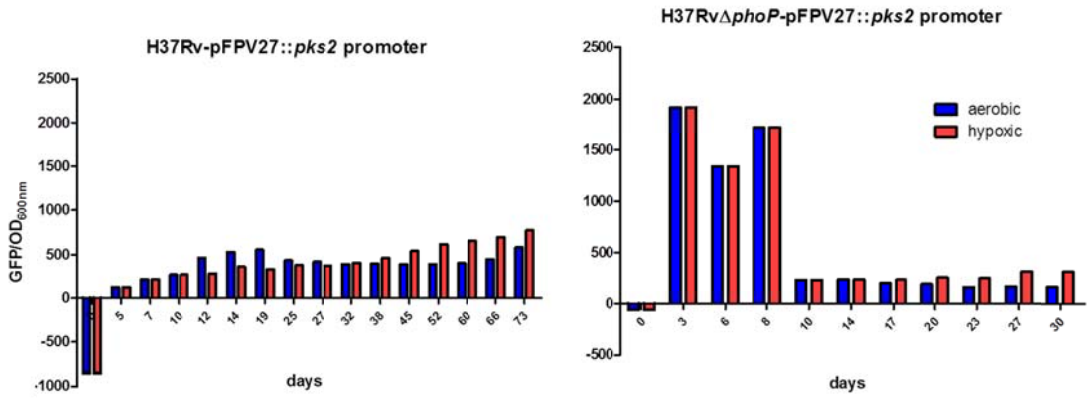

Figure 2. Graphical representation of the effect of hypoxia during growth. The fluorescence registered is proportional to the activation of the *pks2* promoter and it is normalized against the OD_{600nm} of the cultures at each point. No remarkable profile of expression was registered for *pks2* gene in hypoxic cultures. This is a representative graph from a duplicate experiment.

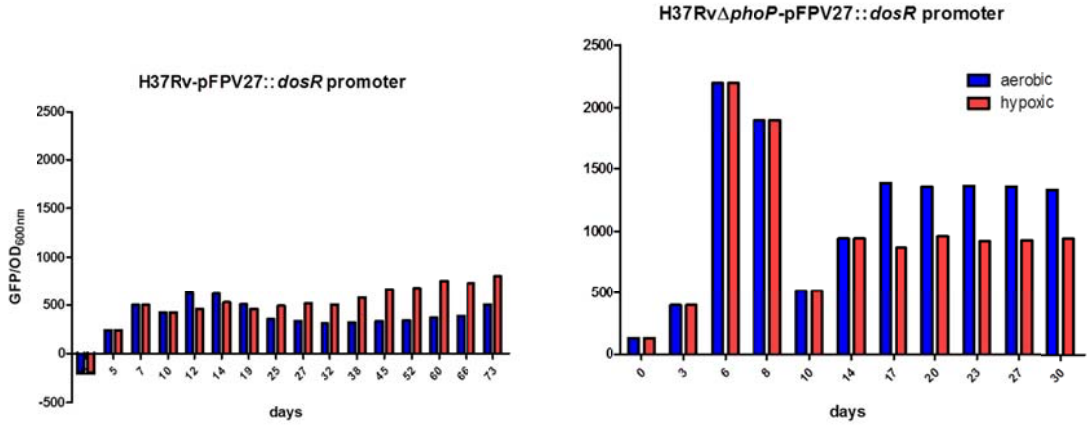

Figure 3. Graphical representation of the effect of hypoxia during growth. The fluorescence registered is proportional to the activation of the *dosR* promoter and it is normalized against the OD_{600nm} of the cultures at each point. The DosR gene has been described to be activated under hypoxic conditions in a PhoP-independent pathway. This is a representative graph from a duplicate experiment.

Growth medium with different concentration of ions.

Different concentrations of various ions were added to the culture medium. The role of salts and ions in balancing the proton and electron gradients that accompany phagosome acidification and oxidative burst has been extensively studied, demonstrating the importance of the phagosomal lumen content in the antimicrobial mechanisms [5]. We designed assays considering broad range of Zn^{2+}, Cu^{2+}, Ca^{2+} and Mg^{2+} concentrations in order to analyze the response of the PhoP-regulated genes [6, 7]. The profile of fluorescence registered and ergo, of the *pks2* activity did not show any remarkable differences comparing both wild type and *phoP* mutant strains in the presence of Zn^{2+}, Cu^{2+} or Mg^{2+} (Figures 4, 5 and 7). In the presence of low concentrations of Ca^{2+} (Figure 6), an increase in the *pks2* promoter activity was registered in the wild type strain, but not in the *phoP* mutant one, showing it could be PhoP-mediated; nevertheless, when we performed the assay with a low range of Ca^{2+} concentrations (Figure 8), no remarkable differences in the profile of fluorescence were registered.

Zinc

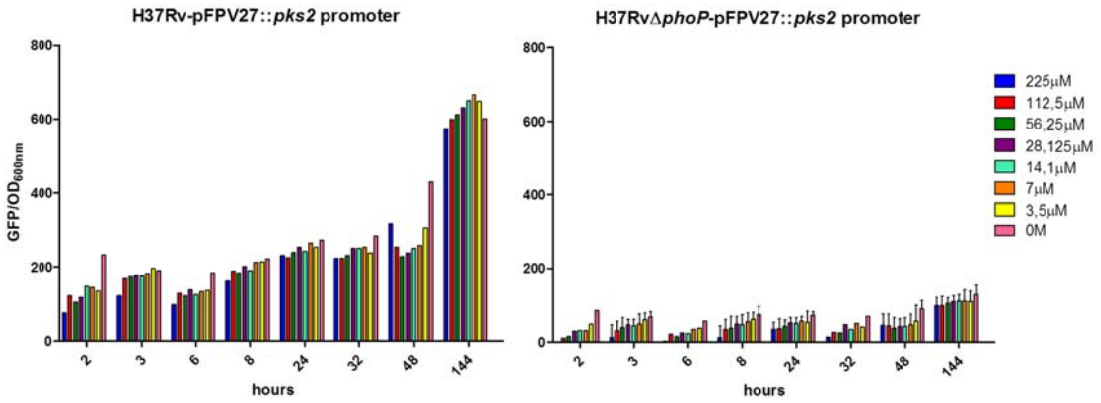

Figure 4. Graphical representation of the effect of the presence of Zn^{2+} in the culture medium. The fluorescence registered is proportional to the activation of the *pks2* promoter and it is normalized against the OD_{600nm} of the cultures at each point. No remarkable profile of expression was registered for *pks2* gene. This is an average graph from a duplicate experiment.

Cupper

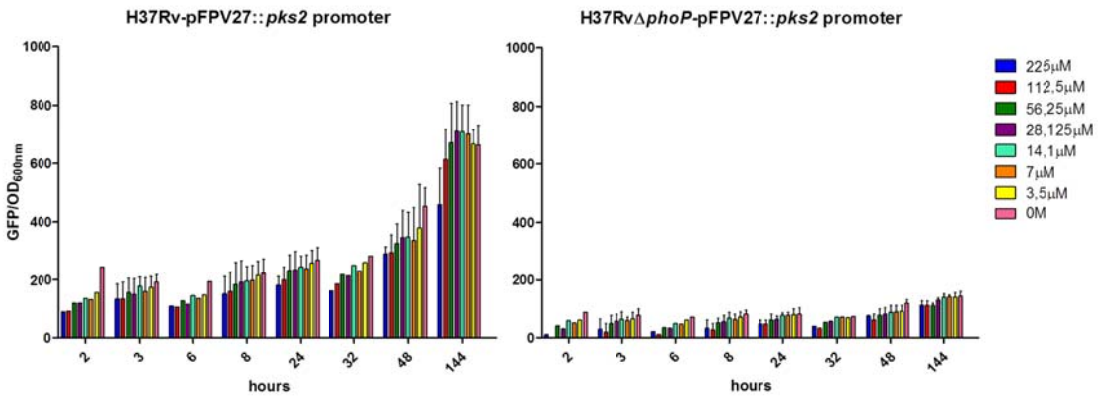

Figure 5. Graphical representation of the effect of the presence of Cu^{2+} in the culture medium. The fluorescence registered is proportional to the activation of the *pks2* promoter and it is normalized against the OD_{600nm} of the cultures at each point. No remarkable profile of expression was registered for *pks2* gene. This is an average graph from a duplicate experiment.

Calcium.

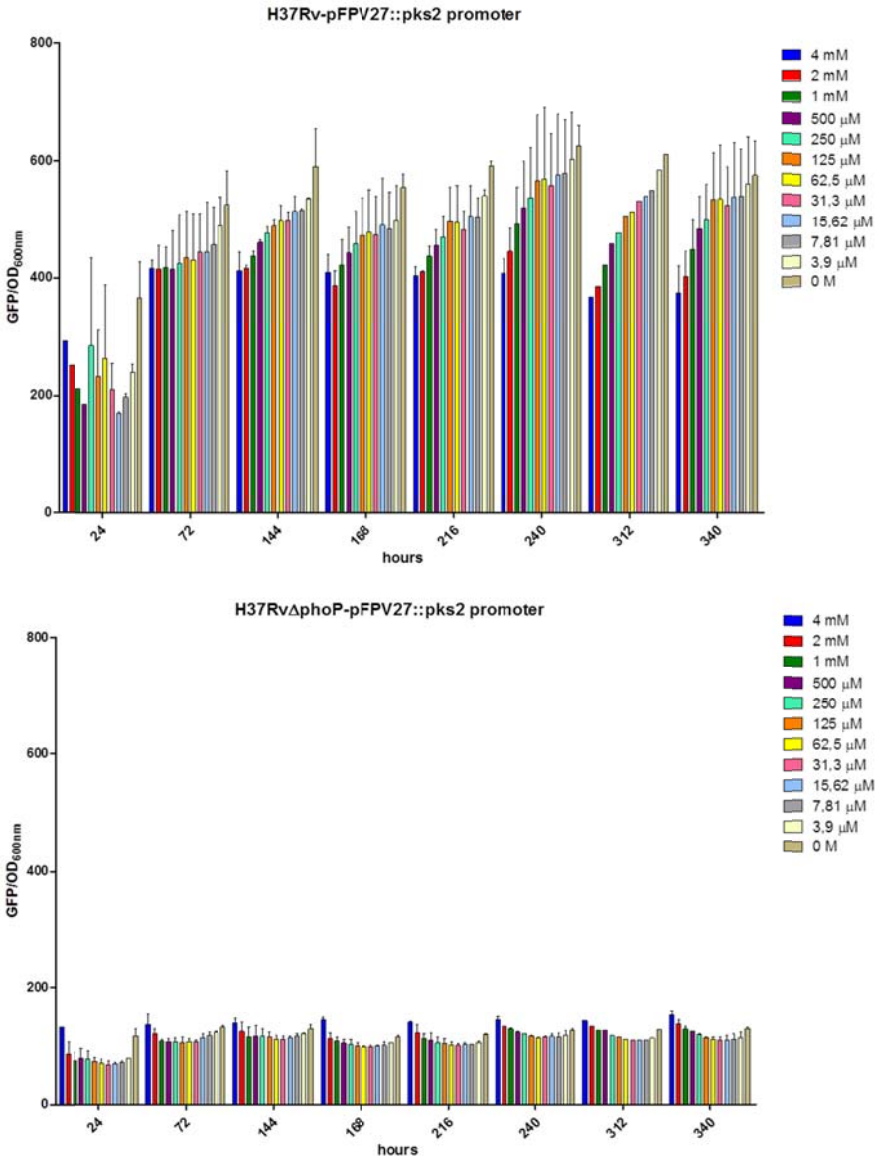

Figure 6. Graphical representation of the effect of the presence of Ca^{2+} in the culture medium. The fluorescence registered is proportional to the activation of the *pks2* promoter and it is normalized against the OD_{600nm} of the cultures at each point. There is an increase in the activity of the *pks2* promoter registered when exposed to low concentrations of Calcium that is not observed in the *phoP* mutant strain. This is an average graph from a duplicate experiment.

Magnesium.

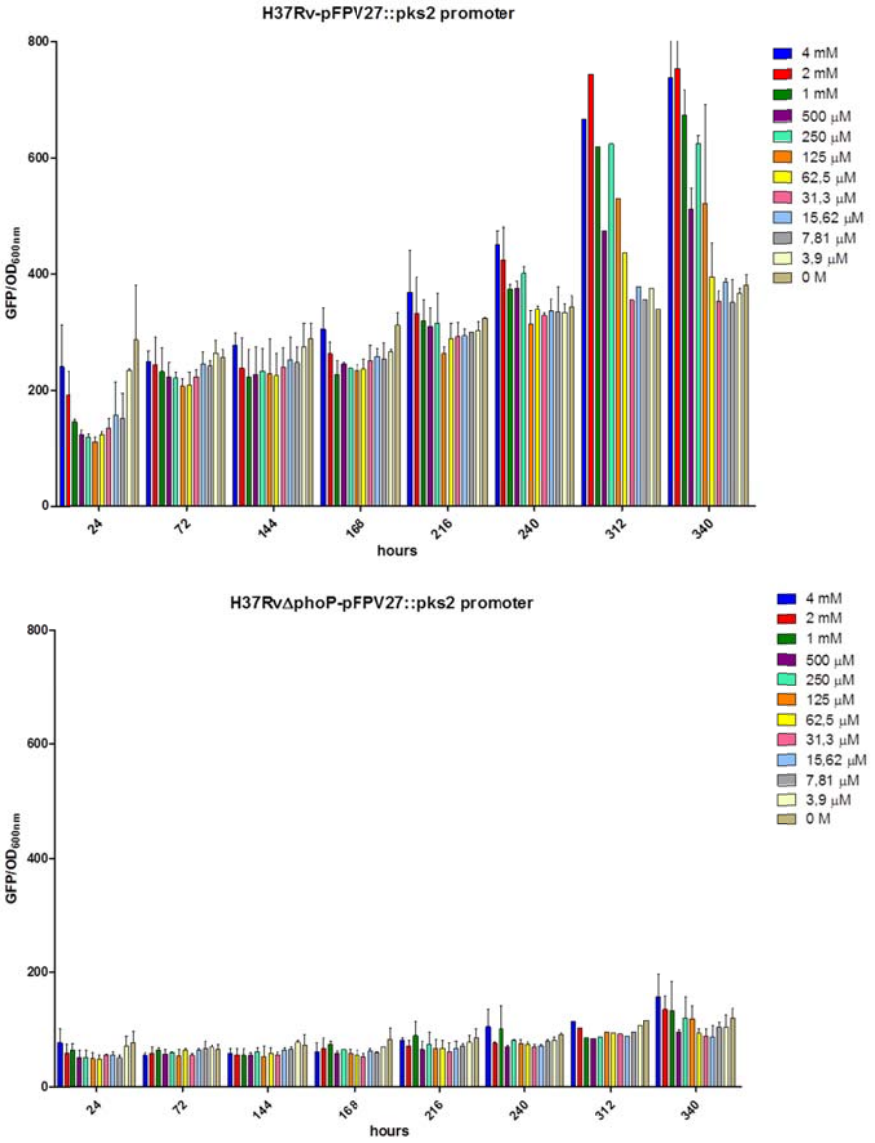

Figure 7. Graphical representation of the effect of the presence of Mg^{2+} in the culture medium. The fluorescence registered is proportional to the activation of the *pks2* promoter and it is normalized against the OD_{600nm} of the cultures at each point. No remarkable profile of expression was registered for *pks2* gene. This is an average graph from a duplicate experiment.

Calcium in low concentrations.

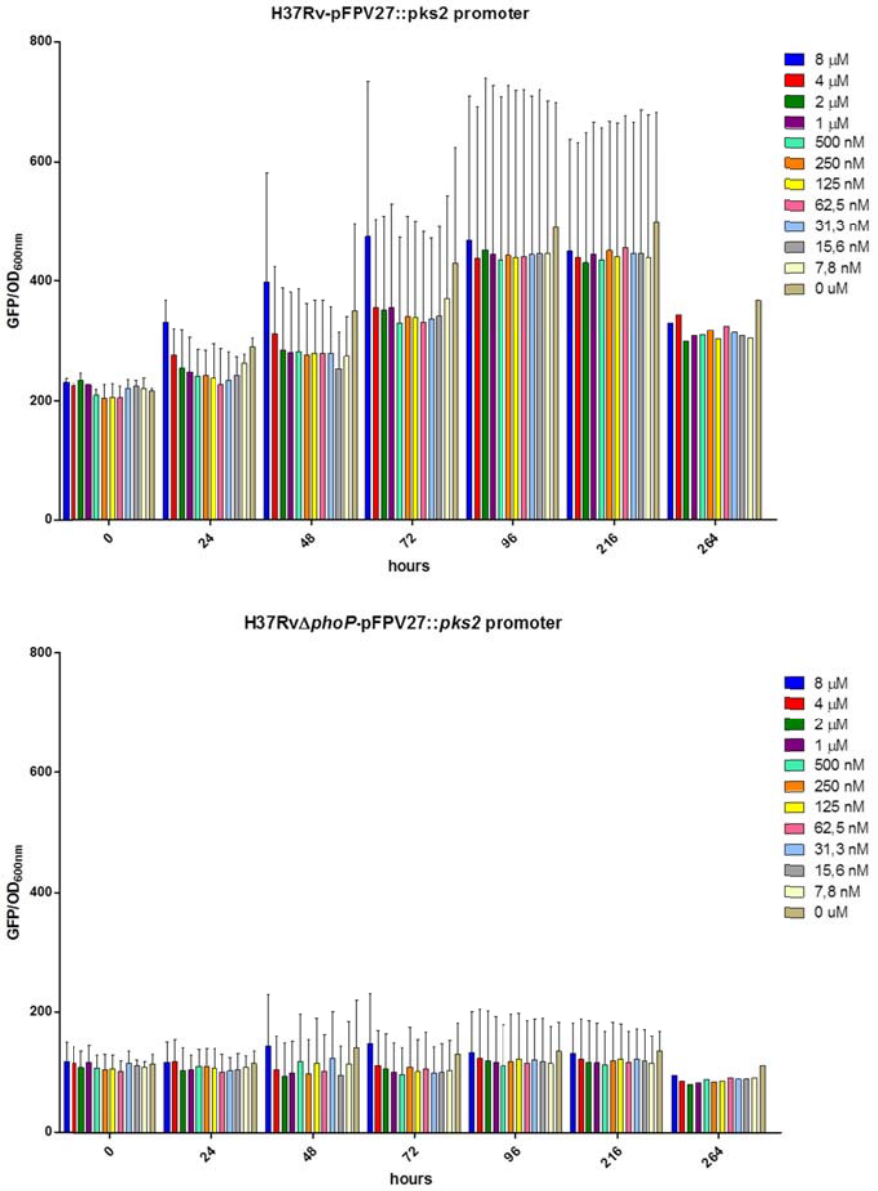

Figure 8. Graphical representation of the effect of the presence of low concentrations of Ca^{2+} in the culture medium. The fluorescence registered is proportional to the activation of the *pks2* promoter and it is normalized against the OD_{600nm} of the cultures at each point. Despite in the assays with Ca^{2+} differences in expression were registered at low concentrations of Calcium in the wild-type strain but not in the phoP mutant, no remarkable profile of expression was registered when low concentrations of Ca^{2+} were assayed for *pks2* gene. This is an average graph from a duplicate experiment.

Oxidative stress.

Another major arm of the phagocyte anti-microbial arsenal is the production of toxic reactive oxygen and nitrogen intermediates (ROI and RNI). A growing number of studies link the production of ROI, its effects on the phagosomal milieu and an indirect impact on bacterial killing [5, 8]. We decided to add different concentration of H_2O_2 to the culture medium to mimic the oxidative stress and analyze the response of the PhoP-regulon. The fluorescence profile registered and ergo, the activity of *pks2* promoter did not show any differences between strains, wild type and *phoP* mutant.

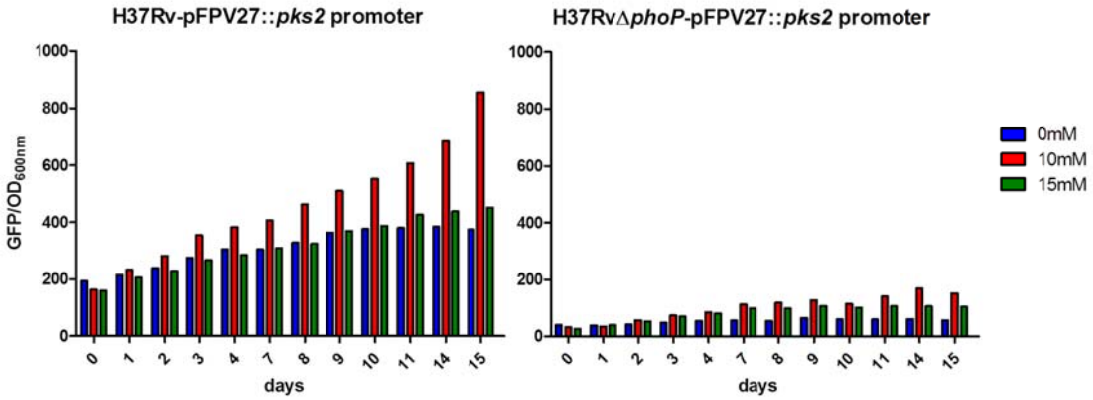

Figure 9. Graphical representation of the effect of the presence of H_2O_2 in the culture medium. The fluorescence registered is proportional to the activation of the *pks2* promoter and it is normalized against the OD_{600nm} of the cultures at each point. No remarkable profile of expression was registered for *pks2* gene. This is representative graph from a duplicate experiment.

Culture at different temperatures.

Even being 37^{o}C the physiological temperature the regular culture temperature, we decided to incubate cultures at 42^{o}C and room temperature trying to mimic different situations, like fever, that could stress the bacteria and analyze the response of the PhoP-regulon. The profile of fluorescence registered for both wild type and *phoP* mutant strains did not show any remarkable difference, meaning that temperatures might not be triggering any response in PhoP-regulon activity.

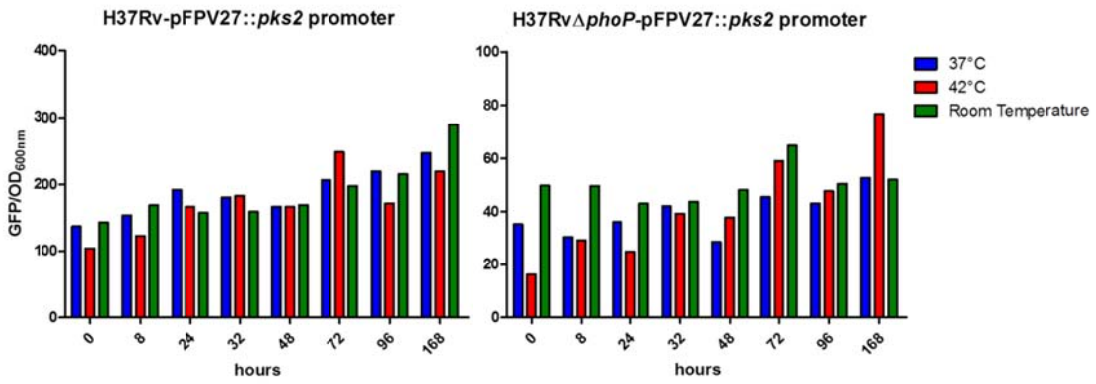

Figure 10. Graphical representation of the effect of different temperatures. The fluorescence registered is proportional to the activation of the *pks2* promoter and it is normalized against the OD_{600nm} of the cultures at each point. No remarkable profile of expression was registered for *pks2* gene. This is representative graph from a duplicate experiment.

Gene expression in presence of fatty acids in the culture medium.

It has been shown that *M. tuberculosis* uses host lipids, in particular, fatty acids and cholesterol, as energy sources during intracellular growth and persistence [9]. In order to study the response of PhoP-regulon to fatty acids, we incubated cultures of *M. tuberculosis* with culture medium in presence of oleic, palmitic and estearic acids. In this assay we did not use the GFP::promoter reporter system, in return we extracted bacterial RNA at the selected points and the expression of *pks2* was directly measured by qRT-PCR. The expression profile registered for both wild type and *phoP* mutant strains did not show any remarkable difference, meaning that the presence of fatty acids might not be the activator of the PhoP-regulon.

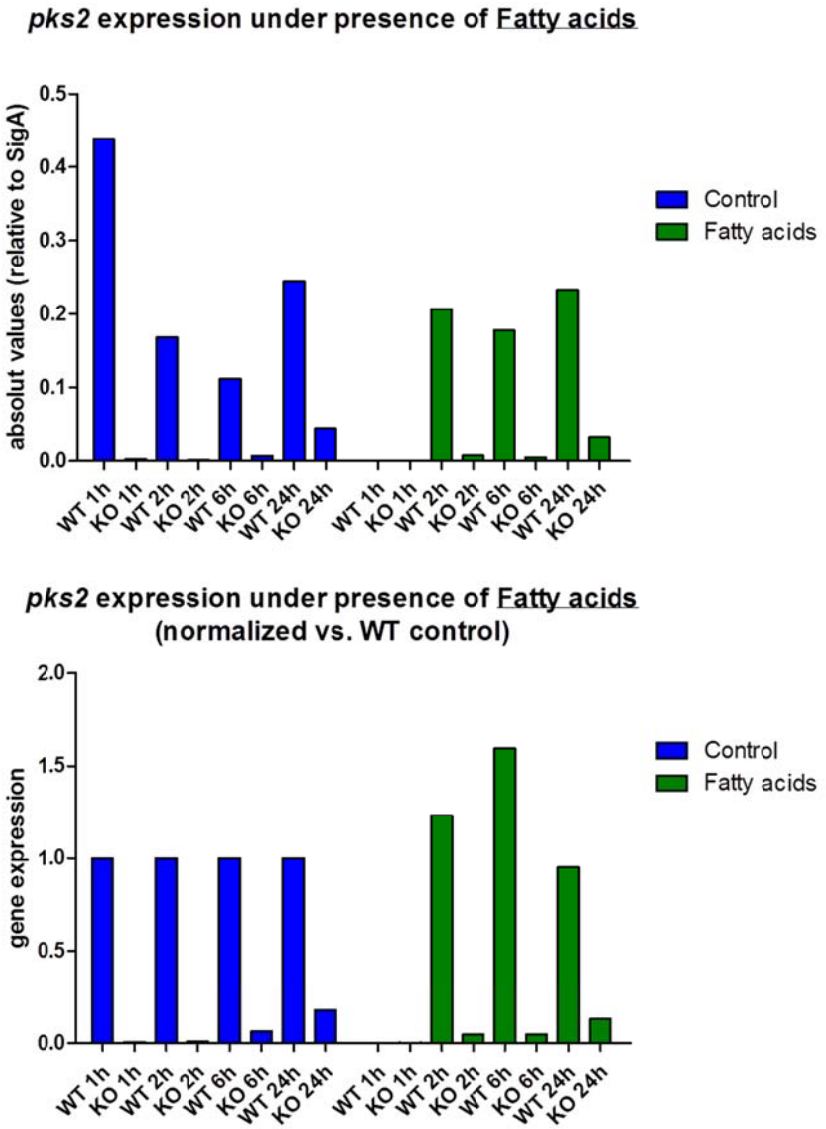

Figure 11. Graphical representation of the effect of the presence of different fatty acids, oleic, palmitic and estearic acids, in the culture medium. The fluorescence registered is proportional to the activation of the *pks2* promoter and it is normalized against the OD_{600nm} of the cultures at each point. No remarkable profile of expression was registered for *pks2* gene. This is a representative graph from a duplicate experiment.

REFERENCES

1. Munoz-Elias, E.J., et al., *Role of the methylcitrate cycle in Mycobacterium tuberculosis metabolism, intracellular growth, and virulence.* Mol Microbiol, 2006. **60**(5): p. 1109-22.
2. Eoh, H. and K.Y. Rhee, *Methylcitrate cycle defines the bactericidal essentiality of isocitrate lyase for survival of Mycobacterium tuberculosis on fatty acids.* Proc Natl Acad Sci U S A, 2014. **111**(13): p. 4976-81.
3. Kendall, S.L., et al., *The Mycobacterium tuberculosis dosRS two-component system is induced by multiple stresses.* Tuberculosis (Edinb), 2004. **84**(3-4): p. 247-55.
4. Leistikow, R.L., et al., *The Mycobacterium tuberculosis DosR regulon assists in metabolic homeostasis and enables rapid recovery from nonrespiring dormancy.* J Bacteriol, 2010. **192**(6): p. 1662-70.
5. Soldati, T. and O. Neyrolles, *Mycobacteria and the intraphagosomal environment: take it with a pinch of salt(s)!* Traffic, 2012. **13**(8): p. 1042-52.
6. Botella, H., et al., *Mycobacterial p(1)-type ATPases mediate resistance to zinc poisoning in human macrophages.* Cell Host Microbe, 2011. **10**(3): p. 248-59.
7. Botella, H., et al., *Metallobiology of host-pathogen interactions: an intoxicating new insight.* Trends Microbiol, 2012. **20**(3): p. 106-12.
8. Aussel, L., et al., *Salmonella detoxifying enzymes are sufficient to cope with the host oxidative burst.* Mol Microbiol, 2011. **80**(3): p. 628-40.
9. Rodriguez, J.G., et al., *Global adaptation to a lipid environment triggers the dormancy-related phenotype of Mycobacterium tuberculosis.* MBio, 2014. **5**(3): p. e01125-14.